A MICROCONTINUUM ANALYSIS OF SOME LUBRICATION PROBLEMS

By

CHANDAN SINGH

DEPARTMENT OF MATHEMATICS

INDIAN INSTITUTE OF TECHNOLOGY, KANPUR

MARCH, 1981

A MICROCONTINUUM ANALYSIS OF SOME LUBRICATION PROBLEMS

A Thesis Submitted
in Partial Fulfilment of the Requirements
for the Degree of
DOCTOR OF PHILOSOPHY

By

CHANDAN SINGH

to the
DEPARTMENT OF MATHEMATICS
INDIAN INSTITUTE OF TECHNOLOGY, KANPUR

MARCH, 1981

DEDICATION

TO MY

FATHER - SRI BACHI SINGH PATWAL

MOTHER - SMT. TULSI DEVI

AND

ELDER BROTHER

SRI DAN SINGH PATWAL

CERTIFICATE

This is to certify that the matter embodied in the thesis entitled "A Microcontinuum Analysis of Some Lubrication problems" by Mr. Chandan Singh for the award of the degree of Doctor of Philosophy of the Indian Institute of Technology, Kanpur, is a record of bonafide research work carried out by him under my supervision and guidance. The thesis has, in my opinion, reached the standard fulfilling the requirements of the Ph.D. degree. The results embodied in this thesis have not been submitted to any other University or Institute for the award of any degree or diploma.

Prawal Sinha.
30/3/81.

(Prawal Sinha)
Thesis Supervisor
Department of Mathematics
Indian Institute of Technology
KANPUR-208016, U.P.
INDIA.

March- 1981.

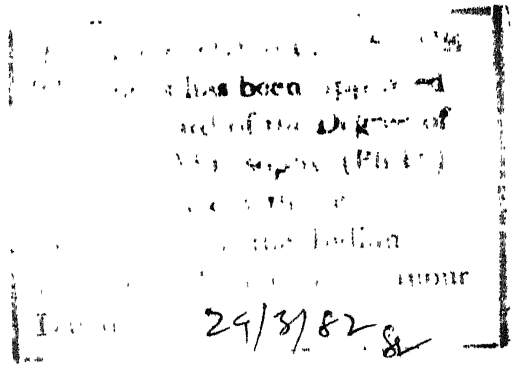

ACKNOWLEDGEMENTS

I shall ever remain deeply indebted and extremely grateful to my supervisor, Dr. Prawal Sinha, Department of Mathematics, I.I.T. Kanpur, who has guided me throughout this work and without whose invaluable inspiration and encouragement the investigations contained in this thesis would not have been possible. The affection bestowed upon me by him, would be a cherished possession of my life.

I take this opportunity to thank Prof.J.B.Shukla, Head of the Department of Mathematics, I.I.T.Kanpur, who inspired me to work in the field of Tribology. His example and precept both have taught me.

I am thankful to Prof.J.N.Kapur and Prof.R.K.Jain, Department of Mathematics, I.I.T.Kanpur, for their encouragement and inspiration from time to time.

I shall be failing in my duty if I do not unreservedly acknowledge my indebtedness to my colleagues, Mr. Axay Kumar Mishra, Mr.A. Nautiyal, Mr.T.S. Nailwal, Mr. K.R.K.Prasad and Mr. S.C.Pandey, for their unfailing cooperation, both academically and non-academically, in and out of the campus, during various stages of my research. Their close association, I will remember for years to come.

I humbly dedicate this work to my parents, Sri Bachi Singh Patwal and Smt. Tulsi Devi, and my elder brother, Sri Dan Singh Patwal, who have with great devotion apart from sustaining me through many

difficult times with tender care and affection, worked untiringly all these years to provide an opportunity for higher education.

The thanks are also due to I.I.T. Kanpur and CSIR, New Delhi, India, for providing the financial assistance during this period.

Finally, the author expresses his thanks to Mr.A.K.Bhatia for his unfailing patience in type - cutting the stencils, to Mr. G.L.Misra and Mr. S.K.Tewari for their careful symbol filling and to Mr. A.N.Upadhyaya for neat cyclostyling. The pains taken by Mr. B.N.Srivastava in drawing the figures is also sincerely acknowledged.

Chandan Singh

March-1981. (CHANDAN SINGH) 30/3/81

ABSTRACT

The need for a proper theoretical explanation of the residual film, reported by various workers, has led to the development of microcontinuum theory of lubrication. Even after a decade this theory seems to be in a preliminary state. Scores of lubrication problems are yet to be analysed from this view point. For example, little work has appeared on dynamically loaded bearings and porous bearings from the microcontinuum view point. Moreover, no attempt has so far been made to study the impact of the micropolarity on finite dimensional bearings and bearings with rough surfaces.

Thus, in this thesis, an endeavour is made to study these lubrication problems using the micropolar fluid theory. The thesis is divided into IX Chapters.

Chapter I is of introductory type, wherein are discussed important experimental evidences, which establish the existence of the residual film (rheological abnormalities). It also emphasizes the fact that the origin of the so called rheological abnormalities may lie in the micro-mechanical motion of the fluid element. Thus this Chapter lays the foundation for the present work.

In Chapter II, the basic equations for the micropolar fluid are given. Attention is restricted to a three dimensional laminar flow of an incompressible micropolar fluid in a finite slider type

bearing. Application of usual lubrication assumptions and a subsequent detailed order of magnitude analysis reduces the governing equations to two systems of coupled ordinary differential equations to be solved for velocity distributions and microrotation velocities (no paper, published so far, gives such a detailed order of magnitude analysis for the three dimensional problem). Generalized Reynolds equation is then obtained in a conventional manner by integrating the continuity equation. Also given in this Chapter are expressions for flow fluxes and shear stresses.

In Chapter III, the generalized Reynolds equation, obtained in Chapter II, is applied to analyse the problem of two dimensional squeeze film of a ball in a spherical seat and to some three dimensional non-cyclic squeeze films, in an effort to study the effects of rigid particle additives for the three dimensional micropolarity model.

In Chapter IV, dynamically loaded short journal bearings are studied. Reynolds equation for the general case, where both wedge and squeeze films are active, is derived. Detailed consideration is given to the dynamic behaviour of squeeze film in a short journal bearing subject to a sinusoidal loading with no journal rotation.

Chapter V, also gives an analysis of dynamically loaded bearings. The problem considered is that of the roller bearing in combined rolling, sliding and normal motion, under cavitation boundary conditions.

In Chapter VI, the micropolar theory is applied to the analysis of bearings with rough surfaces. Generalized forms of Reynolds equation are derived for three cases of roughness, namely, longitudinal, transverse and isotropic, using the stochastic approach. These equations are subsequently applied to the problem of infinitely long journal bearing whose stationary surface (bearing) is assumed to be rough, in an order to study the interaction of micropolarity with surface asperities, using the half Sommerfeld boundary conditions.

In Chapter VII, the generalized Reynolds equations, obtained in Chapter VI, are applied to study the squeezing between parallel plates. Three geometries, namely, infinitely long parallel plates, circular plates and finite rectangular plates are considered.

In Chapter VIII, the problem of synovial joints lubrication is studied, by approximating the joints by a spherical bearing, the cartilage surface as porous (but rigid) and the lubricating synovial fluid as micropolar. A modified form of Reynolds equation is derived using the slip boundary conditions.

Chapter IX is of conclusive nature wherein are presented the main conclusions of the work done in the thesis and the conclusions are compared with the various experimental evidences. The one overall conclusion that emerges is the existence of increased effective viscosity in the proximity of a solid surface. This increase is further enhanced when the surfaces are rough.

A part of the work presented in this thesis has been accepted for publication in the form of following research papers.

(1) Theoretical Effects of Rigid Particle Additives in Non-Cyclic Squeeze Films, 'TRANS.ASME,J.Lub.Tech'.

(2) Dynamic Loading in Micropolar Fluid Lubricated Short Bearings. 'J.Mech.Engng.Sci.,Instn. of Mech. Engrs'.

LIST OF PAPERS

During the research tenure (December 1977 to March 1981) thirty (30) research problems were finalized. These are listed in two categories.

(1) Category A - Related to the thesis

(2) Category B - Not related to the thesis

The details of each category is as follows

CATEGORY A - WORK RELATED TO THE THESIS

The work presented in the thesis has been accepted/communicated for publication in the forms of the following research papers:

(i) Papers Accepted

(1) Theoretical Effects of Rigid Particle Additives in Non-Cyclic Squeeze Films.
TRANS.ASME,J.Lub.Tech., (IN PRESS).

(2) Dynamic Loading in Micropolar Fluid Lubricated Short Bearings.
J.Mech.Engng.Sci.,Instn.Mech.Engrs. (IN PRESS).

(ii) Papers Communicated

(3) Three Dimensional Reynolds Equation for Micropolar Fluid Lubricated Bearings.

(4) Lubrication of Roller Bearing in Combined Rolling,Sliding and Normal Motion With Additives.

(5) Lubrication of Rough Surfaces - A Microcontinuum Analysis.

(6) Microcontinuum Analysis of Squeeze Films Between Rough Surfaces.

(7) Micropolar Squeeze Films Between Rough Rectangular Plates.

(8) Lubrication of Human Joints - A Microcontinuum Approach.

CATEGORY B-WORK NOT RELATED TO THE THESIS

Apart from the work presented in the thesis a number of other research problems were finalized. Details are as follows:

(i) Papers Published

(9) The Effect of Additives in the Lubricant of a Composite Bearing with an Inclined Stepped Surface.
Wear, Vol.66, No.1, 1981, p.17-26.

(10) Effect of Viscosity Variation Due to Lubricant Additives in Journal Bearings.
Wear, Vol.66, No.1, 1981.

(11) Couple Stresses in Journal Bearing Lubricants and the Effect of Cavitation.
Wear, Vol.67, No.1, 1981, p.15-24.

(12) Couple Stresses in the Lubrication of Rolling Contact Bearings Considering Cavitation.
Wear, Vol.67, No.1, 1981, p.85-97.

(ii) Papers Accepted

(13) Lubrication of a Cylinder on a Plane With a Non-Newtonian Fluid Considering Cavitation.
TRANS.ASME, J.Lub.Tech. (IN PRESS).

(14) Non-Newtonian Squeeze Films in Journal Bearings.
Wear. (IN PRESS).

(15) Couple Stresses in the Elastohydrodynamic Film in Roller Bearings.
Wear. (IN PRESS).

(16) Non-Newtonian Squeeze Films in Spherical Bearings.
Wear. (IN PRESS).

(iii) Papers Communicated

(17) Non-Newtonian Power-Law Fluid Lubrication of Lightly Loaded Cylinders With Normal and Rolling Motion.

(18) Cyclic Squeeze Film in Porous Bearing Using Velocity Slip Conditions.

(19) A Microcontinuum Analysis of the Self Propulsion of the Spermatozoa in the Cervical Canal.

(20) Elastohydrodynamic Lubrication of Circular Plate Thrust Bearing With Power Law Lubricants.

(21) Viscosity Variation in Journal Bearing Lubricant With Additives Considering Cavitation.

(22) Effect of Additives on Finite Step Bearing Lubricant.

(23) Non-Newtonian Lubrication Theory for Rough Surfaces : Application to Rigid and Elastic Rollers.

(24) Effects of Surface Roughness and Additives in Lubrication : Generalized Reynolds Equation and Its Application to Elastohydrodynamic Film.

(25) Non-Newtonian Theory for Rough Squeeze Films.

(26) Dynamically Loaded Rough Journal Bearings.

(27) Radial and Frictional Forces in Misaligned Radial Face Seals With Non-Newtonian Fluids.

(28) Hydrostatic Pressure Effects in Misaligned Radial Face Seals With Non-Newtonian Fluids.

(29) Elastohydrostatic Forces in Misaligned Radial Face Seals.

(30) Micropolar Squeeze Films in Porous Hemispherical Bearings.

CONTENTS

CHAPTER		PAGE
	CERTIFICATE	i
	ACKNOWLEDGEMENTS	ii
	ABSTRACT	iv
	LIST OF PAPERS	viii
	NOMENCLATURE	xiii
I :	GENERAL INTRODUCTION	1
	1.1 Why lubrication	1
	1.2 Early days in lubrication	2
	1.3 Classification of lubrication	4
	1.4 Lubrication and rheology	5
	1.5 Experimental evidences	7
	1.6 Developments in theoretical rheology	13
	1.7 Microcontinuum analysis of fluid flows	17
II :	BASIC EQUATIONS AND GENERALIZED REYNOLDS EQUATION FOR MICROPOLAR FLUIDS	21
	2.1 Introduction	21
	2.2 Balance equations for micropolar fluids	22
	2.3 Lubrication problem-Assumptions and basic equations	25
III:	TWO AND THREE DIMENSIONAL NON-CYCLIC SQUEEZE FILMS	37
	3.1 Introduction	37
	3.2 Spherical bearings	38
	3.3 Sliders and rectangular plates	42
	3.4 Elliptical plates	44
	3.5 Miscellaneous configurations	45
	3.6 Results and discussion	50
IV :	DYNAMICALLY LOADED SHORT JOURNAL BEARINGS	65
	4.1 Introduction	65
	4.2 The problem and analysis	67
	4.3 Results and discussion	75
V :	LUBRICATION OF ROLLER BEARINGS IN COMBINED ROLLING, SLIDING AND NORMAL MOTION	86
	5.1 Introduction	86
	5.2 The problem and theoretical analysis	87
	5.3 Results and discussion	96

VI : LUBRICATION THEORY FOR ROUGH SURFACES AND ITS APPLICATION TO A JOURNAL BEARING 108

6.1 Introduction 108
6.2 Modified Reynolds equation for rough surfaces 110
6.3 Bearing characteristics 116
6.4 Modified Reynolds equation applied to a journal bearing 118
6.5 Non-dimensional forms 123
6.6 Results and discussion 126

VII : SQUEEZE FILMS BETWEEN ROUGH SURFACES 138

7.1 Introduction 138
7.2 Mathematical analysis 141
7.3 Squeeze films between rough infinitely long parallel plates 143
7.4 Squeeze film between rough circular plates 147
7.5 Squeezing between rough rectangular plates 151
7.6 Numerical results 157
7.7 Results and discussion 158

VIII : LUBRICATION OF HUMAN JOINTS 170

8.1 Introduction 170
8.2 Anatomy of a synovial joint 176
8.3 Theoretical formulation-Assumptions and equations 176
8.4 Normal motion of human joint 186
8.5 Results and discussion 191

IX : SUMMARY AND CONCLUSIONS 207

REFERENCES 217

NOMENCLATURE

a_1	eccentricity for spherical bearing
a_2	x-dimension of rectangular plate (or slider bearing)
A	area of rectangular plate
A_1	major axis of elliptical plate
b	half total range of random film thickness variable
b_2	z-dimension of rectangular plate (or slider bearing)
B	roughness parameter
B_1	minor axis of elliptical plate
B_F	quantity, defined by eqn. (5.23)
c	bearing clearance
C_F	quantity defined by eqn. (5.24)
$\bar{C}_R$	coefficient of friction parameter
D	diameter of the journal bearing
e	eccentricity of the journal bearing
E(f)	expected or mean value of f
$f(h_s)$	roughness distribution function
$f(N,\ell,h)$	defined by eqn. (2.52) for Chapters III, IV and V, and defined by eqn. (2.55) for Chapters VI and VII
F	frictional force
$F_{1,2}$	frictional forces on the plane and cylindrical surface, respectively
F_{R_1}, F_{R_2}	frictional force ratio parameters
$\bar{F}_R$	frictional drag ratio parameter

$\vec{F}^*$	body force per unit mass
$F(N,L,H)$	defined by eqn. (3.14)
$F_1(N,L,B)$	defined by eqn. (7.15)
$F_2(N,L,H_n,B)$	defined by eqn. (7.19)
$F_3(N,L,B)$	defined by eqn. (7.27)
$F_4(N,L,H_n,B)$	defined by eqn. (7.28)
$g(N,\ell,h)$	defined by eqn. (2.61) for Chapters III, IV and V ; and by eqn. (2.64) for Chapters VI and VII
$G(N,L,H)$	defined by eqn. (5.20)
$G(N,L,H,B)$	defined by eqn. (6.55)
h	film thickness
h_o	minimum/final film thickness
h_1	initial film thickness
h_n	nominal (average) film thickness
h_m	film thickness corresponding to $x = x_m$
h_s	random part of the film thickness
h_{n_i}	initial (nominal) film thickness
H,H_n,H_m,H_s,H_1	non-dimensional form of h,h_n,h_m,h_s,h_1 ; respectively
j	microinertia constant
J	defined by eqn. (5.20)
ℓ	characteristic material length defined by eqn. (2.18)
ℓ_1	half x-dimension of infinitely long parallel plate
L	characteristic length ratio parameter
$\vec{L}^*$	body couple
L_o	length of the short journal bearing (in axial direction)

m	$\frac{N}{\ell}$
$m_{k\ell}$	couple stress tensor
N	coupling number, defined by eqn. (2.18)
n	revolutions per unit time
p	hydrodynamic pressure
P	non-dimensional pressure
P_o	unit loading, $\frac{p}{L_o D}$
q	velocity ratio parameter, defined by eqn. (5.6)
$\vec{q}$	flow flux (in vector form)
q_x, q_z, q_θ	fluxes along x,z and θ directions, respectively
r	radial co-ordinate
r_1, r_2	radii of circular plates
R	radius of journal/cylinder/sphere
R_1	larger radius of conical seat
R_2	smaller radius of conical seat
Re	modified Reynolds number
Re'	defined by eqn. (2.25)
S	Sommerfeld number
t	time
$t_{k\ell}$	stress tensor
T	non-dimensional time
T_R	time ratio parameter
u,v,w	velocity components
U	velocity of the journal

U_1, U_2	velocity of the plane and cylindrical surface, respectively
V	normal relative velocity of the cylindrical surfaces
$\vec{V}$	velocity vector
$\vec{V}_B$	velocity vector on the solid boundary
V_p	velocity of the fluid towards porous region
W	load capacity
$W(t)$	load capacity as a function of time
W_b	amplitude of the applied load
$W_o, W_{\frac{\pi}{2}}$	load components along and perpendicular to the line of centers, respectively
$\overline{W}_R$	load capacity ratio parameter
x, y, z	cartesian co-ordinates
X, X_m	non-dimensional form of x and x_m , respectively
θ	angular co-ordinate (latitude angle)
θ^*	angle at which p = o
ϕ	angle between load line and line of centers
ϕ_a	porosity of the cartilage surface
ϕ_p	non-dimensional porosity parameter
ϕ_s	non-dimensional slip parameter
ψ	angle between the vertical line and load line
$\alpha, \beta, \gamma, \chi$	viscosity coefficients for a micropolar fluid
α_1	semi-vertical angle of cone
β_1	angle subtended by the radii r_1 and r_2 , at the center of circular sector
ε	eccentricity ratio

$\varepsilon_o, \varepsilon_1$	eccentricity ratios corresponding to the final and initial film thickness
$\varepsilon_{k\ell r}$	alternating tensor
λ , μ	Newtonian viscosity coefficients
μ_ν	dynamic viscosity coefficient
μ_f	coefficient of friction
$\vec{\nu}$	microrotation vector
$\vec{\nu}_B$	microrotation vector on the boundary
ν_1, ν_2, ν_3	components of the microrotation vector
ν_A	aspect ratio
ν_c	critical aspect ratio
ω	angular velocity of the journal
ω_L	frequency of the rotation of the applied load ; $\frac{d\psi}{dt}$
ω_p	frequency of oscillation
ρ	mass density
σ	standard deviation
τ	shear stress
τ_x, τ_z	shear stresses along x-direction and z-direction, respectively
Ω	angular velocity of the cylinder
ξ	random variable
Π^*	thermodynamic pressure
ζ	longitudinal angle (used for spherical polar co-ordinates)
Δ	slip parameter
	A bar above a variable denotes the corresponding non-dimensional variable.

CHAPTER I

GENERAL INTRODUCTION

1.1 WHY LUBRICATION

Lubrication plays a most vital role in our great and complex civilization. To estimate the importance of this role one need only consider that every moving part of every machine is subjected to friction and wear. Throughout the centuries from ox-cart axles to grinding wheel spindles, one of man's most persistent problems has centered around reduction and control of friction and wear. Friction consumes and wastes energy. Wear causes changes in dimensions and eventual breakdown of the machine element and the entire machine and all that depends upon it.

Today the constituent parts of modern high speed engines are frequently subjected to a very high rate of wear, which can lead to serious operational disturbances, if not to the total deterioration and destruction of engines. The need for continuous engine operation today necessitates the timely removal and replacement of worn engine parts, which can be a costly operation. A nation's economy can be seriously impaired through excessive losses of engine and machine parts due to wear, so that an intensive campaign against friction and wear is in the best of interest of increased production and national efficiency.

So whether one is concerned with reducing the waste of world's production of energy, conserving a nation's critical natural resources,

maintaining production schedules in a plant, creating a larger margin of profit in plant operation, or even making the family automobile run longer and better, one must be interested in the study of lubrication.

1.2 EARLY DAYS IN LUBRICATION

Lubrication, in one sense, is as old in civilization as the wheel and axles. When a tomb was opened in Egypt, some years ago, one of the chariots still had some of the original lubricant on the axle. This was analyzed and found to be sticky and slightly greasy [1]. It contained road dirt such as quartz sand, compounds of aluminum, iron, and lime. It had a melting point of 120°F, which suggests that it might have been mutton or beef tallow, either of which would have proved suitable for axle lubrication in that warm country.

Until comparatively recent years all lubricants were largely of animal, vegetable, or marine origin : mutton tallow, lard, gooze grease, fish oils, castor oil, cottonseed oil and other vegetable oils, etc. The use of mineral oils dates back principally a little over a hundred years.

Pioneering work in the field of lubrication dates back to the year 1847, when Adams [2] developed and patented several rather good designs for railway axle bearings. Many of the plans show a remarkable comprehension of the fundamentals of proper bearing design.

The new science of lubrication, however, based on hydrodynamics and oil flow, was not recognized as such until 1883, when Petrov [3] made the first significant attempt to analyze theoretically the friction

effect of film lubrication. It was then recognized that the film rather than the bearing material could be a prime consideration.

In the same year that Petrov published his theory, unexpected experimental results were reported by Tower [4] . He demonstrated that a loaded, oil-lubricated journal bearing is subject to local pressures substantially higher than its mean pressure. Three years later Reynolds [5] , unaware of Petrov's theory, was able to explain Tower's results. From the properties of a thin laminar fluid film he derived and published not only the descriptive differential equation, which even today bears his name, but also certain solutions to this equation that agree well with the experimental measurements of Tower [4] . Several years later in 1904, Sommerfeld [6] , provided elegant theoretical extensions to the journal bearing lubrication problem.

Of the thousands of papers on film lubrication which have appeared since 1886, in the wake of Reynolds classical work on lubrication theory, few have offered modification of the theory. In general, papers on film lubrication have extended the application of the fundamentals, as set forth by Reynolds, to a variety of bearing shapes with steady and transient films of variable viscosity, density and temperature. In 1928, Boswall [7] summarized the theory of film lubrication to that date. By now, however, much additional information about lubricating films has been developed. A proper historical review of the same would be a Herculean task and beyond the scope of the present thesis.

Inspite of the rapid growth of the lubrication theory in the 20^{th} century, the picture is far from complete. A perfect correlation between theory and practice has not yet been obtained. This is fundamentall because the basic assumptions frequently circumscribe a rather tight circle within which the applicability of the theory is valid.

1.3 CLASSIFICATION OF LUBRICATION

In surveying the entire field of lubrication with its many vital physical and chemical manifestations, the one phenomenon that occurs most frequently and persistently and which probably has by far the most value is the creation of a load-carrying fluid film. For the builders and users of machinery and mechanism of various kinds, development of this fluid film is quite a natural action and serves them obediently and tirelessly if given even the slightest encouragement. It is obvious that much of our industrial life would grind to a screeching halt without this lubrication phenomenon.

The thickness of the fluid film not only determines between the various kinds of lubrication but also the regime of applicability of the theory. At one extreme is the thick film lubrication, where the bearing surfaces are completely separated by a continuous fluid film of the order of 10^{-3} cm. and the bearing characteristics mainly depend on the viscosity of the lubricant in bulk. At the other extreme is the boundary lubrication, where a fluid film only a few molecular layer thick is left between the bearing surfaces. Between these two extremes, lies, the region of thin film or mixed lubrication. The fluid

film is very thin, of the order of 10^{-6} cm. so that the load is partly supported by the roughness asperities and partly by the fluid film. The region of thin film lubrication is an indeterminate state in which the strict laws of hydrodynamic lubrication are no longer valid. Some of the most exciting research is being done in this field. It is actually a meeting place for a chemist and an engineer as well as a metallurgist and a mathematician. It is in this region that the rheology plays an important role. It is in this region that the proximity of a solid surface drastically modifies the properties of the lubricant. It is also an area of great endeavour, where the experimental facts are to be correlated with theory.

1.4. LUBRICATION AND RHEOLOGY

Interaction between the fields of lubrication and rheology has become increasingly important within the past few years with the growing awareness of the complexity of the lubricant reaction to severe and transient stress conditions, the continued demand for well lubricated, high speed, highly loaded machine elements, extensive use of synthetic lubricants and use of additives.

The general definition of rheology is the science that deals with the deformation and flow of materials. Similarly, one may state, that the primary objective of lubrication is to separate rubbing surfaces by a layer of lubricant to prevent excessive friction and wear. It is clea that the lubricant during the lubrication process will be subjected to a quite high shearing stresses and velocity gradients. The rheological

properties of the lubricants are, therefore, likely to have an important effect on its action.

In early lubrication work, only the Newtonian viscosity of the lubricant was important. However the applied stresses have increased and the range of environmentation conditions, under which the lubricant should work, have become more extreme. The fact that many mineral base oils also manifest non-Newtonian behaviour under the severe shear conditions they often encounter in practice also support this point of view.

Non-Newtonian behaviour is also almost invariably observed in various lubrication systems, when additives are used. These additives are put into the lubricant for a variety of purposes and do a great deal to improve the lubricating oils which nature and the refiner produce. Modern lubricating-oil additives, based on years of scientific research, designed to meet the extreme demands of modern machines and for high performance ratings, under actual working conditions, have become indispensable in many applications.

The ever growing trend to transmit greater power through mechanisms smaller in size and weight imposes an increasing burden on the lubricant. New combustion problems, greater surface loadings, wider range of operating temperatures and often greater stalling or sliding speeds in bearings, all subject the lubricants to higher operating temperatures, loads and overall abuses.

These examples show just a few areas where a knowledge of the rheological properties of the lubricant is likely to be important. For

a proper comprehension, one must look for the experimental evidences where such properties have been found, or have been sought for and found lacking. Hence in the next section a brief summary of such experimental studies is given.

1.5 EXPERIMENTAL EVIDENCES

The manner in which a liquid in contact with a solid surface is influenced by the proximity of that surface has been the subject of intensive study and a matter of controversy. It appears obvious that the molecules of the liquid in the immediate vicinity or those adhering to the surface, or of the adsorbed layers on the surface must necessarily behave different from the adjacent molecules of the liquid in bulk. However the nature of this surface influence and the depth to which it penetrates is not yet properly understood and the experimental results have given rise to widely divergent opinions. It is generally accepted that the surface zone of a liquid is not merely a monomolecular layer but a multimolecular layer [8,9] , i.e. the molecular orientation extends effectively to many molecular lengths.

From a practical point of view, however, the important question is not whether deep molecular orientation exists, but whether it gives rise to rheological abnormalities in the neighbourhood of a solid surface i.e. - whether a fluid in the immediate vicinity of a solid surface, deve properties significantly different from the adjacent molecules in bulk. The experimental evidences are viewed from this angle.

Kingsbury [10] seems to be among the earliest investigators of the question of existence of rheological abnormalities in proximity of a solid surface. He observed an enhanced viscosity in that part of the fluid which is in the region of attraction of the surface molecules of the metals. This enhancement may range from a small increase in viscosity to rigidity and the depth of the affected zone ranges from 10^{-7} mm to 10^{-3} mm.

Hardy and Nottage [11-13] offer proofs that the liquid film must at least be of 0.007 to 0.010 mm in thickness, if any of the liquid is to be beyond the range of surface influence. Willson and Barnard [14] found that capillaries as large as 0.3 mm diameter would gradually clog up under the flow of oils and would close completely if a small percentage of oleic or stearic acid were added to the oil. This clogging was attributed to the gradual building up of adsorbed films on the walls of the capillaries. Bulkley [15] in a carefully conducted series of experiments with capillaries of approximately the same size as those used by Willson and Barnard [14], was however able to show that the clogging was due to the fact that the oil had not been thoroughly filtered. From further experiments with highly filtered oils, Bulkley concluded that there is no rigidity in clean liquid at distances of 0.3×10^{-4} mm from a solid boundary. This, although in accordance with the two experiments of Bastow & Bowden [16,17], who detected no evidence of non-Newtonian behaviour upto a distance of 10^{-4} mm, is in contradiction to Griffiths [18], who claimed to have found evidence

of rigidity in hydrocarbons of low molecular weight with gap between 10^{-3} mm to 2 x 10^{-3} mm. Results similar to this have also been obtained by Tausz and Szekely [19], who found that a film of lubricating oil under a steel ball dipped into mercury was remarkably stable. Non-polar oils gave a film about 5000 Å (5 x 10^{-5} mm) which broke only after two days. Films of polar oils maintained themselves for as long as sixty five days. Terzaghi [20] found the viscosity of water to be many times the bulk value in the passage between glass plates 10^{-5} mm apart. Macaulay [21] also found a similar increase in viscosity.

Of great importance and interest is the work of Needs [22] in 1940, who squeezed fluids between two steel plates and found that a stable residual film was formed. Needs' critics expended most of their energy on deciding that the fluids used were contaminated with solids. Needs' defence partially allays this situation at least for olive and castor oils. Though one must view Needs' work with some reservation, it appears very reasonable that an alteration in the liquid film occured making it substantially more viscous than in the bulk.

In 1949 Henniker [8] published an extensive review paper which included 174 references, largly experimental ones, in support of his conclusion that the surface zone of a liquid is not merely a monomolecular layer, but a multimolecular layer. More recently, but much more briefly, Adamson [23] in 1960 admitted that although all the evidence of deep surface orientation is more or less circumstantial,

nevertheless deep molecular orientation does occur, probably as a result of perturbations passed on from molecule to molecule.

An important class of problems where the evidence of a greatly enhanced viscosity in thin films close to a solid surface is strongest, is when small proportion of a surface active compound is added to the fluid. In fact, some maintenance practices recommend the addition of a small amount of used oil to new oil that may be placed in a lubrication system. The improved performance due to used mineral oil, as boundary lubricant, is probably due to some oxidation of the oil and the formation of long chain acids in the oil. The advantages derived from adding small amounts of long chain acids to a mineral oil were recognized as early as 1920 by Wells and Southcombe [24]. A little later in 1921, Hardy and Doubleday [25,26] have reported the effect of chain length of additives in the lubricant. They observed a definite relationship between the coefficient of friction and the length of molecule ; longer the molecule lower the coefficient of friction. Beeok et.al [27], who used a very slow running four ball machine, showed that a coherent oil film, separating the surfaces, was promoted by the addition of a small proportion of oleic acid to white oil.

Perhaps the most telling support for Needs observation is that provided by Fuks [28-29] . He performed a number of experiments with apparatus very similar to that used by Needs. The resemblances to Needs' data are striking. It is of interest that an addition of o.1% of stearic acid to a chromatographically separated naphthene-paraffin fraction oil

(MS-20) increased the residual film thickness. It is equally interesting to note that lower molecular weight hydrocarbons such as benzene, hexane, cyclohexane, isooctane and decane, exhibited no residual film. Fuks investigated many properties of the film and it was observed that film thickness increased with fatty acid concentration, with surface energy of the solid substrate and with increasing hydrocarbon chain length of both solvent and fatty acid.

The works of Needs [22] and Fuks [28-29] have been a matter of great controversy and criticism for a long time by many workers, most recently by Hayward and Isdale [30]. It has been suggested that asperities on the solid surface might account for the residual film. Also dirt and undissolved material in the fluid have been invoked as explanations. According to Drauglis et.al [31] (who conducted a series of experiments with utmost care and observed residual films similar to Needs and Fuks), if the data of Fuks are all to be explained on the basis of dirt, then one must postulate dirt which changes its properties with temperature, length of additive molecule, concentration of additive, but such a dirt would be a most unusual material.

Derjaguin [32-33], who is regarded as the leading modern exponent of the view that molecular orientation in depth occurs near solid boundaries and gives rise to significant rheological effects, devised an experimental method in order to avoid any possible interference by dirt particles. Increase in viscosity was observed where traces of polar or surface active substances are present (including ordinary lubricat oils).

More recently Cameron and his coworkers [34-37] have also studied the influence of surface active compounds in various lubrication systems. The lubricants were pure paraffins, mainly hexadecane, and the additives consisted of various long chain polar compounds. It was found that the oil film was markedly influenced by the additive. The scuffing load was found to increase with chain length of additive and solvent. Squeeze film studies similar to Fuks [28-29] were also made. The plates came to rest at a separation of about 2×10^{-4} mm, with all fluids, even with pure cetane. In addition, it was found that the increase in surface viscosity was greatest when additives and carriers were matched in terms of chain length and shape. The results presented in these studies are most easily explicable by postulating the presence of a surface film some 10^{-5} mm to 10^{-3} mm thick which has a much larger viscosity than the bulk of the fluid.

Thus, although there may be some controversy, as to the existence of rheological anomalies (like viscosity enhancement) in the neighbourhood of solid boundaries, the evidence on whole seems positive. It is evident that such zones of enhanced viscosity, giving rise to a residual film, would have important effects in the lubrication of practical machinery.

Ordinary mineral lubricating oils contain various polar compounds, many of them surface active, in a non-polar hydrocarbon medium and thus belong to the class of liquids for which the evidence of the effect, viscosity enhancement, is strongest. The rheological anomalies could therefore have a considerable effect on the minimum film thickness, which in turn influences wear and fatigue failure of machine components.

1.6 DEVELOPMENTS IN THEORETICAL RHEOLOGY

A proper theoretical explanation of the residual film, reported by various workers, is clearly needed for a better understanding of thin film lubrication technology. An attempt in this direction is the work of Allen and Drauglis [9], who developed a theory of boundary films based on the ordered liquid model, in which the wall forces, though not strong enough to bind more than a few molecular layer, induce long range order in the fluid. In this model, films on solid substrates are assumed to behave as liquids of special type, that is, they can flow as an ordinary liquid but have an internal order much like that in a crystal. This model fits qualitatively for all of the data of Fuks [28-29]. A beginning of a quantitative theory based on molecular consideration is made in [9] and pursued further in [38] .

These detailed studies, although necessary for a fundamental understanding of physical and chemical phenomena involved in the formation of these films, are hardly justified for an engineering purpose. In such situations it may be sufficient to take into consideration the local degree of freedom in some reasonable average sense. For example, the local rotation and spin of clusters and their stretch, in addition to classical degree of freedom, associated with a continuum may provide an adequate next step.

Motivated by these considerations, attempts have been made by many researchersto extend the range of applicability of continuum mechanics (particularly in the study of fluid behaviour of rheologically complex fluid

in situation where micromotion plays an important role) using the field theory approach to describe the macroscopic manifestation of microscopic events, i.e. microelement motions and deformations.

The inadequacy of classical continuum approach to describe the mechanics of complex fluids has led to the development of theories of microcontinua in which continuous media are regarded as sets of structured particles possessing not only mass and velocity but also a substructure with which is associated a moment of inertia density and micro-deformation tensor. This extension of fluid mechanics required a reappraisal of classical concepts (e.g. the symmetry of stress tensor, the absence of couple stresses, etc.) in order to account for local structural aspects and micromotions. In fact, while many of the principles of classical continuum mechanics remain valid for this new class of fluids they had to be augmented with additional balance laws and constitutive relations. The presence of microscopic elements in a fluid gives rise not only to classical Cauchy stresses but also to couple stresses due to the microelement interactions. Further the orientation of the elements comprising the microcontinuum had to be considered as well as the production of internal angular momentum due to their rotational motions.

No attempt is made in the present thesis to give an account of the historical development of the theory of microcontinua, as an excellant review has been given by Ariman, Turk and Sylvester [39] , and a reference may be made to that.

The earliest formulation of a consistent general theory of fluid

microcontinua is attributed to Eringen [40-41] , in which the mechanics of fluids with deformable microelements are considered. The basis of Eringen's theory of "Simple Microfluids" was his work with Suhubi [42-43] . Although these papers were concerned with a nonlinear theory of microelastic solids, their treatment of motion, balance of moments, conservation of energy and entropy production is applicable to all continuous media where microelements are considered.

In these papers [42-43] the authors develop a physical model in which each continuum particle is assigned a substructure, i.e. each material macrovolume element contains microvolume elements which can translate, rotate and deform independently of the motion of the macrovolume ; however each deformation of the microvolume element can be expected to produce a subsequent deformation of the macrovolume elements. Thus a mechanism is provided in the theory to treat materials, which are capable of supporting local stress moments and body moments, and in addition are influenced by the microelement spin inertia.

The field equations (i.e. balance of momenta, conservation of mass and energy etc.) of Eringen's microcontinuum mechanics have been developed by applying Cauchy's law of motion and the classical conservation statements of mass and energy in the forms of volume and surface integral operators to each microelement contained in a material microvolume element. Simple statistical average of these global balance and conservation laws have been taken over the entire

macrovolume element, resulting in the fundamental laws of microcontinua. The laws of classical continuum mechanics have been augmented with additional equations, which account for conservation of microinertia moments and balance of first stress moment which arise due to consideration of microstructure. The key point to note in the Eringen's theory of microcontinuum mechanics is the introduction of new kinematic variables, e.g. the gyration tensor and microinertia moment tensor, and the addition of the concepts of body moments, stress moments and microstress averages, to classical continuum mechanics.

The microfluid theory [40] is however too complicated and the underlying mathematical problem is not easily amenable to the solution of non-trivial problems in this field. This led Eringen [44] to postulate a subclass of these microfluids, called micropolar fluids, which would still exhibit the effects arising from particle micromotion but would produce considerable mathematical ease. Under these assumptions deformation of the fluid microelement is ignorned. Nevertheless, microrotatic effects are still present and surface and body couples are permitted. In this theory two independent kinematic vector fields are introduced, the vector field representing the translation velocities of the fluid particles and the vector field representing the angular (or spin) velocities of the particle (i.e. microrotation vector).

Many theories similar to Eringen's micropolar fluid theory have been advanced by various research workers in recent years from different view point. However the resulting field equations can be reduced to

those of Eringen [44] (for a detailed comparison see ref. 39).

Physically, the theory of micropolar fluids may serve as a satisfactory model for description of the flow behaviour of polymer fluids and fluid suspensions, where micromotion may play an important role. Another class of problems where micropolar fluid theory may provide an answer is when the wave length of an acoustical disturbance becomes comparable to the mean grain-size or distance in a body. In such situations diffraction patterns appear which can not be reconciled on the classical mechanical grounds. Under these circumstances the molecular or granular constituents of the medium are excited individually and the intrinsic motion of the material constituents must be taken into account. This situation could be thought of as one, representing the phenomena associated with thin films in proximity of a solid surface.

1.7 MICROCONTINUUM ANALYSIS OF FLUID FLOWS

The theory of micropolar fluids has been applied extensively to describe the non-Newtonian behaviour of real fluids such as colloidal solutions, fluid suspensions and sometimes blood. A review of all such published work till 1974 was made by Ariman et.al. [45] , who listed over a hundred references. Since then scores of other papers have been published and no attempt is made to list them in a chronological manner.

This section is restricted, basically to the discussion of those flow problems, which give evidence of rheological effects in the flow of micropolar fluids through narrow passages.

Increased viscosity due to the presence of microstructure in the fluid have been reported by Kline and Allen [46-48] . Cowin [49] and coworkers [50-51] , while studying the polar fluids [49] (a fluid identical to Eringen's micropolar fluid), have analyzed a special class of flows, called creeping flows. The most significant result of their work is that the polar fluid exhibits a resistance to motion, greater than or equal to that of the viscous fluid in the traditional flow situations. Willson [52] and Peddieson and McNitt [53] have also demonstrated increased effective viscosity in boundary layers in micropolar fluids.

The origin of rheological abnormalities is then to be investigated on the basis of the theory of micro-mechanical motions, as there is a distinct possibility that micropolar fluid theory, which takes into account the intrinsic motion of the material constituents, may provide answer to some of the questions concerning these thin films, at least in a macroscopic sense.

Motivated by these considerations lubrication theory for micropolar fluids has been developed by many authors. The earliest work in this direction is by Allen and Kline [54] , who, using their own model, gave an approximate solution of the slider bearing problem . Similar theories were developed by Agrawal et.al. [55], Balaram and Shastri [56] , Shukla and Isa [57] and Prakash and Sinha [58] using Eringen's [44] model for micropolar fluids.

Application of these theories has been made to various traditional lubrication problems. The slider bearing problems have been solved by

Datta [59], Maiti [60], Shukla and Isa [57], Isa and Zaheeruddin [61], Agrawal [62] and Sinha and Singh [63]. Prakash and Sinha [58,64,65], Mahanti [66] and Isa and Zaheeruddin [67] have solved the problem of one-dimensional journal bearings. The squeezing flow in parallel plates and curved plates have been solved by Agrawal et.al. [55], Balaram [68], Prakash and Sinha [69-70], Ramanaiah and Dubey [71], Zaheeruddin and Isa [72] and Tandon and Jaggi [73-74]. Prakash and Sinha [75] and Sinha [76] have studied the dynamically loaded infinitely long journal bearings. Hydrostatic and externally pressurized bearings have been analyzed by Khader and Vachon [77], Shukla and Isa [78] and Isa and Zaheeruddin [79]. Prakash and Christensen [80] and Sinha [81] have analyzed the problem of rolling contact bearings. The elastohydrodynamic zone of roller bearing has been analyzed by Prakash and Christensen [82]. The inertia effects in squeeze bearings and thrust bearings have been studied by Mahanti and Ramanaiah [83].

The earlier theories were based upon the assumption that the Newtonian viscosity and micropolar viscosity coefficients are constant across the lubricant film. Recently Tipei [84] has given a more generalized form of Reynolds equation which assumes the viscosity coefficients to be function of all co-ordinates. However, Tipei [84] too, has solved problem of short bearings under the assumption of constancy of viscosity coefficients.

The results obtained by using micropolar fluid as lubricant are encouraging and illustrate the capabilities of this theory in explaining the phenomenon of the enhancement of effective viscosity in thin films. However, the results in general are grossly exaggerated due to the inadmissible values of the governing parameters.

Even after a decade this theory seems to be in a preliminary state. Scores of lubrication problems have yet to be solved from this view point. For example, little work has appeared on dynamically loaded bearings and porous bearings from the microcontinuum view point. Moreover, the problems of finite dimensional bearings and bearings with rough surfaces from this view point are yet to be analyzed.

Hence, in this thesis, an attempt is made to study these lubrication problems from the microcontinuum point of view.

CHAPTER II

BASIC EQUATIONS AND GENERALIZED REYNOLDS EQUATION FOR MICROPOLAR FLUIDS

2.1 INTRODUCTION

The theory of microfluids introduced by Eringen [40] deals with the class of fluids which respond to certain microscopic effects arising from the presence of microstructure and are influenced by spin inertia. This theory was later simplified to the theory of micropolar fluids [44] in which the deformation of microelement is ignored. These fluids contain a suspension of rigid particles with individual motion which support stresses and body moments [40,44] . This subclass is obtained from the general microfluid theory by imposing skew symmetric property of the gyration tensor, in addition to a condition of microisotropy.

In view of the inadequacies of the classical Newtonian theory, lubrication theory for micropolar fluids has been developed by many authors [54,55,56,58] for two dimensional bearings, and by Shukla and Isa [57] and Tipei [84] for three dimensional bearings. Apart from the analysis of Prakash and Sinha [58] , for the two dimensional case, no paper gives a detailed order of magnitude study for the three dimensional problem. Hence in this Chapter, a detailed order of magnitude study is made and a generalized type of Reynolds equation is obtained for the three dimensional case.

2.2 BALANCE EQUATIONS FOR MICROPOLAR FLUIDS

The balance equations governing the behaviour of micropolar fluids have been derived by Eringen [44] and the results are simply presented here.

(i) Field Equations

The field equations for micropolar fluids in vectorial form are [44]

$$\frac{\partial \rho}{\partial t} + \vec{\nabla} \cdot (\rho \vec{V}) = 0 \tag{2.1}$$

$$(\lambda + 2\mu)\, \vec{\nabla}\vec{\nabla} \cdot \vec{V} - \frac{1}{2}(2\mu+\chi)\, \vec{\nabla} \times (\vec{\nabla} \times \vec{V}) + \chi \vec{\nabla} \times \vec{v} - \vec{\nabla} \Pi^{*} + \rho \vec{F}^{*} = \rho \frac{D\vec{V}}{Dt} \tag{2.2}$$

$$(\alpha+\beta+\gamma)\, \vec{\nabla}\vec{\nabla} \cdot \vec{v} - \gamma \vec{\nabla} \times (\vec{\nabla} \times \vec{v}) + \chi \vec{\nabla} \times \vec{V} - 2\chi \vec{v} + \rho \vec{L}^{*} = \rho\, j \frac{D\vec{v}}{Dt} \tag{2.3}$$

The first equation is the principle of conservation of mass and the others are the conservation of linear and angular momentum, ρ is the mass density, $\vec{V}$ is the velocity vector, $\vec{v}$ is the microrotation velocity vector, Π^{*} is the thermodynamic pressure, $\vec{F}^{*}$ is the body force per unit mass, $\vec{L}^{*}$ is the body couple, j is the microinertia constant, λ, μ are the viscosity coefficients of the classical fluid mechanics and $\chi, \alpha, \beta, \gamma$ are the new viscosity coefficients for micropolar fluids.

$\frac{D}{Dt}$ denotes material differentiation.

For incompressible fluids $\vec{\nabla} \cdot \vec{V} = 0$, and Π^{*} is replaced by the hydrodynamic pressure p, to be determined from the boundary conditions.

The quantities $\lambda, u, \chi, \alpha, \beta, \gamma$ and j are constants and characterize the particular fluid under consideration. It may be emphasized that the constant χ links together, through these field equations, the velocity vector $\vec{V}$, and the microrotation vector $\vec{\nu}$. If mass, time and length are denoted by M, L and T respectively, then λ, μ, and χ are all of dimension $ML^{-1}T^{-1}$, while α, β and γ are all of dimension MLT^{-1} and j of dimension L^2.

(ii) Constitutive Equations

Constitutive equations for the stress tensor $t_{k\ell}$ and the couple stress tensor $m_{k\ell}$, are given in cartesian co-ordinates as

$$t_{k\ell} = (-\Pi^* + \lambda V_{r,r})\,\delta_{k\ell} + (\mu - \tfrac{1}{2}\chi)\,(V_{k,\ell} + V_{\ell,k}) + \chi(V_{\ell,k} - \epsilon_{k\ell r}\,\nu_r) \tag{2.4}$$

$$m_{k\ell} = \alpha \nu_{r,r}\,\delta_{k\ell} + \beta \nu_{k,\ell} + \gamma \nu_{\ell,k} \tag{2.5}$$

where $\epsilon_{k\ell r}$ is an alternating tensor. An index followed by a comma represents partial differentiation with respect to the space variable x_k.

(iii) Boundary Conditions

The boundary conditions are

$$\vec{V}(X_B, t) = \vec{V}_B \tag{2.6}$$

$$\vec{\nu}(X_B, t) = \vec{\nu}_B \tag{2.7}$$

where x_B is a point on the solid boundary having prescribed velocity $\vec{V}_B$ and prescribed microrotation velocity $\vec{\nu}_B$. The zero spin or hyperstick

condition, Cowin [49] and Allen and Kline [54], represents the extreme case in which the wall acts to completely inhibit microrotation. The zero spin boundary condition permits recovery of classical results by passing to the limit as a suitable measure of substructure size tends to zero.

(iv) Three Dimensional Flow

For subsequent study, attention is restricted to three dimensional steady motion of an incompressible micropolar fluid under the following assumptions

(1) Body forces and body couples are negligible

(2) all the characteristic coefficients are y-independent.

Thus the velocity, the microrotation velocity and the pressure have the forms

$$\vec{V} = (u(x,y,z),\ v(x,y,z),\ w(x,y,z)) \tag{2.8}$$

$$\vec{v} = (v_1(x,y,z),\ v_2(x,y,z),\ v_3(x,y,z)) \tag{2.9}$$

$$p = p(x,y,z) \tag{2.10}$$

The balance equations (2.1) - (2.3) reduce to

$$\frac{\partial u}{\partial x} + \frac{\partial v}{\partial y} + \frac{\partial w}{\partial z} = 0 \tag{2.11}$$

$$\frac{1}{2}(2\mu + \chi)\left(\frac{\partial^2 u}{\partial x^2} + \frac{\partial^2 u}{\partial y^2} + \frac{\partial^2 u}{\partial z^2}\right) + \chi\left(\frac{\partial v_3}{\partial y} - \frac{\partial v_2}{\partial z}\right) - \frac{\partial p}{\partial x}$$

$$= \rho\left(u\frac{\partial u}{\partial x} + v\frac{\partial u}{\partial y} + w\frac{\partial u}{\partial z}\right) \tag{2.12}$$

$$\frac{1}{2}(2\mu+\chi)\left(\frac{\partial^2 v}{\partial x^2}+\frac{\partial^2 v}{\partial y^2}+\frac{\partial^2 v}{\partial z^2}\right)+\chi\left(\frac{\partial \nu_1}{\partial z}-\frac{\partial \nu_3}{\partial x}\right)-\frac{\partial \bar{p}}{\partial y}$$

$$=\rho\left(u\frac{\partial v}{\partial x}+v\frac{\partial v}{\partial y}+w\frac{\partial v}{\partial z}\right) \qquad (2.13)$$

$$\frac{1}{2}(2\mu+\chi)\left(\frac{\partial^2 w}{\partial x^2}+\frac{\partial^2 w}{\partial y^2}+\frac{\partial^2 w}{\partial z^2}\right)+\chi\left(\frac{\partial \nu_2}{\partial x}-\frac{\partial \nu_1}{\partial y}\right)-\frac{\partial p}{\partial z}$$

$$=\rho\left(u\frac{\partial w}{\partial x}+v\frac{\partial w}{\partial y}+w\frac{\partial w}{\partial z}\right) \qquad (2.14)$$

$$\gamma\left(\frac{\partial^2 \nu_1}{\partial x^2}+\frac{\partial^2 \nu_1}{\partial y^2}+\frac{\partial^2 \nu_1}{\partial z^2}\right)+\chi\left(\frac{\partial w}{\partial y}-\frac{\partial v}{\partial z}\right)-2\chi\nu_1$$

$$=\rho j\left(u\frac{\partial \nu_1}{\partial x}+v\frac{\partial \nu_1}{\partial y}+w\frac{\partial \nu_1}{\partial z}\right) \qquad (2.15)$$

$$\gamma\left(\frac{\partial^2 \nu_2}{\partial x^2}+\frac{\partial^2 \nu_2}{\partial y^2}+\frac{\partial^2 \nu_2}{\partial z^2}\right)+\chi\left(\frac{\partial u}{\partial z}-\frac{\partial w}{\partial x}\right)-2\chi\nu_2$$

$$=\rho j\left(u\frac{\partial \nu_2}{\partial x}+v\frac{\partial \nu_2}{\partial y}+w\frac{\partial \nu_2}{\partial z}\right) \qquad (2.16)$$

$$\gamma\left(\frac{\partial^2 \nu_3}{\partial x^2}+\frac{\partial^2 \nu_3}{\partial y^2}+\frac{\partial^2 \nu_3}{\partial z^2}\right)+\chi\left(-\frac{\partial v}{\partial x}-\frac{\partial u}{\partial y}\right)-2\chi\nu_3$$

$$=\rho j\left(u\frac{\partial \nu_3}{\partial x}+v\frac{\partial \nu_3}{\partial y}+w\frac{\partial \nu_3}{\partial z}\right) \qquad (2.17)$$

2.3 LUBRICATION PROBLEM-ASSUMPTIONS AND BASIC EQUATIONS

To state the lubrication assumptions a three dimensional slider type of bearing is shown in Fig.2.1 as it is the simplest load carrying mechanism and an easier geometry to visualize the properties of more complicated films. U is the velocity of upper plate along x-direction carrying a load W, h is the film thickness, a_2 is the x-dimension and b_2 is

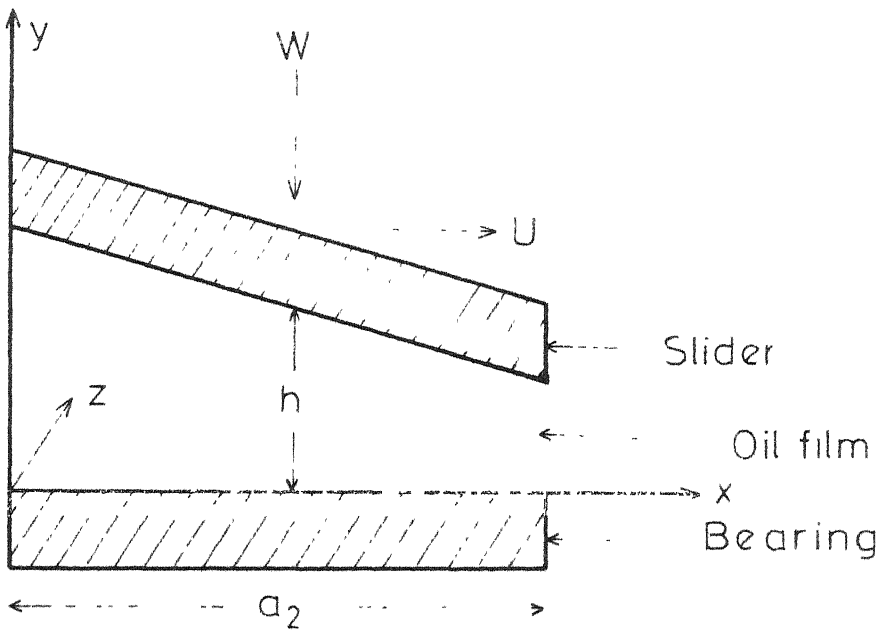

Fig. 2.1 Slider bearing configuration

the z-dimension of the plate. The fluid is an incompressible micropolar fluid.

The lubrication films to be analyzed are assumed to comply with usual assumptions [85,86] made in deriving the Reynolds equation

1. Flow is laminar ; no vortex and no turbulence occur anywhere in the film.
2. Body forces are neglected, e.g. the gravitational or magnetic field is assumed to be negligible.
3. The film is thin enough as compared to the length and span of the bearing. This permits us to ignore the curvature of the fluid film and the rotational velocities may be replaced by translational velocities.
4. No slip on the bearing surfaces.

Apart from the above mentioned conventional lubrication assumptions, three more assumptions must be emphasized. Later on, in Chapters VI, VII and VIII, the first two will be violated.

1. Bearing surfaces are smooth, i.e. there is no surface roughness.
2. Bearing surfaces are non-porous.
3. The bearing surfaces are rigid, i.e. they are not deformed under pressure caused by fluid film.

Equations (2.12) - (2.17) can be simplified with the help of above mentioned assumptions and following non-dimensional scheme.

$$\bar{x} = \frac{x}{a_2}, \ \bar{y} = \frac{y}{h}, \ \bar{z} = \frac{z}{b_2}, \ \bar{u} = \frac{u}{U}, \ \bar{v} = \frac{v}{U}, \ \bar{w} = \frac{w}{U}$$

$$\bar{\nu}_i = \frac{\nu_i h}{U}, \ \bar{p} = \frac{ph^2}{Ua_2(\mu + \frac{1}{2}\chi)}, \ \delta_1 = \frac{h}{a_2}, \ \delta_2 = \frac{h}{b_2}, \ \delta_3 = \frac{b_2}{a_2},$$

$$L = \frac{h}{\ell}, \ \ell = \left(\frac{\gamma}{4\mu}\right)^{1/2}, \ N = \left(\frac{\chi}{2\mu+\chi}\right)^{1/2}, \ i = 1,2,3 \qquad (2.18)$$

The equations (2.12) - (2.17) in dimensionless form are

$$\{\delta_1^2 \frac{\partial^2 \bar{u}}{\partial \bar{x}^2} + \frac{\partial^2 \bar{u}}{\partial \bar{y}^2} + \delta_2^2 \frac{\partial^2 \bar{u}}{\partial \bar{z}^2}\} + 2N^2 \{\frac{\partial \bar{\nu}_3}{\partial \bar{y}} - \delta_2 \frac{\partial \bar{\nu}_2}{\partial \bar{z}}\}$$

$$- \frac{\partial \bar{p}}{\partial \bar{x}} = \mathrm{Re}\ \{\delta_1 \bar{u} \frac{\partial \bar{u}}{\partial \bar{x}} + \bar{v} \frac{\partial \bar{u}}{\partial \bar{y}} + \delta_2 \bar{w} \frac{\partial \bar{u}}{\partial \bar{z}}\} \qquad (2.19)$$

$$\{\delta_1^2 \frac{\partial^2 \bar{v}}{\partial \bar{x}^2} + \frac{\partial^2 \bar{v}}{\partial \bar{y}^2} + \delta_2^2 \frac{\partial^2 \bar{v}}{\partial \bar{z}^2}\} + 2N^2 \{\delta_2 \frac{\partial \bar{\nu}_1}{\partial \bar{z}} - \delta_1 \frac{\partial \bar{\nu}_3}{\partial \bar{x}}\}$$

$$- \frac{1}{\delta_1} \frac{\partial \bar{p}}{\partial \bar{y}} = \mathrm{Re}\ \{\delta_1 \bar{u} \frac{\partial \bar{v}}{\partial \bar{x}} + \bar{v} \frac{\partial \bar{v}}{\partial \bar{y}} + \delta_2 \bar{w} \frac{\partial \bar{v}}{\partial \bar{z}}\} \qquad (2.20)$$

$$\{\delta_1^2 \frac{\partial^2 \bar{w}}{\partial \bar{x}^2} + \frac{\partial^2 \bar{w}}{\partial \bar{y}^2} + \delta_2^2 \frac{\partial^2 \bar{w}}{\partial \bar{z}^2}\} + 2N^2 \{\delta_1 \frac{\partial \bar{\nu}_2}{\partial \bar{x}} - \frac{\partial \bar{\nu}_1}{\partial \bar{y}}\}$$

$$- \frac{1}{\delta_3} \frac{\partial \bar{p}}{\partial \bar{z}} = \mathrm{Re}\ \{\delta_1 \bar{u} \frac{\partial \bar{w}}{\partial \bar{x}} + \bar{v} \frac{\partial \bar{w}}{\partial \bar{y}} + \delta_2 \bar{w} \frac{\partial \bar{w}}{\partial \bar{z}}\} \qquad (2.21)$$

$$\{\delta_1^2 \frac{\partial^2 \bar{\nu}_1}{\partial \bar{x}^2} + \frac{\partial^2 \bar{\nu}_1}{\partial \bar{y}^2} + \delta_2^2 \frac{\partial^2 \bar{\nu}_1}{\partial \bar{z}^2}\} + \frac{N^2 L^2}{2(1-N^2)} \{\frac{\partial \bar{w}}{\partial \bar{y}} - \delta_2 \frac{\partial \bar{v}}{\partial \bar{z}}\}$$

$$- \frac{N^2 L^2}{(1-N^2)} \bar{\nu}_1 = \mathrm{Re}\ \{\delta_1 \bar{u} \frac{\partial \bar{\nu}_1}{\partial \bar{x}} + \bar{v} \frac{\partial \bar{\nu}_1}{\partial \bar{y}} + \delta_2 \bar{w} \frac{\partial \bar{\nu}_1}{\partial \bar{z}}\} \qquad (2.22)$$

$$\{\delta_1^2 \frac{\partial^2 \bar{\nu}_2}{\partial \bar{x}^2} + \frac{\partial^2 \bar{\nu}_2}{\partial \bar{y}^2} + \delta_2^2 \frac{\partial^2 \nu_2}{\partial \bar{z}^2}\} + \frac{N^2L^2}{2(1-N^2)}\{\delta_2 \frac{\partial \bar{u}}{\partial \bar{z}} - \delta_1 \frac{\partial \bar{w}}{\partial \bar{x}}\}$$

$$- \frac{N^2L^2}{(1-N^2)} \bar{\nu}_2 = Re' \{\delta_1 \bar{u} \frac{\partial \bar{\nu}_2}{\partial \bar{x}} + \bar{v} \frac{\partial \bar{\nu}_2}{\partial \bar{y}} + \delta_2 \bar{w} \frac{\partial \bar{\nu}_2}{\partial \bar{z}}\} \quad (2.23)$$

$$\{\delta_1^2 \frac{\partial^2 \bar{\nu}_3}{\partial \bar{x}^2} + \frac{\partial^2 \bar{\nu}_3}{\partial \bar{y}^2} + \delta_2^2 \frac{\partial^2 \bar{\nu}_3}{\partial \bar{z}^2}\} + \frac{N^2L^2}{2(1-N^2)}\{\delta_1 \frac{\partial \bar{v}}{\partial \bar{x}} - \frac{\partial \bar{u}}{\partial \bar{y}}\}$$

$$- \frac{N^2L^2}{(1-N^2)} \bar{\nu}_3 = Re' \{\delta_1 \bar{u} \frac{\partial \bar{\nu}_3}{\partial \bar{x}} + \bar{v} \frac{\partial \bar{\nu}_3}{\partial \bar{y}} + \delta_2 \bar{w} \frac{\partial \bar{\nu}_3}{\partial \bar{z}}\}$$

(2.24)

where

$$Re = \frac{2\rho hU}{2\mu+\chi}, \quad Re' = \frac{\rho j U h}{4\mu \ell^2} \quad (2.25)$$

The parameters N and ℓ characterize the micropolarity of the fluid and distinguish a micropolar fluid from a Newtonian fluid. The parameter N, called coupling number, couples equations (2.2) and (2.3). For $\chi \to o, N \to o$, and these equations become uncoupled and (2.2) reduces to the usual Navier - Stokes equation. Thermodynamic restrictions require that $o \leq N^2 < \frac{1}{2}$ [84,87].

The parameter ℓ has the dimensions of length and can be thought of as a fluid property depending upon the size of the fluid molecule. In this sense the parameter $L(= h/\ell)$ characterizes interaction between the geometry and the fluid. The case $L \to \infty$ (in which the substructure size is negligible as compared to the bearing clearance) gives Newtonian results.

It may be noted that Eringen [44], Shukla and Isa [57] and Tipei [84] and other authors have used the parameter NL (where $L = h/\ell$) as one parameter, in discussing the micropolar fluids, but this product characterizes a combination of effects, which are considered separately in this thesis. These parameters are discussed in more details in next Chapter.

Re is the modified Reynolds number where μ has been replaced by $\mu + \frac{1}{2}\chi$ and this number is always smaller than the classical Reynolds number. For lubrication problem $Re \ll 1$, generally of the order of 10^{-3}. Also it is reasonable to assume that $Re' \ll 1$, since j, is the square of the length typical of the microstructure and comparable to ℓ^2. If a requirement that microrotation velocity identically equal to the local fluid vorticity should be a possible solution of the balance equation, is imposed, it can be shown that $j = \ell^2$ [47]. This requirement seems to be a natural one and has the desirable effect of reducing the number of constitutive coefficients.

Further, δ_1 and δ_2 are of order 10^{-3}, δ_3 is of order unity. Using these order of magnitude study and the above requirements, eqns. (2.19) to (2.24) reduce to

$$\frac{\partial^2 \bar{u}}{\partial \bar{y}^2} + 2N^2 \frac{\partial \bar{v}_3}{\partial \bar{y}} - \frac{\partial \bar{p}}{\partial \bar{x}} = 0 \qquad (2.26)$$

$$\frac{\partial \bar{p}}{\partial \bar{y}} = 0 \qquad (2.27)$$

$$\frac{\partial^2 \bar{w}}{\partial \bar{y}^2} - 2N^2 \frac{\partial \bar{v}_1}{\partial \bar{y}} - \frac{1}{\delta_3} \frac{\partial \bar{p}}{\partial \bar{z}} = o \tag{2.28}$$

$$\frac{\partial^2 \bar{v}_1}{\partial \bar{y}^2} + \frac{N^2 L^2}{2(1-N^2)} \times \frac{\partial \bar{w}}{\partial \bar{y}} - \frac{N^2 L^2}{(1-N^2)} \times \bar{v}_1 = o \tag{2.29}$$

$$\frac{\partial^2 \bar{v}_2}{\partial \bar{y}^2} - \frac{N^2 L^2}{1-N^2} \times \bar{v}_2 = o \tag{2.30}$$

$$\frac{\partial^2 \bar{v}_3}{\partial \bar{y}^2} - \frac{N^2 L^2}{2(1-N^2)} \frac{\partial \bar{u}}{\partial \bar{y}} - \frac{N^2 L^2}{(1-N^2)} \times \bar{v}_3 = o \tag{2.31}$$

From equation (2.27), $p = p(x,z)$, and when (2.30) is solved with zero boundary conditions [49,54], $v_2 = o$.

(i) Velocity Distribution

To solve for velocity components and microrotation velocity components, we revert equations (2.26) - (2.31) to corresponding dimensional form.

The equations are

$$(\mu + \tfrac{1}{2}\chi) \frac{\partial^2 u}{\partial y^2} + \chi \frac{\partial v_3}{\partial y} - \frac{\partial p}{\partial x} = o \tag{2.32}$$

$$(\mu + \tfrac{1}{2}\chi) \frac{\partial^2 w}{\partial y^2} - \chi \frac{\partial v_1}{\partial y} - \frac{\partial p}{\partial z} = o \tag{2.33}$$

$$\gamma \frac{\partial^2 v_1}{\partial y^2} - 2\chi v_1 + \chi \frac{\partial w}{\partial y} = o \tag{2.34}$$

$$\gamma \frac{\partial^2 \nu_3}{\partial y^2} - 2\chi\nu_3 - \chi\frac{\partial u}{\partial y} = 0 \qquad (2.35)$$

The four differential equations (2.32 to 2.35) form two systems of simultaneous equations. One consists of (2.32) and (2.35) and the other of (2.33) and (2.34). The solution of first system will yield expressions for u and ν_3. The second system will yield expressions for w and ν_1. It is seen that the second system becomes identical to the first system if we replace ν_1 by $-\nu_1$. Hence it is necessary to solve only the first system for u and ν_3, and the expressions for w and ν_1 can be written in a similar way.

The boundary conditions for velocity and microrotation velocity are

$$u = U_{11},\ w = U_{12},\ \nu_1 = 0,\ \nu_3 = 0, \text{at } y = 0 \qquad (2.36)$$

$$u = U_{21},\ w = U_{22},\ \nu_1 = 0,\ \nu_3 = 0, \text{at } y = h \qquad (2.37)$$

The solutions are

$$u = \frac{1}{\mu}\left(\frac{\partial p}{\partial x}\frac{y^2}{2} + A_{11}y\right) - \frac{2N^2}{m}\{A_{21}\sinh my + A_{31}\cosh my\} + A_{41} \qquad (2.38)$$

$$\nu_3 = -\frac{1}{2\mu}\left(\frac{\partial p}{\partial x}y + A_{11}\right) + A_{21}\cosh my + A_{31}\sinh my \qquad (2.39)$$

$$w = \frac{1}{\mu}\left(\frac{\partial p}{\partial z}\frac{y^2}{2} + A_{12}y\right) - \frac{2N^2}{m}\{A_{22}\sinh my + A_{32}\cosh my\} + A_{42} \qquad (2.40)$$

$$\nu_1 = -\left\{-\frac{1}{2\mu}\left(\frac{\partial p}{\partial z}y + A_{12}\right) + A_{22}\cosh my + A_{32}\sinh my\right\} \qquad (2.41)$$

where A_{1j}, $i = 1,2,3,4$; $j = 1,2$; are constants and given by

$$A_{1j} = \left[(U_{2j} - U_{1j}) \sinh mh - \frac{h}{2\mu} \frac{\partial p}{\partial x_j} \{ h \sinh mh + \frac{2N^2}{m}(1 - \cosh mh) \} \right] / A_5 \tag{2.42}$$

$$A_{2j} = \frac{A_{1j}}{2\mu} \tag{2.43}$$

$$A_{3j} = \frac{1}{\mu} \left[(U_{2j} - U_{1j}) \frac{(1 - \cosh mh)}{2} + \frac{h}{2\mu} \frac{\partial p}{\partial x_j} \{ \frac{h}{2} (\cosh mh - 1) + (h - \frac{N^2}{m} \sinh mh) \} \right] / A_5 \tag{2.44}$$

$$A_{4j} = U_{1j} + \frac{2N^2}{m} A_{3j} \tag{2.45}$$

$$A_5 = \frac{h}{\mu} \{ \sinh mh - \frac{2N^2}{mh} (\cosh mh - 1) \} \tag{2.46}$$

in which

$$x_1 = x, \; x_2 = z, \; m = \frac{N}{\ell} \tag{2.47}$$

(ii) Flow Flux

The volume flow rates q_x and q_z, along x and z axes, are given by

$$q_x = \int_o^h u \, dy \tag{2.48}$$

and

$$q_z = \int_o^h w \, dy \tag{2.49}$$

or

$$q_x = \frac{h}{2}(U_{11}+U_{21}) - \frac{h^3 f(N,\ell,h)}{\mu}\frac{\partial p}{\partial x} \tag{2.50}$$

and

$$q_z = \frac{h}{2}(U_{12}+U_{22}) - \frac{h^3 f(N,\ell,h)}{\mu}\frac{\partial p}{\partial z} \tag{2.51}$$

where

$$f(N,\ell,h) = \frac{1}{12} + \frac{\ell^2}{h^2} - \frac{N\ell}{2h}\coth\frac{Nh}{2\ell} \tag{2.52}$$

It should be noted that for convenience in Chapters VI and VII the flow fluxes are defined as follows

$$q_x = \frac{h}{2}(U_{11}+U_{21}) - \frac{f(N,\ell,h)}{\mu}\frac{\partial p}{\partial x} \tag{2.53}$$

$$q_z = \frac{h}{2}(U_{21}+U_{22}) - \frac{f(N,\ell,h)}{\mu}\frac{\partial p}{\partial z} \tag{2.54}$$

where

$$f(N,\ell,h) = \frac{h^3}{12} + h\,\ell^2 - \frac{N\ell h^2}{2}\coth\frac{Nh}{2\ell} \tag{2.55}$$

(iii) Generalized Reynolds Equation

Integrating the equation of continuity (2.11) across the film and using (2.50) and (2.51) (or eqn s.2.53 and 2.54) together with (2.36) and (2.37) the generalized Reynolds equation for micropolar fluid in three dimensions is obtained as

$$\frac{\partial}{\partial x}\{q_x\} + \frac{\partial}{\partial z}\{q_z\} = U_{21}\frac{\partial h}{\partial x} + U_{22}\frac{\partial h}{\partial z} + V_o - V_h \tag{2.56}$$

where V_h and V_o are the normal velocity components of the surfaces at $y = h$ and $y = o$, respectively.

Similar equation was obtained by Shukla and Isa [57] and Tipei [84] under the assumption of constancy of characteristic coefficients across the film. However the parameters N and ℓ are different from the parameters used by [57,84] .

For infinitely long bearings, along z-axis, the two dimensional Reynolds equation is given by [58] .

(iv) Frictional Torques

The shear stresses along x-direction and z-direction, from equation (2.4), are

$$\tau_x = (\mu + \frac{1}{2}\chi) \frac{\partial u}{\partial x} + \chi v_3 \tag{2.57}$$

and

$$\tau_z = (\mu + \frac{1}{2}\chi) \frac{\partial w}{\partial z} - \chi v_1 \tag{2.58}$$

and on the surfaces $y = o$ and $y = h$ these assume the form

$$(\tau_x)_{o,h} = \mp \frac{h}{2} \frac{\partial p}{\partial x} + \frac{\mu (U_{21} - U_{11})}{hg(N,\ell,h)} \tag{2.59}$$

$$(\tau_z)_{o,h} = \mp \frac{h}{2} \frac{\partial p}{\partial z} + \frac{\mu (U_{22} - U_{12})}{hg(N,\ell,h)} \tag{2.60}$$

where

$$g(N,\ell,h) = 1 - \frac{2N\ell}{h} \tanh \frac{Nh}{2\ell} \tag{2.61}$$

The frictional drags are obtained by integrating the shearing stresses over the bearing surfaces.

It should be noted that for convenience in Chapters VI and VII the shear stresses are defined as follows

$$(\tau_x)_{o,h} = \mp \frac{h}{2}\frac{\partial p}{\partial x} + \frac{\mu(U_{21}-U_{11})}{g(N,\ell,h)} \tag{2.62}$$

$$(\tau_z)_{o,h} = \mp \frac{h}{2}\frac{\partial p}{\partial z} + \frac{\mu(U_{22}-U_{12})}{g(N,\ell,h)} \tag{2.63}$$

where

$$g(N,\ell,h) = h - 2N\ell \tanh \frac{Nh}{2\ell} \tag{2.64}$$

CHAPTER III

TWO AND THREE DIMENSIONAL NON-CYCLIC SQUEEZE FILMS

3.1 INTRODUCTION

In recent years many workers have analyzed the problems of micropolar fluid lubricated non - cyclic squeeze films [55,68-71,83] and cyclic squeeze films [75-76] . The problem of porous non-cyclic squeeze films have also been solved using micropolar fluid as lubricant [72-74] . The prominent feature of using micropolar fluid as lubricant was an increase in load carrying capacity and squeeze time.

Though some of the geometries, such as circular plates, considered were finite dimensional, but due to non-variation of pressure along circumferential direction, the problems solved were essentially two dimensional. It is thus imperative to study the effects of micropolarity on three dimensional squeeze films problems.

In this Chapter, an application of micropolar fluid theory is made to study some hitherto untouched two dimensional important problems and to some three dimensional configurations.

The problem considered is that of the so called 'non-cyclic squeeze films'. The squeeze velocity V is imparted by a load W, which will be considered constant in magnitude and direction and symmetrically placed, with respect to the boundaries of the system. Various geometries

are considered , namely , spherical bearings, slider and rectangular plates, conical bearings and some miscellaneous configurations. The approach is similar to that of Pinkus and Sternlicht [85]. Detailed numerical results are obtained for the spherical bearings, whereas for the three dimensional case only the dimensionless response time is obtained.

3.2 SPHERICAL BEARINGS

The film geometry for squeeze film in spherical bearing is shown in Fig. 3.1(a). Here we shall consider the case of hemispherical seat.

From the geometry, given by Fig.3.1(a), the film thickness is given by

$$h = r - R - a_1 \cos\theta \tag{3.1}$$

which can be rewritten as

$$h = c(1 - \epsilon \cos\theta) \tag{3.2}$$

where

$$c = r - R, \quad \epsilon = \frac{a_1}{r-R} \tag{3.3}$$

For a sphere the amount of fluid passing through a conical element of surface is given by

$$q_\theta = \int_0^h (2\pi R \sin\theta)\, u \, dy \tag{3.4}$$

where u is the velocity of the fluid. For zero tangential velocities

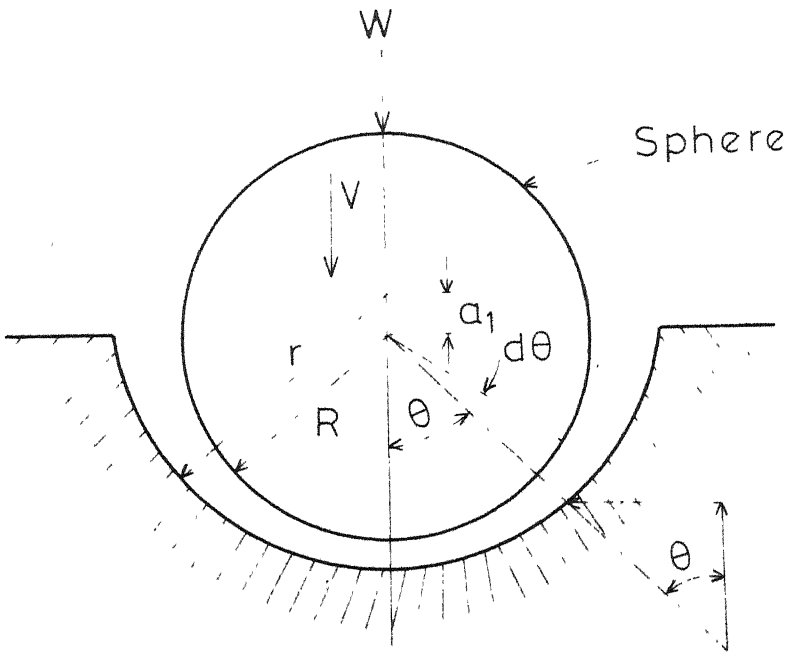

Fig. 3.1(a) Spherical bearing configuration.

the expression for u, equation (2.38), reduces to

$$u = \frac{1}{\mu R}\frac{dp}{d\theta}\left(\frac{y^2}{2} - \frac{N^2 h}{m}\frac{\cosh my - 1}{\sinh mh}\right) - \frac{h}{2\mu R}\frac{dp}{d\theta}\left[y - \frac{N^2}{m} \times \right.$$

$$\left. \times \left\{\sinh my - \frac{(\cosh my - 1)(\cosh mh - 1)}{\sinh mh}\right\}\right] \qquad (3.5)$$

in which x is replaced by $R\theta$.

Substitution of u, equation (3.5) in equation (3.4), yields

$$q_\theta = 2\pi R \sin\theta \left\{-\frac{h^3}{\mu R}\frac{dp}{d\theta} f(N,\ell,h)\right\} \qquad (3.6)$$

where m, N and ℓ are given by eqn. (2.18) and $f(N,\ell,h)$ is defined by eqn. (2.52).

The displacement of the fluid at any point in the seat is [88],

$$q_\theta = \pi V R^2 \sin^2\theta \qquad (3.7)$$

where V is the relative normal velocity of the surfaces, responsible for squeeze film action and is given by

$$V = c\frac{d\varepsilon}{dt} \qquad (3.8)$$

Equating (3.6) and (3.7)

$$\frac{dp}{d\theta} = -\frac{\mu V R^2 \sin\theta}{2h^3 f(N,\ell,h)} \qquad (3.9)$$

The pressure distribution with the boundary conditions

$$p\left(\pm\frac{\pi}{2}\right) = 0 \qquad (3.10)$$

becomes

$$p(\theta) = \frac{\mu VR^2}{2} \int_{\theta}^{\frac{\pi}{2}} \frac{\sin\theta \, d\theta}{h^3 f(N,\ell,h)} , \quad o \leq \theta \leq \frac{\pi}{2} \tag{3.11}$$

since the prescure distribution is symmetric for the regions $-\frac{\pi}{2} \leq \theta \leq o$ and $o \leq \theta \leq \frac{\pi}{2}$.

Non-dimensionalizing, using

$$H = \frac{h}{c} = (1 - \varepsilon \cos\theta), \quad L = \frac{c}{\ell} , \quad P = \frac{p}{\frac{\mu VR^2}{2c^3}} \tag{3.12}$$

the non-dimensional pressure is

$$P(\theta) = \int_{\theta}^{\pi/2} \frac{\sin\theta \, d\theta}{H^3 F(N,L,H)} \tag{3.13}$$

where

$$F(N,L,H) = \frac{1}{12} + \frac{1}{(LH)^2} - \frac{N}{2LH} \coth \frac{NLH}{2} \tag{3.14}$$

The load capacity for a hemisphere is

$$W = 2\pi R^2 \int_{o}^{\pi/2} p \sin\theta \cos\theta \, d\theta = \frac{\pi\mu VR^4}{2} \int_{o}^{\pi/2} \frac{\sin^3\theta \, d\theta}{h^3 f(N,\ell,h)} \tag{3.15}$$

The non-dimensional load is

$$\bar{W} = \frac{W}{\left(\frac{\pi\mu VR^4}{2c^3}\right)} = \int_{o}^{\pi/2} \frac{\sin^3\theta \, d\theta}{H^3 F(N,L,H)} \tag{3.16}$$

The time of approach, t, from an initial film thickness h_1 to a final film thickness $h_o (h_1 > h_o)$ in terms of corresponding values of eccentricity ratio can be evaluated using (3.15) and (3.8).

Thus

$$t = \frac{\pi \mu c R^4}{2W} \int_{\varepsilon_o}^{\varepsilon_1} \int_{o}^{\pi/2} \frac{\sin^3 \theta \, d\theta \, d\varepsilon}{h^3 f(N,\ell,h)} \tag{3.17}$$

The non-dimensional time of approach is

$$T = \frac{t}{\left(\frac{\pi \mu R^4}{2c^2 W}\right)} = \int_{\varepsilon_o}^{\varepsilon_1} \int_{o}^{\pi/2} \frac{\sin^3 \theta \, d\theta \, d\varepsilon}{H^3 F(N,L,H)} \tag{3.18}$$

3.3. SLIDERS AND RECTANGULAR PLATES

The rectangular plate poses a three dimensional problem, and we must return to the basic differential equation of a viscous flow of micropolar fluid for a solution.

The differential equation governing the pressure distribution in three-dimensions, equation (2.56), for h = constant, is

$$\frac{\partial^2 p}{\partial x^2} + \frac{\partial^2 p}{\partial z^2} = \frac{\mu V}{h^3 f(N,\ell,h)} \tag{3.19}$$

Equation (3.19) is Poisson's equation, the solution of which is assumed of the form

$$p(x,z) = \sum_{n=1,3,5}^{\infty} \left(A_n \cos \frac{n\pi x}{a_2}\right) Z(z) \tag{3.20}$$

where $Z(z)$ is the function of z alone and A_n is a constant to be determined. a_2 is the x-dimension of plate. Substituting (3.20) into (3.19) and using the relation

$$\frac{\pi}{4} = \sum_{n=1,3,5}^{\infty} (-1)^{\frac{(n-1)}{2}} \frac{1}{n} \cos \frac{n\pi x}{a_2} \tag{3.21}$$

we have

$$- \sum_{n=1,3,5}^{\infty} \left(\frac{n\pi}{a_2}\right)^2 A_n \cos \frac{n\pi x}{a_2} Z(z) +$$

$$+ \sum_{n=1,3,5}^{\infty} A_n \cos \frac{n\pi x}{a_2} \frac{d^2 Z(z)}{dz^2}$$

$$= \frac{4}{\pi} \frac{\mu V}{h^3 f(N,\ell,h)} \sum_{n=1,3,5}^{\infty} (-1)^{\frac{(n-1)}{2}} \frac{1}{n} \cos \frac{n\pi x}{a_2} \tag{3.22}$$

which is satisfied if

$$A_n \frac{d^2 Z(z)}{dz^2} - \left(\frac{n\pi}{a_2}\right)^2 A_n Z(z) = \frac{4}{\pi} \frac{\mu V}{h^3} \frac{(-1)^{\frac{(n-1)}{2}}}{f(N,\ell,h)} \tag{3.23}$$

A particular solution is given by

$$Z(z) = B_m \sinh \frac{n\pi z}{a_2} + C_n \cosh \frac{n\pi z}{a_2} - \frac{4\mu a_2^2 V}{\pi^3 h^3 f(N,\ell,h)} \frac{(-1)^{\frac{(n-1)}{2}}}{n^3 A_n} \tag{3.24}$$

Putting (3.24) into (3.20) and using the boundary conditions

$$p = o \text{ at } z = \pm \frac{b_2}{2} \tag{3.25}$$

where b_2 is the z-dimension of the plate and by the requirement of symmetry in z-direction, the pressure distribution is

$$p(x,z) = \frac{+4\mu a_2^2 V}{\pi^3 h^3 f(N,\ell,h)} \sum_{n=1,3,5}^{\infty} \frac{(-1)^{\frac{n-1}{2}}}{n^3} \left[\frac{\cosh \frac{n\pi z}{a_2}}{\cosh \frac{n\pi b_2}{2a_2}} - 1\right] \tag{3.26}$$

The total load is given by

$$W = + \frac{16\mu a_2^3 V}{\pi^4 h^3 (N,\ell,h)} \sum_{n=1,3,5}^{\infty} \left(\frac{a_2}{n^5\pi} \tanh \frac{n\pi b_2}{2a_2} - \frac{b_2}{2n^4} \right) \qquad (3.27)$$

Using $V = -\frac{dh}{dt}$, the time of approach from an initial film thickness h_1 to a final film thickness $h_o (h_1 > h_o)$ is given by

$$t = \frac{16\mu a_2^3}{\pi^4 W} \sum_{n=1,3,5}^{\infty} \left(\frac{b_2}{2n^4} - \frac{a_2}{n^5\pi} \tanh \frac{n\pi b_2}{2a_2} \right) \int_{h_o}^{h_1} \frac{dh}{h^3 f(N,\ell,h)} \qquad (3.28)$$

Non-dimensionlizing, using

$$H = \frac{h}{h_1}, \quad H_o = \frac{h_o}{h_1}, \quad L = \frac{h_1}{\ell}, \quad T = \frac{t}{\left(\frac{16\mu a_2^3}{\pi^4 W h_1^2} \right)},$$

$$S_n = \sum_{n=1,3,5}^{\infty} \left(\frac{b_2}{2n^4} - \frac{a_2}{n^5\pi} \tanh \frac{n\pi b_2}{2a_2} \right) \qquad (3.29)$$

the non-dimensional time of approach is

$$T = \int_{H_o}^{1} \frac{dH}{H^3 F(N,L,H)} \qquad (3.30)$$

3.4 ELLIPTICAL PLATES

For an elliptic plate

$$\frac{x^2}{A_1^2} + \frac{z^2}{B_1^2} = 1 \qquad (3.31)$$

the pressure distribution with the help of governing differential equation (3.19) can be written as

$$p(x,z) = C_1\left(\frac{x^2}{A_1^2} + \frac{z^2}{B_1^2} - 1\right),\ C_1 \text{ is a constant} \tag{3.32}$$

where the pressure boundary condition is p = o on the boundary of the ellipse given by equation (3.31).

Substituting equation (3.32) into (3.19), we get the pressure distribution

$$p(x,z) = -\frac{\mu V A_1^2 B_1^2}{2(A_1^2+B_1^2)h^3 f(N,\ell,h)}\left(\frac{x^2}{A_1^2} + \frac{z^2}{B_1^2} - 1\right) \tag{3.33}$$

The load capacity and time of approach from an initial film thickness h_1 to a final thickness h_o are given by

$$W = +\frac{\mu\pi V}{4h^3 f(N,\ell,H)}\frac{A_1^3 B_1^3}{(A_1^2+B_1^2)} \tag{3.34}$$

and

$$t = \frac{1}{4W}\frac{\pi\mu A_1^3 B_1^3}{(A_1^2+B_1^2)}\int_{h_o}^{h_1}\frac{dh}{h^3 f(N,\ell,h)} \tag{3.35}$$

Circular plates are special case of elliptical plates and the bearing characteristics can be obtained directly from above expression by putting $A_1=B_1=r$, Prakash and Sinha [69].

3.5 MISCELLANEOUS CONFIGURATIONS

By the methods similar to those described above, results for

other shapes, of falling plates, can be extracted. Some of these are given by

(i) Circular rings of inner radius r_1 and outer radius r_2

$$W = \frac{\pi \mu V}{8h^3 f(N,\ell,h)} \left[r_2^4 - r_1^4 - \left[\frac{(r_2^2 - r_1^2)^2}{\log(\frac{r_2}{r_1})} \right] \right] \tag{3.36}$$

putting $V = -\frac{dh}{dt}$

$$t = \frac{\pi\mu}{8W} \left[r_2^4 - r_1^4 - \frac{(r_2^2 - r_1^2)^2}{\log(\frac{r_2}{r_1})} \right] \int_{h_o}^{h_1} \frac{dh}{h^3 f(N,\ell,h)} \tag{3.37}$$

(ii) Circular sector of angle β_1 and bounded by radii r_1 and r_2

$$W = \frac{8\mu\beta_1 V}{\pi^2 h^3 f(N,\ell,h)} \sum_{1,3,5}^{\infty} \left[\frac{r_2^4 - r_1^4}{4n^2(2-\frac{n\pi}{\beta_1})^2} - \right.$$

$$\left. - \frac{2\pi}{n\beta_1} \frac{1}{\left[4-(\frac{n\pi}{\beta_1})^2 \right]^2} \frac{r_2^{2+\frac{n\pi}{\beta_1}} - r_1^{2+\frac{n\pi}{\beta_1}}}{r_2^{\frac{2n\pi}{\beta_1}} - r_1^{\frac{2n\pi}{\beta_1}}} \right] \tag{3.38}$$

and

$$t = \frac{8\beta_1\mu}{\pi^2 W} \sum_{n=1,3,5}^{\infty} \left[\frac{r_2^4 - r_1^4}{4n^2(2-\frac{n\pi}{\beta_1})^2} - \frac{r_2^{2+\frac{n\pi}{\beta_1}} - r_1^{2+\frac{n\pi}{\beta_1}}}{r_2^{\frac{2n\pi}{\beta_1}} - r_1^{\frac{2n\pi}{\beta_1}}} \frac{2\pi}{n\beta_1\{4-(\frac{n\pi}{\beta})^2\}^2} \right] \times$$

$$\times \int_{h_o}^{h_1} \frac{dh}{h^3 f(N,\ell,h)} \tag{3.39}$$

Letting $r_1 \to o$ in equations (3.38) and (3.39) the characteristics for full sector can be obtained.

(iii) A circle of radius r_1, a portion of which has been cut out by another full circle of radius r_2 (Fig. 3.1(b))

$$W = \frac{\mu V}{8h^3 f(N,\ell,h)} \left[(2r_1^4 - 4r_1^2 r_2^2 - r_2^4) \cos^{-1} \frac{r_2}{2r_1} + \right.$$

$$\left. + \frac{r_2}{2}(r_1^2 + \frac{7}{2} r_2^2)(4r_1^2 - r_2^2)^{1/2} \right] \qquad (3.40)$$

and

$$t = + \frac{\mu}{8W} \left[(2r_1^4 - 4r_1^2 r_2^2 - r_2^4) \cos^{-1} \frac{r_2}{2r_1} + \frac{r_2}{2}(r_1^2 + \frac{7}{2} r_2^2) \times \right.$$

$$\left. \times (4r_1^2 - r_2^2)^{1/2} \right] \int_{h_o}^{h_1} \frac{dh}{h^3 f(N,\ell,h)} \qquad (3.41)$$

Letting $r_2 \to o$, the case of full circle is obtained, Prakash and Sinha [69].

(iv) Full Conical Seats

In case of complete cone (Fig.3.1(c)),

$$W = \frac{\pi \mu R_1^4 V}{8h^3 f(N,\ell,h) \sin^4 \alpha_1} \qquad (3.42)$$

where α_1 is the semi-vertical angle and R_1 is the radius of base and

$$t = + \frac{\pi \mu R_1^4}{8W \sin^4 \alpha_1} \int_{h_o}^{h_1} \frac{dh}{h^3 f(N,\ell,h)} \qquad (3.43)$$

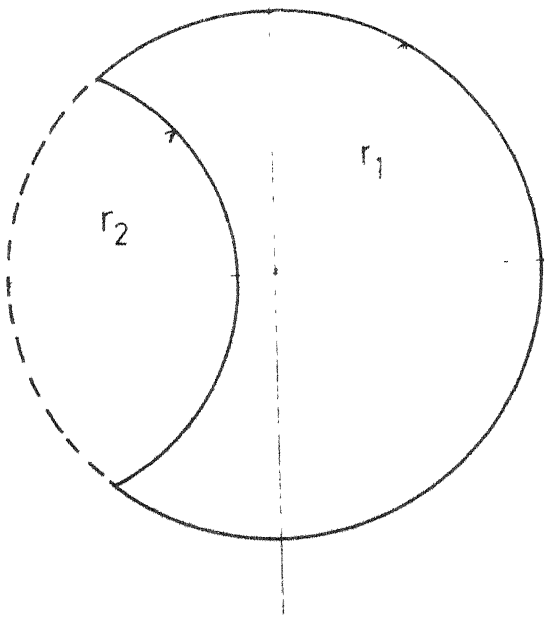

Fig 3 1(b) Configuration of circle of radius r_1, a portion of which is cut out by another circle of radius

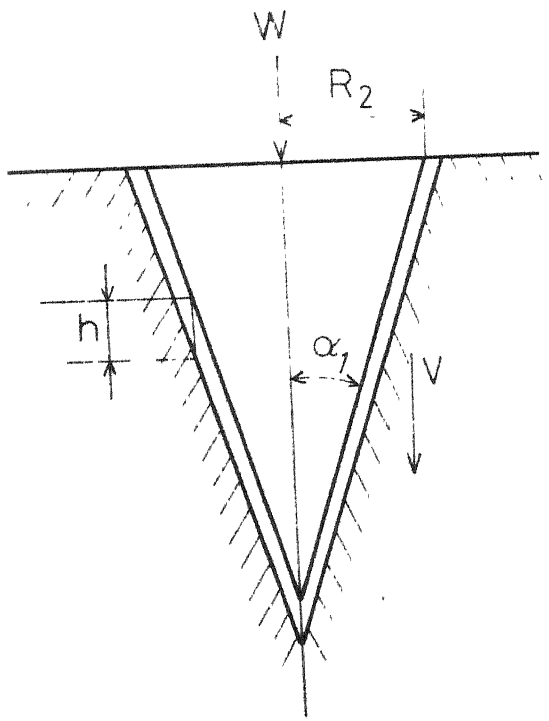

Fig 3.1(c) Full conical seat configuration

(v) Truncated Conical Seats

For truncated cone (Fig. 3.1(d)), whose smaller radius is R_2 and larger radius is R_1,

$$W = \frac{\pi\mu V}{8h^3 f(N,\ell,h)\ \sin^4\alpha_1}\left[\ R_1^4 - R_2^4 - \frac{(R_1^2-R_2^2)^2}{\log(\frac{R_1}{R_2})}\ \right] \tag{3.44}$$

and

$$t = \frac{\pi\mu}{8W\sin^4\alpha_1}\left[R_1^4 - R_2^4 - \frac{(R_1^2-R_2^2)^2}{\log\ (\frac{R_1}{R_2})}\right]\int_{h_o}^{h_1} \frac{dh}{h^3 f(N,\ell,h)} \tag{3.45}$$

The dimensionless response time in each of the above cases is governed by integral

$$\int_{H_o}^{1} \frac{dH}{H^3 F(N,L,H)} \tag{3.46}$$

This integral is therefore integrated numerically for rectangular plates and represented graphically. This integral is similar to the one obtained by Prakash and Sinha [69] .

3.6 RESULTS AND DISCUSSION

(i) Dimensionless Parameters

The micropolar fluid is characterized by three physical constants, μ , χ and γ as compared to a Newtonian fluid which only

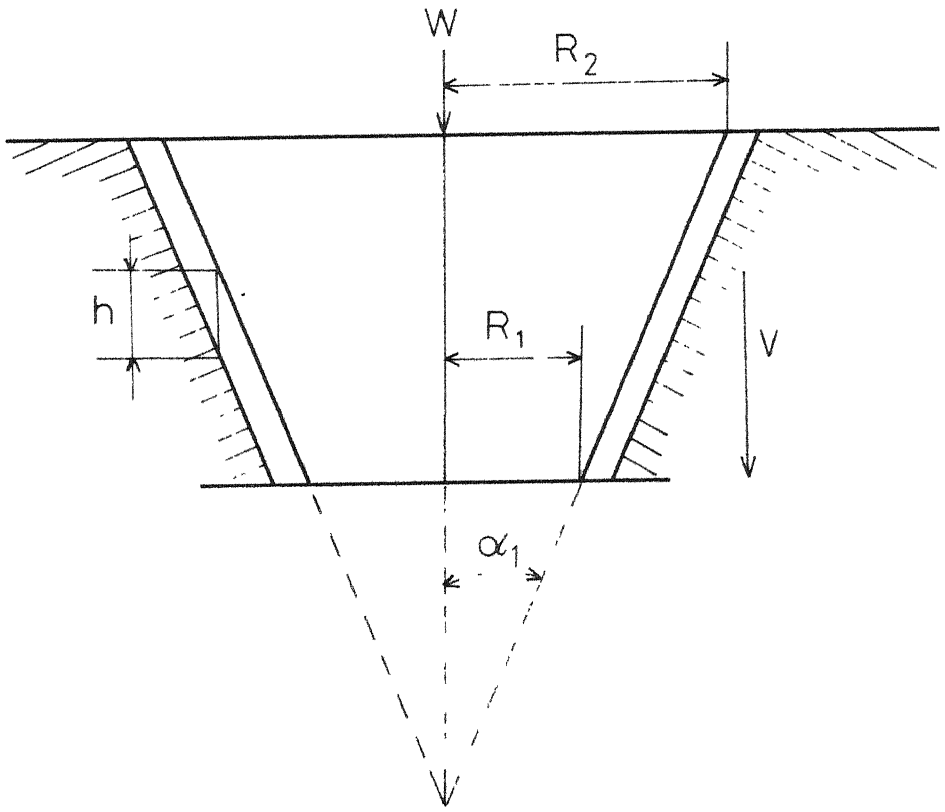

Fig 3 1(d) Truncated conical seat configuration

has one constant μ, the Newtonian viscosity. This arises as a consequence of resistance to linear motion, whereas the parameter χ, which has the dimensions of viscosity may be visualized, to be a consequence of resistance to the micromotion of the fluid molecule. The third coefficient γ, which has the dimension $L^2[\mu]$, gives rise to a very important parameter, when compared with the Newtonian viscosity μ, i.e. the parameter $\ell = (\frac{\gamma}{4\mu})^{1/2}$. This ℓ has the dimensions of length and may be thought of as a material parameter, called the material characteristic length, depending upon the molecular size of the fluid or the chain length of the rigid particle additive.

Thus these three physical constants, μ, χ, and γ give rise to two-dimensionless parameters defined as

$$N = (\frac{\chi}{2\mu+\chi})^{1/2} \text{ and } L = \frac{c}{\ell}, \quad \ell = (\frac{\gamma}{4\mu})^{1/2} \tag{3.47}$$

called the coupling number and the length ratio. These parameters are not encountered in the usual Newtonian theory, and are likely to be of great value in discussing the effects arising due to the presence of rigid particle additives in the lubricant.

The coupling number N, characterizes the coupling of the linear and rotational motions arising due to the micro-motions of the fluid molecules or the additive molecules. Thus the number N signifies a coupling between Newtonian and rotational viscosity. Since the apparent or equivalent dynamic viscosity μ is a derived magnitude including χ and another independent constant μ_ν, called dynamic

viscosity, $\mu = \mu_v + \frac{1}{2}\chi$ [44] . Thus the expression for N becomes

$$N^2 = \frac{\chi}{2(\mu_v + \chi)} \tag{3.48}$$

Thermodynamic restrictions require that μ_v , $\chi \geq o$ [40,44] , it is thus evident that $o \leq N^2 < \frac{1}{2}$.

The second parameter L, defined as the ratio of the clearance width to the characteristic material length ℓ , characterizes interaction between the geometry and the fluid and may be considered to be a property depending upon the size of lubricant molecule, say, the chain length of the molecule.

It is expected that the effects of micropolarity will be of importance either when the characteristic material length is large, corresponding to a large size of lubricant molecule or when the clearance width is small. The second case is of importance in lubrication theory where c is usually small and hence comparable with ℓ. Recalling that $L = c/\ell$ and keeping c fixed an increase in ℓ means a decrease in L, so lower the value of L, larger the chain length of molecule and higher should be the effects due to micropolarity. In fact it is seen that as $L \to o$, the expressions for velocity and other flow characteristics reduce to their equivalents in the Newtonian theory, with μ everywhere replaced by $(\mu + \frac{1}{2}\chi)$. Thus indicating an increased effective viscosity. This observation supports the experimental evidence of increased effective viscosity [8,22,28-36] in the presence

of additives having large chain length and as well as in the case of thin films. Since a small value of L corresponds also to a small clearance width provided ℓ is kept as constant. A large value of L, on the other hand, signifies a large clearance width, i.e. a case of hydrodynamic lubrication or a small material characteristic length and the effects of the micropolarity are not likely to be significant. It is seen that as L tends to ∞, ℓ would tend to zero, and the individuality of the microelement is lost and once again the Newtonian results are obtained.

(ii) Bearing Characteristics

Out of the various cases that have been treated in this Chapter, the numerical results are obtained in detail for the case of spherical bearings (Fig. 3.2 to 3.7) whereas for the three-dimensional rectangular plates only the response time is plotted (Figs. 3.8 and 3.9).

Non-dimensional pressure distribution curves are shown in Fig. 3.2 (N = 0.7 and various values of L) and Fig.3.3(L = o.o and various values of N). Since the pressure curve is symmetric about $\theta = o$, only half of the pressure curve is shown $(o \leq \theta \leq \frac{\pi}{2})$. $L \to \infty$(Fig. 3.2) and $N \to o$ (Fig. 3.3) show the Newtonian pressure curves. As the value of L is decreased, which corresponds to a small clearance or a large size of additive molecule, the pressure begins to rise (Fig. 3.2) and for L = o.o, the maximum pressure is obtained. As the coupling number increases

(Fig. 3.3) the additives play a significant role. The pressure in all cases is higher than the Newtonian pressure.

Fig. 3.4 and Fig. 3.5 show the graphs for dimensionless load capacity as a function of micropolar parameters N and L. The load also is seen to increase as the value of N increases and L decreases. The Newtonian curves are straight lines as the load remains unaffected by the variation in N and L in this case.

Figs. 3.6 to 3.9 are the curves for response time for various values of N and L. Response time is actually the most important squeeze film characteristic. This gives us the time that will elapse for an oil film to be reduced to some minimum value, a value which may have been established as the thinnest permissible film for a particular bearing. The time required to reduce the film thickness can then be compared with the length of the time the load is actually applied.

Fig. 3.6 shows the time-height relationship for a fixed value of N($N = 0.7$) and various values of L. For large values of H, i.e. for large film thickness, the effect of additive on response time is not significant. But as the surfaces further approach each other, the value of H decreases and a marked discrepancy is observed between the Newtonian and micropolar curves. This discrepancy is conspicuous for $H < 0.3$ and for low values of L. A similar result was obtained by Needs [22] in his experiments on squeeze films. This discrepancy indicates that for low values of L and H, the time of approach is

increased, which in turn indicates the enhancement of effective viscosity, which is a confirmed experimental fact when additives are used in lubricants. Similar interpretations can be made regarding Fig. 3.7.

Figs. 3.8 and 3.9 depict the response time curves for various values of L and N for rectangular plate squeeze film (three-dimensional problem). The qualitative effects of micropolarity on response time is same as that in two-dimensional problems which can be easily ascertained from these graphs.

It can thus be concluded that the theoretical effects of additives on three-dimensional lubrication problem are almost identical to those in two dimensions, at least qualitatively.

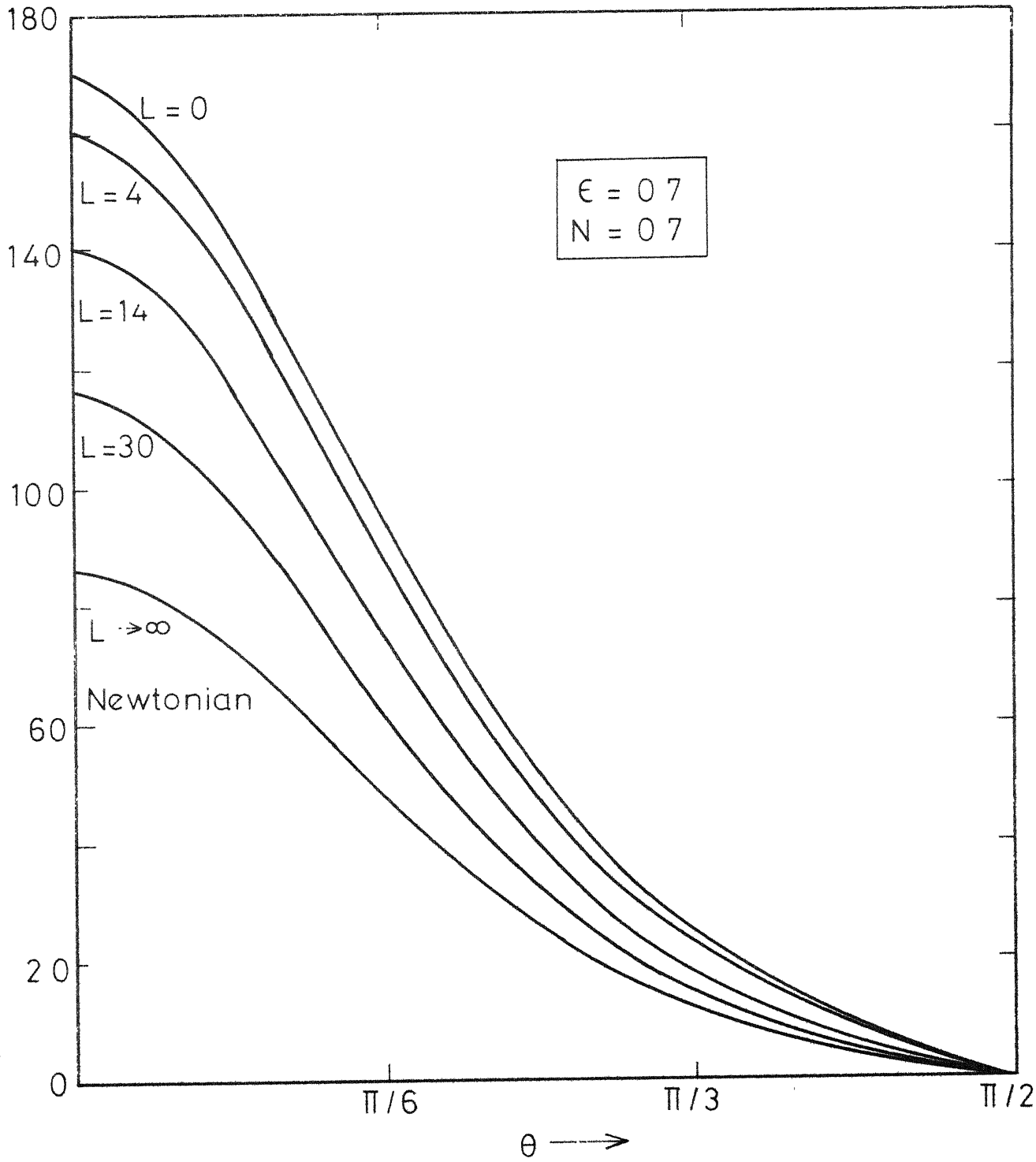

Fig. 3·2 Non dimensional pressure distribution for various values of L at N=0·7 and ϵ=0·7

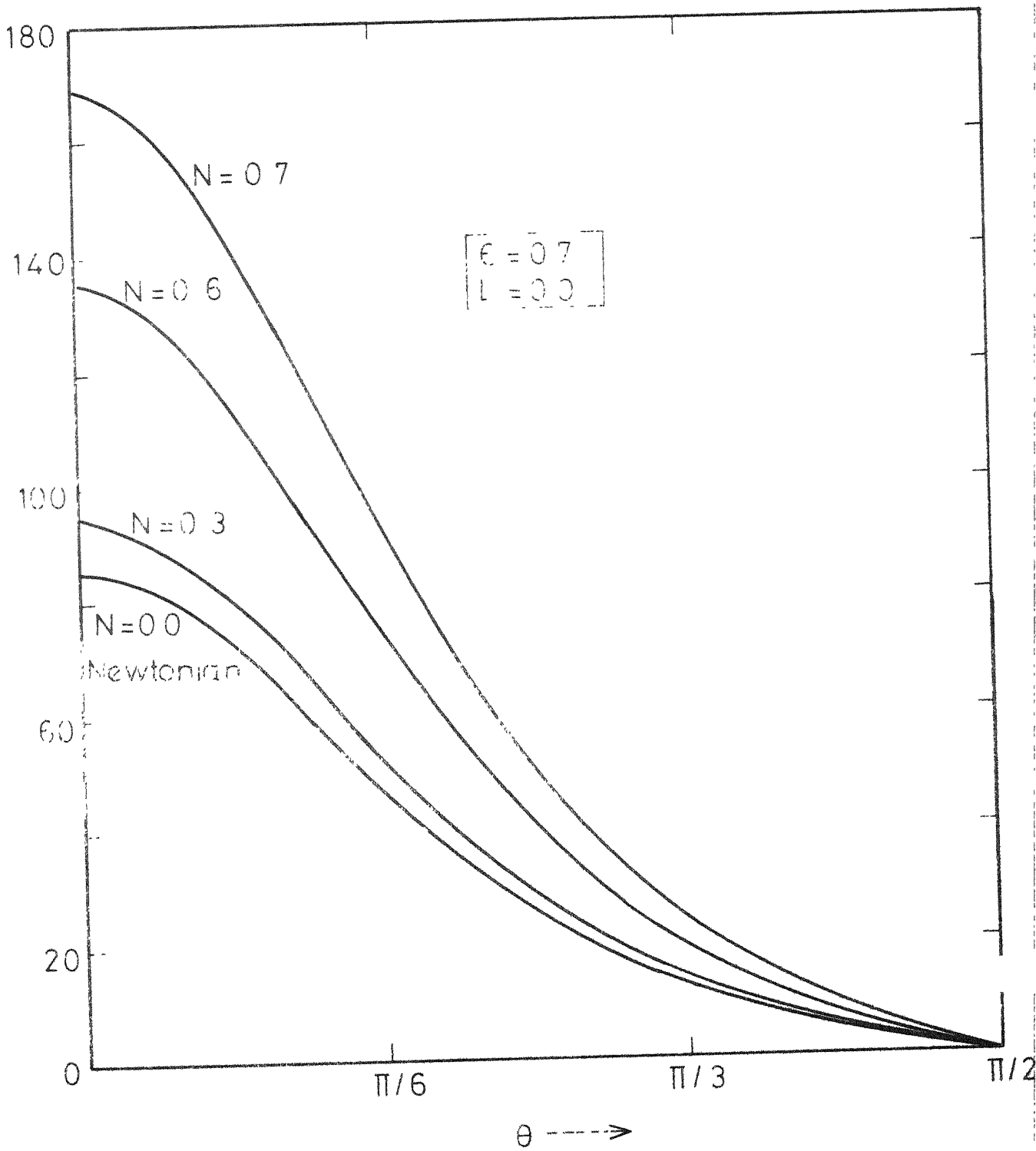

Fig. 3·3 Non-dimensional pressure distribution for various values of N at L=0·0 and ϵ=0·7

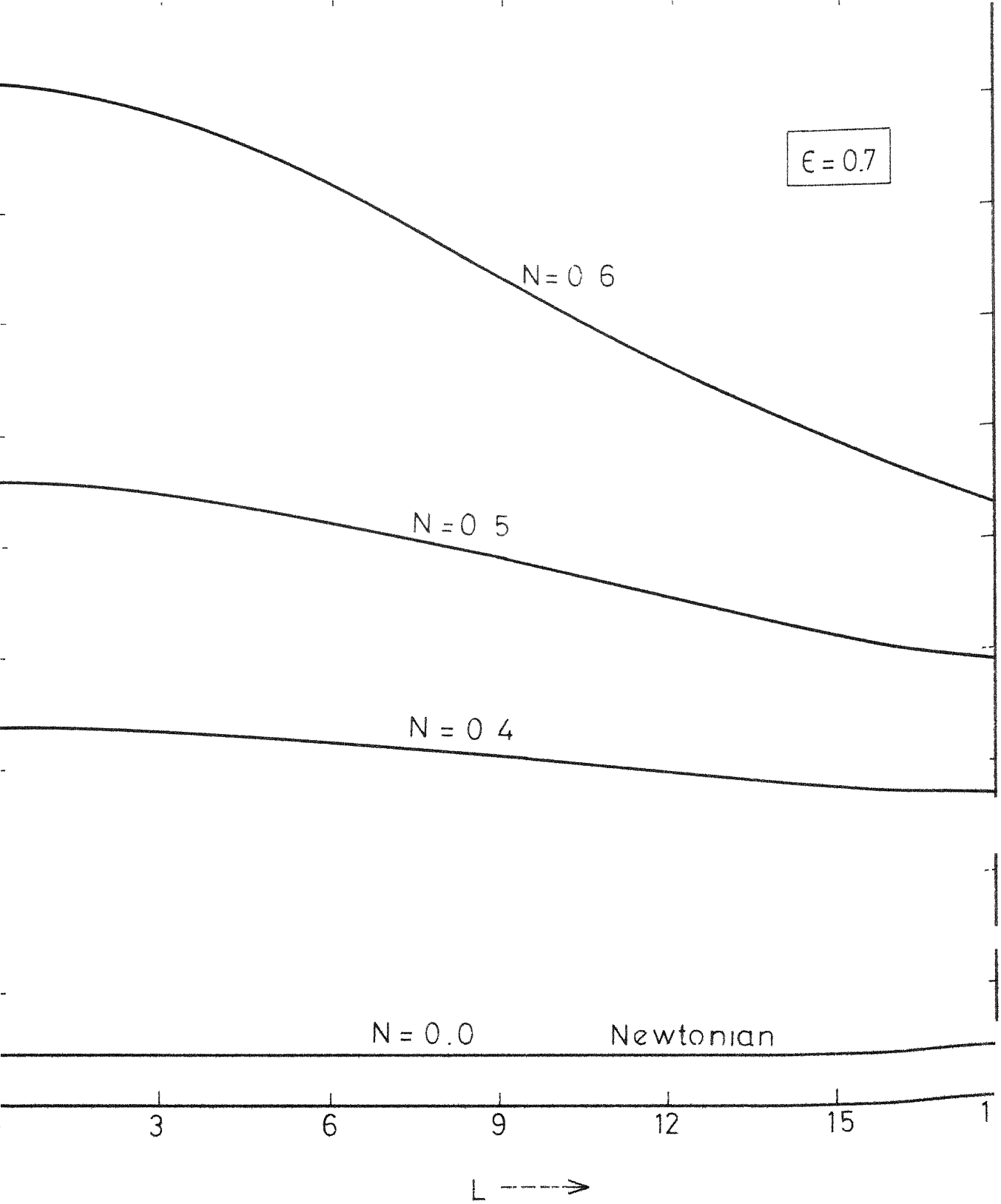

Fig. 3·4 Non-dimensional load vs. L for various values of N at $\epsilon = 0{\cdot}7$

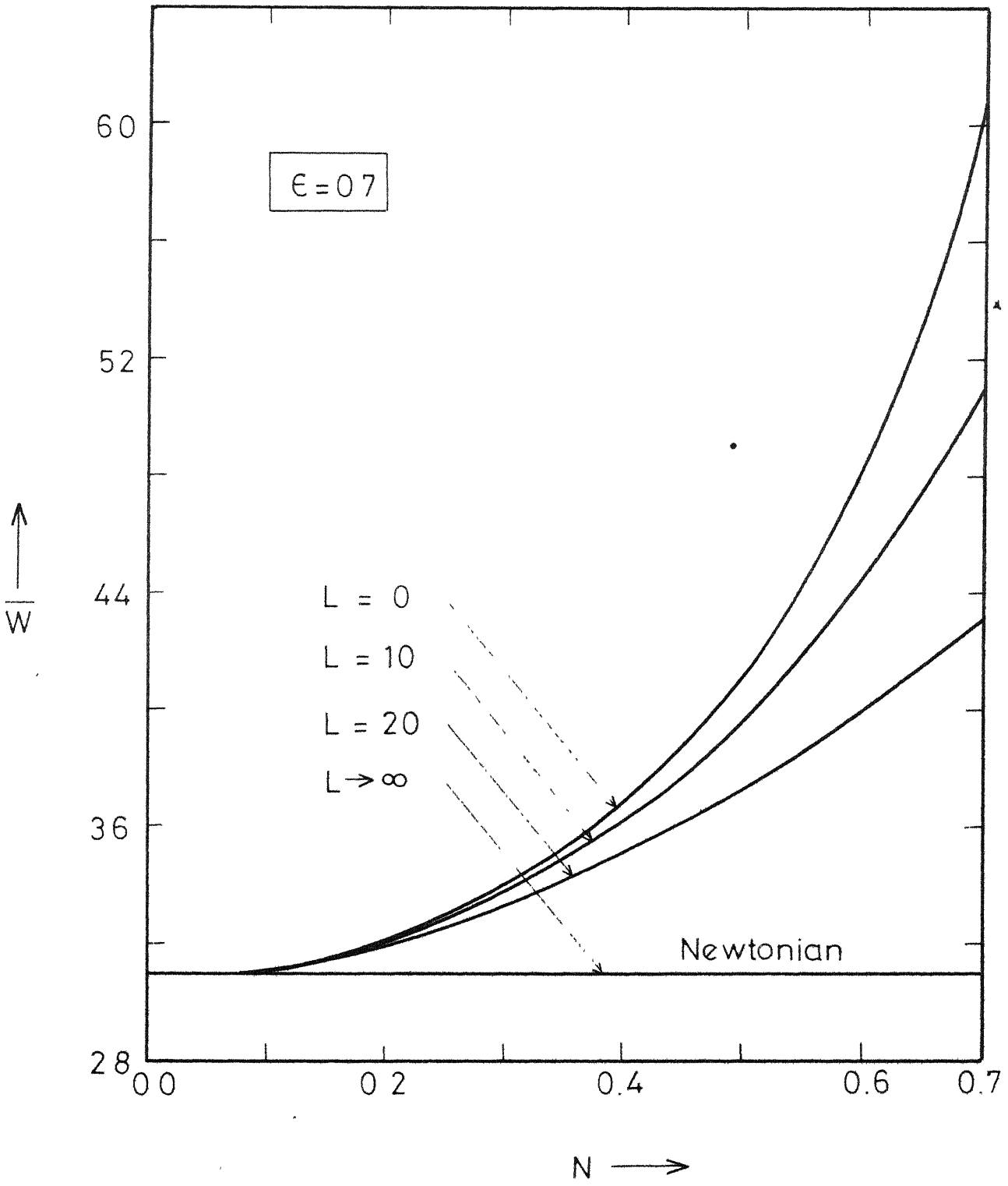

Fig. 3·5 Non-dimensional load vs. N for various values of L at $\epsilon = 0.7$

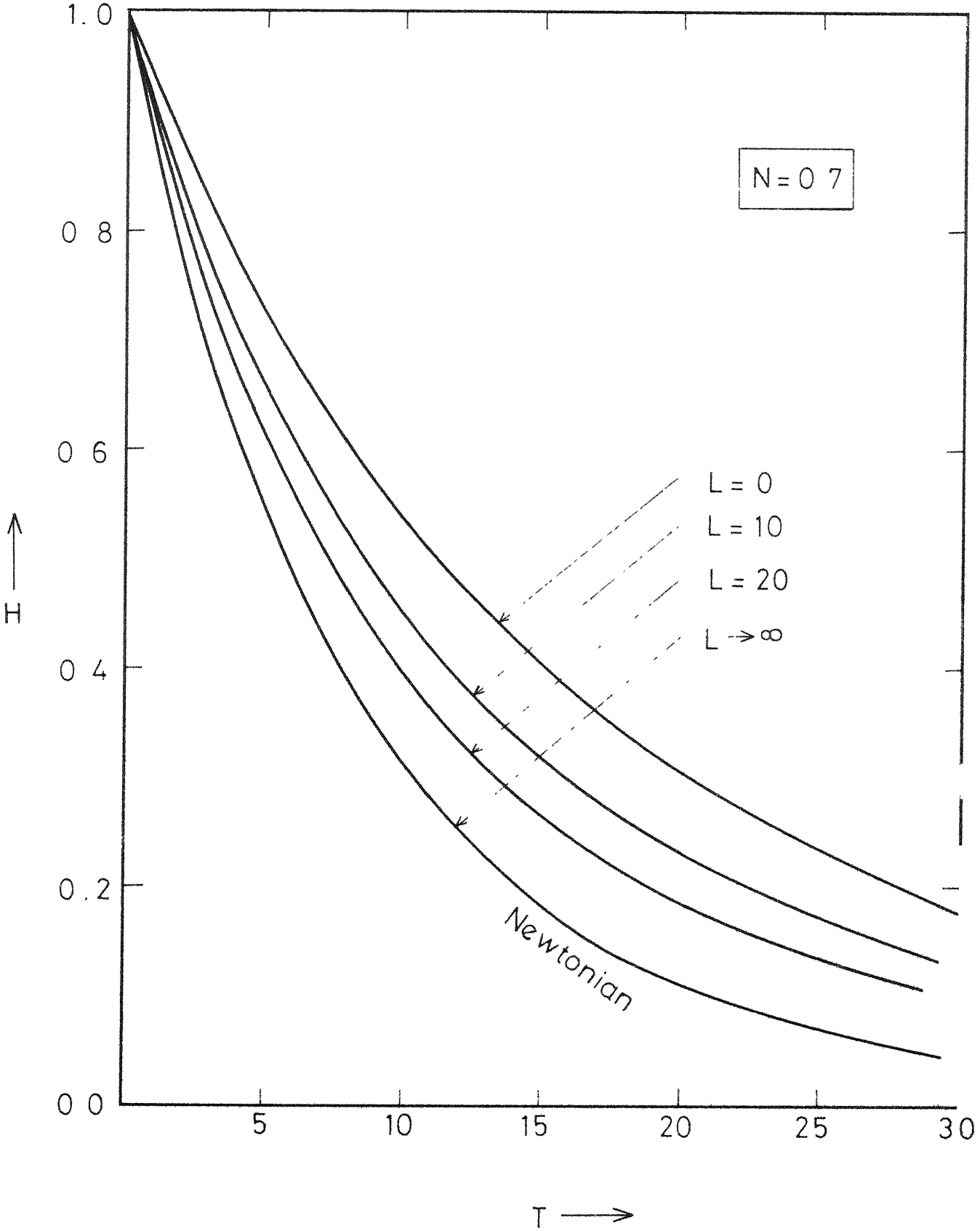

Fig. 3·6 Non-dimensional height vs. non-dimensional time of approach for various values of L at N = 0·7

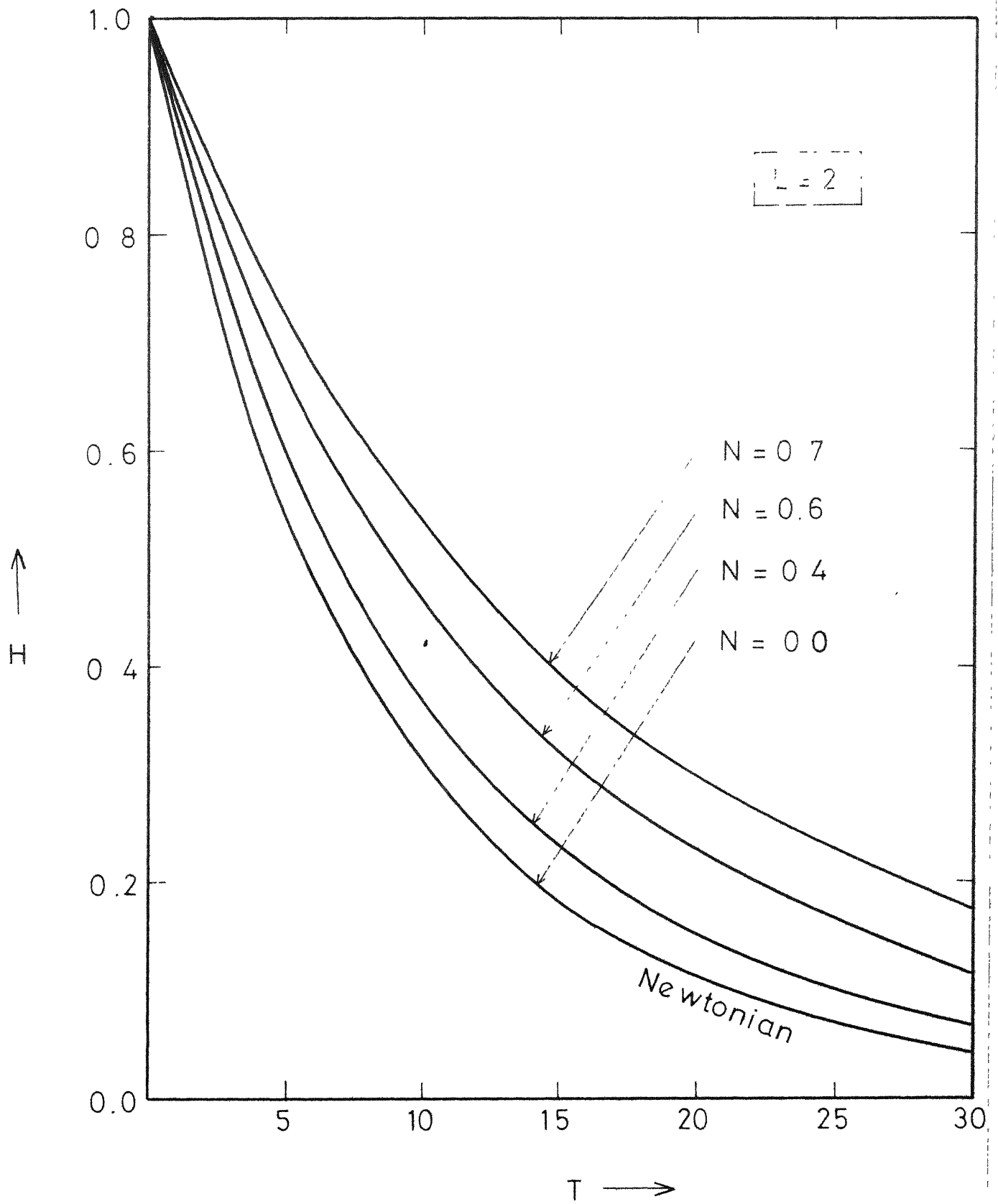

Fig. 3·7 Non-dimensional height vs. non-dimensional time of approach for various values of N at L=2·0

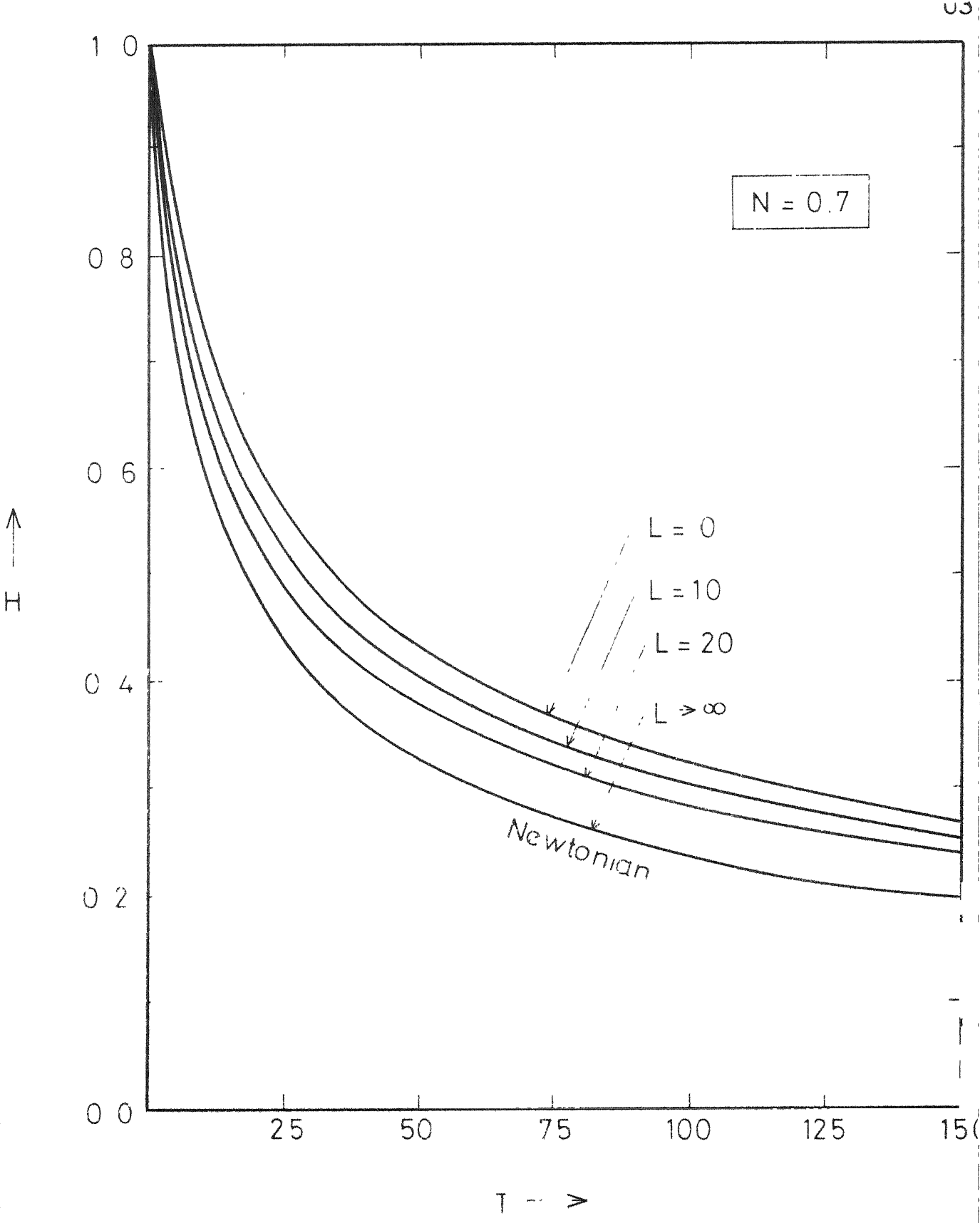

Fig. 3·8 Non-dimensional height vs non-dimensional time of approach for various values of L at N = 0·7 (Rectangular plate)

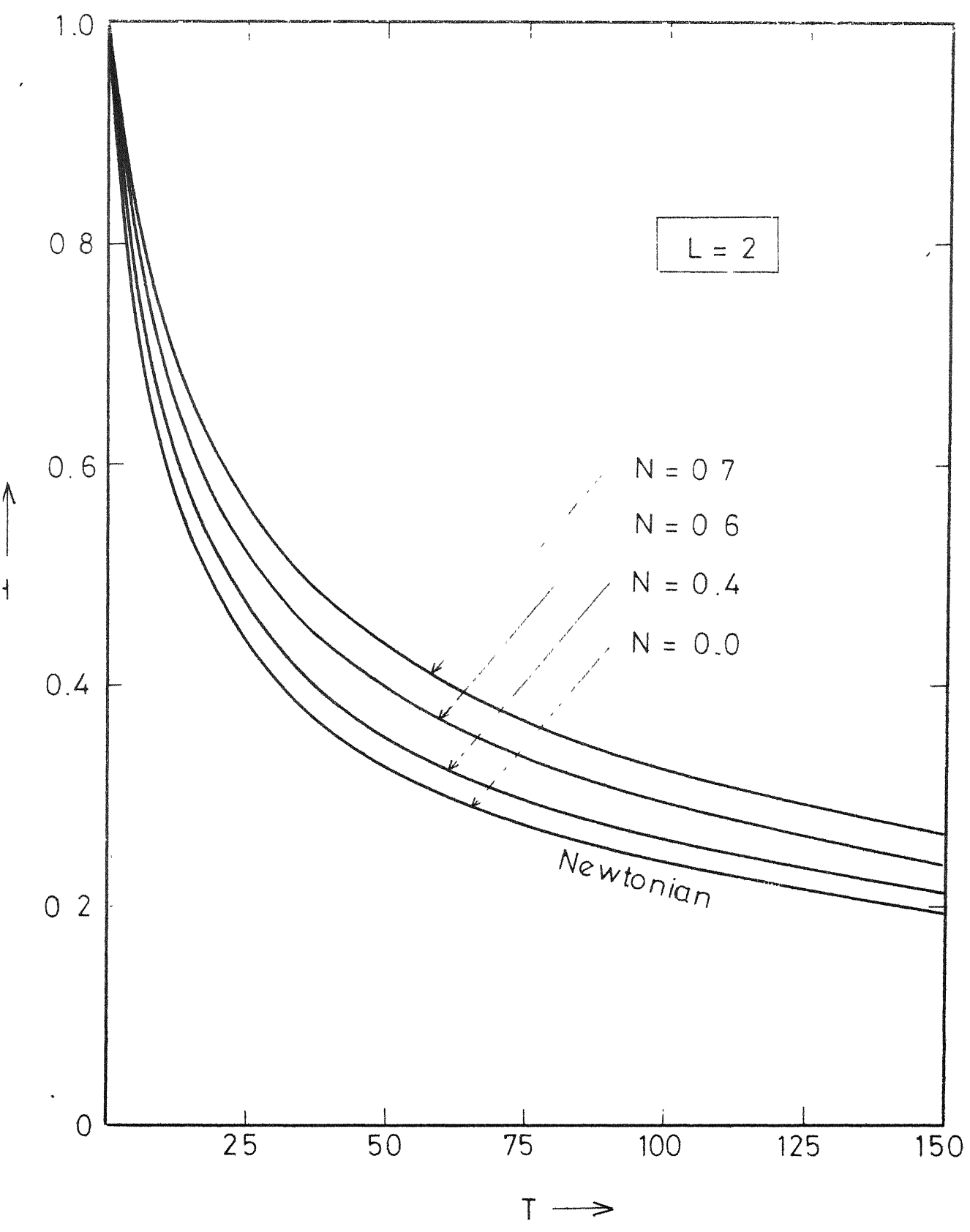

Fig. 3·9 Non-dimensional height vs non-dimensional time of approach for various values of N at L=2·0 (Rectangular plate)

CHAPTER IV

DYNAMICALLY LOADED SHORT JOURNAL BEARINGS

4.1 INTRODUCTION

Dynamically loaded bearings in which the load alternates or rotates has been subject of much interest, conjecture and research. Dynamic situations where both wedge and squeeze films are active, arise in the bearings of almost all reciprocating machines, especially in steam engines, automobile and aircraft piston engines and various machine tools. Even the human joints can be approximated by dynamically loaded bearings.

The load-carrying phenomenon in such bearing arises due to the fact that a viscous lubricant cannot be instantaneously squeezed from between the two approaching surfaces. Because of the resistance of the lubricant to extrusion, pressure is built up and the load is supported by the oil film. When the load is relieved or reversed, the oil film thickness can recover its thickness before the next cycle, if the bearing has been designed to permit this build up.

This phenomenon is found in reciprocating machines where the bearings are subjected to fluctuating, impulsive or dynamic loads and therefore present problems not met in the normal operation of steady load bearings. In general, lubricating oils in the bearing subjected to reciprocating loads are highly vulnerable to contamination,

by both dirt and metal particles. The lubricant may then behave as a fluid suspension. Moreover, the use of additives is a common practice not only for the enhancement of viscosity and a consequent increase in the load carrying capacity, but also to increase the working range of temperature. These additives, through chemical reactions, with the metal surfaces form solid surface films and thus protect the bearing surfaces from damage and wear.

Little work has been reported [75,76] on the lubrication of the dynamically loaded bearings from this view point. It is thus felt that the application of the concept of micropolar fluid lubrication to bearings operating under dynamic conditions would lead to a better understanding of bearing operation and could yield results in conformity more to practice than those obtained by the Newtonian theory. The application of the present work may also be found in the lubrication of human joints, which can be approximated by dynamically loaded bearings. These joints are lubricated by synovial fluid, which has long chain hyaluronic acid molecules and can thus be thought of as a micropolar fluid.

In earlier works, by Prakash and Sinha [75] and Sinha [76], the problems solved were restricted to infinitely long journal bearings. However, for practice, the short bearings are better approximation to finite journal bearings [89]. Hence, in this Chapter, we solve the problem of dynamically loaded short journal bearings lubricated with micropolar fluid.

We start with the general case of dynamic loading in which the load and speed of rotation vary both in magnitude and in direction with time. Various bearing characteristics for an infinitely short journal bearings are obtained in the form of integrals. The equation for determining the journal locus is rather complicated and therefore only a particular case is considered in detail, namely, pure squeeze films with no journal rotation. The case of a fluctuating (sinusoidal) load without rotation is considered. Under this loading condition, the journal may be thought to act like a piston in hydraulic damping mechanism. Physically this implies that, as the load is applied in one direction, the fluid is squeezed out on one side and sucked in on the other. Before the piston comes in contact with the bearing, the load reverses its direction and the oil on the other side begins to take the load. Thus, assuming a continuous fluid film to exist from o to 2π the bearing response to sinusoidal loading is studied and the micropolar effects are elaborated graphically.

4.2 THE PROBLEM AND ANALYSIS

The problem considered is that of dynamically loaded journal bearings (Fig.4.1) in which the load is a function of time. The journal is in combined tangential motion U and normal motion V_o, where U and V_o are both functions of time.

Equation (2.56), governing the pressure distribution, for the type of flow mentioned above, assumes the form

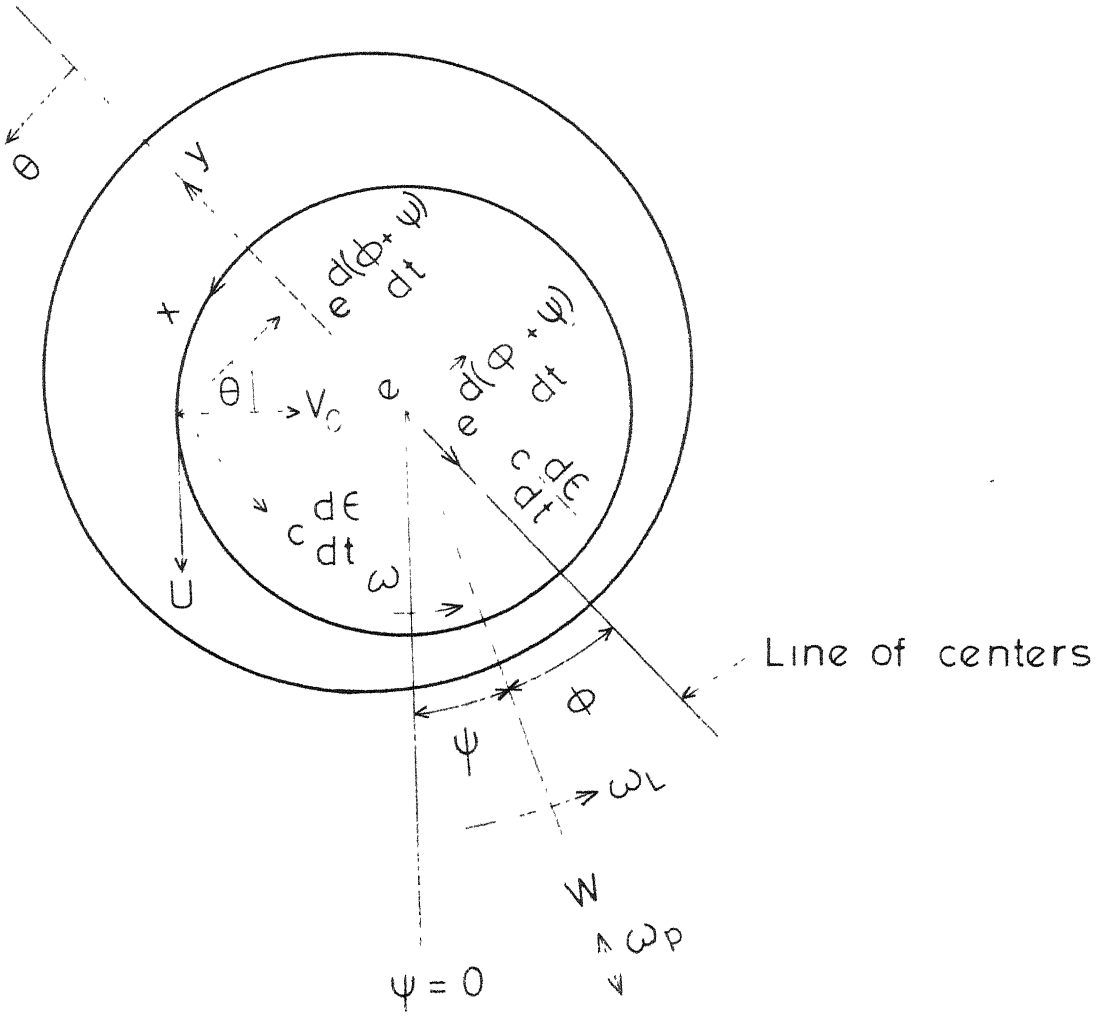

Fig. 4.1 Journal bearing configuration under dynamic loading

$$\frac{\partial}{\partial x}\left\{\frac{h^3}{\mu} f(N,\ell,h)\ \frac{\partial p}{\partial x}\right\} + \frac{\partial}{\partial z}\left\{\frac{h^3}{\mu} f(N,\ell,h)\ \frac{\partial p}{\partial z}\right\}$$

$$= \frac{U}{2}\frac{\partial h}{\partial x} + \frac{h}{2}\frac{\partial U}{\partial x} + V_o \qquad (4.1)$$

where N and ℓ are given by eqn. (2.18) and $f(N,\ell,h)$ is defined by eqn. (2.52).

The first term in the r.h.s. of eqn. (4.1) represents the action of the journal rotating with a velocity U over a wedge shaped fluid film given by $h(x)$, the second term implies a variation of tangential velocity along the bearing surface and the last term is the expression for velocity of the shaft centre and is responsible for squeeze film action.

Assuming the bearing to be fixed, the shaft centre will have instantaneous radial and tangential velocities. Referring to the vertical line $\psi = o$, those will be $c\frac{d\varepsilon}{dt}$ and $e\frac{d(\phi+\psi)}{dt}$. Thus U and V_o are given by

$$U = R\omega + c\frac{d\varepsilon}{dt}\sin\theta - c\varepsilon\frac{d(\phi+\psi)}{dt}\cos\theta \qquad (4.2)$$

and

$$V_o = c\frac{d\varepsilon}{dt}\cos\theta + c\varepsilon\frac{d(\phi+\psi)}{dt}\sin\theta \qquad (4.3)$$

Substituting for U and V_o in equation (4.1) and considering that, [85], $x = R\theta$, $\frac{c}{R} << 2$ and $\frac{e}{R}\cos\theta << 2$ and

$$2c\varepsilon \frac{d(\phi+\psi)}{dt} \sin\theta = -2\frac{d(\phi+\psi)}{dt} \frac{dh}{d\theta} \tag{4.4}$$

one obtains, the Reynolds equation for the general case of dynamic loading for micropolar fluids,

$$\frac{1}{R^2}\frac{\partial}{\partial\theta}\left\{\frac{h^3 f(N,\ell,h)}{\mu}\frac{\partial p}{\partial\theta}\right\} + \frac{\partial}{\partial z}\left\{\frac{h^3 f(N,\ell,h)}{\mu}\frac{\partial p}{\partial z}\right\}$$

$$= \frac{1}{2}\left[\left\{(\omega - 2\omega_L - 2\frac{d\phi}{dt})\frac{dh}{d\theta}\right\} + 2c\frac{d\varepsilon}{dt}\cos\theta\right] \tag{4.5}$$

For short journal bearings, eqn. (4.5) reduces to

$$\frac{d^2p}{dz^2} = \frac{\mu}{2h^3 f(N,\ell,h)}\left\{(\omega - 2\omega_L - 2\frac{d\phi}{dt})\frac{dh}{d\theta} + 2c\frac{d\varepsilon}{dt}\cos\theta\right\} \tag{4.6}$$

where ω is the angular velocity of the journal and $\omega_L\,(=\frac{d\psi}{dt})$ is the frequency of rotation of applied load.

Integrating eqn. (4.6) twice, using the boundary conditions

$$p(\pm\frac{L_o}{2}) = o \tag{4.7}$$

the pressure distribution is obtained as

$$p(\theta,z) = \frac{\mu}{4h^3 f(N,\ell,h)}\left\{(\omega - 2\omega_L - 2\frac{d\phi}{dt})\frac{dh}{d\theta} + 2c\frac{d\varepsilon}{dt}\cos\theta\right\}(z^2 - \frac{L_o^2}{4}) \tag{4.8}$$

The load component, $W_{\frac{\pi}{2}}$, normal to the line of centers is given by

$$W_{\frac{\pi}{2}} = W \sin\phi = 2 \int_{o}^{\frac{L_o}{2}} \int_{o}^{2\pi} p(\theta,z) \sin\theta R \, d\theta \, dz \tag{4.9}$$

Substituting the value of p and integrating, we get

$$W_{\frac{\pi}{2}} = W \sin\phi = -\frac{\mu\varepsilon c L_o^3 R}{24}(\omega - 2\omega_L - 2\frac{d\phi}{dt}) \int_{o}^{2\pi} \frac{\sin^2\theta . d\theta}{h^3 f(N,\ell,h)} \tag{4.10}$$

The load component, W_o, along the line of centers, is given by

$$W_o = W \cos\phi = -2 \int_{o}^{\frac{L_o}{2}} \int_{o}^{2\pi} p(\theta,z) \cos\theta R \, d\theta \, dz \tag{4.11}$$

which after simplification becomes

$$W_o = \frac{c\mu L_o^3 R}{12} \frac{d\varepsilon}{dt} \int_{o}^{2\pi} \frac{\cos^2\theta \, d\theta}{h^3 f(N,\ell,h)} \tag{4.12}$$

Equations (4.10) and (4.12) give a relation between the applied load and the motion of shaft center. In these equations W, ω and ω_L can be functions of time. This makes the integration of these equations more complicated, but, when accomplished this would, through the relation between ε and ϕ, yield the cyclic locus of the shaft center, as well as the instantaneous resultant hydrodynamic force.

(i) Cyclic Squeeze Films in Journal Bearings

In this section, the study is restricted to the particular case of dynamic loading, in which the journal does not rotate about its center but moves under a variable unidirectional load. The load vector is fixed in the space, and the shaft center follows a path determined by the nature of imposed load.

Here, since

$$\omega = \omega_L = 0 \tag{4.13}$$

we have from eqns. (4.10) and (4.12) that

$$W_{\frac{\pi}{2}} = W \sin\phi = \frac{\mu \varepsilon c L_o^3 R}{12} \frac{d\phi}{dt} \int_0^{2\pi} \frac{\sin^2\theta \, d\theta}{h^3 f(N,\ell,h)} \tag{4.14}$$

and

$$W_o = W \cos\phi = \frac{\mu c L_o^3 R}{12} \frac{d\varepsilon}{dt} \int_0^{2\pi} \frac{\cos^2\theta \, d\theta}{h^3 f(N,\ell,h)} \tag{4.15}$$

Dividing, we get

$$\frac{d\varepsilon}{d\phi} \tan\phi = \varepsilon \frac{f_1(\varepsilon)}{f_2(\varepsilon)} \tag{4.16}$$

where

$$f_1(\varepsilon) = \int_0^{2\pi} \frac{\sin^2\theta \, d\theta}{h^3 f(N,\ell,h)} \tag{4.17}$$

and

$$f_2(\varepsilon) = \int_0^{2\pi} \frac{\cos^2\theta \, d\theta}{h^3 f(N,\ell,h)} \tag{4.18}$$

Integrating (4.16), we get

$$\sin\phi = A \exp\left[\int \frac{d\varepsilon}{\varepsilon f_3(\varepsilon)}\right] \tag{4.19}$$

where A is the constant of integration and

$$f_3(\varepsilon) = \frac{f_1(\varepsilon)}{f_2(\varepsilon)} \tag{4.20}$$

Equation (4.19) describes the locus of the shaft centre under a unidirectional load, which depends upon the costant of integration A, determined by the initial position of the journal. Equation (4.19) is independent of load which shows that the journal centre once located on a given path will always remain there regardless of the magnitude and nature of the applied load. The effect of load will only be upon the amplitude and speed on that fixed path. The substitution of ϕ from eqn.(4.19) into either of the equations (4.14) and (4.15) would yield the relation between the load and eccentricity.

(ii) Bearing Response to Sinusoidal Loading

We now consider the case of shaft travelling along the vertical centre line(ϕ= o), with an oscillatory load.

$$W(t) = W_b \sin \omega_p(t) \tag{4.21}$$

where W_b is the amplitude of applied load and ω_p is the frequency of oscillation.

Equation (4.15) now becomes

$$W_b \sin\omega_p t = \frac{\mu c L_o^3 R}{12} \frac{d\varepsilon}{dt} \int_o^{2\pi} \frac{\cos^2\theta \, d\theta}{h^3 f(N,\ell,h)} \tag{4.22}$$

which after simplification becomes

$$\frac{d\varepsilon}{dt} = \frac{12 W_b \sin\omega_p t}{\mu R c L_o^3} \frac{1}{f_2(\varepsilon)} \tag{4.23}$$

Using the non-dimensional scheme

$$H = \frac{h}{c} = 1 + \varepsilon \cos\theta, \quad L = \frac{c}{\ell}, \quad T = \omega_p t = \frac{2\pi nt}{60}, \quad P_o = \frac{720 W_b}{L_o D} \tag{4.24}$$

and defining the Sommerfeld number, S, for an infinitely short bearing as

$$S\left(\frac{L_o}{D}\right)^2 = \frac{\mu n}{P_o}\left(\frac{L_o}{c}\right)^2 \tag{4.25}$$

eqn. (4.23) reduces to

$$\frac{d\varepsilon}{dT} = \frac{\sin T}{\pi S \left(\frac{L_o}{D}\right)^2 \bar{f}_2(2\pi)} \tag{4.26}$$

where, $D = 2R$, and

$$\bar{f}_2(2\pi) = \int_o^{2\pi} \frac{\cos^2\theta \, d\theta}{F(N,L,H)} \tag{4.27}$$

and

$$F(N,L,H) = \frac{1}{12} + \left(\frac{1}{LH}\right)^2 - \frac{N}{2LH} \coth \frac{NLH}{2} \tag{4.28}$$

Equations (4.26) and (4.27) are integrated numerically to yield the time variation of the eccentricity ratio over the region of T from o to 2π . The resulting response curves for various values of N,L and S are shown in Figs. 4.2 to 4.10. The value of $(\frac{L_o}{D})^2$ is taken to be o.o5.

4.4 RESULTS AND DISCUSSION

One of the most important bearing characteristics is the response time, i.e. the time that will elapse for an oil film to be reduced to some minimum value, say a value which may have been established as the thinnest permissible film for the safe performance of a particular bearing.

Figs. 4.2 to 4.4 illustrate the journal centre locus for various combinations of the micropolar parameters N and L and the Sommerfeld number S. The value of $(\frac{L_o}{D})^2$ is kept fixed $((\frac{L_o}{D})^2 = o.o5)$. For smaller values of N and larger values of L the effects are not significant . But for higher values of N and smaller values of L (where the micropolarity is significant) the effects are quite significant. This shows that the micropolarity causes the fluid to offer more resistance to journal motion, thereby allowing for smaller eccentricities (higher film thickness) for a constant load.

The velocity of approach, $d\varepsilon/dT$, is plotted against time, T, in Figs.4.5 to 4.7, over a half cycle. It can easily be seen

that the velocity of approach decreases for micropolar fluid for those values of T which are near to $\pi/2$, but for those values of T which are close to T = o or T = π, the trend is almost same. The velocity of approach is highest for a Newtonian fluid but for micropolar fluid this velocity decreases. Thus indicating an increased effective viscosity.

The maximum eccentricity ratio, ε_{max}, is a measure of minimum permissible film thickness, and thus its study is essential. The maximum eccentricity ratio is plotted against L in Fig. 4.8, against S in Figs. 4.9 and Fig. 4.10. In these figures it is seen that for larger values of N or smaller values of L, the maximum eccentricity ratio decreases. For the Newtonian case it is highest. It implies that the same amount of load is now being carried with a smaller eccentricity (or at a larger film thickness). This means that the system can be used to sustain much higher loads, or, conversely, the same load can be used for a longer period of time without any malfunctioning.

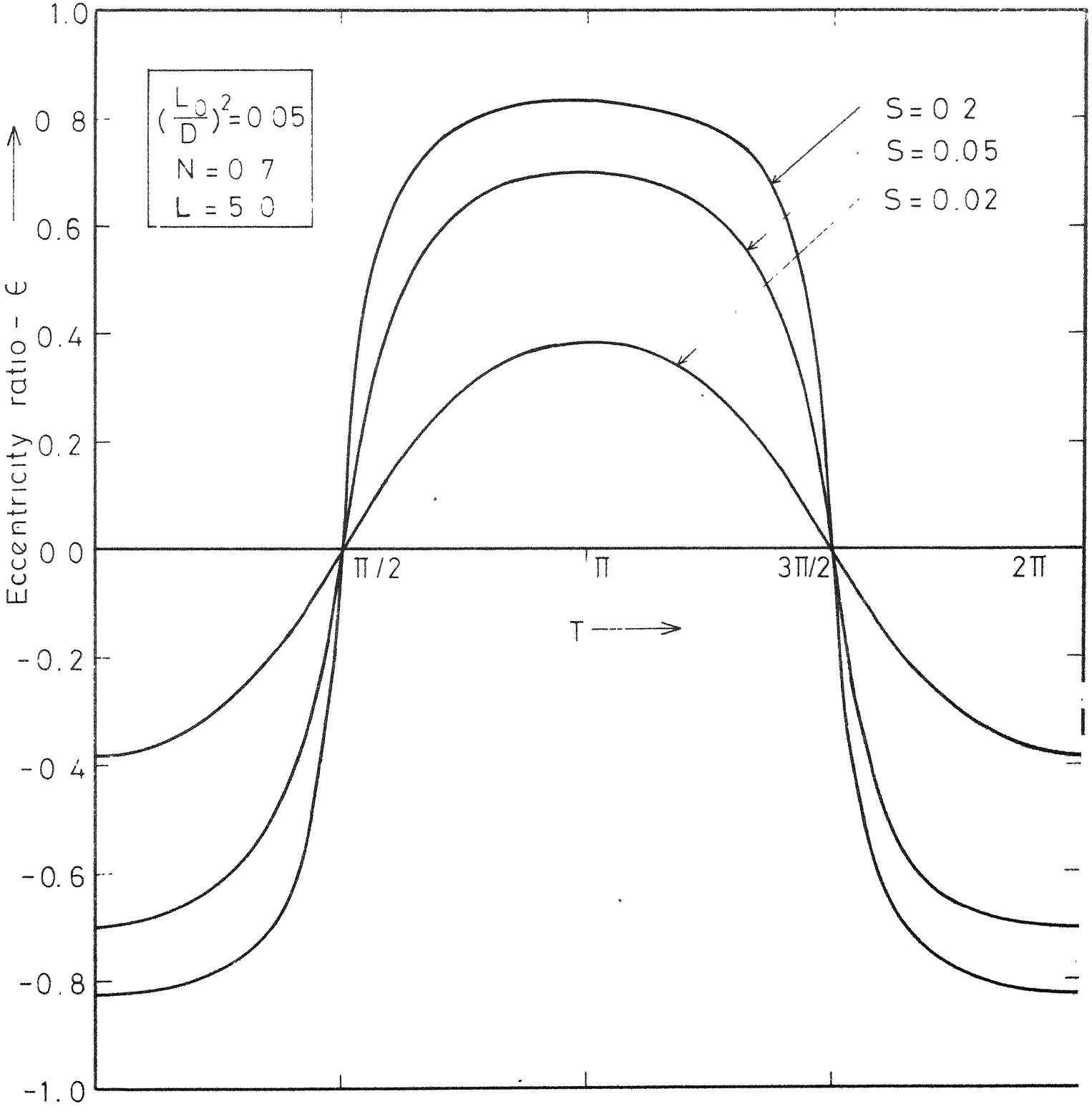

Fig 4 2 Path of the journal centre over one cycle of sine loading for various values of Sommerfeld number

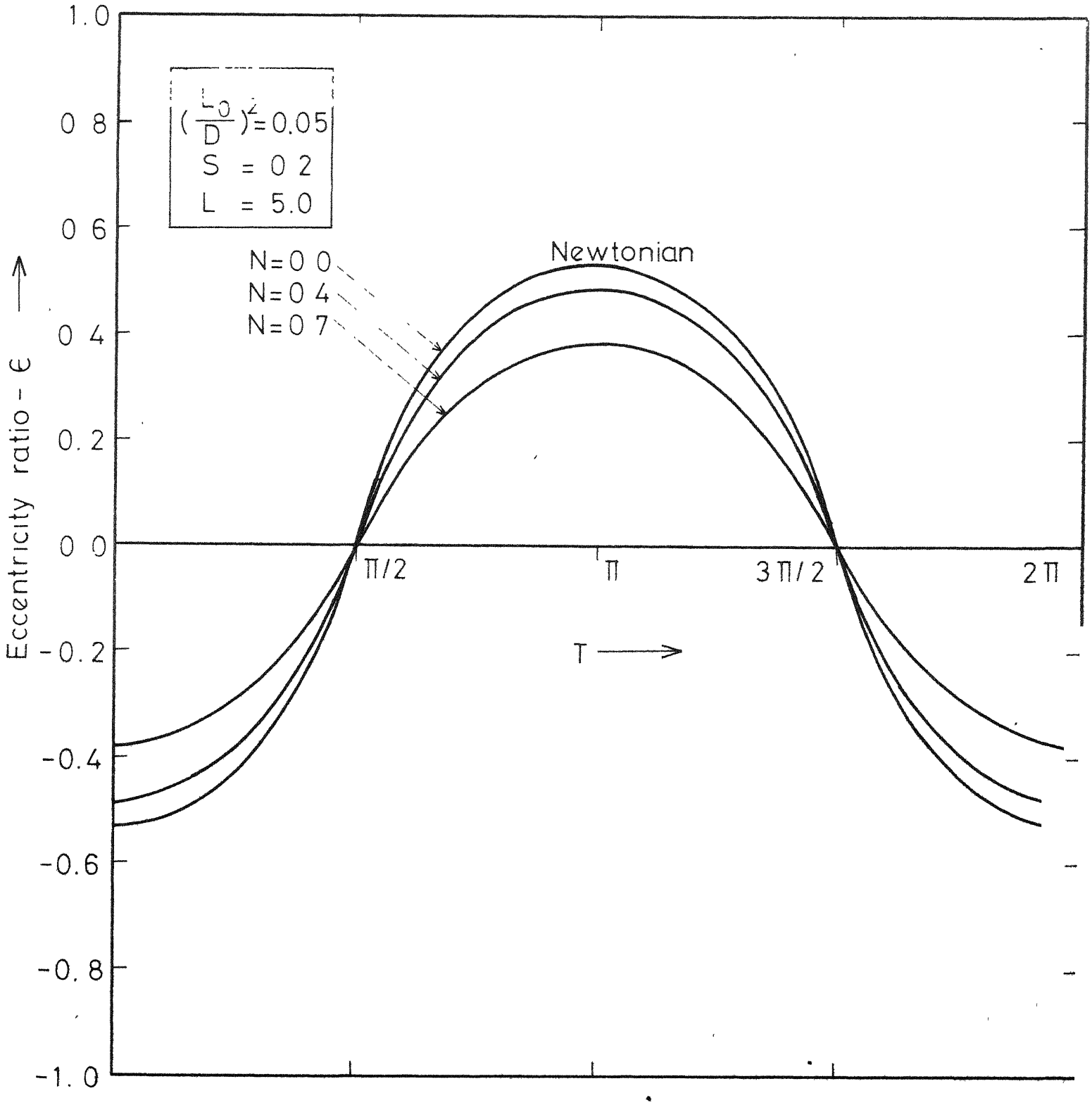

Fig 4.3 Path of the journal centre over one cycle of sine loading for various values of coupling number

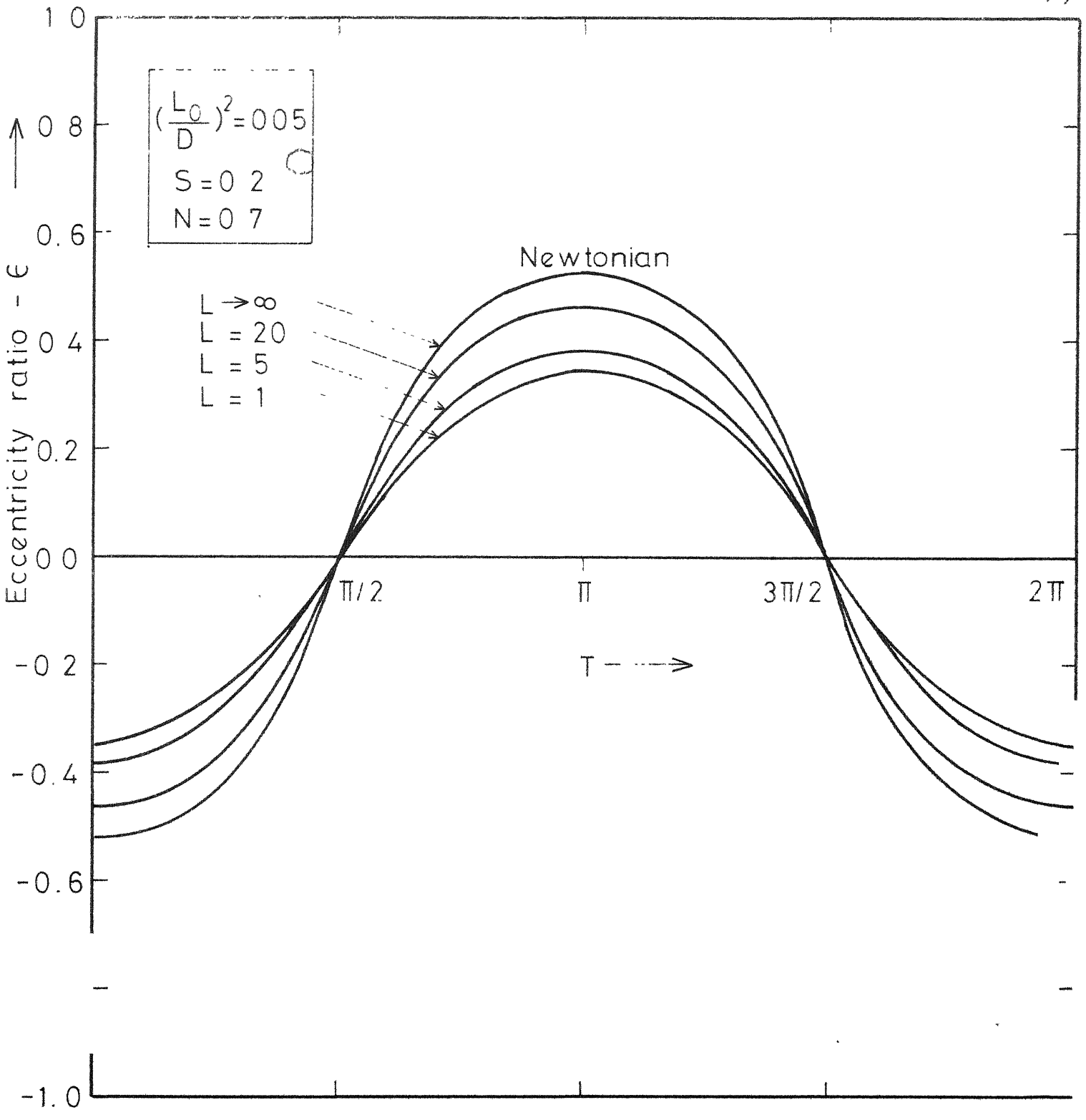

Fig. 4 4 Path of the journal centre over one cycle of sine loading for various values of length ratio

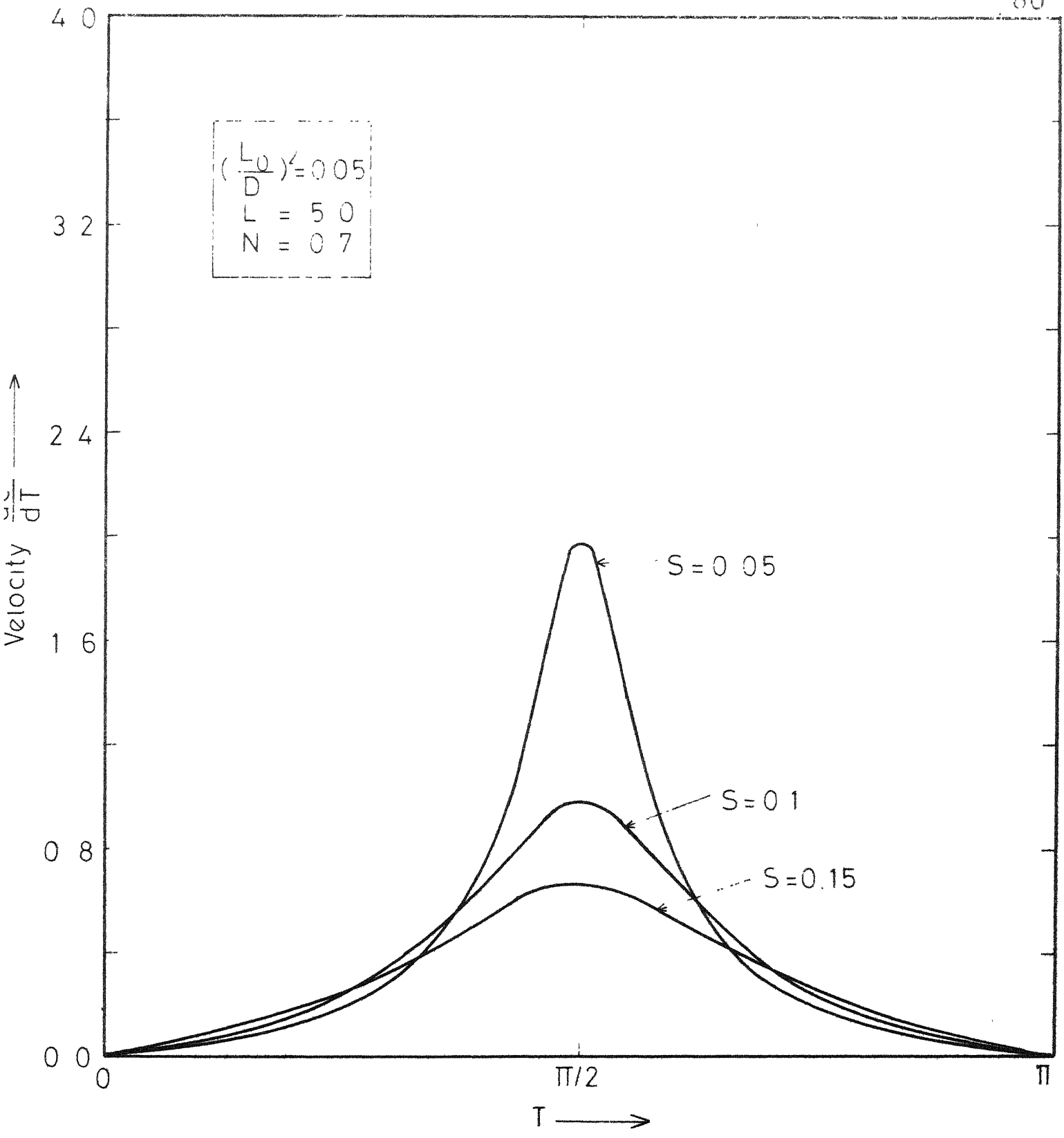

Fig 4 5 Velocity of journal centre over one half cycle of sine loading for various values of Sommerfeld number

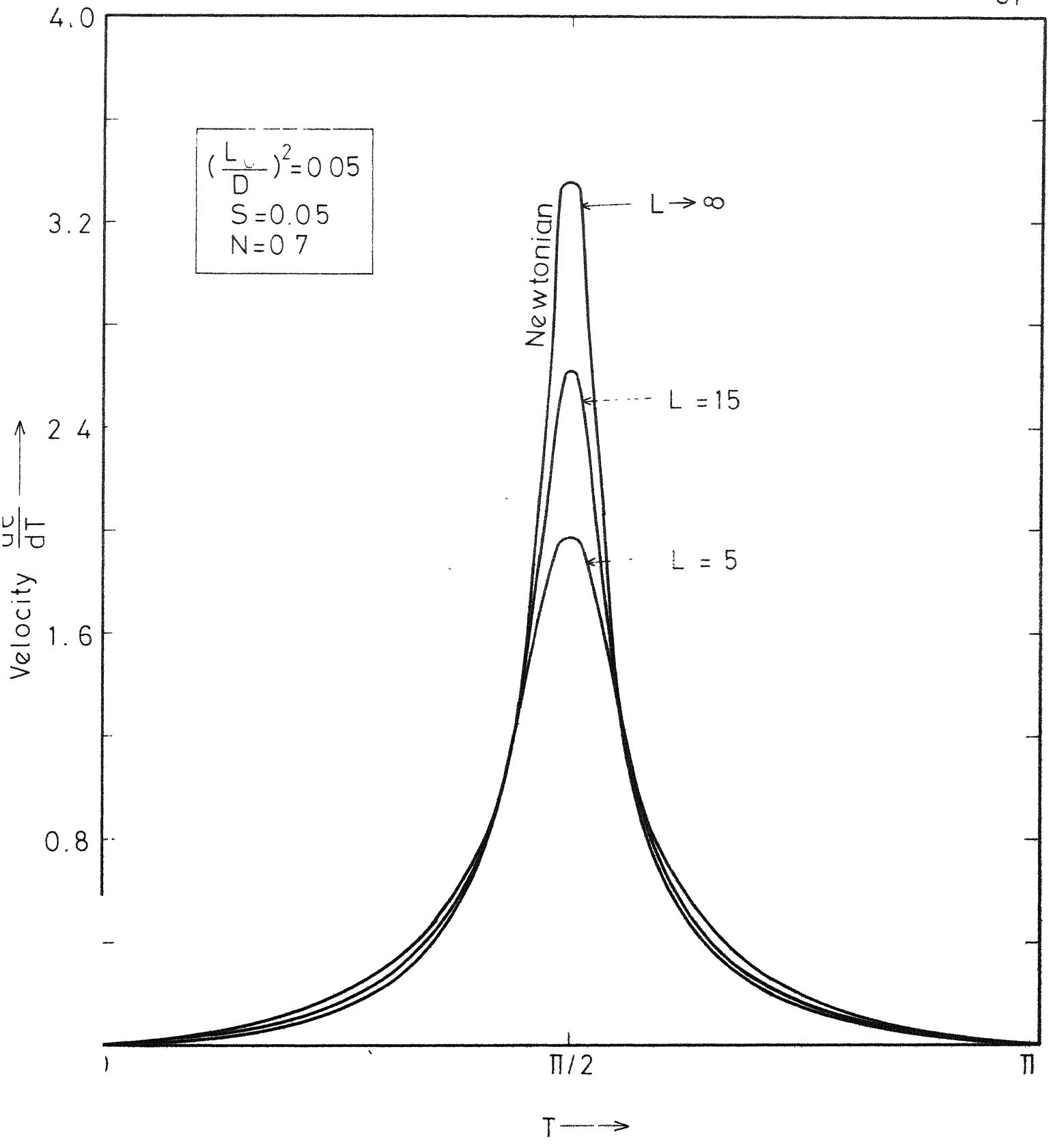

Fig. 4.6 Velocity of journal centre over one half cycle of sine loading for various values of length ratio.

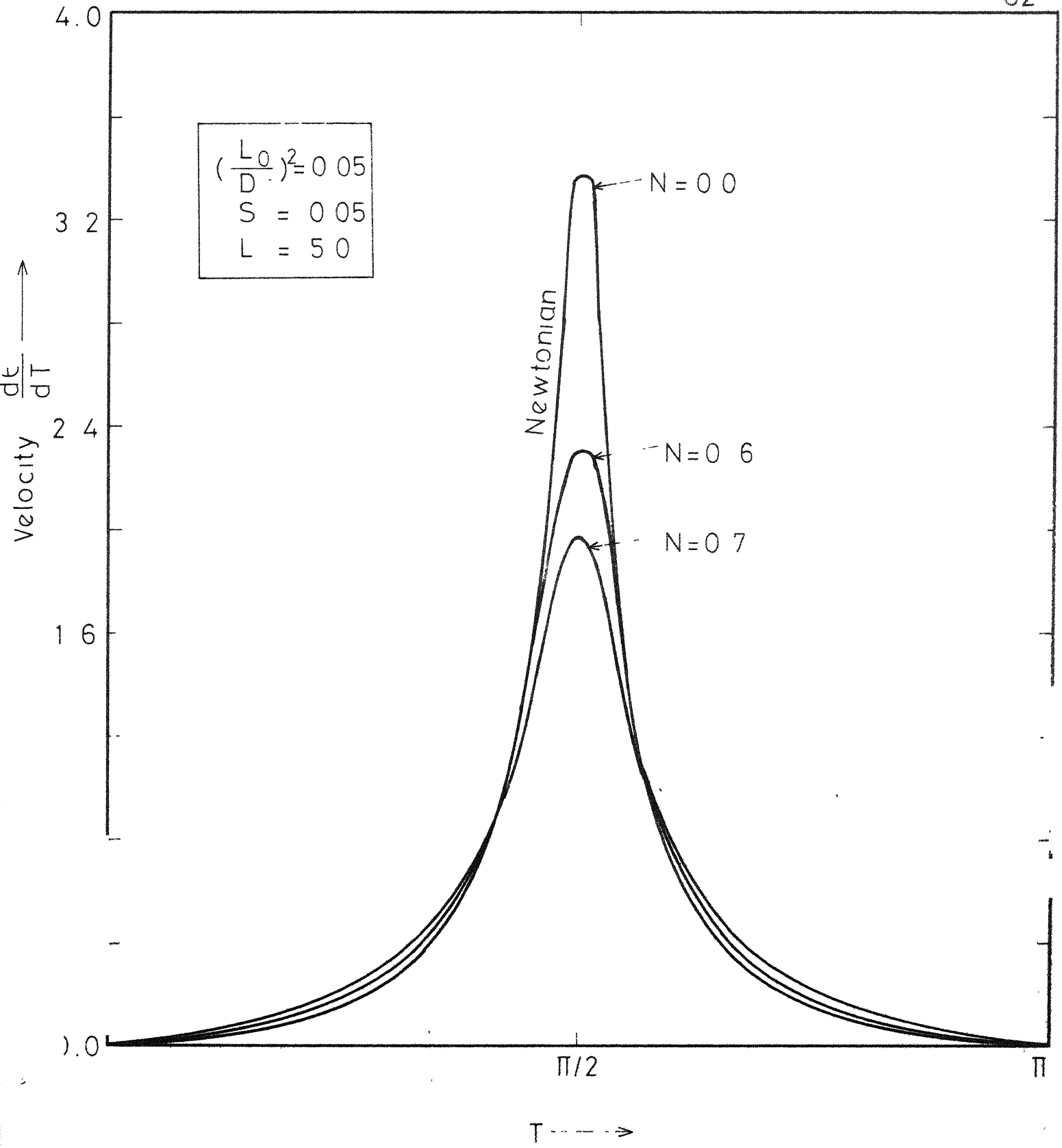

Fig 4.7 Velocity of journal centre over one half cycle of sine loading for various values of coupling number

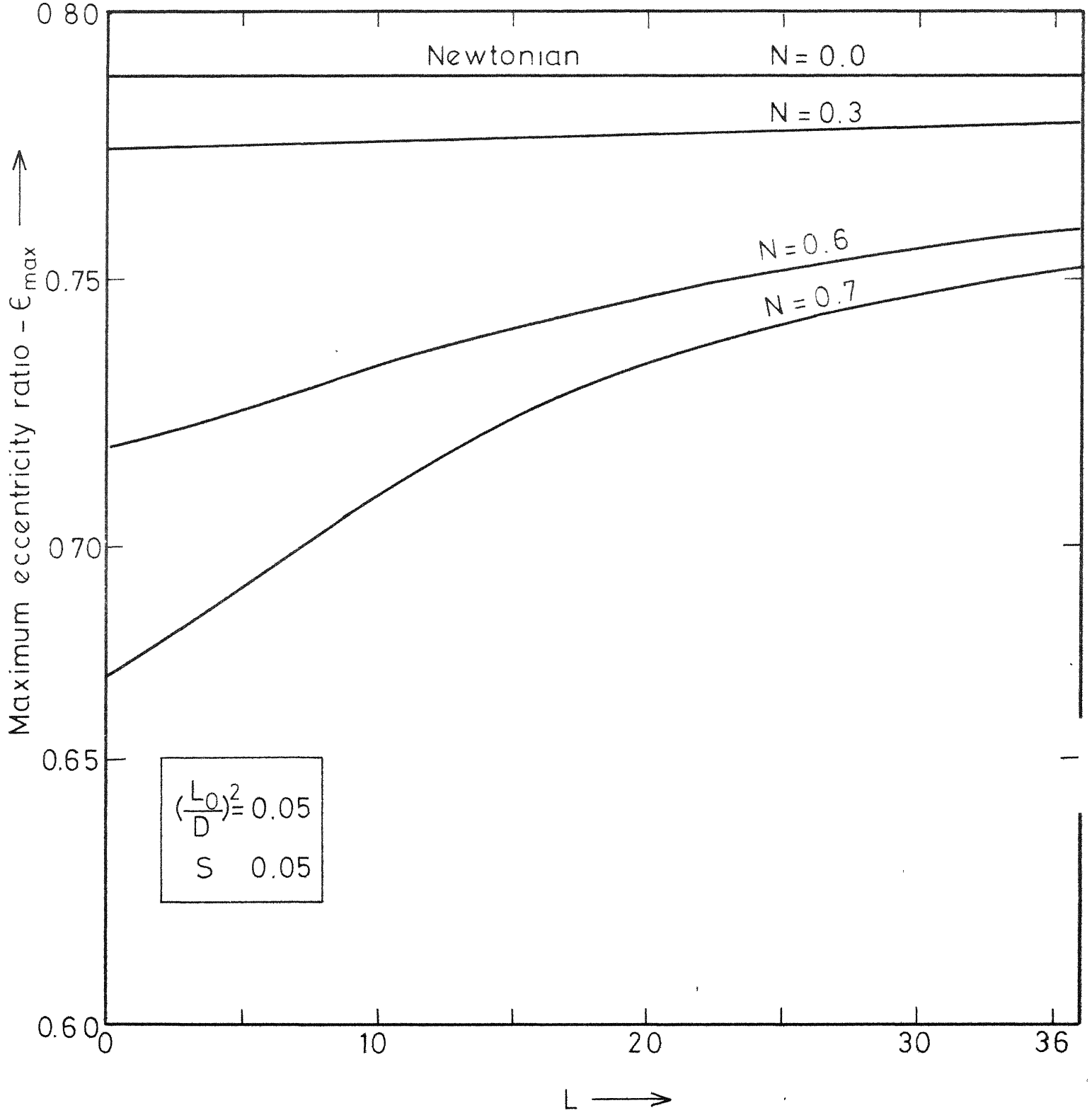

Fig 4.8 Maximum eccentricity ratio vs. length ratio for various values of coupling number

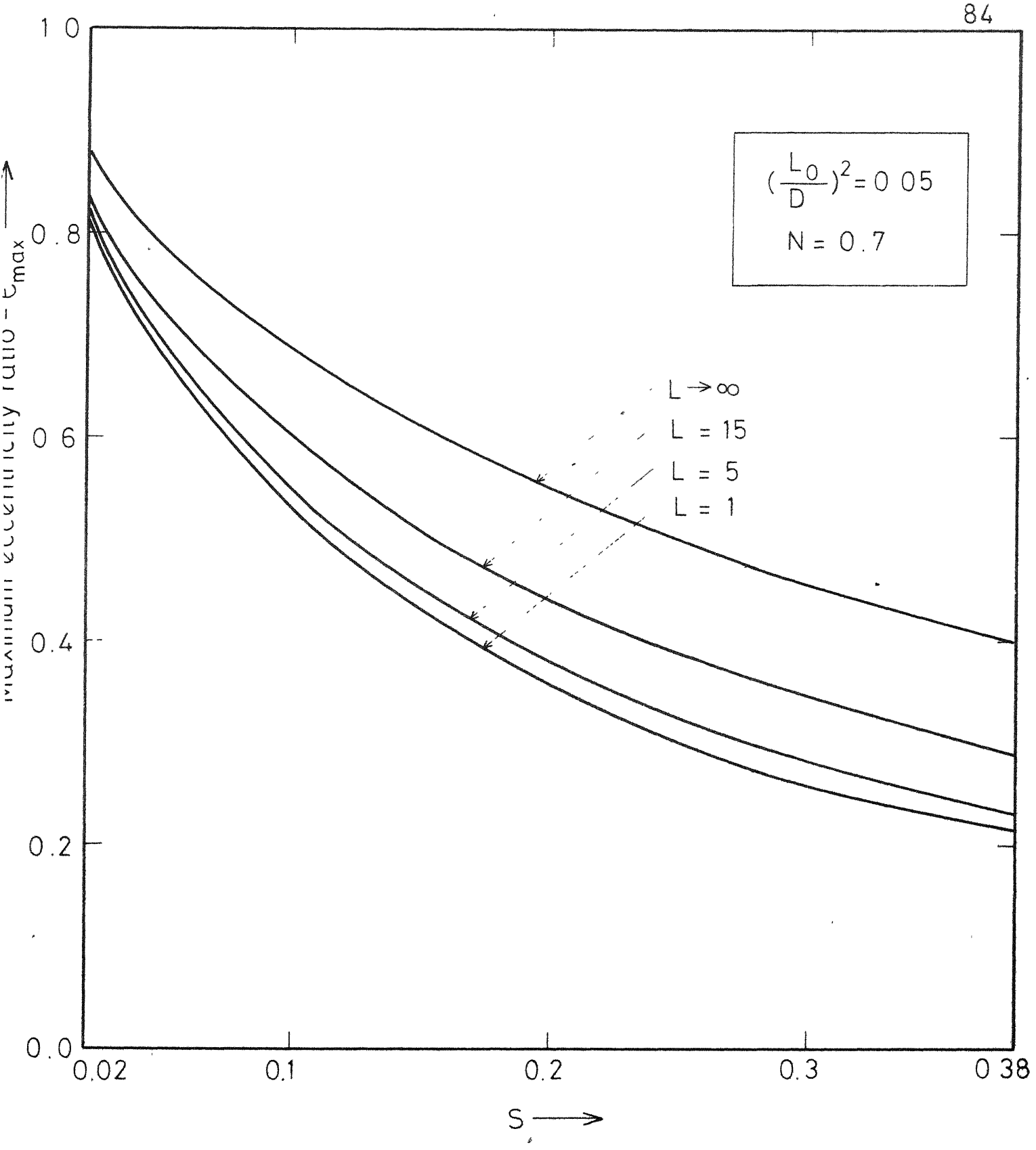

Fig. 4.9 Maximum eccentricity ratio Vs Sommerfeld number for various values of length ratio

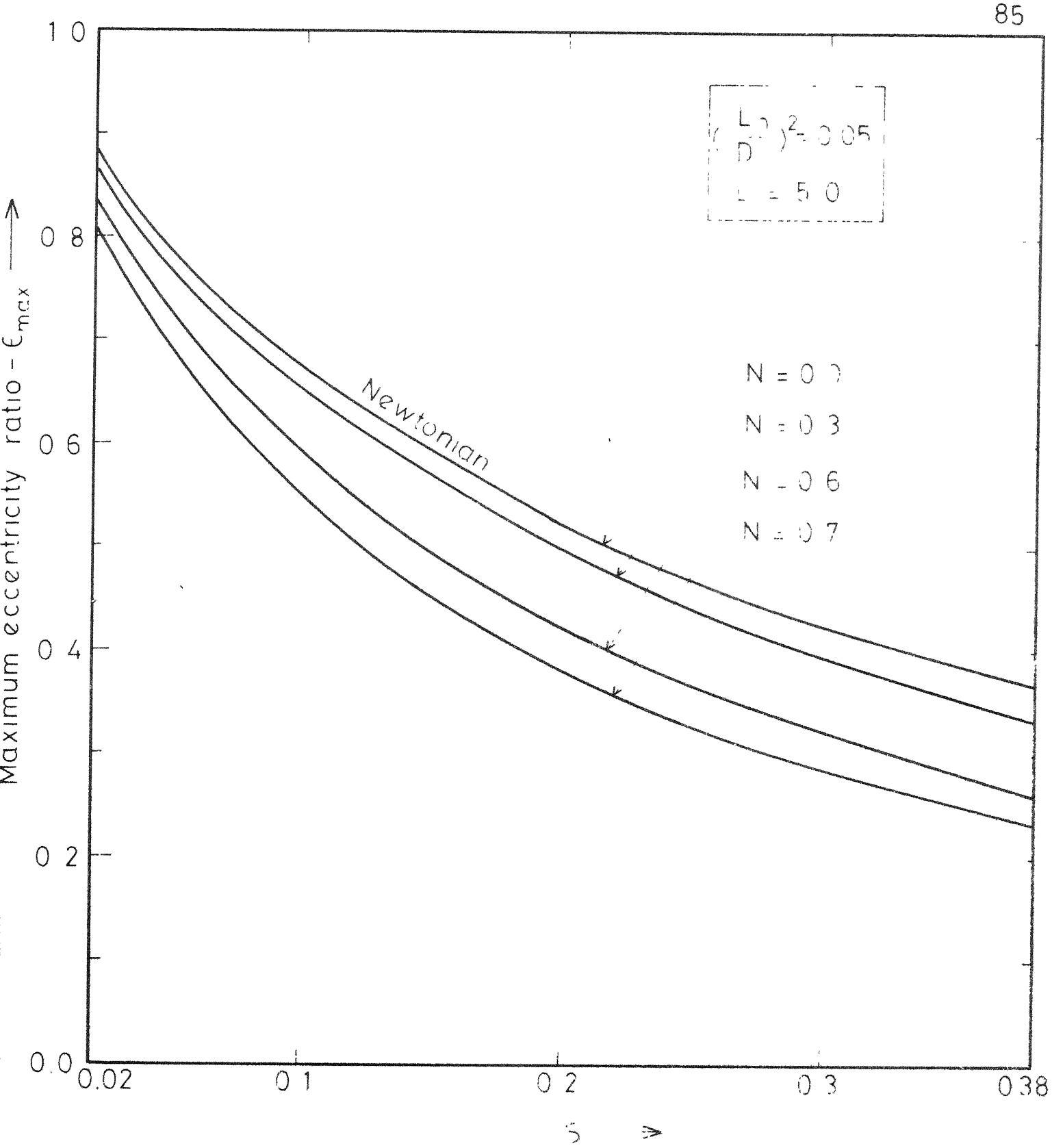

Fig 4 13 Maximum eccentricity ratio vs Sommerfeld number for various values of coupling number

CHAPTER V

LUBRICATION OF ROLLER BEARINGS IN COMBINED ROLLING, SLIDING AND NORMAL MOTION

5.1 INTRODUCTION

Thousands of papers on film lubrication have appeared since 1886 in the wake of Osborne Reynolds classical work on lubrication theory. In general, papers on film lubrication have extended the application of the fundamentals, as set forth by Reynolds, to a variety of bearing shapes with steady and transient films of variable density, viscosity and temperature.

In recent years a lot of attention has been directed towards the study of rolling element bearings. Considerable understanding of the bearing characteristics has been obtained through the studies of elastohydrodynamic lubrication, and for all practical cases theoretical solutions have been published.

Most of earlier work in lubrication have dealt with steady lubricating films in which there existed either an effective tangential surface velocity or a maximum film velocity due to an externally pressurized source. Unfortunately there are few instances where the film are completely steady. Usually there are transient or periodic forces or displacements imposed on the films. Changes in surface velocity result in tangential accelerations which can be important during starting and stopping. However, relative normal

surface motions are of far greater importance. The film must maintain sufficiently precise spacing in the presence of disturbance. Various authors have examined theoretically the bearing behaviour under normal, sliding or rotating motion separately. Sasaki et.al [90] were the first who studied the dynamic behaviour of roller bearing. However the boundary condition applied at the trailing end violates the continuity of flux. Dowson et. al. [91], later on, obtained a detailed theoretical solution of lightly loaded cylindrical bearings subjected to a combined rolling, sliding and normal motion applying a more realistic boundary condition at the film rupture point. A satisfactory agreement was found between theory and experiment [92] .

No attempt has so far been made to analyze this problem [91] from the microcontinuum view point. Thus it is felt that the present analysis may provide a better insight into the lubrication of such bearings when analyzed from microcontinuum point of view. Dowson's et.al. results [91] are obtained as a special case of the present study. It will also be shown that this theory may yield better fit to the experimental curves obtained by Markho and Dowson [92].

5.2 THE PROBLEM AND THEORETICAL ANALYSIS

The problem considered is that of the lubrication of lightly loaded cylinders in combined rolling, sliding and normal motion, with micropolar fluids. The fluid is assumed to be isoviscous. The geometry of the system and the coordinate system are shown in

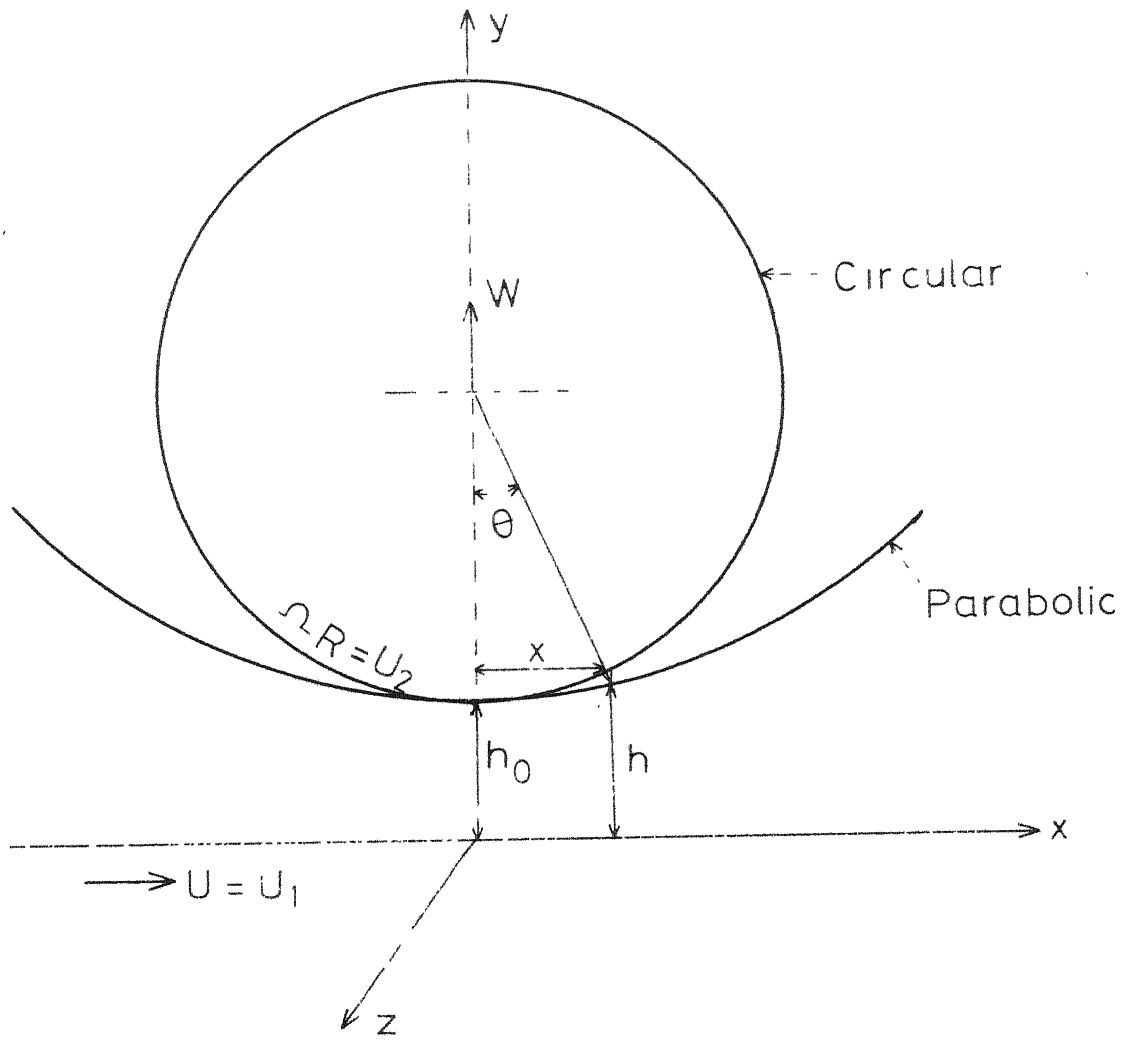

ig 5 1 Geometry , co-ordinate system and surface velocities for a lubricated cylinder near a plane

Fig.5.1.The two cylinders of radii R_1 and R_2, rolling with peripheral velocities U_1 and U_2, respectively, and approaching with a normal velocity V, are separated by a lubricant film of thickness h. The conventional representation of the system is a plane and a cylinder of radius R. Moreover, the circular cylinder can be approximated by a parabolic cylinder with the film thickness h given by [93]

$$h = h_o + \frac{x^2}{2R} \tag{5.1}$$

where

$$\frac{1}{R} = \frac{1}{R_1} + \frac{1}{R_2} \tag{5.2}$$

where h_o is the minimum separation of the oil film between the surfaces.

Assuming the cylinders to be infinitely long in the axial direction, the governing equation for a two dimensional flow field, from eqn. (2.56), is

$$\frac{d}{dx}\left\{h^3 f(N,\ell,h)\frac{dp}{dx}\right\} = \mu\left\{\frac{(U_1+U_2)}{2}\frac{dh}{dx} + V\right\} \tag{5.3}$$

where N and ℓ are given in (2.18) and $f(N,\ell,h)$ by eqn. (2.52). Integrating eqn. (5.3), using the condition

$$\frac{dp}{dx} = o, \text{ at } x = x_m \text{ or } h = h_m = h_o + \frac{x_m^2}{2R} \tag{5.4}$$

the pressure gradient is obtained as

$$\frac{dp}{dx} = \frac{\mu}{h^3 f(N,\ell,h)} \left\{ \frac{U_1+U_2}{2} \left(\frac{x^2-x_m^2}{2R}\right) + V(x-x_m) \right\} \tag{5.5}$$

Non-dimensionalizing, using

$$X = \frac{x}{(2Rh_o)^{1/2}}, \quad X_m = \frac{x_m}{(2Rh_o)^{1/2}}, \quad H = \frac{h}{h_o} = 1 + X^2,$$

$$H_m = 1 + X_m^2, \quad L = \frac{h_o}{\ell}, \quad P = \frac{2ph_o^2}{\mu(U_1+U_2)\sqrt{2Rh_o}},$$

$$q = \frac{V\sqrt{2Rh_o}}{h_o(U_1+U_2)} \tag{5.6}$$

$$\frac{dP}{dX} = \frac{(X^2-X_m^2) + 2q(X-X_m)}{H^3 F(N,L,H)} \tag{5.7}$$

where

$$F(N,L,H) = \frac{1}{12} + \frac{1}{(LH)^2} - \frac{N}{2LH} \coth \frac{NLH}{2} \tag{5.8}$$

Equation (5.7) can be written as

$$\frac{dP}{dX} = \frac{(X-X_m)\ (X+X_m+2q)}{H^3 F(N,L,H)} \tag{5.9}$$

Equation (5.9) shows that the pressure gradient falls to zero at $X = X_m$ and $X = -X_m-2q$. If the latter point is taken at the point of maximum pressure, then at the trailing end

$$P = \frac{dP}{dX} = o \qquad \text{at } X = X_m \tag{5.10}$$

Condition (5.10) is the Swift-Stieber boundary condition applicable when $|q| < 1$ [91] .

The other boundary condition depends on the oil flow through the wedge. If the oil supply is enough and the weight of the oil is neglected, the pressure build up will begin at the start of the wedge, where $X = -\infty$. This is the inlet boundary condition for the pressure, i.e.

$$P = o \qquad \text{at} \quad X = -\infty \tag{5.11}$$

Integrating eqn. (5.9) for the pressure distribution, we have

$$P(X) = \int_{-\infty}^{X} \frac{(2q+X+X_m)\,(X-X_m)\;dX}{H^3 F(N,L,H)} \tag{5.12}$$

The point X_m can be determined using $P(X_m) = o$, i.e.

$$\int_{-\infty}^{X_m} \frac{(2q+X+X_m)\,(X-X_m)\,dX}{H^3 F(N,L,H)} = o \tag{5.13}$$

Solving eqn. (5.13) we can find the values of X_m for different values of the parametersN,L and q.

The load capacity per unit length is

$$W = \int_{-\infty}^{x_m} p\;dx = -\int_{-\infty}^{x_m} x\;\frac{dp}{dx}\;dx \tag{5.14}$$

or, the non-dimensional load capacity is

$$\bar{W} = \frac{2Wh_o^2}{\mu(U_1+U_2)\, R\sqrt{2Rh_o}} = -\int_{-\infty}^{X_m} X \frac{dP}{dX}\, dX \tag{5.15}$$

The shear stresses acting on the plane (y = o) and cylinder (y = h), in regions where oil is filled, are given by eqn. (2.59),

$$\tau_{o,h} = -\frac{h}{2}\frac{dp}{dx} \mp \frac{\mu(U_1-U_2)}{hg(N,\ell,h)} \tag{5.16}$$

where $g(N,\ell,h)$ is defined by eqn. (2.61). In the cavitated region the mean shear stress is [94]

$$\tau_c = \mp \frac{h_m}{h^2} \frac{\mu(U_1-U_2)}{g(N,\ell,h)} \tag{5.17}$$

The surface tractions are

$$F_{1,2} = \int_{-\infty}^{X_m} \left\{ -\frac{h}{2}\frac{dp}{dx} \mp \frac{\mu(U_1-U_2)}{hg(N,\ell,h)} \right\} dx \mp (U_1-U_2)\, h_m \int_{X_m}^{\infty} \frac{dx}{h^2 g(N,\ell,h)} \tag{5.18}$$

or, in non-dimensional form

$$\bar{F}_{1,2} = \frac{2h_o F_{1,2}}{\mu(U_1+U_2)\sqrt{2Rh_o}} = -\int_{-\infty}^{X_m} \frac{1}{2} H \frac{dP}{dX}\, dX$$

$$\mp J\left[\int_{-\infty}^{X_m} \frac{dX}{HG(N,L,H)} + H_m \int_{X_m}^{\infty} \frac{dX}{H^2 G(N,L,H)} \right] \tag{5.19}$$

where

$$G(N,L,H) = 1 - \frac{2N}{LH}\tanh\frac{NLH}{2}, \quad J = \frac{2(U_1-U_2)}{U_1+U_2} \tag{5.20}$$

These surface tractions are put in the form

$$\bar{F}_1 = -[B_F + J C_F] \tag{5.21}$$

$$\bar{F}_2 = -[B_F - J C_F] \tag{5.22}$$

where

$$B_F = \int_{-\infty}^{X_m} \frac{(2q+X+X_m)(X-X_m)}{2H^2 F(N,L,H)}\, dX \tag{5.23}$$

$$C_F = \int_{-\infty}^{X_m} \frac{dX}{HG(N,L,H)} + H_m \int_{X_m}^{\infty} \frac{dX}{H^2 G(N,L,H)} \tag{5.24}$$

The coefficient of friction on the plane is

$$\left(\frac{h_o}{R}\right) \mu_f = \frac{\bar{F}_1}{\bar{W}} \tag{5.25}$$

The numerical solution consists of first solving the equation (5.13) to get the values of X_m for different parameters ; N, L, and q. The equation is solved using Regula falsi method within an appropriate accuracy where the infinite limit has been replaced by a finite but large quantity. (i.e. $-\infty$ is replaced by -10). A comparison is made between the solutions for the steady state case ($q = o$) with the non-steady case ($q \neq o$). For this purpose some ratios for different bearing characteristics are defined.

(i) Location of the Film Rupture or Cavitation Point (X_m)

Let

$$X_{m_R} = \frac{X_m}{(X_m)_{q=o}} \tag{5.26}$$

where X_m represents the general point in which q can take any accepted values and $(X_m)_{q=o}$ is the point of cavitation for sliding or rolling case. For the same minimum film thickness, X_{m_R} is a function of micropolar parameters N and L, and the velocity parameter q.

(ii) Location of Line of Maximum Pressure

It has been already pointed out that if X_m represents the point of cavitation then the expression for determining point of maximum pressure X_{m_p}, say, can be found as

$$X_{m_p} = - 2q - X_m \tag{5.27}$$

and thus the nature of this line would be same. Defining

$$X_{m_{pR}} = \frac{X_{m_p}}{(X_{m_p})_{q=o}} \tag{5.28}$$

where q = o represents the steady state case, $X_{m_{pR}}$ will be a function of N, L and q.

(iii) The Maximum Pressure

Let

$$P_{m_R} = \frac{P_m}{(P_m)_{q=o}} \tag{5.29}$$

where $(P_m)_{q=o}$ is the value of maximum pressure under pure rolling or sliding case for the same instantaneous value of the minimum film thickness, i.e. h_o. This is also seen to be a function of N, L and q.

(iv) Instantaneous Load Carrying Capacity and Surface Tractions

$$\bar{W}_R = \bar{W}/(\bar{W})_{q=o} \tag{5.30}$$

and

$$\bar{F}_{R_1} = \frac{B_F}{(B_F)_{q=o}} \tag{5.31}$$

$$\bar{F}_{R_2} = \frac{C_F}{(C_F)_{q=o}} \tag{5.32}$$

where the term $(\ )_{q=o}$ represents the steady state case, then it can be seen that the functions $\bar{W}_R$, $\bar{F}_{R_1}$ and $\bar{F}_{R_2}$ are dependent on N, L and q.

The numerical solutions have been given for the point of cavitation, the instantaneous load carrying capacity and surface tractions. To have a better insight of the present analysis the pressure distribution, load carrying capacity and coefficient of friction are presented in non-dimensional forms for different values of N, L and q and compared with the Newtonian case (N = o or $L \to \infty$).

5.3 RESULTS AND DISCUSSION

(i) Dimensionless Parameters :

Apart from the micropolar parameters N and L, one more important parameter is encountered in the present study, i.e. the velocity ratio parameter, q, defined by

$$q = \frac{V}{U_1+U_2}\sqrt{2\frac{R}{h_o}} \tag{5.33}$$

which determines the qualitative behaviour of a roller bearing when subjected to a combined rolling, sliding and normal motion. Positive values of q indicate a situation when the surfaces are moving apart normally and negative values signify an approaching case. Numerical solutions have been presented for $-0.9 < q \leq 0.9$, since, it has been pointed out by Dowson [92], that the cavitation occurs for $|q| < 1$.

(iii) Bearing Characteristics :

Non-dimensional pressure distribution curves are shown in Fig. 5.2 for different values of velocity ratio parameter q and the micropolar parameter N for a fixed L. Micropolar curves are shown by dotted lines. From these curves it is seen that the approaching normal velocity (q negative) results in a stronger pressure generation while the separation (q positive) leads to a weaker pressure. The micropolarity ofthe fluid increases the pressure at corresponding points as compared to the Newtonian fluid (N = 0.0).

Non-dimensional load capacity $\bar{W}$ is plotted against the length parameter L for different coupling numbers N and velocity ratio parameter q in Fig. 5.3. It is clearly seen that as L increases the load capacity decreases and its value is seen to approach the Newtonian one for different values of q. For the fixed value of L the load capacity is higher for larger values of N and it is least at N = o.o (which corresponds to the Newtonian case [91] for the corresponding value of q). A similar conclusion can be drawn regarding the parameter q. For negative values of q the load capacity is higher and for positive values of q it is smaller. When the normal motion disappears (q = o), we get the case of pure rolling and sliding.

The variation of the load parameter ratio $\bar{W}_R$ with the modulus of the dimensionless velocity ratio q is shown in Fig. 5.4. for different values of the micropolar parameter N. This figure depicts that the effects of micropolarity are higher for higher values of $|q|$. The parameter $\bar{W}_R$, in case of normal approach, increases as q and N increase and decreases as these decrease (Fig. 5.4). The figure also shows that the load capacity is higher when the surfaces approach each other and it increases as the rate of approach increases or the micropolar parameter N increases. In case of separation the phenomenon is reversed.

The frictional drag parameters $\bar{F}_{R_1}$ and $\bar{F}_{R_2}$, as a function of

N, L and q have been drawn in Fig. 5.5. An interesting feature of these curves is the graph for $\bar{F}_{R_2}$ when the surfaces are either in normal approach or normal separation. It is seen that the parameter $\bar{F}_{R_2}$ first decreases and then increases when the surfaces are moving apart for all values of micropolar parameters. But when the surfaces are in normal approach the function $\bar{F}_{R_2}$ increases slowly. The use of micropolar fluid is seen to reduce this factor. The qualitative behaviour of the parameter $\bar{F}_{R_1}$ is the same as that of load parameter.

The coefficient of friction $(R/h_o)\mu_f$ is plotted against the length parameter L for different values of the coupling number N in Fig. 5.6 ($q = -0.5$), Fig. 5.7 ($q = 0.0$) and Fig. 5.8 ($q = 0.25$). The value of $\bar{J} = \frac{2(U_1-U_2)}{U_1+U_2}$ is taken to be 0.5 in all these three cases. It is seen that the coefficient of friction reduces to the value predicted by the classical lubrication theory for all three limiting cases ($L \to 0$, $L \to \infty$, and $N \to 0$). It is seen that as the coupling number N increases the departure of the coefficient of friction from the classical theory becomes more conspicuous. The most interesting aspect of these curves is the fact that the coefficient of friction decreases rather sharply as L increases from 0 to approximately 10. The minimum value of μ_f is a function of L and N which can be seen directly from the graphs. This observation is true for the case of normal approach and sliding or rolling. It can be also seen that as q decreases from +0.25 (Fig. 5.8) to -0.5 (Fig.5.6)

for fixed value of the coupling number N, the minimum values of coefficient of friction are obtained for smaller values of the length parameter L. Fig. 5.8 is the graph of coefficient of friction in case of separation of surfaces. A peculiar behaviour of coefficient of friction is seen for this case. As L increases the coefficient of friction first increases and attains a maximum value for a fixed coupling number and then decreasesrapidly and reaches a minimum values (a value which is always lesser than Newtonian one) and then increases again slowly. The behaviour is more significant for higher value of N.

Fig. 5.9 is the graph for point of cavitation $\bar{X}_m$ vs. the velocity parameter q. It is seen that as q decreases the point of cavitation increases. The point of cavitation for pure rolling or sliding case is obtained at q = o.o. In case of micropolar fluids the cavitation process is accelerated, i.e. it starts a little earlier.

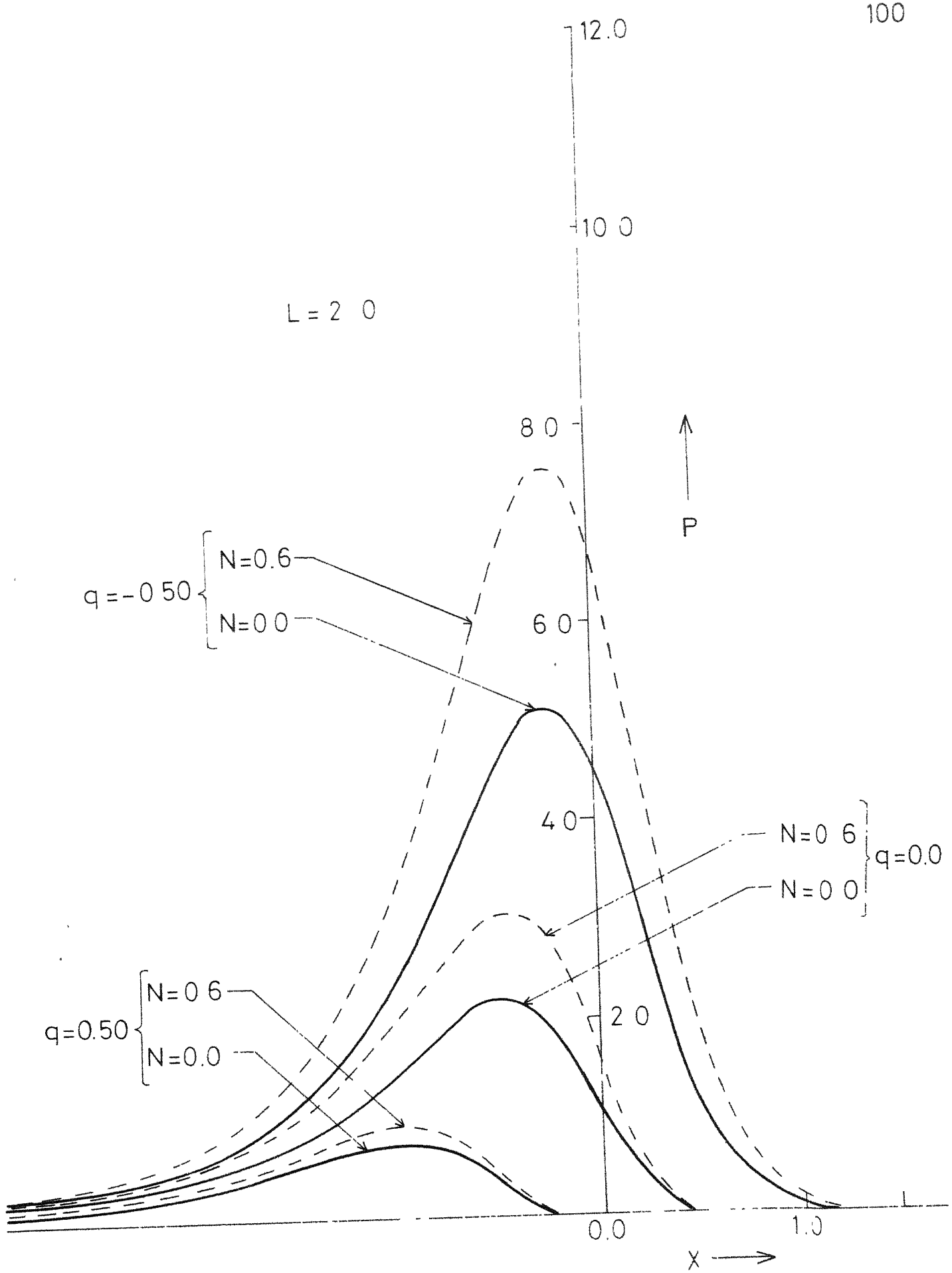

Fig. 5 2 Dimensionless pressure distribution P as a function of the dimensionless velocity ratio q for different coupling number N

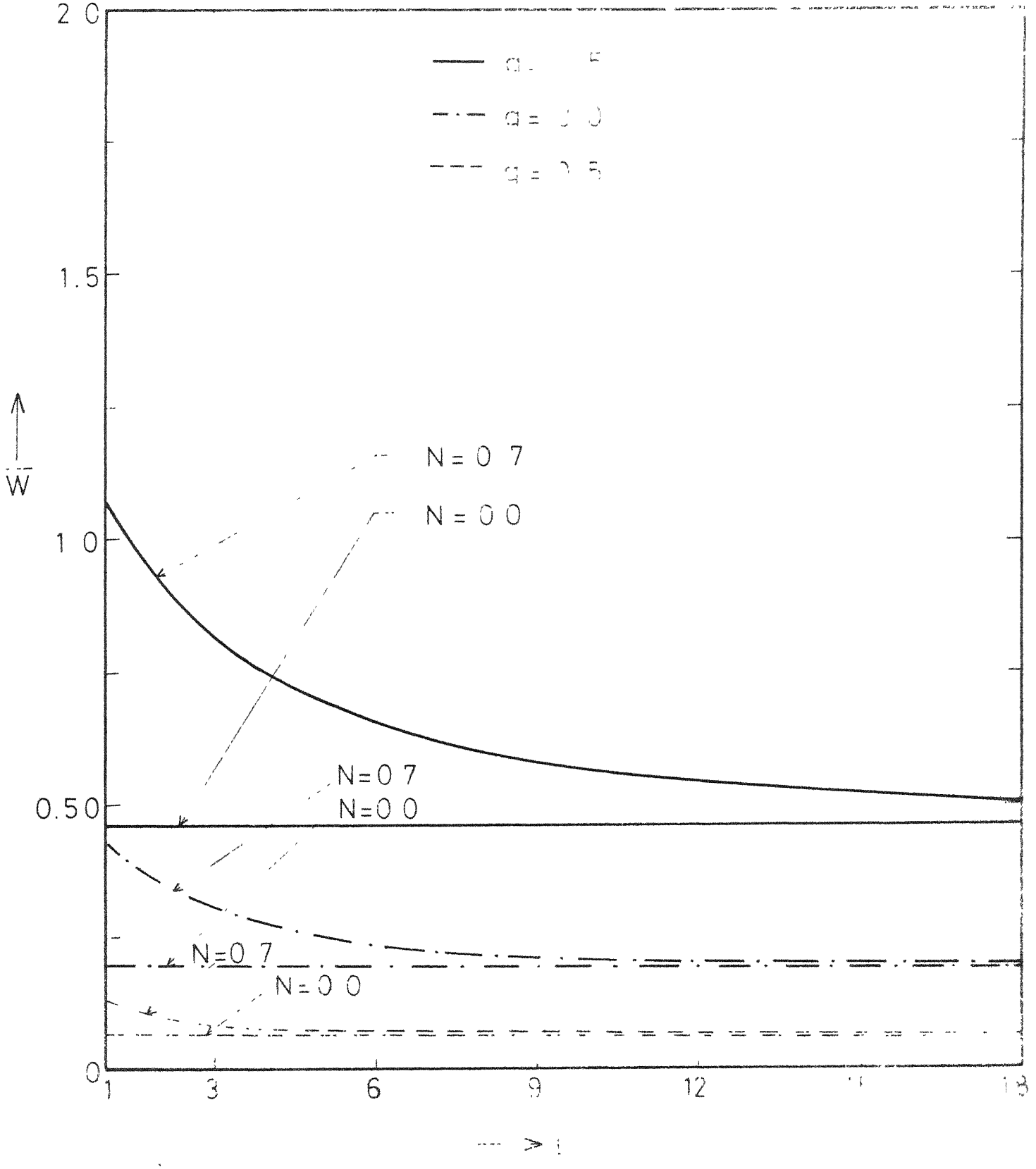

Fig 5 3 Non-dimensional load capacity [illegible] values of q and N

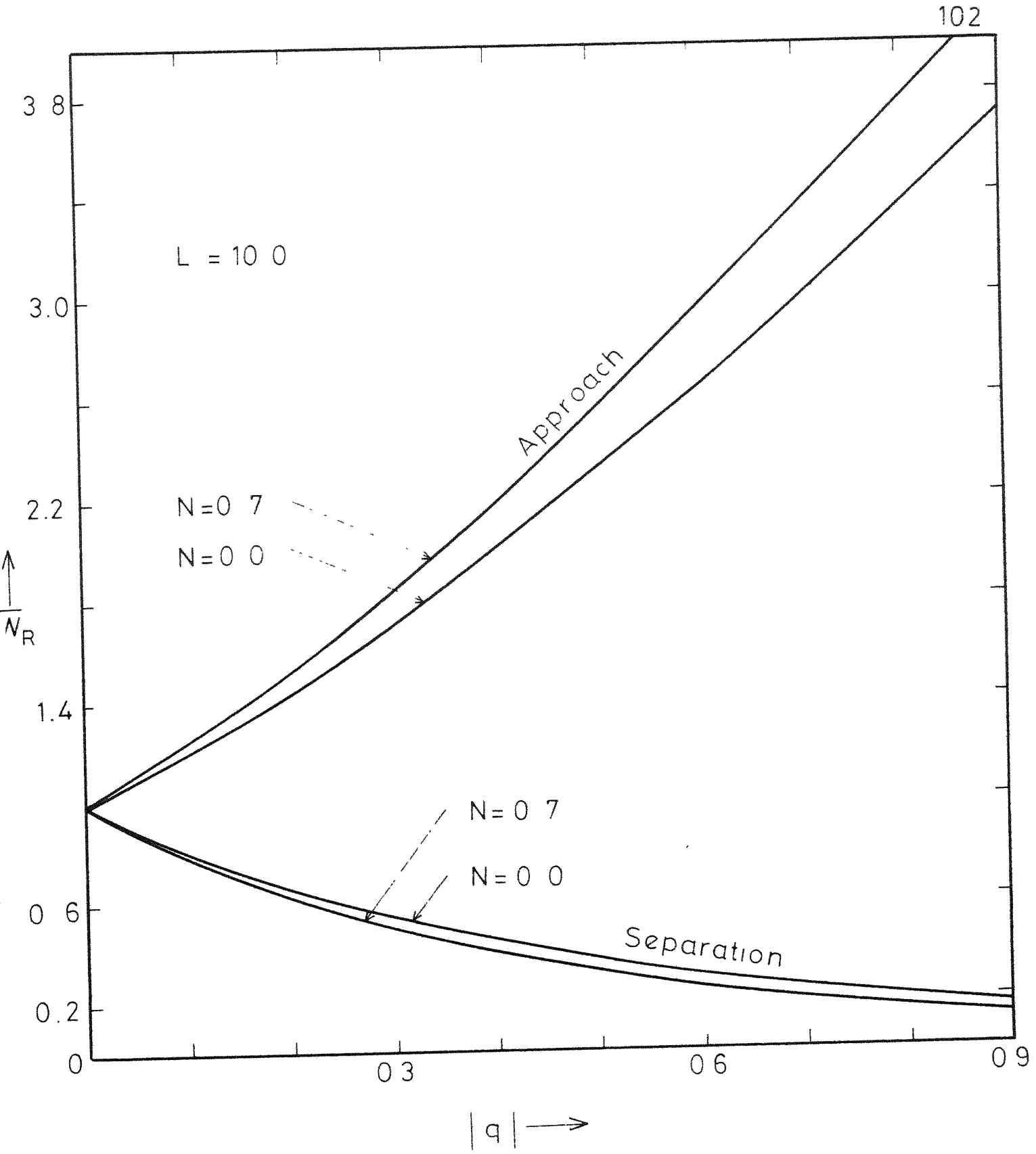

Fig 5 4 Load capacity ratio parameter $\overline{W}_R$ vs |q| for different values of N

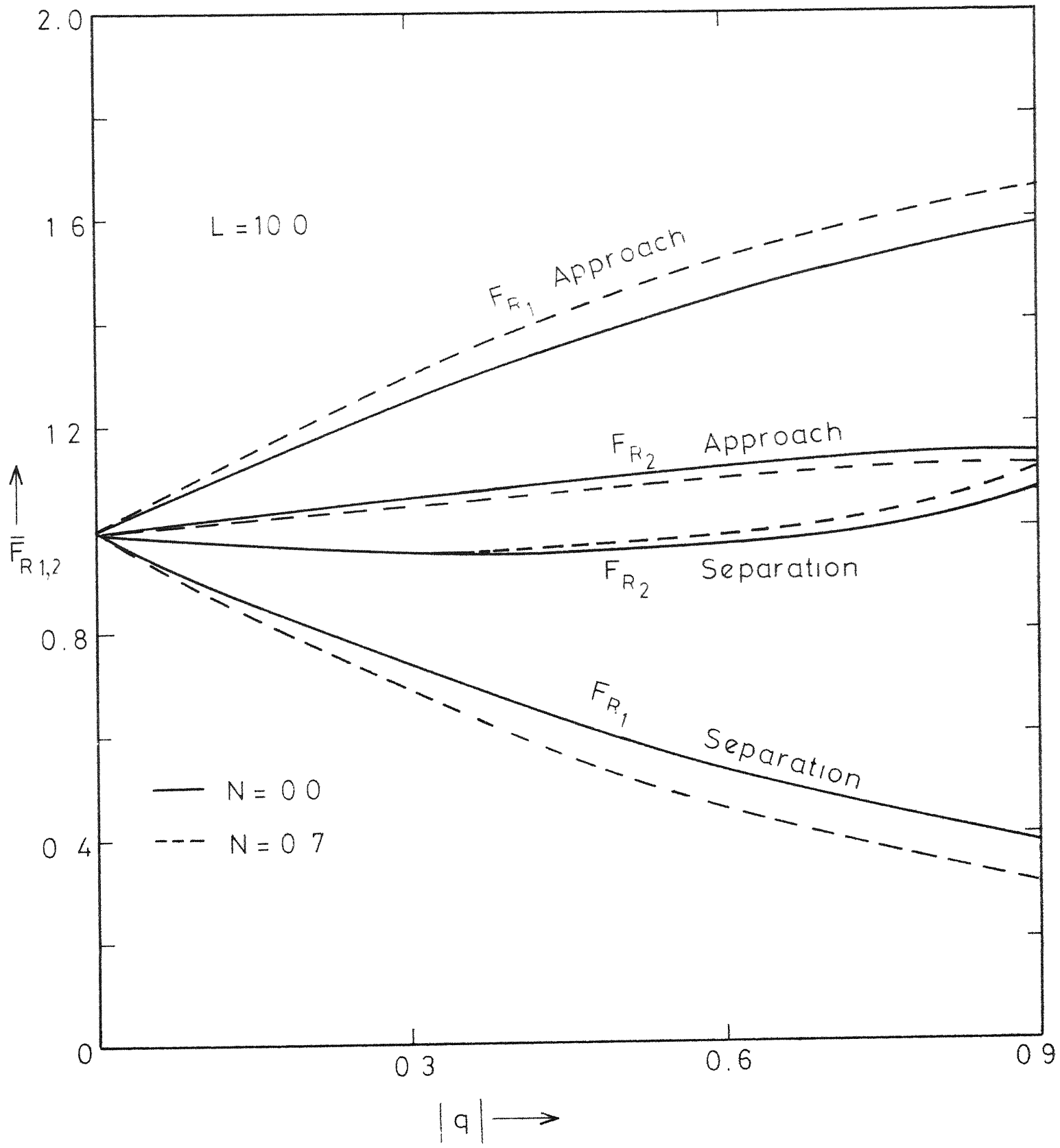

Fig 5.5 Friction coefficient parameter vs |q| for different values of N

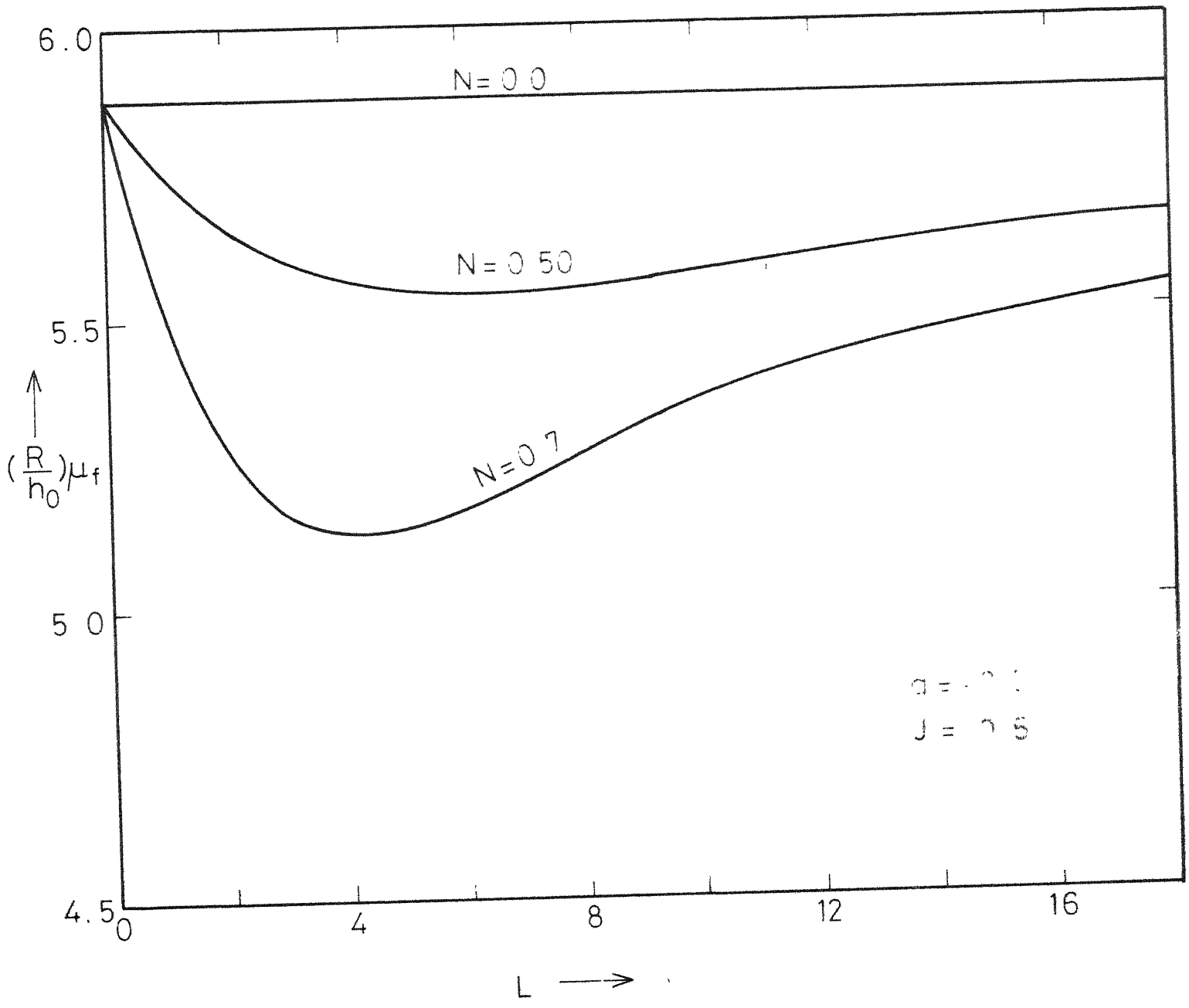

Fig 5.6 Coefficient of friction $(R/h_0)\,\mu_f$ vs L for different values of N(q = - 0 5)

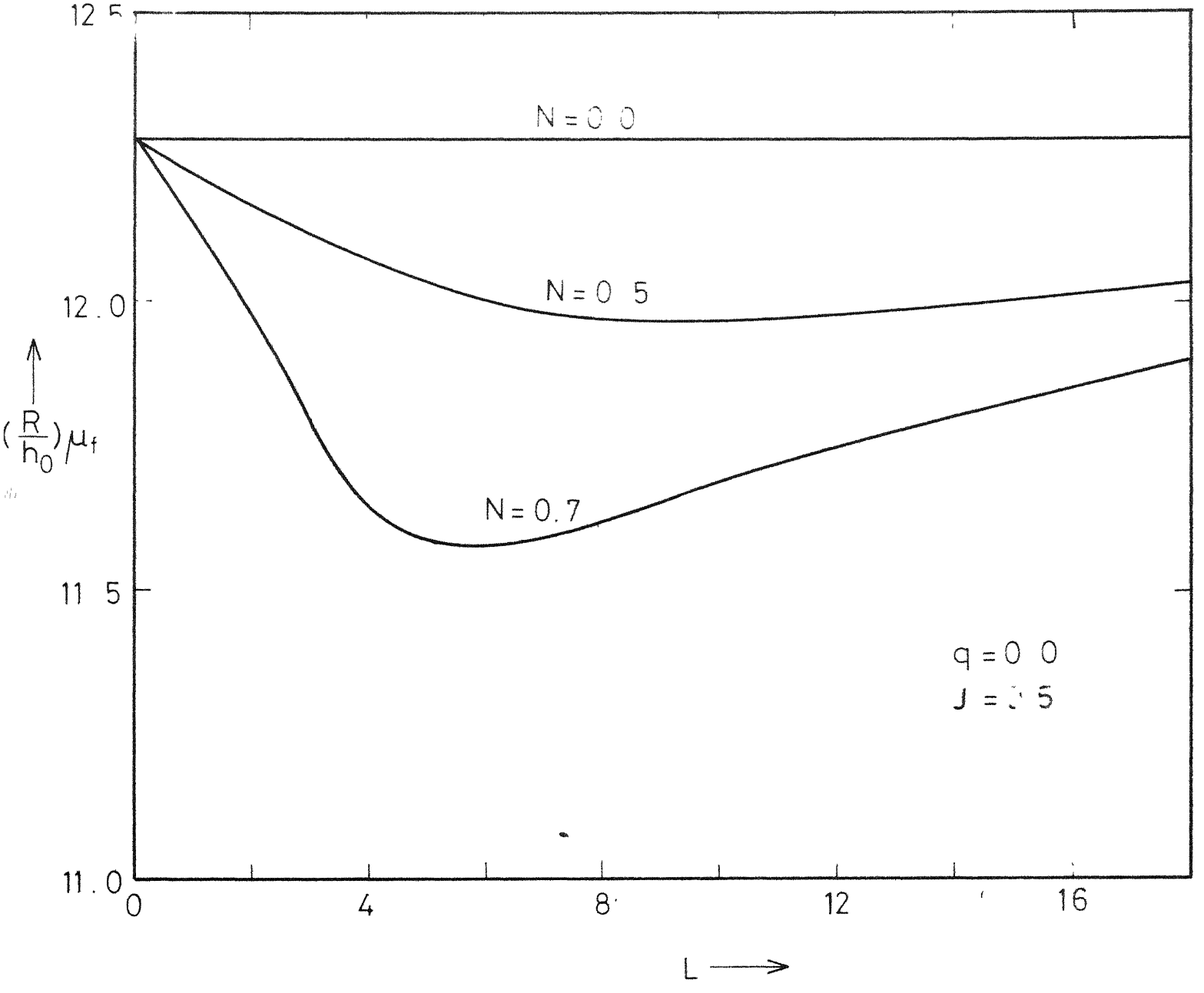

Fig 5 7 Coefficient of friction $(R/h_0)\mu_f$ vs L for different values of N (q = 0 0)

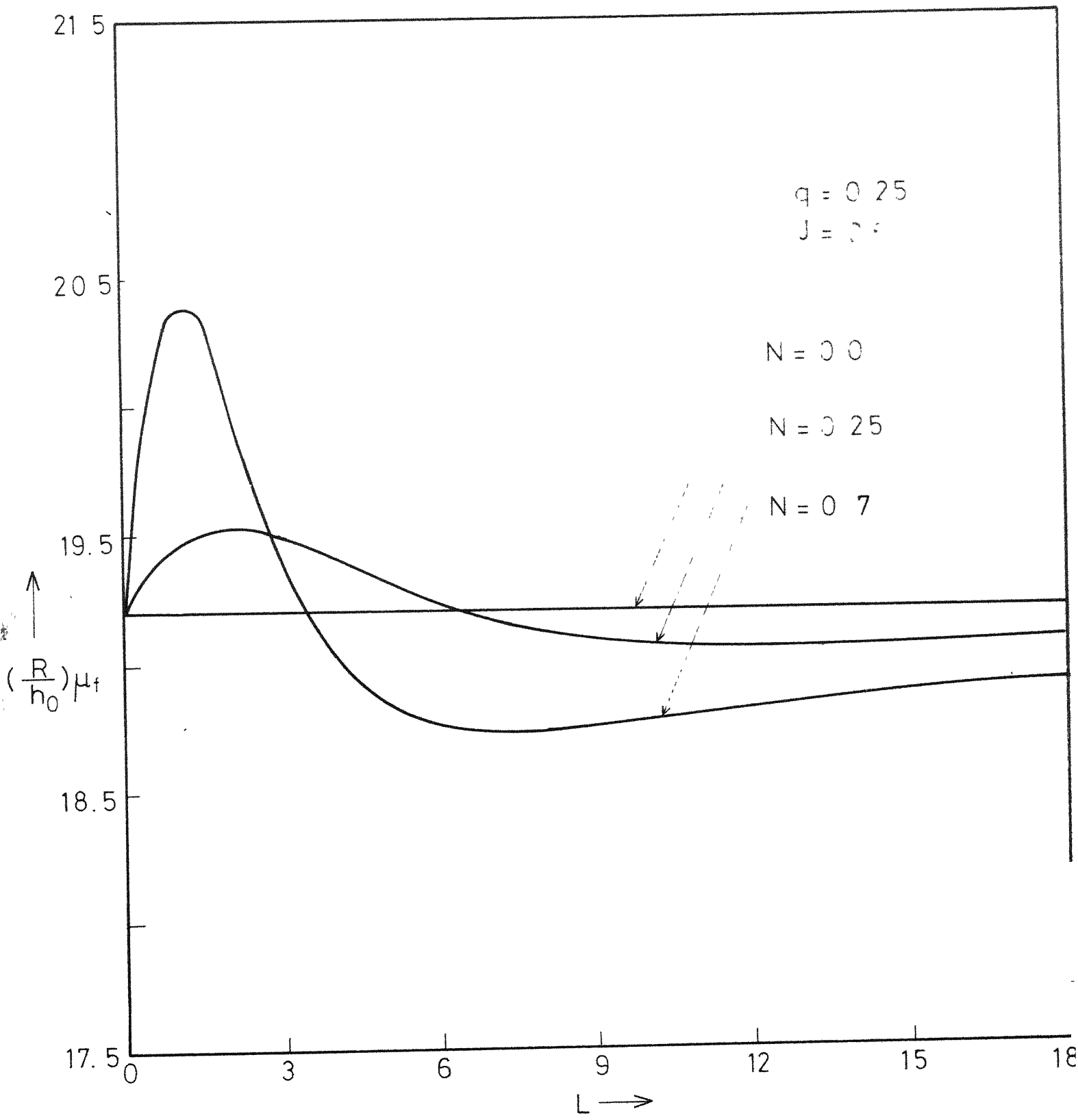

Fig. 5.8 Coefficient of friction $(R/h_0)\,\mu_f$ vs. L for different values of N(q = + 0.25)

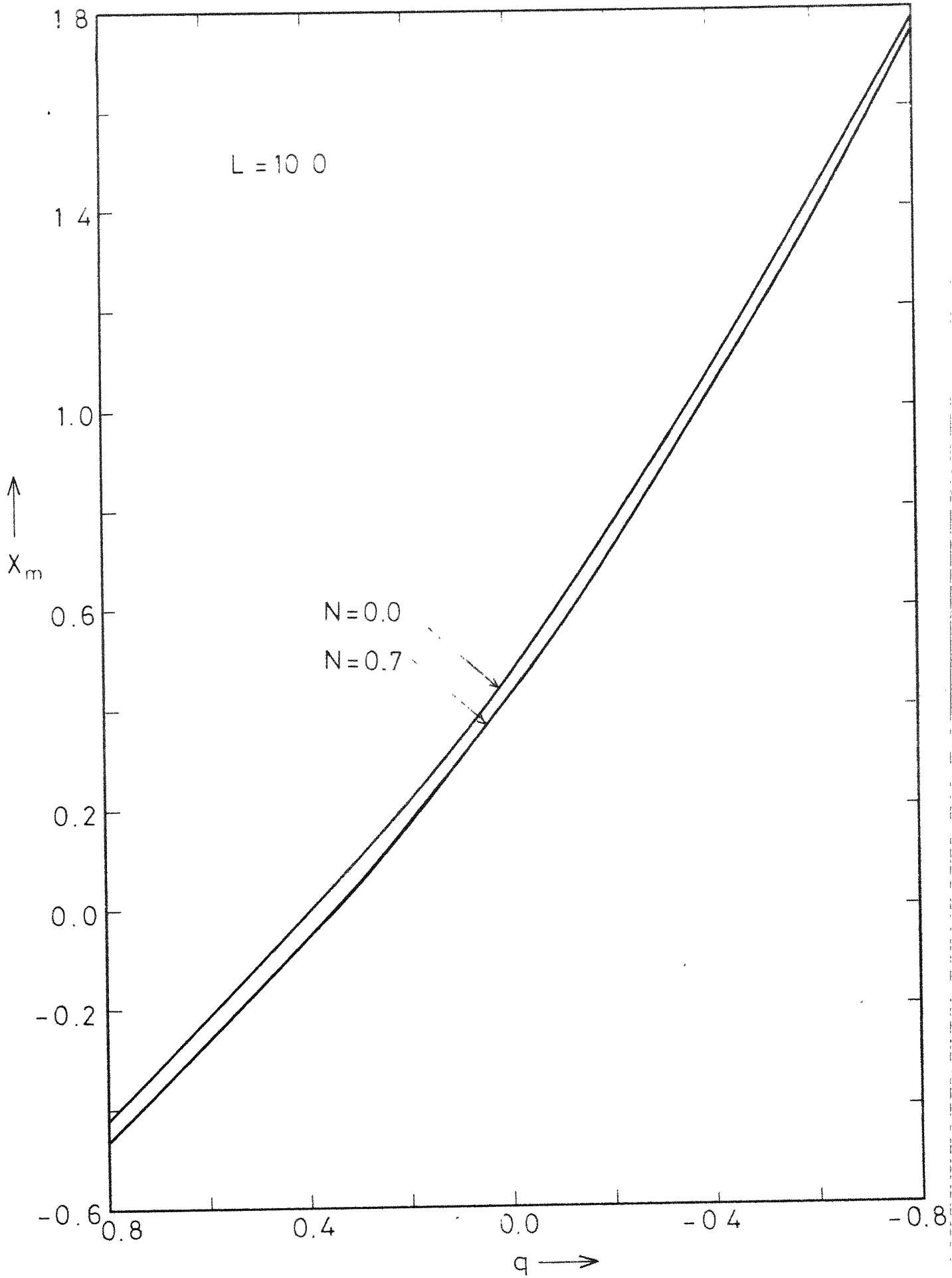

Fig. 5 9 Point of cavitation X_m vs q for different values of N

CHAPTER VI

LUBRICATION THEORY FOR ROUGH SURFACES AND ITS APPLICATION TO A JOURNAL BEARING

6.1 INTRODUCTION

The analysis of surface roughness effects on lubrication has gained considerable attention and has become a subject of intensive study during the last two decades. This is due to their importance in the practical field, its physical significance and also to the great theoretical interest inherent in these problems.

Most theoretical studies on bearing lubrication appearing in the literature make use of the assumption that the bearing surfaces are perfectly smooth. It has long been recognized that owing to machining limitations, this assumption is rather unrealistic, particularly in bearings, where the film thickness is small.

In recent years a major way of analyzing the problem has been the adoption of statistical methods. Two basic approaches have been developed namely the deterministic and stochastic approach. The starting point in each case has been the Reynolds equation. In the deterministic approach the surface roughness was accounted for by postulating a sine (cosine) wave or a series of sine (cosine) waves for the film thickness [95] . More recently Tzeng and Saibel [96,97] have used stochastic concepts to study the surface roughness effects on slider bearing [96] and on short journal bearing [97] . The

analysis was concerned with the problem of two dimensional slider bearing, with one dimensional roughness in the direction transverse to the sliding direction. There are, however, experimental evidences [98] which often exhibit a one-dimensional type of roughness running in the direction of sliding, generally referred to as the longitudinal roughness. Keeping in line with this evidence Christensen and Tonder [99-100] and Christensen [101] presented a stochastic model for hydrodynamic lubrication of rough surfaces. Christensen [101] considered two types of one-dimensional roughness, the longitudinal roughness with its striation parallel to the sliding direction, and the transverse roughness with its striation perpendicular to the sliding direction, and obtained modified Reynolds equations by making two heuristic assumptions about the pressure gradient and flow rate. It was concluded that the longitudinal roughness results in a slight decrease in load carrying capacity and an increase in frictional force thereby causing a significant increase in coefficient of friction. The effect of transverse roughness is, however, to improve the bearing characteristics. Later Elrod [102] improved the Christensen's modified form of Reynolds equation.

Scores of papers have appeared in the wake of the earlier mentioned works on various aspects of the lubrication of rough surfaces. All of the works appeared to date show that the surface roughness may have significant effect when the minimum film thickness is comparable to roughness mean height. The effect is much pronounced

for lower values of film thickness. Inherent in these works was a fundamental assumption that all the lubricants behaved as if they were Newtonian.

Non-Newtonian behaviour is almost invariably observed in lubrication practice and they may be of important consequence when the surfaces are rough. Christensen's models [101] do not account for non-Newtonian situations or where the micropolarity of the fluid is important. A question, therefore, naturally arises as to how the bearing performance would be modified in such situations.

It is the aim of this Chapter to analyze the surface roughness effects from microcontinuum view point. For simplicity it is assumed that the moving surface is smooth and the stationary surface is rough. Three cases of roughness are considered and the theory is applied to the problem of journal bearing under half Sommerfeld boundary conditions.

The present study may be of important consequence where the combined effects of surface roughness and additives are desired.

6.2 MODIFIED REYNOLDS EQUATION FOR ROUGH SURFACES

The Reynolds equation for micropolar fluids for smooth surfaces is of the form (eqn. 2.56)

$$\frac{\partial}{\partial x}\{q_x\} + \frac{\partial}{\partial z}\{q_z\} = \frac{\partial h}{\partial t} \tag{6.1}$$

where

$$q_x = \frac{Uh}{2} - \frac{f(N,\ell,h)}{\mu} \frac{\partial p}{\partial x} \tag{6.2}$$

$$q_z = - \frac{f(N,\ell,h)}{\mu} \frac{\partial p}{\partial z} \tag{6.3}$$

q_x and q_z are obtained from eqns. (2.53) and (2.54) by substituting, $U_{11} = U$, $U_{21} = U_{12} = U_{22} = o$. N and ℓ are defined by eqn. (2.18) and $f(N,\ell,h)$ by eqn. (2.55).

The geometry of the lubricant film can be considered to be constituted of two parts. The first part denotes the nominal (smooth) part of the geometry and can be considered to be a function of space and time co-ordinates. The second part of the film geometry, a randomly varying quantity, arises due to the surface roughness and is measured from the nominal level. Mathematically,

$$h = h_n(x,z,t) + h_s(x,z,\xi) \tag{6.4}$$

ξ, a random variable, determines a definite roughness arrangement, from a large number of similar- but not identical - arrangements having the same statistical properties.

Taking the expected value, equation (6.1) assumes the from

$$\frac{\partial}{\partial x} \{E(q_x)\} + \frac{\partial}{\partial z} \{E(q_z)\} = \frac{\partial E(h)}{\partial t} \tag{6.5}$$

where

$$E(\quad) = \int_{-\infty}^{\infty} (\quad) f(h_s)\, dh_s \tag{6.6}$$

and $f(h_s)$ is the probability density distribution of the random variable h_s. Using (6.6) it is readily seen [101] , that

$$\frac{\partial E(h)}{\partial t} = \frac{\partial h_n}{\partial t} \tag{6.7}$$

where h_n is the smooth part of the film thickness.

To evaluate the average of the fluxes appearing in equation (6.5), subject to a particular, specific model of the roughness, i.e. either along or perpendicular to the sliding direction, two assumptions, similar to those used by Christensen [101] , are made.

(i) The pressure gradient in the roughness direction is assumed to be a stochastic variable with zero (or negligible) variance

(ii) The flux perpendicular to the roughness direction is assumed to be a stochastic variable with zero (or negligible) variance.

A justification of these assumptions for micropolar fluid can be forwarded in a way similar to that of Christensen [101] .

(i) Longitudinal, One-Dimensional Roughness

The roughness is assumed to be running parallel to the sliding direction in the form of long narrow ridges and valleys. Thus the film geometry assumes the form

$$h = h_n(x,z,t) + h_s(z,\xi) \tag{6.8}$$

Taking the average of all terms in equation (6.2) and adopting the first assumption the mean flux in the x-direction is given by

$$E(q_x) = \frac{U}{2} E(h) - \frac{1}{\mu} E(f(l,\ell,h)) \quad \frac{\partial E(p)}{\partial x} \tag{6.9}$$

This is so, because, $\partial p/\partial x$ is a variable with zero variance and $f(N,\ell,h)$ and $\partial p/\partial x$ can be considered (approximately) to be stochastically independent quantities. However, to get the mean flux in z-direction, we divide equation (6.3) by $f(N,\ell,h)$. Taking the expected value of both sides of resulting equation and using the second assumption

$$E(q_z) = - \frac{1}{\mu} \frac{1}{E\left(\frac{1}{f(N,\ell,h)}\right)} \frac{\partial E(p)}{\partial z} \tag{6.10}$$

Substituting the expressions for $E(q_x)$ and $E(q_z)$ in equation (6.1) the modified Reynolds equation becomes

$$\frac{\partial}{\partial x}\{E(f(N,\ell,h)) \frac{\partial E(p)}{\partial x}\} + \frac{\partial}{\partial z}\{(E(f(N,\ell,h)^{-1}))^{-1} \frac{\partial E(p)}{\partial z}\}$$

$$= \frac{\mu}{2}\{U \frac{\partial E(h)}{\partial x} + 2 \frac{\partial E(h)}{\partial t}\} \tag{6.11}$$

(ii) Transverse, One-Dimensional Roughness

In this model, the roughness striation is assumed to be running perpendicular to the sliding direction in the form of long narrow ridges and furrows. The film thickness therefore assumes the following form

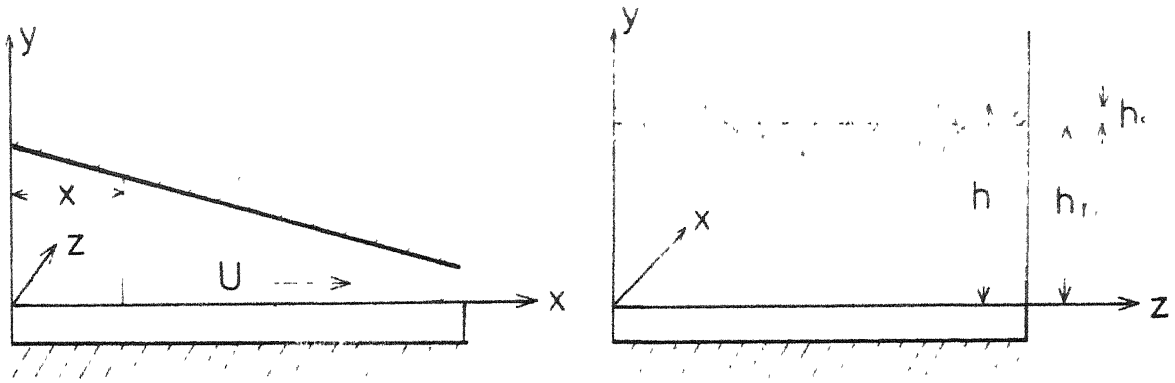

Fig. 6·1(a) Longitudinal roughness

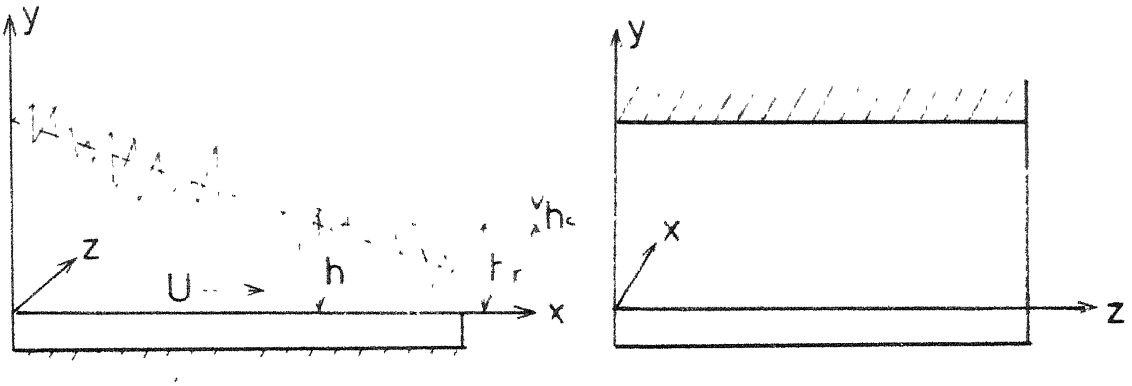

Fig. 6·1(b) Transverse roughness

$$h = h_n(x,z,t) + h_s(x,\xi) \tag{6.12}$$

In a similar way, adopted earlier, the fluxes, along and perpendicular to the sliding direction, are

$$E(q_x) = \frac{U}{2} \frac{E\left(\frac{h}{f(N,\ell,h)}\right)}{E\left(\frac{1}{f(N,\ell,h)}\right)} - \frac{1}{\mu} \frac{\partial E(p)}{\partial x} \left(E(f(N,\ell,h)^{-1})\right)^{-1} \tag{6.13}$$

$$E(q_z) = -\frac{1}{\mu} \frac{\partial E(p)}{\partial z} E(f(N,\ell,h)) \tag{6.14}$$

and the modified Reynolds equation is

$$\frac{\partial}{\partial x}\left[\left(E(f(N,\ell,h)^{-1})\right)^{-1} \frac{\partial E(p)}{\partial x}\right] + \frac{\partial}{\partial z}\left[E(f(N,\ell,h)) \frac{\partial E(p)}{\partial z}\right]$$

$$= \frac{\mu}{2}\left[U \frac{\partial}{\partial x}\left\{\frac{E\left(\frac{h}{f(N,\ell,h)}\right)}{E\left(\frac{1}{f(N,\ell,h)}\right)}\right\} + 2 \frac{\partial E(h)}{\partial t}\right] \tag{6.15}$$

(iii) Uniform, Isotropic Roughness

In this model, the roughness is assumed to be uniformly distributed over the bearing surface with no preferred position or direction on the surface. The film thickness assumes the form

$$h = h_n(x,z,t) + h_s(x,z,\xi) \tag{6.16}$$

Adopting the same hypothesis as in [99] and mathematical reasoning given by Tonder [103] , the fluxes and modified equations are given as follows.

$$E(q_x) = \frac{U}{2} E(h) - \frac{1}{\mu} E(f(N,\ell,h) \frac{\partial E(p)}{\partial x} \tag{6.17}$$

$$E(q_z) = -\frac{1}{\mu} E(f(N,\ell,h) \frac{\partial E(p)}{\partial z} \tag{6.18}$$

$$\frac{\partial}{\partial x} \{E(f(N,\ell,h)) \frac{\partial E(p)}{\partial x}\} + \frac{\partial}{\partial z} \{E(f(N,\ell,h)) \frac{\partial E(p)}{\partial z}\}$$

$$= \frac{\mu}{2} \{U \frac{\partial E(h)}{\partial x} + 2 \frac{\partial E(h)}{\partial t}\} \tag{6.19}$$

(iv) Distribution of Roughness Heights

The roughness distribution function which is generally used to evaluate the several expected values is [101]

$$f(h_s) = \frac{35}{32b^7} (b^2 - h_s^2)^3 \quad -b < h_s < b \tag{6.20}$$

$$= 0 \quad \text{elsewhere}$$

where b is the half total range of random film thickness variable and if σ is the standard deviation, $b = \pm 3\sigma$. The polynomial distribution function (6.20) is an approximation to the Gaussian distribution. The reason for using such a polynomial distribution is that the Gaussian distribution always implies a finite probability of having asperity of very large sizes violating the conditions for hydrodynamic operation.

6.3 BEARING CHARACTERISTICS

Once the modified Reynolds type equation is obtained, for a particular case, the evaluation of the bearing characteristics can be carried out in a way similar to that of the smooth bearing.

(i) Oil Flow

When the roughness is longitudinal the mean flux along and across the direction of sliding is given by equation (6.9) and (6.10), respectively. For transverse roughness these values are governed by (6.13) and (6.14). Equations (6.17) and (6.18) account for these characteristics for the isotropic case. The total flow over the edge of the bearing can be found from the above mentioned equations by integrating in a usual way.

(ii) Load Capacity

The mean load carrying capacity is obtained by integrating the mean pressure over the bearing surface.

$$E(W) = \int_A E(p)\, dA \tag{6.21}$$

(iii) Frictional Drag

The expression for shear stress on the moving surface, from eqn. (2.62), is

$$\tau = \frac{h}{2}\frac{\partial p}{\partial x} + \frac{\mu U}{g(N,\ell,h)} \tag{6.22}$$

where $g(N,\ell,h)$ is defined by eqn. (2.64).

For longitudinal roughness the mean shear stress is given by

$$E(\tau) = \frac{1}{2} E(h) \frac{\partial E(p)}{\partial x} + \mu U E\left(\frac{1}{g(N,\ell,h)}\right) \tag{6.23}$$

When the roughness is transverse the mean shear stress is

$$E(\tau) = \mu U \left[\frac{1}{4}E\left(\frac{h^2}{f(N,\ell,h)}\right) + E\left(\frac{1}{g(N,\ell,h)}\right) - \frac{1}{4}\frac{\left\{E\left(\frac{h}{f(N,\ell,h)}\right)\right\}^2}{E\left(\frac{1}{f(N,\ell,h)}\right)}\right] + \frac{1}{2}\frac{E\left(\frac{h}{f(N,\ell,h)}\right)}{E\left(\frac{1}{f(N,\ell,h)}\right)}\frac{\partial E(p)}{\partial x} \qquad (6.24)$$

The mean frictional drag is

$$E(F) = \int_A E(\tau)\, dA \qquad (6.25)$$

(iv) Coefficient of Friction

The mean coefficient of friction is defined by

$$E(\mu_f) = \frac{E(F)}{E(W)} \qquad (6.26)$$

6.4 MODIFIED REYNOLDS EQUATION APPLIED TO A ROUGH JOURNAL BEARING

The modified Reynolds equation derived above will now be applied to the lubrication of one-dimensional rough journal bearing under half Sommerfeld boundary conditions.

The configuration of the system is shown in Fig. 6.1(c). Here the bearing is assumed to be rough and journal to be smooth. The two cases of roughness, i.e. longitudinal and transverse, are treated separately.

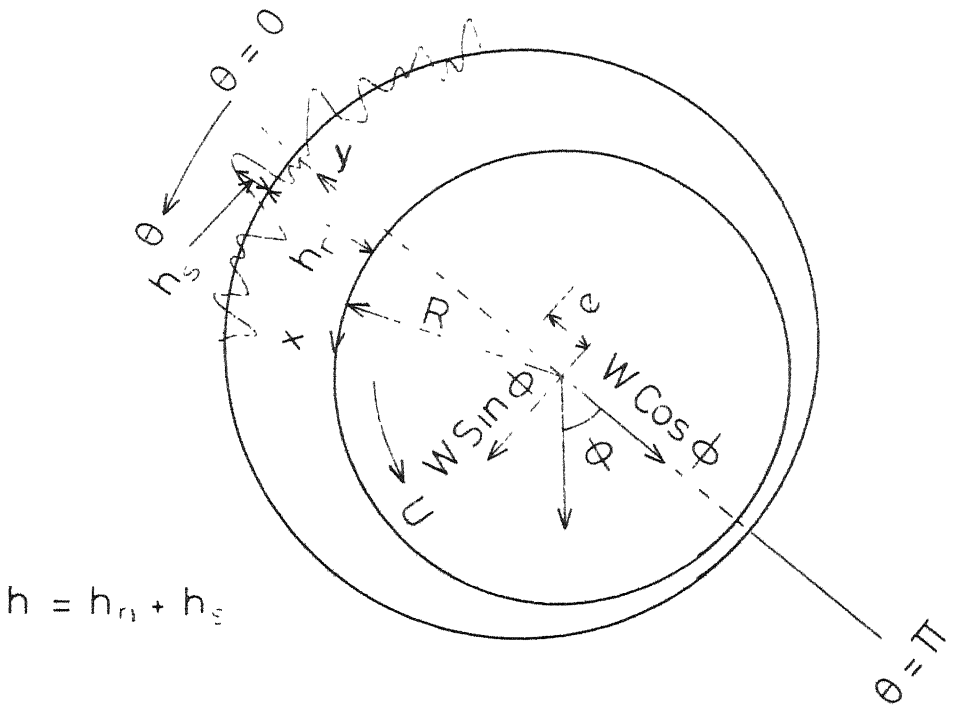

Fig 6 1(c) Geometry of rough journal bearing

(i) Longitudinal, One-Dimensional Roughness

Since $x = R\theta$, equation (6.11) assumes the form

$$\frac{d}{d\theta}\left\{E(f(N,\ell,h))\,\frac{dE(p)}{d\theta}\right\} = \frac{\mu UR}{2}\,\frac{dE(h)}{d\theta} \tag{6.27}$$

The smooth part of the film thickness is

$$h_n = c(1 + \varepsilon\cos\theta) \tag{6.28}$$

and

$$E(h) = h_n \tag{6.29}$$

The boundary conditions for pressure are

$$E(p) = o, \text{ at } \theta = o \text{ and } \pi \tag{6.30}$$

The mean pressure distribution is given by

$$E(p(\theta)) = \frac{1}{2}\mu UR\int_o^\theta \frac{(h_n - h_{n_o})\,d\theta}{E(f(N,\ell,h))} \tag{6.31}$$

where

$$h_{n_o} = \frac{\int_o^\pi \frac{h_n\,d\theta}{E(f(N,\ell,h))}}{\int_o^\pi \frac{d\theta}{E(f(N,\ell,h))}} \tag{6.32}$$

The mean load components per unit length, along and perpendicular to the line of centers, are obtained by integrating the mean pressure around the bearing surface from $\theta = o$ to $\theta = \pi$. Thus the mean load component normal to the line of centers per unit length is given by

$$E(W_{\frac{\pi}{2}}) = E(W) \sin\phi = \int_0^{\pi} E(p(\theta)) \sin\theta \, R \, d\theta \tag{6.33}$$

Substituting the value of $E(p(\theta))$ from eqn. (6.31) and integrating we get

$$E(W_{\frac{\pi}{2}}) = \frac{1}{2} \mu U R^2 \int_0^{\pi} \frac{(h_n - h_{n_o}) \cos\theta \, d\theta}{E(f(N,\ell,h))} \tag{6.34}$$

Similarly, the mean load component along the line of centers is given

$$E(W_o) = E(W) \cos\phi = \frac{1}{2} \mu U R^2 \int_0^{\pi} \frac{(h_n - h_{n_o}) \sin\theta \, d\theta}{E(f(N,\ell,h))} \tag{6.35}$$

The resultant mean load capacity is given by

$$E(W) = \{ (E(W_{\frac{\pi}{2}}))^2 + (E(W_o))^2 \}^{\frac{1}{2}} \tag{6.36}$$

The expression for mean shear stress assumes the form

$$E(\tau) = \frac{E(h)}{2R} \frac{dE(p)}{d\theta} + \mu U E\left(\frac{1}{g(N,\ell,h)} \right) \tag{6.37}$$

The mean frictional drag, $E(F)$, per unit length is given by

$$E(F) = \int_0^{\pi} \frac{h_n}{2R} \frac{dE(p)}{d\theta} R \, d\theta + \mu U \int_0^{2\pi} E\left(\frac{1}{g(N,\ell,h)} \right) R \, d\theta \tag{6.38}$$

or, using eqn. (6.31),

$$E(F) = \frac{1}{4}\mu UR\left\{\int_0^{\pi} \frac{h_n(h_n - h_{n_o})\,d\theta}{E(f(N,\ell,h))} + 4\int_0^{2\pi} E\left(\frac{1}{g(N,\ell,h)}\right) d\theta\right\} \qquad (6.39)$$

The coefficient of friction is obtained according to equation (6.26).

(ii) Transverse, One-Dimensional Roughness

For this roughness the Reynolds equation is

$$\frac{d}{d\theta}\left[\left(E(f(N,\ell,h)^{-1})\right)^{-1} \frac{dE(p)}{d\theta}\right] = \frac{1}{2}\mu UR \frac{d}{d\theta}\left\{\frac{E\left(\frac{h}{f(N,\ell,h)}\right)}{E\left(\frac{1}{f(N,\ell,h)}\right)}\right\} \qquad (6.40)$$

In a way similar to the case of longitudinal roughness, the mean value of pressure distribution, load carrying capacity, frictional drag and coefficient of friction are

$$E(p(\theta)) = \frac{\mu UR}{2}\int_0^{\theta}\left\{E\left(\frac{h}{f(N,\ell,h)}\right) - h_{n_1} E\left(\frac{1}{f(N,\ell,h)}\right)\right\} d\theta \qquad (6.41)$$

$$E\left(W_{\frac{\pi}{2}}\right) = \frac{\mu UR}{2}\int_0^{\pi}\left\{E\left(\frac{h}{f(N,\ell,h)}\right) - h_{n_1} E\left(\frac{1}{f(N,\ell,h)}\right)\right\}\cos\theta\, d\theta \qquad (6.42)$$

$$E(W_o) = \frac{\mu UR}{2}\int_0^{\pi}\left\{E\left(\frac{h}{f(N,\ell,h)}\right) - h_{n_1} E\left(\frac{1}{f(N,\ell,h)}\right)\right\}\sin\theta\, d\theta \qquad (6.43)$$

$$E(F) = \frac{\mu UR^2}{2}\left[\frac{1}{2}\int_0^{\pi}\frac{E\left(\frac{h}{f(N,\ell,h)}\right)}{E\left(\frac{1}{f(N,\ell,h)}\right)}\left\{E\left(\frac{h}{f(N,\ell,h)}\right) - h_{n_1} E\left(\frac{1}{f(N,\ell,h)}\right)\right\} d\theta\right.$$

$$\left. + 2\int_0^{2\pi}\left\{3E\left(\frac{h^2}{f(N,\ell,h)}\right) + E\left(\frac{1}{g(N,\ell,h)}\right) - 3\frac{\left\{E\left(\frac{h}{f(N,\ell,h)}\right)\right\}^2}{E\left(\frac{1}{f(N,\ell,h)}\right)}\right\} d\theta\right] \qquad (6.44)$$

where

$$h_{n_1} = \frac{\int_0^{\pi} E\left(\frac{h}{f(N,\ell,h)}\right) d\theta}{\int_0^{\pi} E\left(\frac{1}{f(N,\ell,h)}\right) d\theta} \qquad (6.45)$$

The coefficient of friction is obtained as usual.

(iii) Isotropic Roughness

For one dimensional case the isotropic roughness will be equivalent to longitudinal roughness.

6.5 NON-DIMENSIONAL FORMS

To obtain the results numerically the following non-dimensional scheme is adopted,

$$h = \frac{h_n}{c} = 1 + \varepsilon\cos\theta,\ H_o = \frac{h_{n_o}}{c},\ H_{o_1} = \frac{h_{n_1}}{c},\ H_s = \frac{h_s}{c},\ B = \frac{b}{c}$$

$$L = \frac{c}{\ell},\quad E(P) = \frac{2E(p)c^2}{\mu UR},\ \overline{E(W)} = \frac{2E(W)c^2}{\mu UR^2},\ \overline{E(F)} = \frac{2E(F)c}{\mu UR} \qquad (6.46)$$

The non-dimensional average values of bearing characteristics for longitudinal and transverse roughness are given as follows.

Longitudinal, one-dimensional roughness

$$E(P(\theta)) = \int_0^{\theta} \frac{(H-H_o)\, d\theta}{S_1(N,L,H,B)} \qquad (6.47)$$

$$\overline{E(W_{\frac{\pi}{2}})} = \overline{E(W)} \sin\phi = \int_0^{\pi} \frac{(H-H_o)\cos\theta\, d\theta}{S_1(N,L,H,B)} \qquad (6.48)$$

$$\overline{E(W_o)} = \overline{E(W)} \cos\phi = \int_0^{\pi} \frac{(H-H_o)\sin\theta\, d\theta}{S_1(N,L,H,B)} \qquad (6.49)$$

$$\overline{E(F)} = \frac{1}{2}\int_0^{\pi} \frac{H(H-H_o)\,d\theta}{S_1(N,L,H,B)} + 2\int_0^{\pi} G(N,L,H,B)\,d\theta \tag{6.50}$$

$$\overline{E(W)} = \left(\overline{E(W_{\frac{\pi}{2}})}^2 + \overline{E(W_o)}^2\right)^{\frac{1}{2}} \tag{6.51}$$

$$\frac{R}{c}(E(\mu_f)) = \frac{\overline{E(F)}}{\overline{E(W)}} \tag{6.52}$$

where

$$H_o = \frac{\int_0^{\pi} \frac{H\,d\theta}{S_1(N,L,H,B)}}{\int_0^{\pi} \frac{d\theta}{S_1(N,L,H,B)}} \tag{6.53}$$

$$S_1(N,L,H,B) = \frac{H^3}{12} + \frac{B^2}{36}H + \frac{H}{L^2} - \frac{35N}{64B^7L}\int_{-B}^{B} (H+H_s)^2(B^2-H_s^2)^3 \coth\frac{NL}{2}(H+H_s)\,dH_s \tag{6.54}$$

$$G(N,L,H,B) = \frac{35}{32B^7}\int_{-B}^{B} \frac{(B^2-H_s^2)^3\,d\,H_s}{\{(H+H_s) - \frac{2N}{L}\tanh\frac{NL}{2}(H+H_s)\}} \tag{6.55}$$

Transverse, one-dimensional roughness

$$E(P(\theta)) = \int_0^{\theta} \{S_3(N,L,H,B) - H_{o1}\,S_2(N,L,H,B)\}\,d\theta \tag{6.56}$$

$$\overline{E(W_{\frac{\pi}{2}})} = \int_0^{\pi} \{S_3(N,L,H,B) - H_{o1}\,S_2(N,L,H,B)\}\cos\theta\,d\theta \tag{6.57}$$

$$\overline{E(W_o)} = \int_0^{\pi} \{S_3(N,L,H,B) - H_{o1}\,S_2(N,L,H,B)\}\sin\theta\,d\theta \tag{6.58}$$

$$\overline{E(F)} = \frac{1}{2}\int_0^{\pi} \left\{\frac{S_3^2(N,L,H,B)}{S_2(N,L,H,B)} - H_{o1}S_3(N,L,H,B)\right\} d\theta + 2\int_0^{2\pi} \left\{3S_4(N,L,H,B) + G(N,L,H,B) - 3\,\frac{S_3^2(N,L,H,B)}{S_2(N,L,H,B)}\right\} d\theta \tag{6.59}$$

where

$$H_{ol} = \frac{\int_0^{\pi} S_3(N,L,H,B)\, d\theta}{\int_0^{\pi} S_2(N,L,H,B)\, d\theta} \tag{6.60}$$

$$S_i(N,L,H,B) = \frac{420}{32B^7}\int_{-B}^{B} \frac{(H+H_s)^{i-2}(B^2-H_s^2)^3\, d\,H_s}{\left[(H+H_s)^3 + 12\,\frac{(H+H_s)}{L^2} - \frac{6N}{L}(H+H_s)^2 \coth\frac{NL}{2}(H+H_s)\right]}, \quad i=2,3,4 \tag{6.61}$$

To determine the rate of change of bearing characteristics for a rough bearing as compared to the smooth theory the following bearing parameters are defined to study the micropolar effects.

(iii) Mean Load Ratio Parameter

The mean load ratio parameter is defined by

$$\bar{W}_R = \frac{\overline{E(W)} - \overline{(E(W))}_{B=o}}{\overline{(E(W))}_{B=o}} \tag{6.62}$$

(iv) Mean Frictional Drag Ratio Parameter

The mean frictional drag ratio parameter is defined by

$$\bar{F}_R = \frac{\overline{E(F)} - \overline{(E(F))}_{B=o}}{\overline{(E(F))}_{B=o}} \tag{6.63}$$

(v) Mean Coefficient of Friction Ratio Parameter

The mean coefficient of friction ratio parameter is defined by

$$\bar{C}_R = \frac{E(\mu_f) - (E(\mu_f))_{B=0}}{(E(\mu_f))_{B=0}} \qquad (6.64)$$

In all the above parameters $(\quad)_{B=0}$ denotes the corresponding value for smooth surfaces.

6.6 RESULTS AND DISCUSSION

(i) Dimensionless Parameters

Three dimensionless parameters are of important consequence in context with the present study, namely, N, L and B, defined by equations (2.18) and (6.46).

The parameters N and L have already been discussed in Chapter III.

The parameter $B(=\frac{b}{c})$ is a characteristic of bearing geometry and arises due to the surface roughness. It is obvious that the bearing characteristics would be prominent when b becomes comparable to c. A detailed discussion and limitation of this parameter are given in [99,100,101] . Here it suffices to say that $o \leq B < 1$.

(ii) Limiting Cases

The present study can be considered as a generalization of the works of Christensen [101] and Prakash and Sinha [58] , because their results can be obtained from the present analysis by

considering certain limiting cases.

Christensen's results are obtained in the limit $L \to \infty$ or $N \to o$, as both of these cases correspond to the Newtonian results. The results of Prakash and Sinha are obtained in the limit $B \to o$, since $B \to o$ signifies a smooth surface.

(iii) Bearing Characteristics

The analysis of surface roughness effects from a microcontinuum view point, yields bearing characteristics which are functions, not only of the roughness parameter B, but also of the micropolar parameters N and L.

The load ratio parameter $\bar{W}_R$, friction ratio parameter $\bar{F}_R$ and the coefficient of friction ratio parameter $\bar{C}_R$ have been plotted as a function of the roughness parameter B for various values of the coupling number N($\varepsilon = o.5$, L = 30) in Figs.6.2to 6.4. It is seen that, akin to the Newtonian lubricants, the transverse roughness leads to a significant increase in load carrying capacity Fig. 6.2. and the frictional drag, Fig. 6.3 whereas the coefficient of friction decreases significantly, Fig. 6.4. The percentage rate of increase or decrease is higher for higher values of N. In case of longitudinal roughness there is a slight decrease in load carrying capacity, Fig. 6.2, and a slight increase in frictional drag, Fig. 6.3 consequently the coefficient of friction increases for all values of N. Again it is seen that the rate of increase is further enhanced

by large values of N.

Figs.6.5 to 6.7 show the variation of the parameters $\bar{W}_R$, $\bar{F}_R$ and $\bar{C}_R$ versus L for various values of N(ϵ = 0.5, B=0.49) for longitudinal roughness. It is seen that the parameter $\bar{W}_R$ is lower for higher values of N and intermediate values of L whereas $\bar{F}_R$ is always higher. The reduction in $\bar{W}$ and increase in $\bar{F}$ leads to a significant increase in coefficient of friction and the rate of decrease or increase is always higher for micropolar fluid. However, the limits L → o and L → ∞ give rise to the Newtonian values for these parameters.

Figs. 6.8 to 6.10 are the variations of the parameters $\bar{W}_R$, $\bar{F}_R$ and $\bar{C}_R$ for transverse roughness. $\bar{W}_R$ and $\bar{F}_R$ are positive showing that the load capacity and frictional drag are higher for rough bearing. However, negative values of $\bar{C}_R$ show the reduction in coefficient of friction. The rate of increase of load capacity and frictional drag is higher for micropolar fluids. On the other hand the coefficient of friction parameter $\bar{C}_R$ shows a typical trend. From Fig. 6.10 it can be concluded that for smaller values of L the rate of decrease of coefficient of friction (μ_f) is smaller for micropolar fluids. However for higher values of L the decrease is higher and then comes to the Newtonian rate (corresponding to L → ∞).

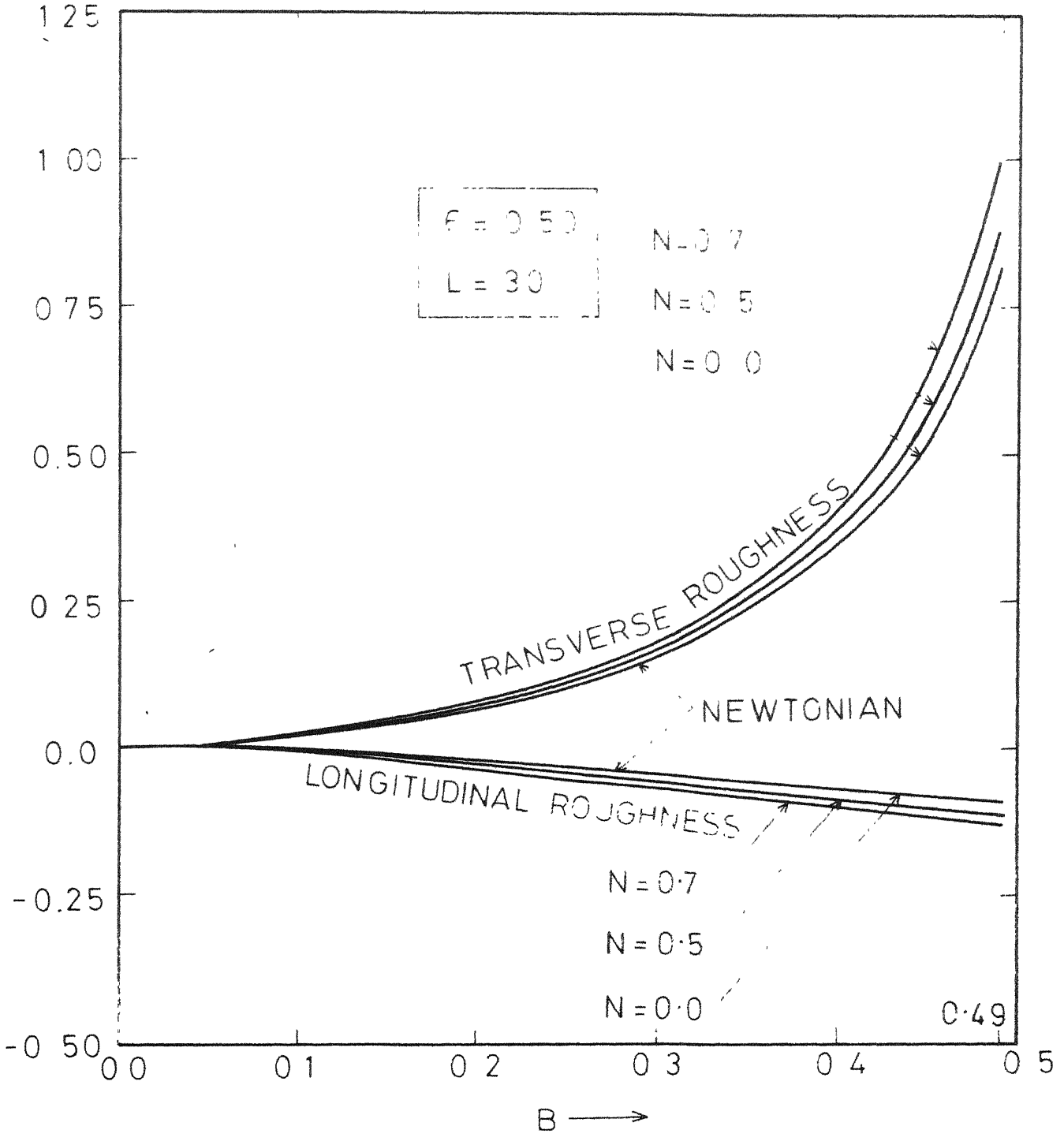

Fig 6.2 Load parameter $\bar{W}_2$ vs roughness parameter B for various values of coupling number N

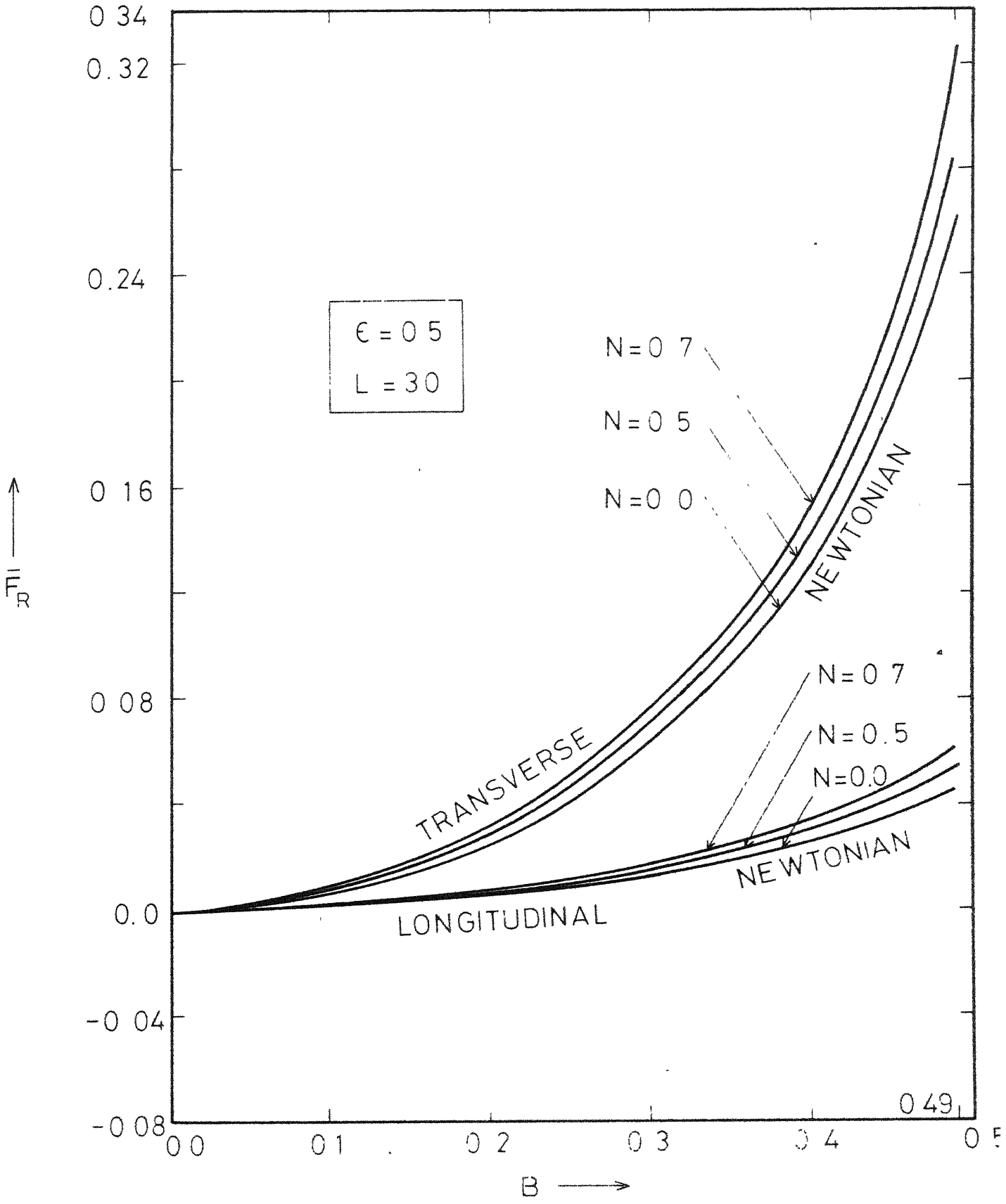

Fig. 6·3 Frictional drag parameter $\bar{F}_R$ vs. roughness parameter B for various values of coupling number N

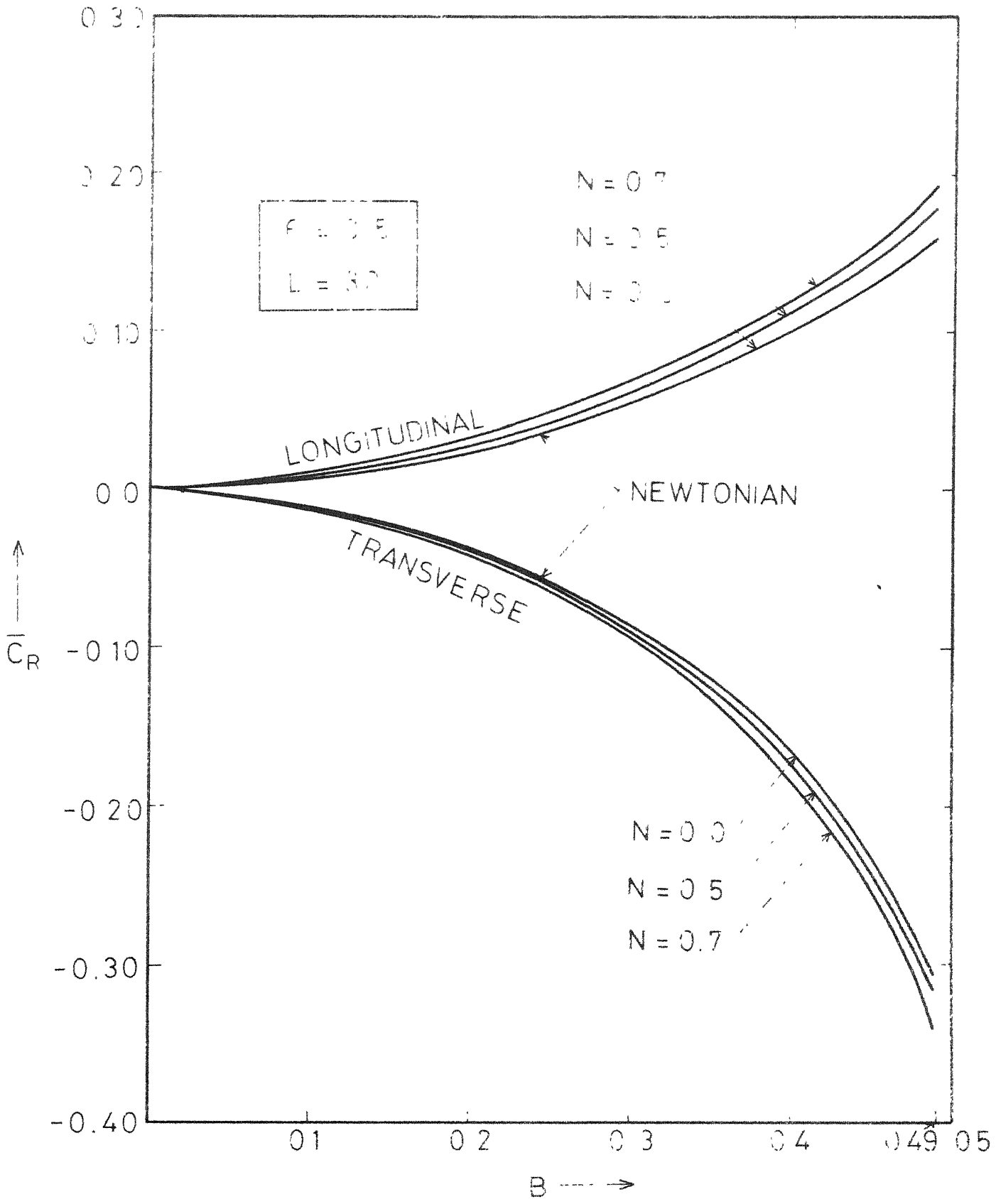

Fig. 6·4 Coefficient of friction parameter $\bar{C}_R$ vs. roughness parameter B for various values of coupling number N

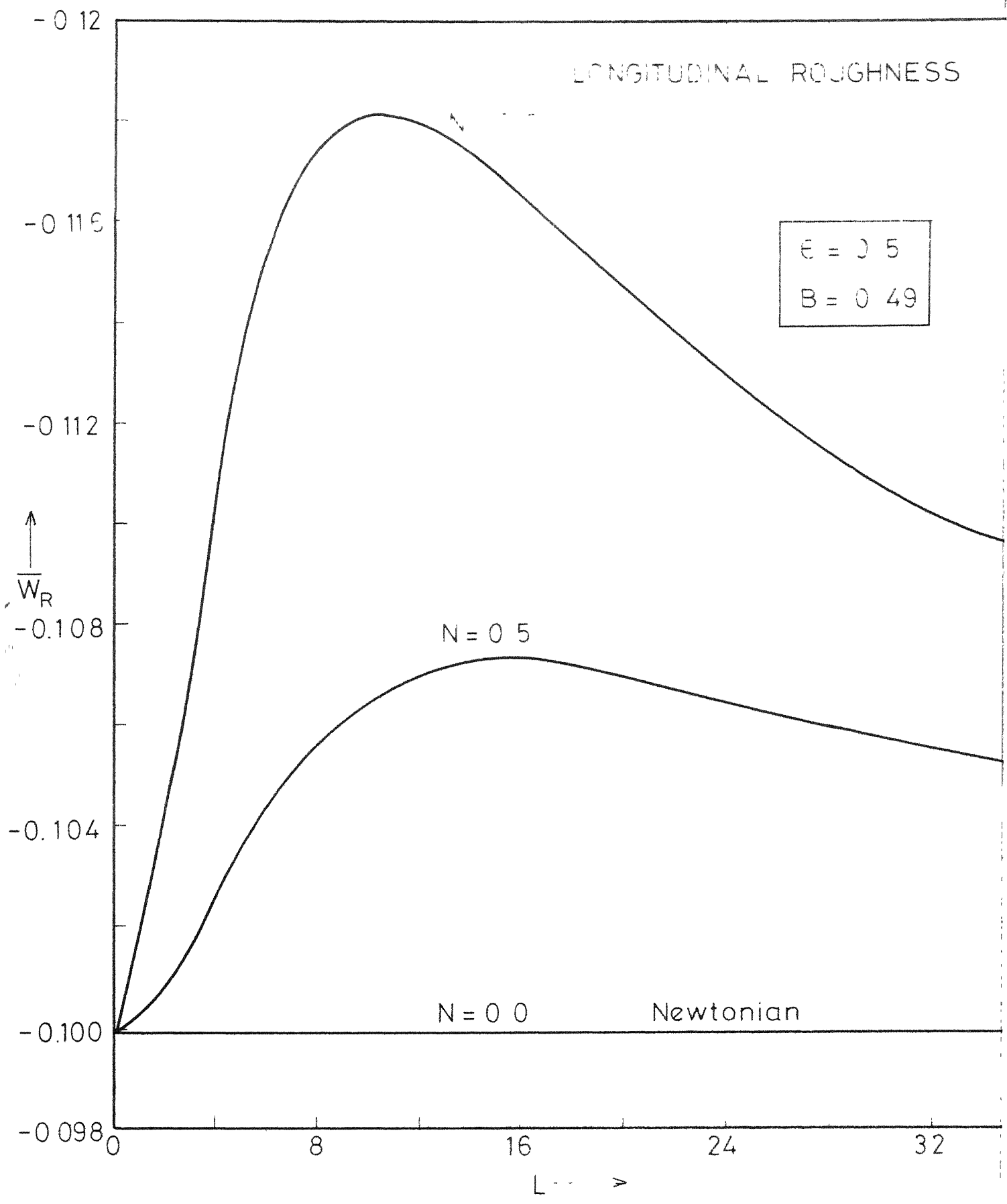

Fig. 6-5 Load parameter $\bar{W}_R$ vs. length ratio parameter L for various values of coupling number N (B=0·49, longitudinal roughness)

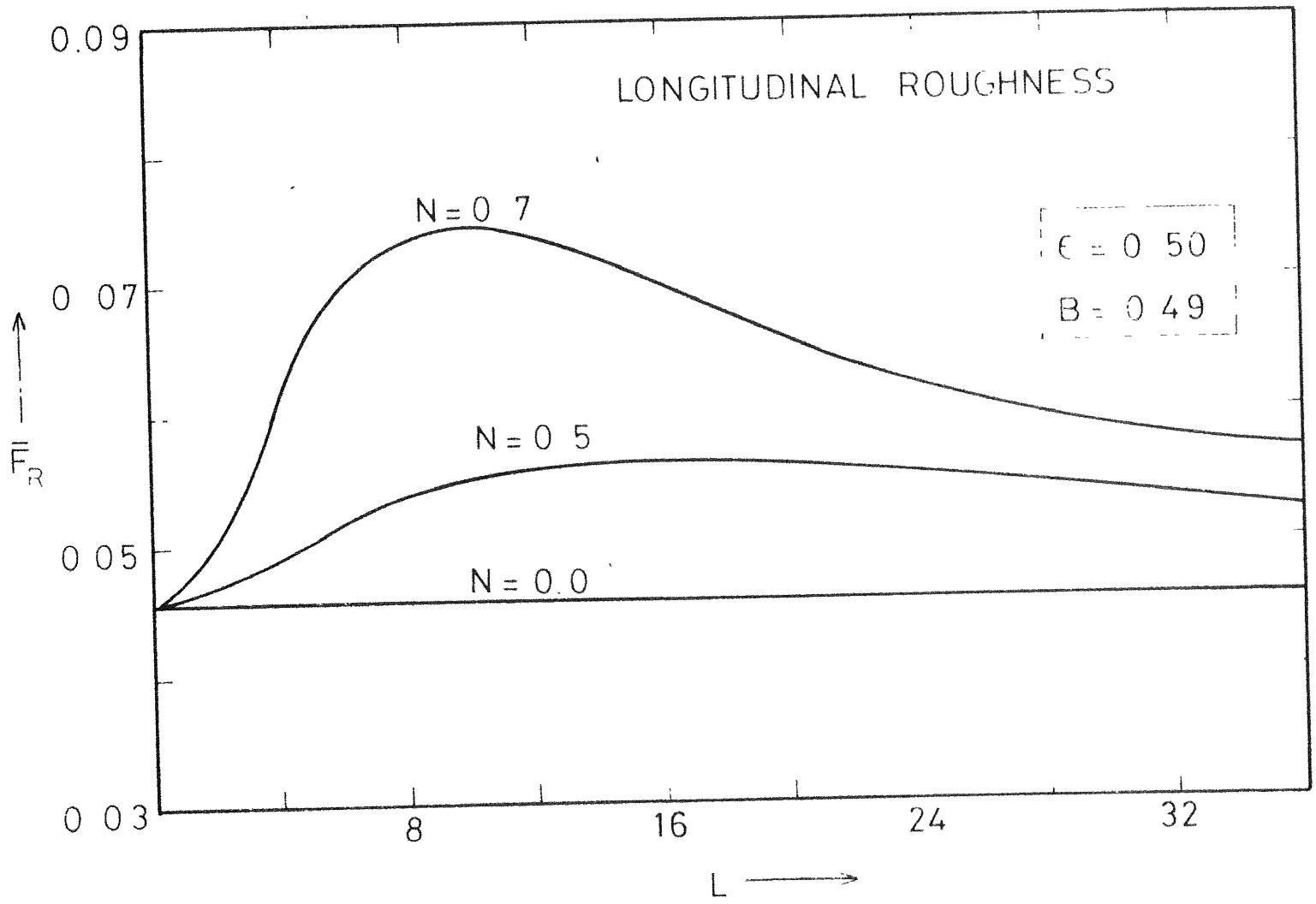

Fig.6·6 Frictional drag parameter $\bar{F}_R$ vs. length ratic parameter L for various values of coupling number N (B = 0·49 longitudinal roughness)

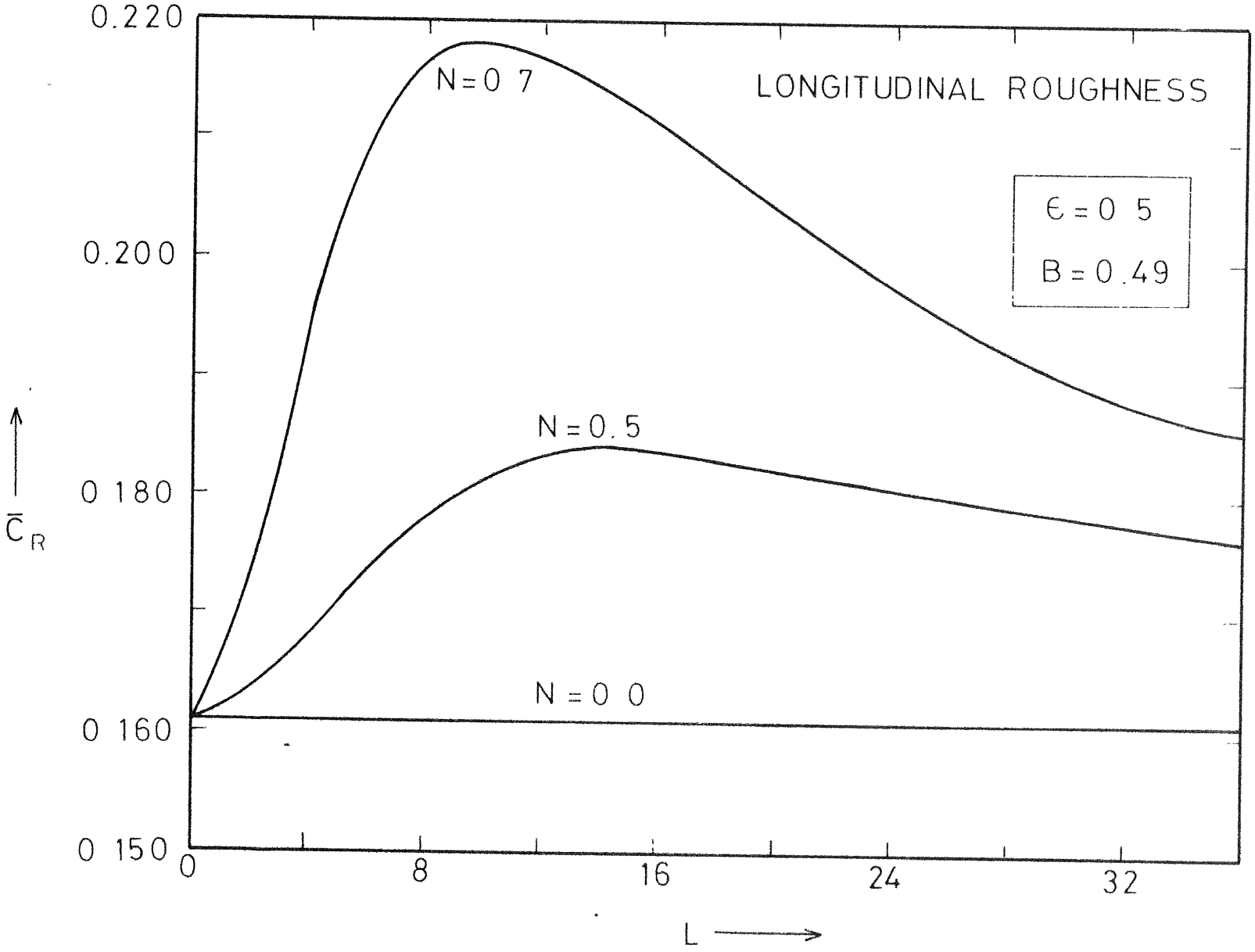

Fig.6·7 Coefficient of friction parameter $\bar{C}_R$ vs. length ratio parameter L for various values of coupling number N (B=0·49, longitudinal roughness)

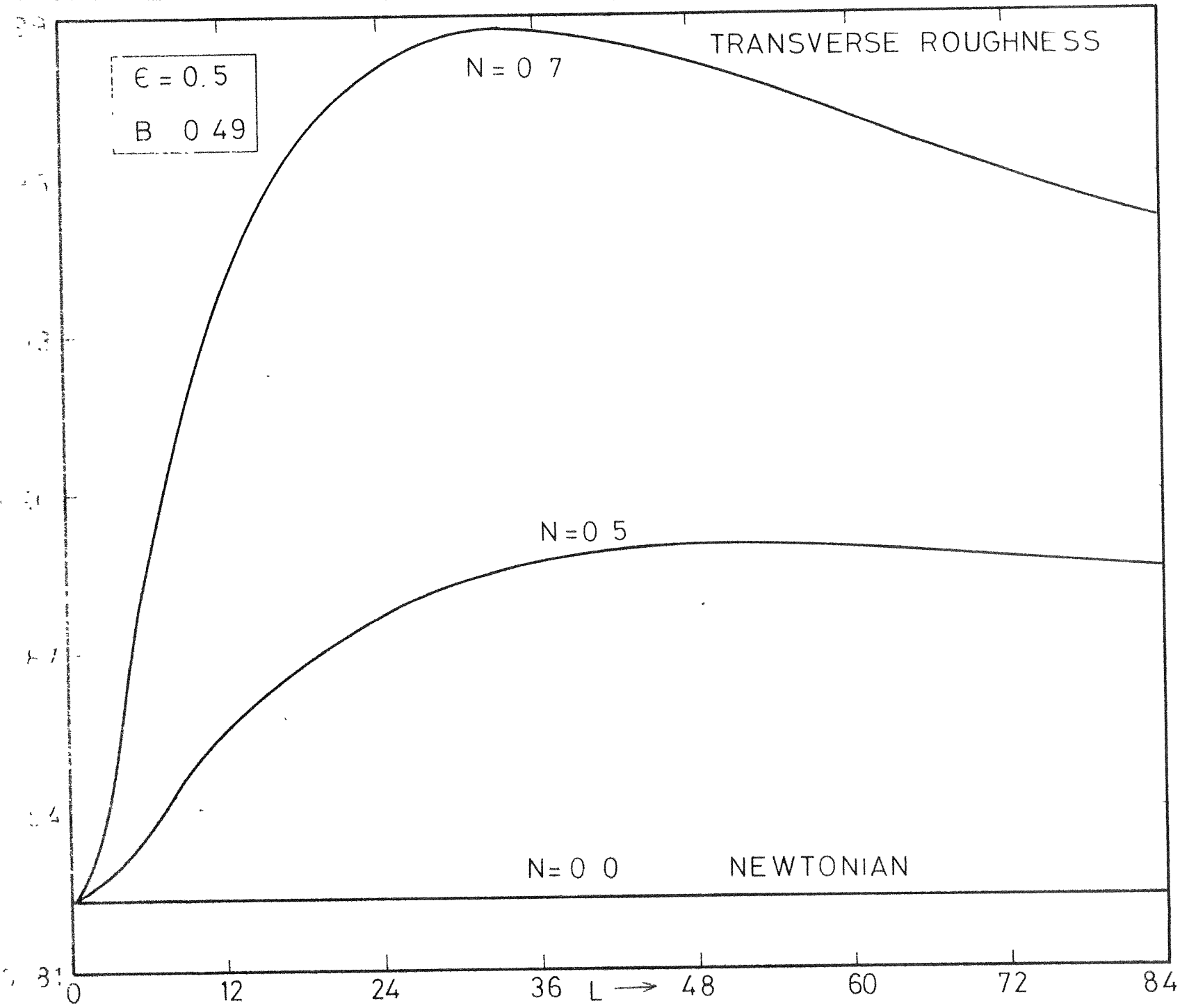

Fig. 8 Load parameter $\overline{W}_R$ vs. length ratio parameter L for various values of coupling number N (B=0·49, transverse roughness)

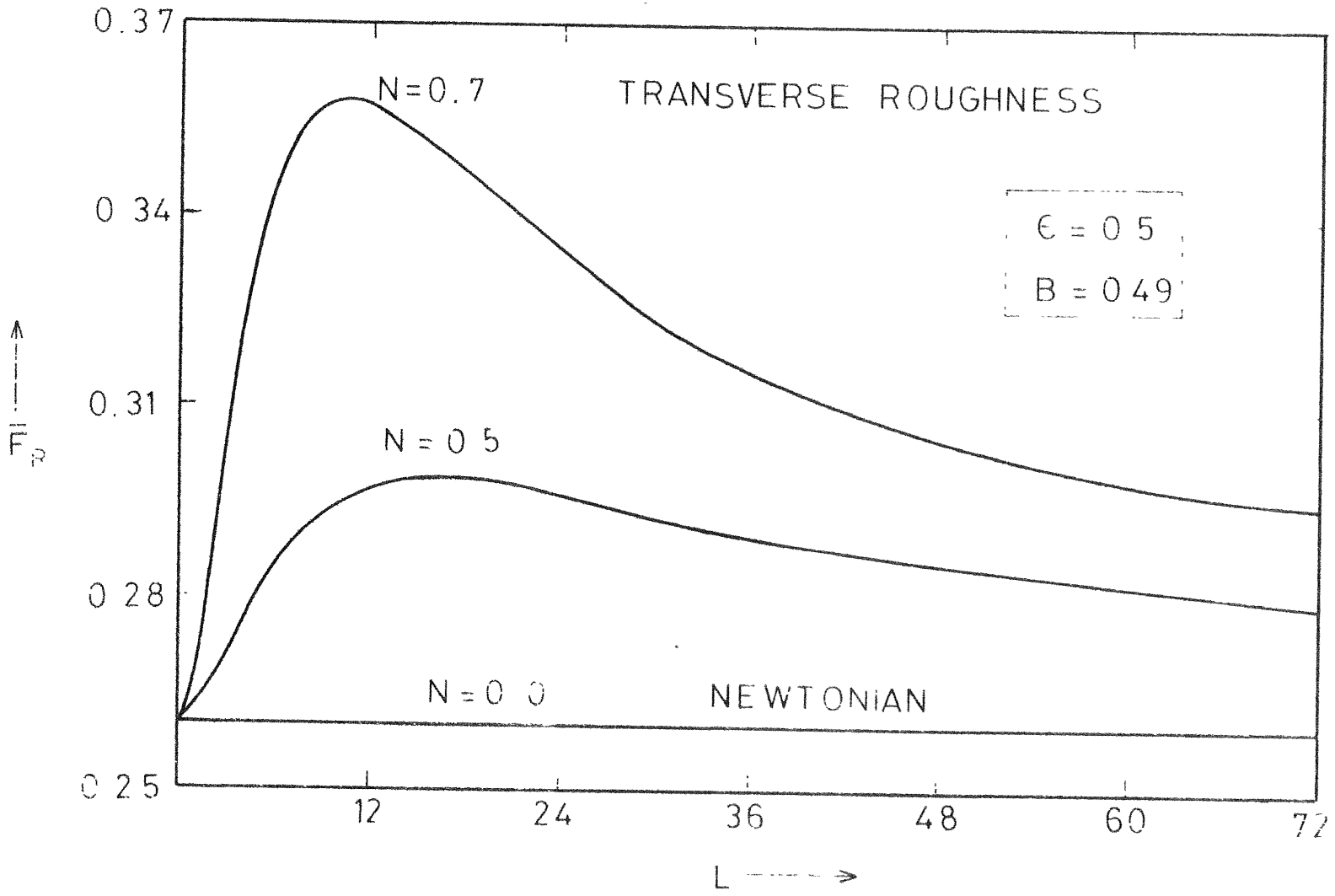

Fig.6·9 Frictional drag parameter $\bar{F}_R$ vs length ratio parameter L for various values of coupling number N (B=0·49 transverse roughness)

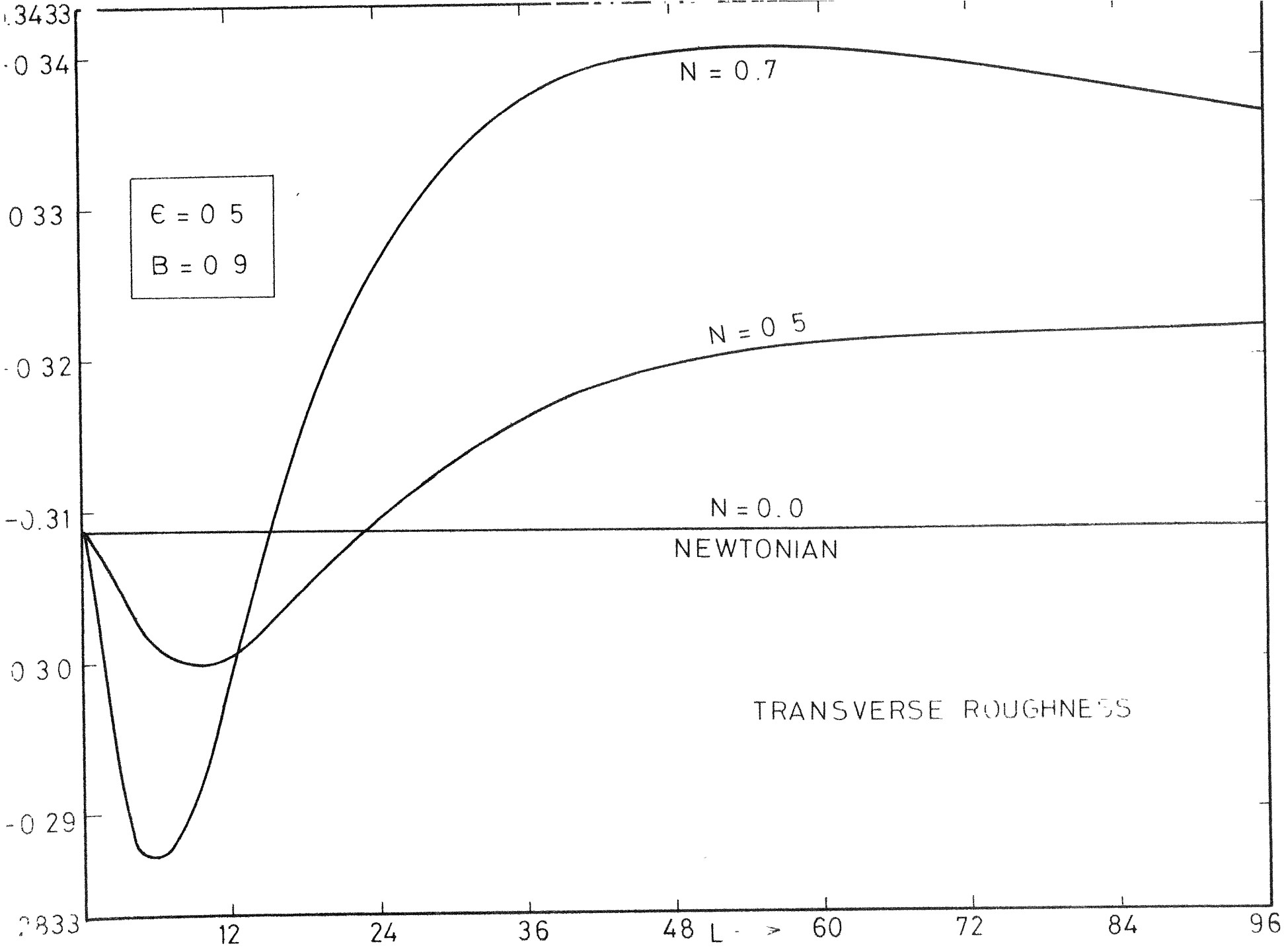

Fig.6.10 Coefficient of friction parameter $\bar{C}_R$ vs. length ratio parameter L for various values of coupling number N (B = 0·49 transverse roughness)

CHAPTER VII

SQUEEZE FILMS BETWEEN ROUGH SURFACES

7.1 INTRODUCTION

A number of experiments in which the evidence of rheological abnormalities, like enhancement of viscosity, has been rather extensive and convincing, are of squeeze film type. For example Needs [22] conducted a series of experiments to detect the influence of boundary surface on the viscosity of lubricant films between two optically plane parallel circular disks approaching each other with no tangential velocity. He measured film thickness down to 0.000635 mm. For values less than 0.00127 mm an increasing discrepancy appeared between measured and theoretical (as predicted by the classical Newtonian theory) intervals of time. It actually took longer time for plates to approach than what was predicted by the theory, indicating that the effective viscosity of the lubricant in such thin films had somehow increased. Effective viscosity in the boundary film nearly five times the bulk value was observed. No conclusive explanation could be offered except to suggest that the proximity of the metal surfaces influenced the viscosity of the fluid, causing the fluid to become more rigid.

Experiments by Fuks [28,29] also fall under the same category. Various fluids (like solution of pure fatty acids in

pure hydrocarbon solvent) were squeezed between two plates submerged in the fluid and measuring the gap between the plates as a function of time. It was observed that even after squeezing for a very long time a residual film remained between the plates.

More recent experiments of this type are by Drauglis et.al [31] and Askwith, Cameron and Gohar [36] . In the experiment of Drauglis et.al. results similar to Fuks [28,29] were obtained, residual films were observed only in the presence of additives. However in Askwith et.al [36] squeeze film studies showed that the plates came to rest at a separation of about 2×10^{-4} mm with all fluids, even pure Cetane.

It has been suggested that asperities on the solid surface might account for the residual film. Also dirt and undissolved materials in the films have been invoked as the explanation for this residual film [30] . According to Drauglis et.al [31] "if the data of Fuks are all to be explained in this manner, then one must postulate dirt which changes its properties with temperature length of molecule of additive and concentration of additive but such dirt would be a most unusual material".

A proper theoretical explanation of the residual film reported by various workers is therefore clearly needed for a better understanding of thin film lubrication technology , especially when the height of the roughness asperities is of the same order as that of the thin films.

Motivated by these considerations the squeeze film problems have been studied by various authors [55,68-71,75,76] from **microcontinuum** view point. Inherent in all earlier theoretical analyses for squeeze films including those from the microcontinuum view point was a fundamental assumption of perfectly smooth surfaces. It has long been recognized that owing to machining limitations, this assumption is rather unrealistic, particularly in bearings where the bearing clearance is very small. Of interest, in this direction are the works of Prakash and Tonder [104] who studied squeeze films between rough circular plates and Prakash and Christensen [105] who studied squeeze films between rough rectangular plates. In analyzing the roughness effects use was made of the stochastic models for hydrodynamic lubrication of rough surfaces developed by Christensen and Tonder [99,100] and Christensen [101] for Newtonian fluids.

Hence in this Chapter, the lubrication theory for micropolar fluid for rough surfaces, advanced in Chapter VI, is applied to the squeezing between parallel plates. Three standard geometries have been analyzed, i.e. two dimensional parallel plates (Fig.7.1(a)), circular plates and rectangular plates (Fig.7.1(b)) (three dimensional). It is our strong belief that this theory could provide a proper theoretical explanation to the existence of residual films.

The application of this theory may be found in the lubrication of rough surfaces where long chain length additives are used in

lubricants. An example to this context is the skidding of a rolling pneumatic tyre, even at low vehicle velocities on a wet surface. The main feature contributing to this skidding is the existence of a squeeze film in the contact area between tyre and surface. This could be done by minimizing the sinkage time. The behaviour of a tyre element in this zone may be idealized by the parallel plate squeeze film onto a rough surface and the fluid in between as a micropolar fluid on account of suspension of rigid particle additives (e.g. dirt particles). A theoretical and experimental study of such a situation has been made by Moore [106] , where the asperity height of a randomly rough surface have all been assumed same.

Further application of this study may be found in human joint lubrication where the mechanism is of squeeze film type. The lubricating synovial fluid in joints can be considered as a micropolar fluid and the cartilage surfaces rough (a detailed justification is given in Chapter VIII).

7.2 MATHEMATICAL ANALYSIS

The generalized forms of Reynolds equation for rough surfaces from the microcontinuum approach have been derived in Chapter VI. For squeezing, equations (6.11), (6.15) and (6.19) reduce, respectively, to the following ,

Longitudinal, one-dimensional roughness,

$$\frac{\partial}{\partial x}\{E(f(N,\ell,h))\frac{\partial E(p)}{\partial x}\}+\frac{\partial}{\partial z}\{(E(f(N,\ell,h)^{-1}))^{-1}\frac{\partial E(p)}{\partial z}\}$$

$$=\mu\frac{\partial E(h)}{\partial t} \tag{7.1}$$

Transverse, one-dimensional roughness,

$$\frac{\partial}{\partial x}\{(E(f(N,\ell,h)^{-1}))^{-1}\frac{\partial E(p)}{\partial x}\}+\frac{\partial}{\partial z}\{E(f(N,\ell,h))\frac{\partial E(p)}{\partial z}\}$$

$$=\mu\frac{\partial E(h)}{\partial t} \tag{7.2}$$

Isotropic roughness,

$$\frac{\partial}{\partial x}\{E(f(N,\ell,h))\frac{\partial E(p)}{\partial x}\}+\frac{\partial}{\partial z}\{E(f(N,\ell,h))\frac{\partial E(p)}{\partial z}\}$$

$$=\mu\frac{\partial E(h)}{\partial t} \tag{7.3}$$

where

$$h = h_n(x,z,t) + h_s(x,z) \tag{7.4}$$

$$E(\ ) = \int_{-\infty}^{\infty} (\ )\, f(h_s)\, dh_s \tag{7.5}$$

$f(h_s)$ is the roughness distribution function of the random variable h_s given by eqn. (6.20). N and ℓ are defined in (2.18) and $f(N,\ell,h)$ by eqn. (2.55).

Since the roughness distribution function is assumed to be symmetric,

$$E(h) = h_n \tag{7.6}$$

7.3 SQUEEZE FILMS BETWEEN ROUGH INFINITELY LONG PARALLEL PLATES

(i) Longitudinal, One-Dimensional Roughness

For this type of roughness, the ridges and valleys are assumed to be running along x-direction.

The film thickness assumes the form

$$h = h_n(t) + h_s(z) \tag{7.7}$$

and the one-dimensional Reynolds equation, from eqn. (7.1), is

$$\frac{d}{dx}\left\{E(f(N,\ell,h)\,\frac{dE(p)}{dx}\right\} = \mu\,\frac{dh_n}{dt} \tag{7.8}$$

The pressure boundary conditions are

$$E(p) = o, \text{ at } x = \ell_1 \tag{7.9}$$

$$\frac{dE(p)}{dx} = o \ (E(p) \text{ maximum}), \text{ at } x = o \tag{7.10}$$

where ℓ_1 is the half x-dimension of the plate. The mean pressure distribution is

$$E(p) = -\frac{1}{2}\,\mu\,\frac{dh_n}{dt}\,(x^2 - \ell_1^2)\,\frac{1}{E(f(N,\ell,h))} \tag{7.11}$$

The expected value of load carrying capacity per unit width is

$$E(W) = 2\int_o^{\ell_1} E(p)\,dx \tag{7.12}$$

or

$$E(W) = -\frac{2}{3}\,\mu\,\ell_1^3\,\frac{dh_n}{dt}\,\frac{1}{E(f_1(N,\ell,h))} \tag{7.13}$$

The non-dimensional load carrying capacity is

$$\overline{E(W)} = \frac{E(W)}{\left(-\frac{2u}{3}\frac{\ell^3}{h_n^3}\frac{1}{dt}\frac{dh_n}{dt}\right)} = \frac{1}{F_1(N,L,B)} \tag{7.14}$$

where

$$F_1(N,L,B) = \frac{35}{32B^7}\int_{-B}^{B}(B^2-H_s^2)^3 \left\{\frac{(1+H_s)^3}{12} + \frac{(1+H_s)}{L^2} - \frac{N}{2L}(1+H_s)^2 \coth\frac{NL}{2}(1+H_s)\right\} dH_s \tag{7.15}$$

and

$$H_s = \frac{h_s}{h_n}, \quad L = \frac{h_n}{\ell}, \quad B = \frac{b}{h_n} \tag{7.16}$$

The time of approach, t, from an initial (nominal) film thickness h_{n_i} to a final (nominal) film thickness h_n, is given by

$$t = -\frac{2}{3}\frac{\mu\ell^3}{E(W)}\frac{1}{\int_{h_{n_i}}^{h_n}\frac{dh_n}{E(f(N,\ell,h))}} \tag{7.17}$$

The non-dimensional time of approach is

$$T = \frac{t}{\frac{1}{h_{n_i}^2}\left(\frac{2}{3}\frac{\mu\ell^3}{E(W)}\right)} = -\int_1^{H_n}\frac{dH_n}{F_2(N,L,H_n,B)} \tag{7.18}$$

where

$$F_2(N,L,H_n,B) = \frac{35}{32B^7} \int_{-B}^{B} (B^2-H_s^2)^3 \left\{ \frac{(H_n+H_s)^3}{12} + \frac{(H_n+H_s)}{L^2} - \frac{N(H_n+H_s)^2}{2L} \coth \frac{NL}{2}(H_n+H_s) \right\} dH_s \qquad (7.19)$$

and

$$H_n = \frac{h_n}{h_{n_i}}, \quad H_s = \frac{h_s}{h_{n_i}}, \quad L = \frac{h_{n_i}}{\ell}, \quad B = \frac{b}{h_{n_i}} \qquad (7.20)$$

(ii) Transverse, One-Dimensional Roughness

In this roughness, the ridges and valleys are assumed to be running perpendicular to x-direction.

The corresponding Reynolds equation, from eqn.(7.2), is

$$\frac{d}{dx}\left\{ (E(f(N,\ell,h)^{-1}))^{-1} \frac{dE(p)}{dx} \right\} = \mu \frac{dh_n}{dt} \qquad (7.21)$$

where

$$h = h_n(t) + h_s(x) \qquad (7.22)$$

Proceeding in a way similar to longitudinal roughness the average value of squeeze film characteristics are given by

$$E(W) = -\frac{2}{3} \mu \ell_1^3 \frac{dh_n}{dt} E\left(\frac{1}{F(N,\ell,h)}\right) \qquad (7.23)$$

$$t = -\frac{2}{3} \frac{\mu \ell_1^3}{E(W)} \int_{h_{n_i}}^{h_n} E\left(\frac{1}{f(N,\ell,h)}\right) dh_n \qquad (7.24)$$

The dimensionless load capacity and squeeze time are

$$E\overline{(W)} = F_3(N,L,B) \tag{7.25}$$

$$T = -\int_1^{H_n} F_4(N,L,H_n,B)\, dH_n \tag{7.26}$$

where

$$F_3(N,L,B) = \frac{105}{8B^7}\int_{-B}^{B} \frac{(B^2-H_s^2)^3\, dH_s}{\left\{(1+H_s)^3+\frac{12(1+H_s)}{L^2}-\frac{6N(1+H_s)^2}{L}\coth\frac{NL}{2}(1+H_s)\right\}} \tag{7.27}$$

$$F_4(N,L,H_n,B) = \frac{105}{8B^7}\int_{-B}^{B} \frac{(B^2-H_s^2)^3\, dH_s}{\left\{(H_n+H_s)^3+12(H_n+H_s)-\frac{6N(H_n+H_s)^2}{L}\coth\frac{NL}{2}(H_n+H_s)\right\}} \tag{7.28}$$

and the other non-dimensional parameters for load capacity are defined according to eqn. (7.16) and for squeeze time as per eqn. (7.20).

(iii) Isotropic Roughness

The roughness is uniformly distributed over the surface of the plate. For two dimensional geometries the isotropic roughness will be equivalent to longitudinal roughness.

7.4 SQUEEZE FILM BETWEEN ROUGH CIRCULAR PLATES

(i) Radial, One-Dimensional Roughness

In this model, the roughness is assumed to have the form of long narrow ridges and valleys running in radial direction, and, therefore, film thickness assumes the form

$$h = h_n(t) + h_s(\theta) \tag{7.29}$$

The governing differential equation, from eqn. (7.1) in polar co-ordinates, is

$$\frac{1}{r}\frac{\partial}{\partial r}\{r\,E(f(N,\ell,h))\,\frac{\partial E(p)}{\partial r}\} + \frac{1}{r^2}\frac{\partial}{\partial \theta}\left(E\left(f(N,\ell,h)^{-1}\right)\right)^{-1}\frac{\partial E(p)}{\partial \theta}\} = \mu\frac{\partial h_n}{\partial t} \tag{7.30}$$

For an axisymmetry case, eqn. (7.30) reduces to

$$\frac{1}{r}\frac{d}{dr}\{rE\,(f(N,\ell,h))\,\frac{dE(p)}{dr}\} = \mu\frac{dh_n}{dt} \tag{7.31}$$

The boundary conditions for average pressure are

$$E(p) = o, \text{ at } \quad r = r_1 \tag{7.32}$$

$$\frac{dE(p)}{dr} = o \ (E(p) \text{ maximum}), \text{ at } r = o \tag{7.33}$$

where r_1 is the radius of the circular plate.

The mean pressure distribution is given by

$$E(p) = -\frac{\mu}{4}\frac{dh_n}{dt}(r_1^2-r^2)\frac{1}{E(f(N,\ell,h))} \tag{7.34}$$

The average instantaneous load capacity and time of squeezing are

$$E(W) = \int_0^{r_1} 2\pi r\, E(p)\, dr$$

$$= -\frac{\pi}{8}\frac{\mu\, dh_n}{dt} r_1^4 \frac{1}{E(f(N,\ell,h))} \tag{7.35}$$

$$t = -\frac{\pi\mu r_1^4}{8E(W)} \int_{h_{n_i}}^{h_n} \frac{dh_n}{E(f(N,\ell,h))} \tag{7.36}$$

The non-dimensional load carrying capacity and squeeze time are

$$\overline{E(W)} = \frac{E(W)}{\left(-\frac{\pi\mu}{8}\frac{dh_n}{dt}\frac{r_1^4}{h_n^3}\right)} = \frac{1}{F_1(N,L,B)} \tag{7.37}$$

$$T = \frac{t}{\left(+\frac{\pi}{8}\frac{\mu r_1^4}{E(W)}\right)\frac{1}{h_{n_i}^2}} = -\int_1^{H_n} \frac{dH_n}{F_2(N,L,H_n,B)} \tag{7.38}$$

where $F_1(N,L,B)$ is defined by eqn. (7.15) and $F_2(N,L,H_n,B)$ by eqn. (7.19) and the non-dimensional parameters for load are according to (7.16) and for squeeze time as per eqn. (7.20).

(ii) Circumferential, One-Dimensional Roughness

In this model, the ridges and valleys are assumed to be running along θ direction. The film thickness is

$$h = h_n(t) + h_s(r) \tag{7.39}$$

The corresponding Reynolds equation, from eqn. (7.2), in polar co-ordinates, is

$$\frac{1}{r}\frac{\partial}{\partial r}\left\{ r\left(E\left(f(N,\ell,h)^{-1}\right)\right)^{-1} \frac{\partial E(p)}{\partial r}\right\}$$

$$+ \frac{1}{r^2}\frac{\partial}{\partial \theta}\left\{E(f(N,\ell,h)) \frac{\partial E(p)}{\partial \theta}\right\} = \mu \frac{\partial h_n}{\partial t} \tag{7.40}$$

For an axisymmetry case eqn. (7.40) reduces to.

$$\frac{1}{r}\frac{d}{dr}\left\{ r\left(E\left(\left(f(N,\ell,h)^{-1}\right)\right)\right)^{-1} \frac{dE(p)}{d\theta}\right\}$$

$$= \mu \frac{dh_n}{dt} \tag{7.41}$$

Proceeding in a similar way as in the case of radial roughness, the load capacity, squeeze time and their non-dimensional forms are given by

$$E(W) = -\frac{\pi}{8} \frac{\mu dh_n}{dt} r_1^4 \, E\left(\frac{1}{f(N,\ell,h)}\right) \tag{7.42}$$

$$t = -\frac{\pi\mu}{8E(W)} r_1^4 \int_{h_{n_i}}^{h_n} E\left(\frac{1}{f(N,\ell,h)}\right) dh_n \tag{7.43}$$

and

$$\overline{E(W)} = \frac{E(W)}{\left(-\frac{\pi}{8}\mu \frac{dh_n}{dt}\frac{r_1^4}{h_n^3}\right)} = F_3(N,L,B) \tag{7.44}$$

$$T = \frac{t}{\left(\frac{\pi \mu r_1^4}{8h_{n_i}^2 E(W)}\right)} = -\int_1^{H_n} F_4(N,L,H_n,B)\, dH_n \tag{7.45}$$

where $F_3(N,L,B)$ is defined by eqn. (7.27) and $F_4(N,L,H_n,B)$ by eqn. (7.28) and the other non-dimensional parameters for load capacity are defined by eqn. (7.16) and for time height relation by eqn. (7.20).

(iii) Isotropic Roughness

The modified form of Reynolds equation, from eqn. (7.3), in polar form, is

$$\frac{1}{r}\frac{\partial}{\partial r}\left\{rE(f(N,\ell,h))\frac{\partial E(p)}{\partial r}\right\} + \frac{1}{r^2}\frac{\partial}{\partial \theta}\left\{E(f(N,\ell,h))\frac{\partial E(p)}{\partial \theta}\right\} = \mu \frac{\partial h_n}{\partial t} \tag{7.46}$$

For axisymmetry case the form of isotropic roughness will be identical to radial roughness.

It is evident that the qualitative and quantitative effects of roughness will be same for both the geometries, i.e.

infinitely long parallel plates and circular plates (axisymmetry case). Hence the results are given only for circular plates.

7.5 SQUEEZING BETWEEN ROUGH RECTANGULAR PLATES

The previous sections were concerned with the one-dimensional problems. Therefore the side leakage effects, the width/length ratio effects for unidirectional roughness were not detected. Moreover the distinction between the isotropic roughness and the one-dimensional roughness could not be made. Hence, in this section, the problem of squeezing between rectangular plates is analyzed in order to study the effects of aspect ratio (width/length ratio) on the lubrication of rough surfaces with micropolar fluids. The geometry of the system is shown in Fig.7.1(b).

Since there is no relative tangential velocity between the surfaces and because of symmetry, the one-form of one-dimensional roughness can be obtained from the other, simply by a rotation of co-ordinate axes. Hence, only the case of one-dimensional roughness, with roughness having forms of long narrow ridges and valleys running in the x-direction is studied. This will be termed as 'Unidirectional Roughness'. The case of isotropic roughness is also analyzed.

(i) Unidirectional Roughness

Since, in this model, the roughness is assumed to have the form of long, narrow ridges and valleys running in the x-direction,

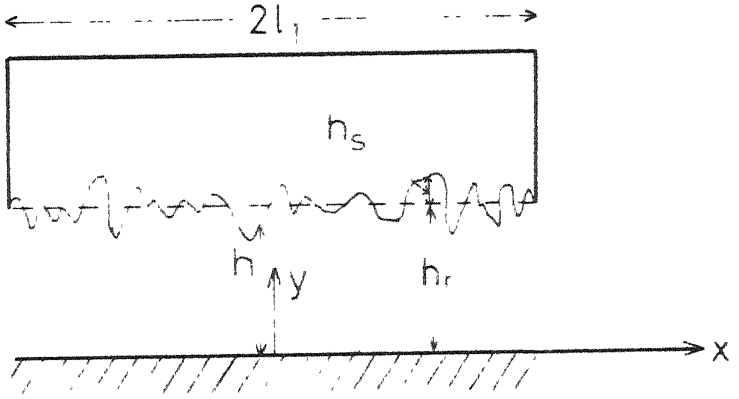

Fig 7·1(a) Schematic diagram of a squeeze plate

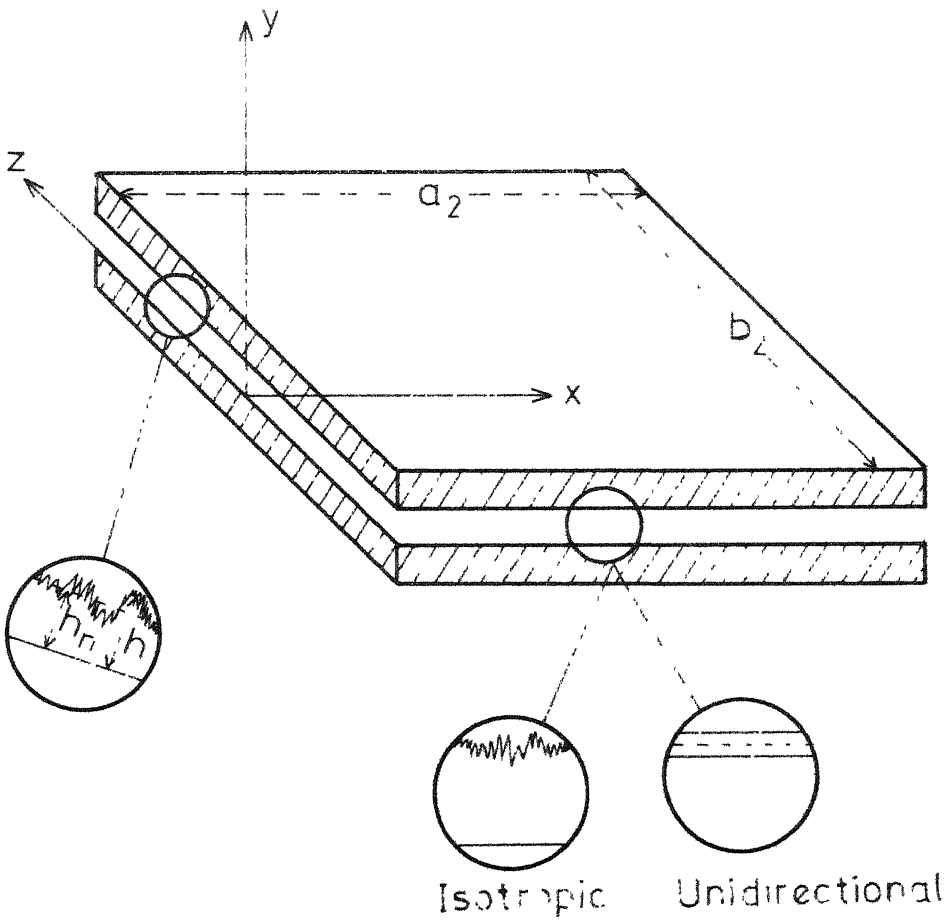

Fig. 7·1 (b) Schematic diagram of a rough rectangular plate

the film thickness assumes the form

$$h = h_n(t) + h_s(z) \tag{7.47}$$

The corresponding Reynolds type equation, from eqn. (7.1), is

$$\frac{\partial}{\partial x}\{E(f(N,\ell,h)\frac{\partial E(p)}{\partial x}\} + \frac{\partial}{\partial z}\{(E(f(N,\ell,h)^{-1}))^{-1}\frac{\partial E(p)}{\partial z}\} = \mu\frac{\partial h_n}{\partial t} \tag{7.48}$$

Equation (7.48) can be written as

$$\frac{\partial^2 E(p)}{\partial x^2} + \delta_R^2\frac{\partial^2 E(p)}{\partial z^2} = \frac{\mu}{E(f(N,\ell,h))}\frac{\partial h_n}{\partial t} \tag{7.49}$$

where

$$\delta_R = \delta_R(N,\ell,h_n) = \{E(f(N,\ell,h)) \times E(\frac{1}{f(N,\ell,h)})\}^{\frac{1}{2}} \tag{7.50}$$

Equation (7.49) is Poisson-type equation and can be solved by usual separation of variable techniques with the boundary conditions

$$E(p) = o \quad \text{at } x = o \text{ and } x = a_2 \tag{7.51}$$

$$E(p) = o \quad \text{at } z = \pm\frac{b_2}{2} \tag{7.52}$$

to give the mean pressure distribution

$$E(p) = \frac{4\mu a_2^2\frac{dh_n}{dt}}{\pi^3 E(f(N,\ell,h))}\sum_{n=1,3,5}^{\infty}\frac{1}{n^3}\left(\frac{\cosh\frac{n\pi z}{a_2\delta_R}}{\cosh\frac{n\pi b_2}{2a_2\delta_R}} - 1\right)\times \sin\frac{n\pi x}{a_2} \tag{7.53}$$

where a_2 is the x-dimension and b_2 is the z-dimension of the rectangular plates.

The mean instantaneous load carrying capacity is

$$E(W) = \int_{-b_2/2}^{b_2/2} \int_{0}^{a_2} E(p)\, dx\, dz \tag{7.54}$$

or

$$E(W) = \frac{16\mu a_2^3}{\pi^4} \left(\frac{dh_n}{dt}\right) \frac{1}{E(f(N,\ell,h))} \times$$

$$\times \sum_{n=1,3,5}^{\infty} \left(\frac{a_2 \delta_R}{n^5 \pi} \tanh \frac{n\pi b_2}{2a_2 \delta_R} - \frac{b_2}{2n^4}\right) \tag{7.55}$$

The non-dimensional load carrying capacity is

$$\overline{E(W)} = \frac{E(W)\, \pi^4 h_n^3}{16\mu A^2 \frac{dh_n}{dt}}$$

$$= \nu_A^{-2} \frac{1}{F_1(N,L,B)} \sum_{n=1,3,5}^{\infty} \left(\frac{\bar{\delta}_R}{n^5 \pi} \tanh \frac{n\pi \nu_A}{2a_1 \bar{\delta}_R} - \frac{\nu_A}{2n^4}\right) \tag{7.56}$$

where

$$\bar{\delta}_R^2 = \frac{1}{F_1 \cdot F_3}, \quad A = a_2 b_2, \quad \nu_A = \frac{b_2}{a_2} \tag{7.57}$$

$F_1(N,L,B)$ is defined by eqn. (7.15), $F_3(N,L,B)$ by eqn. (7.27) and other non-dimensional parameters, i.e. B, L, H_s are defined

according to eqn. (7.16).

The time of approach is

$$t = -\frac{48\mu a_2^3}{\pi^4 E(\mathcal{N})} \int_{h_{n_i}}^{h_n} \frac{1}{E(f(N,\ell,h))} \sum_{n=1,3,5}^{\infty} \left(\frac{a_2 \delta_R}{\pi n^5} \tanh \frac{n\pi\, b_2}{2a_2\delta_R} - \frac{b_2}{2n^4} \right) dh_n \tag{7.58}$$

The non-dimensional time of approach is

$$T = \frac{t\pi^4 E(W) h_{n_i}^2}{48\mu A^2}$$

$$= +\nu_A^{-2} \int_{H_n}^{1} \frac{1}{F_2(N,L,H_n,B)} \sum_{n=1,3,5}^{\infty} \left(\frac{\bar{\delta}_{R_1}}{\pi n^5} \tanh \frac{n\pi\nu_A}{2\bar{\delta}_{R_1}} - \frac{\nu_A}{2n^4} \right) dH_n \tag{7.59}$$

where

$$\bar{\delta}_{R_1}^2 = \frac{1}{F_2 \cdot F_4} \tag{7.60}$$

The parameters H_n, B, H_s and L are defined according to eqn. (7.20) and $F_2(N,L,H_n,B)$ by eqn. (7.19) and $F_4(N,L,H_n,B)$ by eqn. (7.28).

(ii) Isotropic Roughness

The film thickness is

$$h = h_n(t) + h_s(x,z,\xi) \tag{7.61}$$

and the Reynolds-type equation for this type of roughness is

$$\frac{\partial}{\partial x}\{E(f(N,\ell,h))\ \frac{\partial E(p)}{\partial x}\} + \frac{\partial}{\partial z}\{E(f(N,\ell,h))\ \frac{\partial E(p)}{\partial z}\}$$

$$= \mu\ \frac{\partial h_n}{\partial t} \qquad (7.62)$$

or

$$\frac{\partial^2 E(p)}{\partial x^2} + \frac{\partial^2 E(p)}{\partial z^2} = \frac{\mu}{E(f(N,\ell,h))}\ \frac{dh_n}{dt} \qquad (7.63)$$

The various bearing characteristics and their non-dimensional forms are given as

Pressure distribution,

$$E(p) = \frac{4\mu a_2^2}{\pi^3}\ \frac{dh_n}{dt}\ \frac{1}{E(f(N,\ell,h))}\ \sum_{n=1,3,5}^{\infty} \frac{1}{n^3}\left(\frac{\cosh \frac{n\pi z}{a_2}}{\cosh \frac{n\pi b_2}{2a_2}} - 1\right) \sin \frac{n\pi x}{a_2} \qquad (7.64)$$

Load capacity,

$$E(W) = K\ \frac{dh_n}{dt}\ \frac{1}{E(f(N,\ell,h))} \qquad (7.65)$$

where

$$K = \frac{16\mu a_2^3}{\pi^4}\ \sum_{n=1,3,5}^{\infty} \left(\frac{a_2}{n^5} \tanh \frac{n\pi b_2}{2a_2} - \frac{b_2}{2n^4}\right) \qquad (7.66)$$

and is independent of the roughness parameter.

Squeeze time,

$$t = \frac{K}{E(W)} \int_{h_{n_i}}^{h_n} \frac{dh_n}{E(f(N,\ell,h))} \tag{7.67}$$

The load capacity and squeezing time can be put in non-dimensional form as

$$\overline{E(W)} = \frac{E(W)}{K \frac{dh_n}{dt} h_n^3} = \frac{1}{F_1(N,L,B)} \tag{7.68}$$

$$T = \frac{t}{\left(\frac{K}{E(W)h_{n_i}^2}\right)} = - \int_1^{H_n} \frac{dH_n}{F_2(N,L,H_n,B)} \tag{7.69}$$

Thus it is evident that the qualitative effects of isotropic roughness on rectangular plate squeeze films are identical to that of radial one - dimensional roughness in circular plates(or longitudinal roughness in infinitely long parallel plates).

7.5. NUMERICAL RESULTS

The roughness effects on various bearing characteristics are studied through the following parameters

(i) Load Capacity Ratio Parameter

The load ratio parameter, $\bar{W}_R$, is defined by

$$\bar{W}_R = \frac{\overline{E(W)} - \overline{(E(W))}_{B=0}}{\overline{(E(W))}_{B=0}} \tag{7.70}$$

where $\overline{(E(W))}_{B=0}$ is the load capacity for smooth surfaces with the same nominal film thickness.

(ii) Time Ratio Parameter

The time ratio parameter, T_R, is defined by

$$T_R = \frac{T - (T)_{B=0}}{(T)_{B=0}} \tag{7.71}$$

where $(T)_{B=0}$ represents the squeeze time for smooth surfaces to reach to the same nominal film thickness. While calculating this ratio the load is assumed to be same for rough surfaces and smooth surfaces as well.

7.7 RESULTS AND DISCUSSION

(i) Dimensionless Parameters

In addition to the well known parameters for smooth squeeze films, lubricated with Newtonian fluids, four new parameters N, L, B and ν_A are introduced in the present study.

The micropolar parameters N and L have been discussed in Chapter III and the roughness parameter B in Chapter VI. Here it

suffices to say that the effects of surface roughness would be pronounced for large values of B and N and small values of L.

The non-dimensional parameter $\nu_A (= \frac{b_2}{a_2})$ is termed as aspect ratio. In case of unidirectional roughness the role of this parameter might be important because the value of ν_A will determine whether the nature of the unidirectional roughness is longitudinal or transverse.

(ii) Bearing Characteristics

Figs. 7.2 to 7.4 are the graphs for circular plates squeeze film and Figs. 7.5 to 7.7 for rectangular plates squeeze film.

Further, it should be noted that the cases of radial and circumferential roughness for circular plates are equivalent to the cases of longitudinal and transverse roughness, respectively, for the infinitely long parallel plates.

Fig. 7.2 is the graph of $\bar{W}_R$ vs. B where the nominal film height is kept constant. It is seen that when $B \leq 0.3$ the load capacity for rough surfaces does not differ significantly as compared to smooth ones. Even for micropolar fluid this assertion is true. Beyond $B > 0.3$ the roughness effects become prominent and as $B \to 1$ the load capacity is affected significantly. It is seen that the radial roughness decreases the load capacity while circumferential roughness increases it. The load capacity

for circumferential roughness may be $\frac{35}{8}$ times and for radial roughness $\frac{3}{4}$ times the load for corresponding smooth surfaces, as $B \to 1$. These limits are for Newtonian fluid and can be obtained directly from eqn.s (7.44) and (7.37) , respectively by taking the limits $B \to 1$ and $N \to o$. For micropolar fluids the rate of increase or decrease in load capacity is higher and the deviations from Newtonian rate are more prominent at higher values of roughness parameter B and higher values of N.

Fig. 7.3 and Fig. 7.4 are the graphs for T_R vs. non-dimensional film height H_n for B = o.1 and B = o.4, respectively. From Fig. 7.3 it is clear that the effects of roughness are prominent only when the roughness parameter is of the same order as the film thickness, i.e. when $\frac{B}{H_n}$ approaches unity. It is also evident that the circumferential roughness increases the sinkage time while the radial roughness decreases it and the effects of circumferential roughness are more prominent than the radial roughness. The reason being same as that given for load capacity.

Fig. 7.4 shows a similar trend as shown by Fig. 7.3, except for the accentuation of roughness effects.

Fig. 7.5 is the graph between $\bar{W}_R$ and B. It is seen that the roughness effects are significant only for B > o.4 and for values of ν_A not around 1.5. For values of ν_A around 1.5 the roughness effects are significant only for B very close to unity. Further, it is seen that the load capacity for rough plates is higher

than that for smooth plates for smaller values of ν_A (i.e. $\nu_A < 1.5$). For values of ν_A from $\nu = 1.5$ to $\nu_A = 2.0$, approximately, the load capacity decreases first, reaches a minimum, and then increases. For values of ν_A higher than 2.0 the load capacity decreases for almost all values of B. A mathematical reason for Newtonian fluids is given in the following (for micropolar fluids a similar reasoning can be advanced, however, the mathematics involved will be complicated and hence only numerical results are given in this case to illustrate a similar phenomenon).

The unidirectional roughness pattern, with roughness ridges and valleys running in x-direction, tends to increase the x-component of the flow, $E(q_x)$, whereas the flow in z-direction, $E(q_z)$, is reduced, mathematically,

$$E(q_x) = -\frac{1}{12\mu}\left\{h_n^3 + \frac{b^2}{3}h_n\right\}\frac{\partial E(p)}{\partial x} \tag{7.72}$$

and

$$E(q_z) = -\frac{1}{12\mu}\frac{32b^7}{35}\left[3(5h_n^2-b^2)(b^2-h_n^2)\log\frac{h_n+b}{h_n-b} + 2bh_n(15h_n^2-13b^2)\right]^{-1}\frac{\partial E(p)}{\partial z} \tag{7.73}$$

It is obvious from eqn. (7.72) that the flux in x-direction increases and reaches to a maximum value as $b \to h_n$ (or $B \to 1$), which is $\frac{4}{3}$ times the corresponding flux for smooth surfaces. The flux in z-direction decreases as $\frac{b}{h_n}(= B)$ increases and as $b \to h_n$ (or $B \to 1$)

it becomes $\frac{8}{35}$ times the corresponding flux for smooth surfaces.

Further, it must be noted that for a constant area bearing the component of the flow along the smaller dimension would be larger because most of the fluid would have a tendency to escape along smaller dimension. Thus if $\nu_A < 1$, $q_x < q_z$ (for smooth surfaces).

Thus when $\nu_A > \nu_c$ ($\nu_c \approx 1.5$, ν_c may be termed as critical aspect ratio) but not more than 2.0 (approximately), the x-dimension is smaller than the z-dimension and the increase in $E(q_x)$ is more than enough to offset the decrease in $E(q_z)$. This remains true for smaller values of B. For higher values of B, on the other hand, the increase in $E(q_x)$ will not be able to balance the decrease in $E(q_z)$. However when ν_A is sufficiently large, i.e. more than 2.0 (approximately), the effect of decrease in $E(q_z)$ will not be more than the effect of increase in $E(q_x)$, for a constant area bearing.

Also, the roughness effects are more pronounced for micropolar fluids, i.e. the rate of increase (for smaller values of ν_A) and the rate of decrease (for higher values of ν_A) are higher when micropolarity of the fluid is taken into consideration.

Fig. 7.6 is the graph, T_R vs. nominal film height H_n keeping the roughness parameter fixed (B = 0.2). It is seen that for smaller values of ν_A the uni-directional roughness increases the sinkage time, i.e. the behaviour is similar to that of transverse

roughness. It is seen that around $\nu_A = 1.5$ the roughness effects are not prominent. For considerably high values of ν_A, the uni-directional roughness decreases the sinkage time for all values of B.

Fig. 7.7 is the time - height relation for B = 0.4. The trend is similar to Fig. 7.6 except for the accentuation of the roughness effects due to the micropolarity.

For isotropic roughness the load capacity and sinkage time are always lower than the corresponding smooth ones. It is seen that after $\nu_A \geq 15$, the unidirectional roughness and isotropic roughness yield approximately the same results. The case of isotropic roughness from uni-directional roughness can be derived by letting $\nu_A \to \infty$.

It should, however, be remembered that the comparisons here have been made on the basis of nominal film height. Therefore, if h_n is the minimum film thickness for smooth surfaces, $h_n - b$ would be minimum film thickness for rough surfaces and hence the minimum height permissible in order to avoid a surface - to - surface contact would be much less than that in the case of smooth ones.

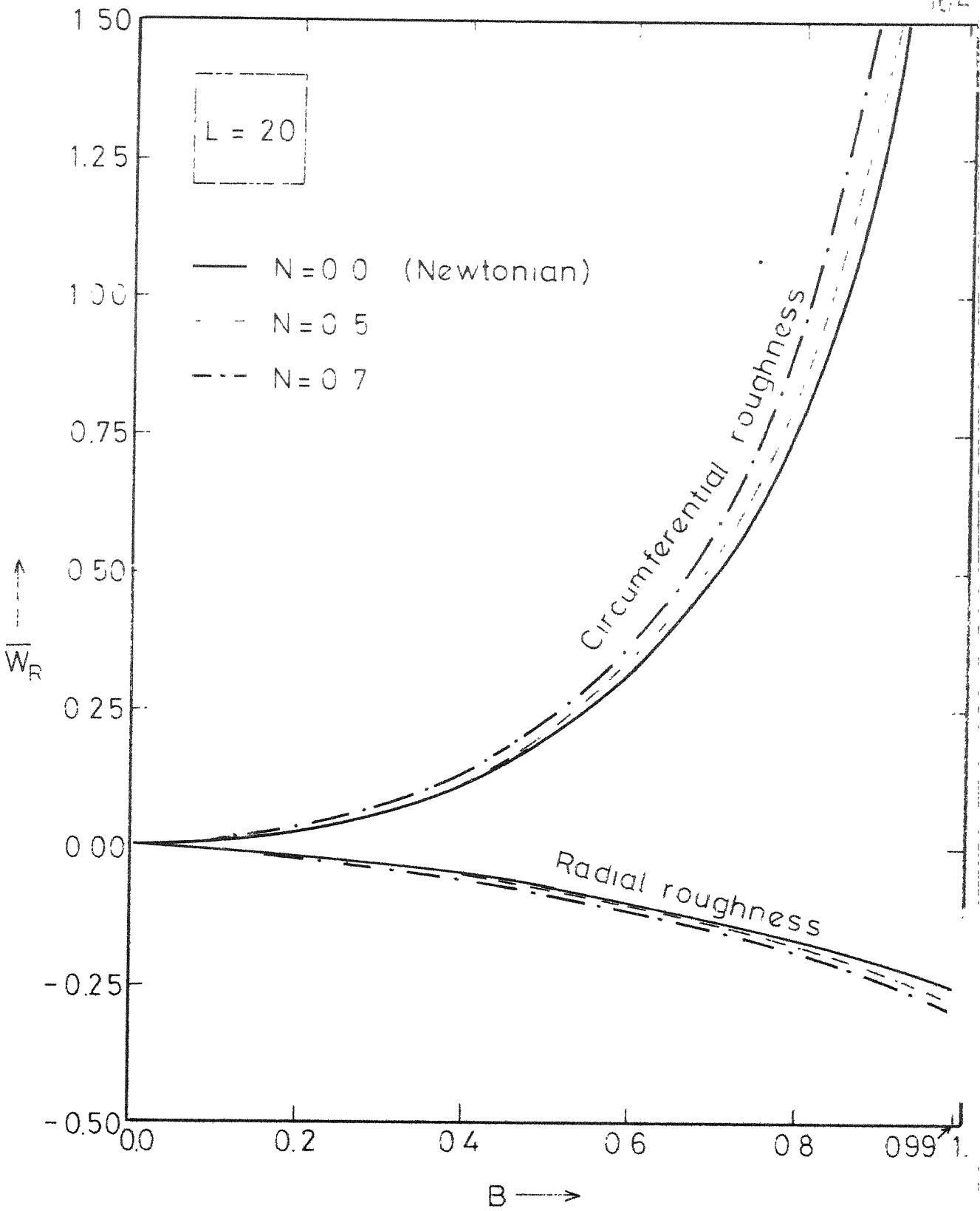

Fig.7-2 Load capacity ratio $\overline{W}_R$ vs. roughness parameter B (circular plate)

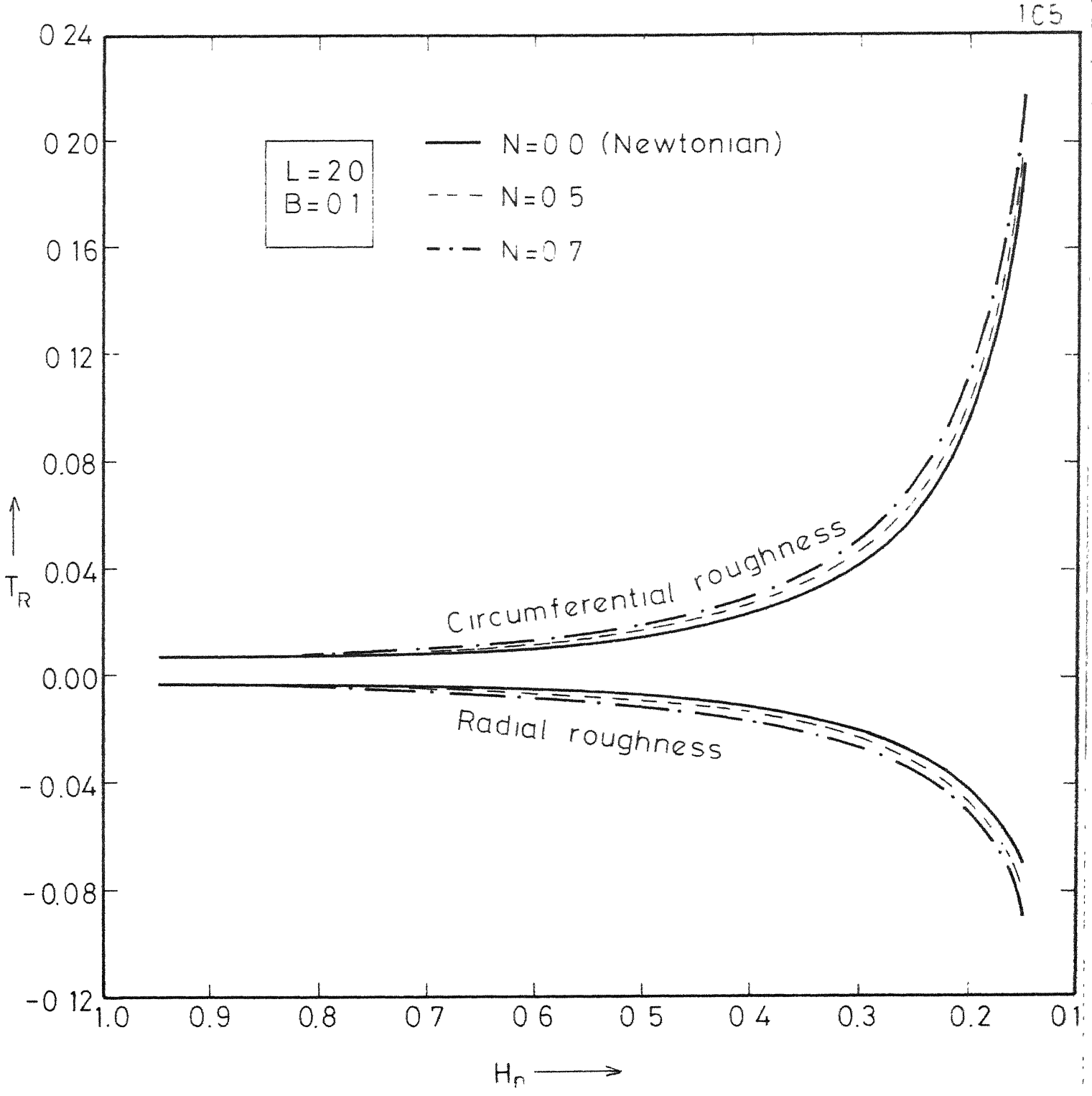

Fig. 7-3 Time ratio parameter T_R vs film thickness H_n
(B = 0·1, Circular plate)

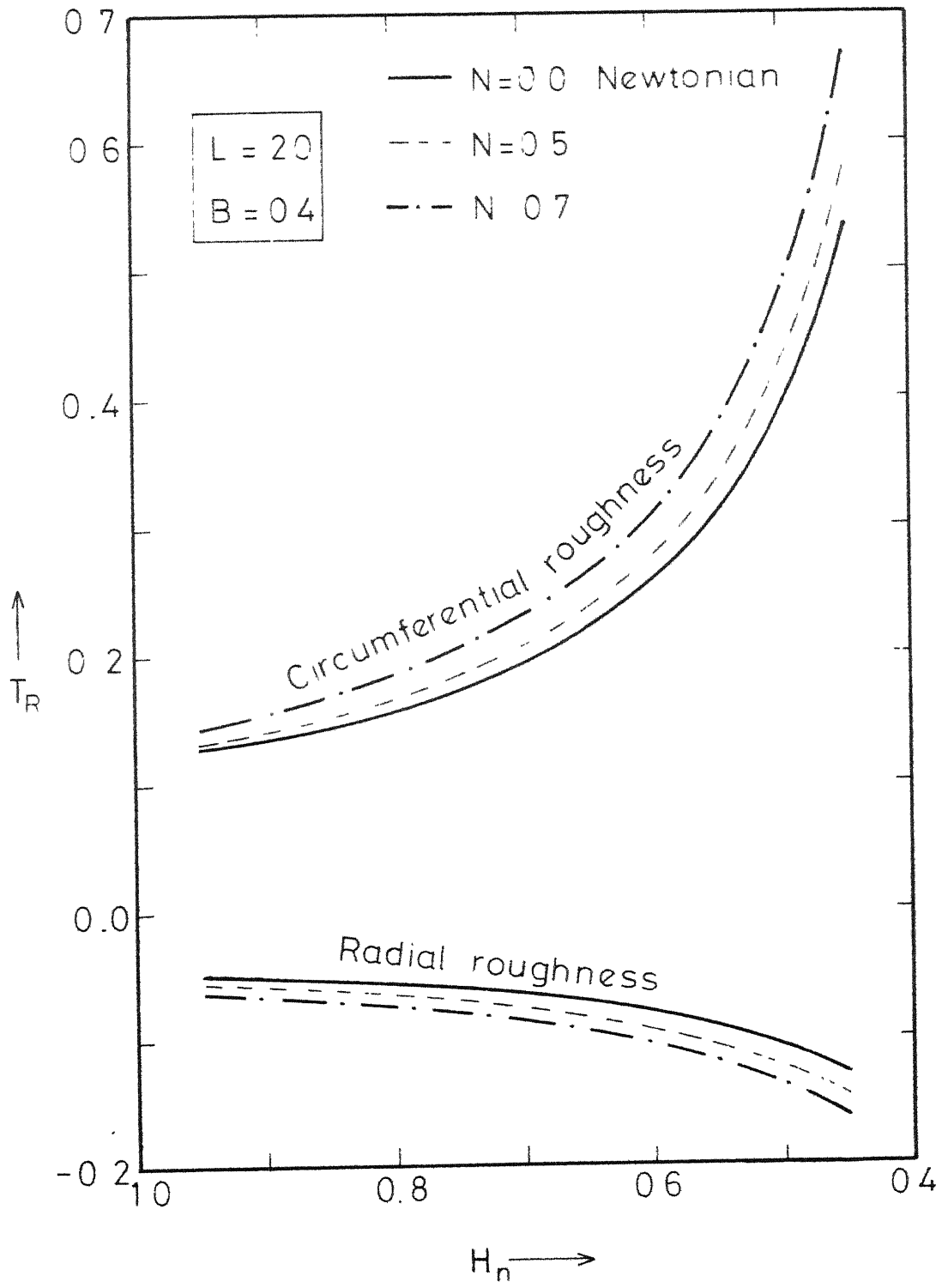

Fig.7·4 Time ratio parameter T_R vs. film thickness H_n (B = 0·4 Circular plate)

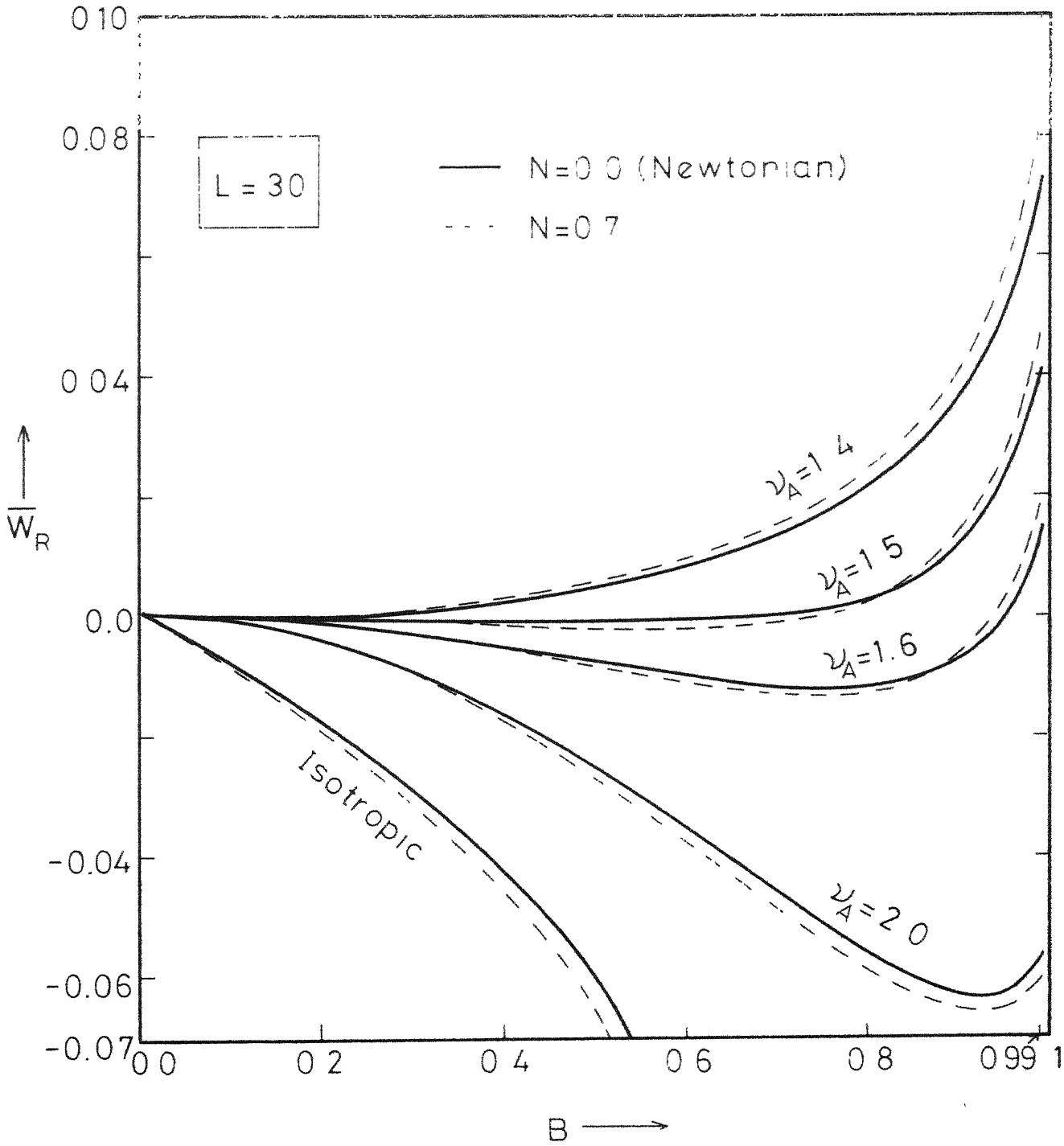

Fig.7.5 Load capacity ratio parameter $\overline{W}_R$ vs. roughness parameter. B (Rectangular plate)

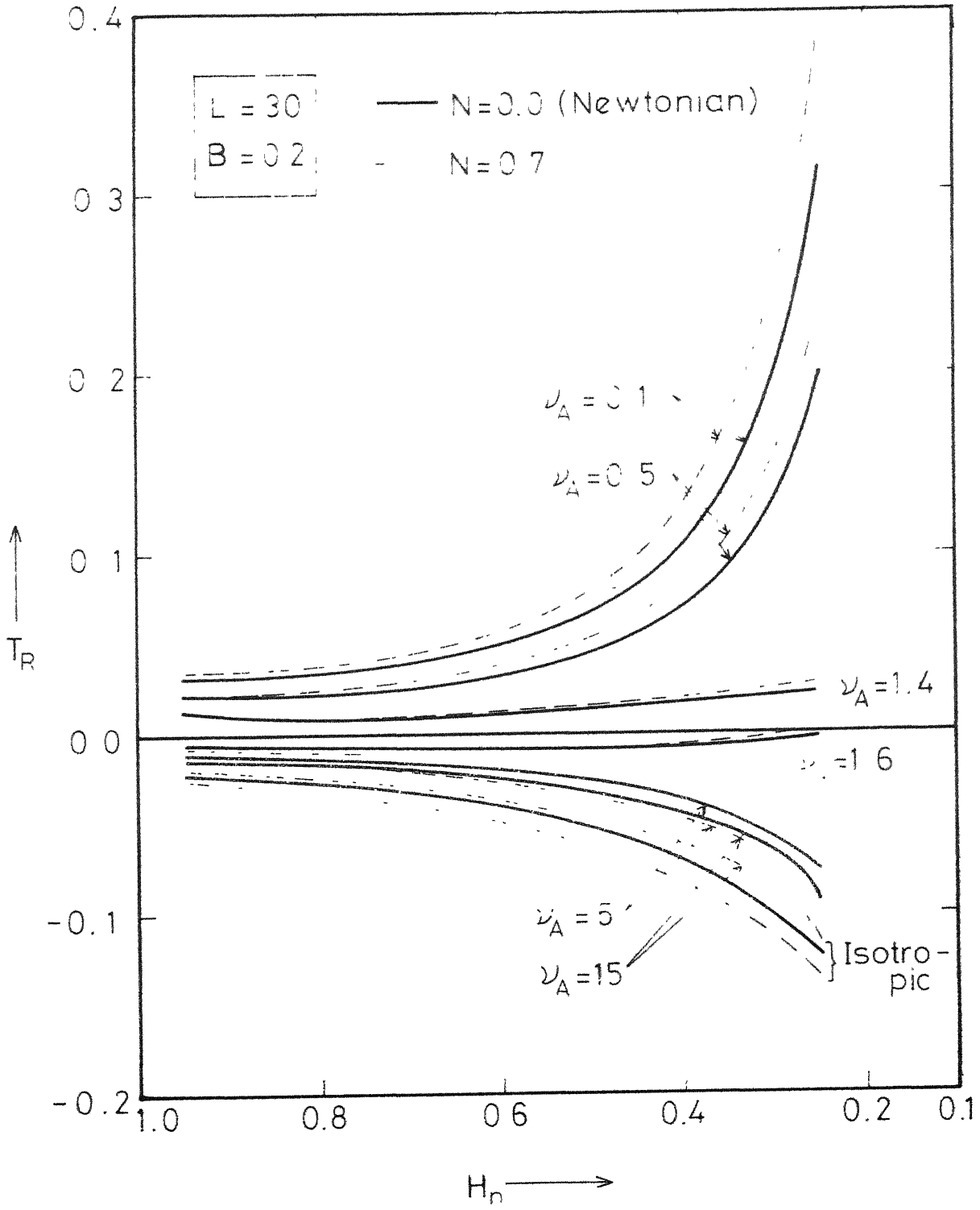

Fig. 7·6 Time ratio parameter T_R vs. film thick
H_r (B=0·2, rectangular plate

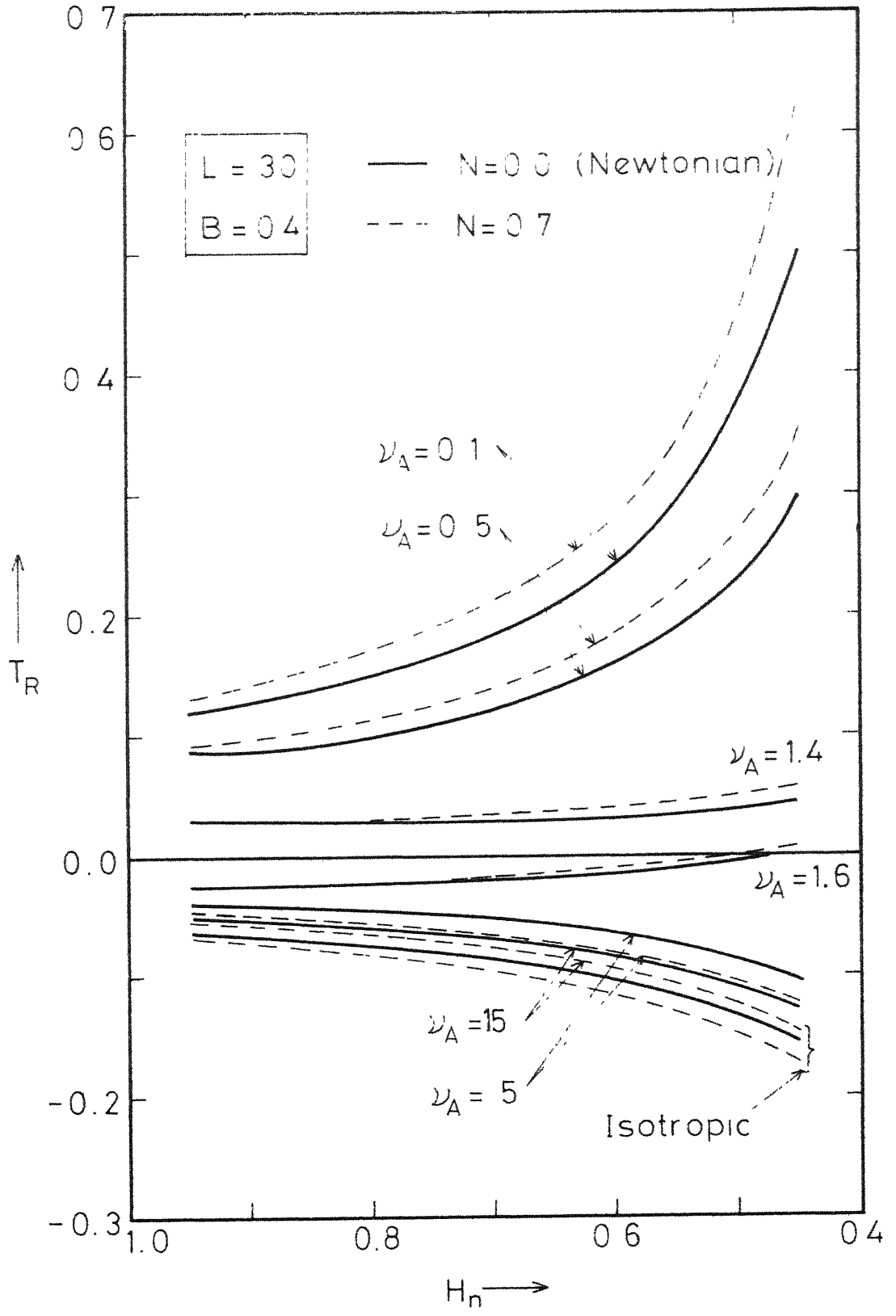

Fig.7·7 Time ratio parameter T_R vs. film thickness. H_n (B = 0·4. rectangular plate)

CHAPTER VIII

LUBRICATION OF HUMAN JOINTS

8.1 INTRODUCTION

Two centuries of study has failed to unravel completely the mysteries of the mechanism of human joints, although from the engineers point of view they represent one of the closest points of approach between the inventions of man and the work of nature.

The synovial joints provided by the nature in the human body to carry out the trouble free motion of one bone past another, have long been identified as bearing systems. With the exception of the joints of the middle ear and that between the lower jaw and the skull, all synovial joints are potentially weight-bearing, although some exercise this function more often than others. These joints function as excellent bearings in the biological conditions and generally support considerable load, while providing, low friction service over a long span of one's life time. There exists no mechanical device which yields as low a coefficient of friction as that found in the synovial joints. Thus a clear visualization of the synovial joints is likely not only to provide a guide-line to improve the existing mechanical bearings but also help in the replacement of a faulty human joint.

The human joint, of course, is an excessively complicated

system from an engineering view point and it is not possible to build as a mechanical replica in which all the features of the real thing are represented, nor indeed is it possible to device a mathematical description that is completely comprehensive. It is more practical and probably more logical to commence investigation in the opposite manner, i.e. to start with the most simple squeeze film and to introduce complicating features one at a time, until either a situation of sufficient complexity is reached or the engineering and computational aspects inhibit further progress.

This fundamental approach has led to the development of various theories of human joint lubrication. Serious study of the lubrication mechanism in human joints dates back to almost half a century ago. MacConaill [107] suggested as early as 1932, that the synovial joints function as the hydrodynamically lubricated bearings. Charney [108] challenged this view in 1959. His experimental evidence supported a boundary lubrication action. Charney observed a chemical affinity of hyaluronic acid molecules with the cartilage surface. McCutchen [109-112] introduced the porous nature of the cartilage into the lubrication concept, when he proposed his "weeping lubrication" ideas. Dintenfass [113] put forward the concept of elastohydrodynamic lubrication for synovial joints, which was later supported by Tanner [114]. Any possibility of boundary lubrication was ruled out by Dintenfass, while Tanner indicated a slight possibility of boundary lubrication

at the asperity contacts.

However, it was only in 1967 that Dowson [115] realized that one mode of lubrication is insufficient to explain the joint mechanism. He concluded that "the major lubrication mechanism would seem to be some form of elastohydrodynamic action determined by sliding or squeeze film-action between porous surfaces with boundary lubrication providing the surface protection in cases of severe loading and little movement". A little later in 1968, Walker et.al [116], suggested a new concept of joint lubrication, i.e. "Boosted lubrication". According to this concept of lubrication, squeeze-film action leads to a concentration of hyaluronic acid-protein complex in the lubricant as a result of diffusion of water and low molecular weight substances through the porous cartilage, and the restricated gap between the approaching cartilage surfaces. The increased concentration of hyaluronic acid molecule would give rise to an increase in viscosity of the synovial fluid in accordance with the findings of Negami [117] and the proposal is also consistent with the formation of gels on the cartilage surface (Maroudas [118]). Other work in this direction is by Higginson and Norman [119] who inferred that elastohydrodynamic lubrication plays a significant role. Unsworth et.al [120] and Wright and Dowson [121] have strongly suggested boundary lubrication.

Though, Dintenfass [113], Tanner [114] and Dowson [115] had made some numerical calculations for the fluid film thickness,

Fein [122] was probably the first to give a mathematical model for synovial joints. The joints system was considered to be elastically equivalent to sphere-on-a flat system. Mow and Ling [123] made use of Biot's formulation of poroelastic theory for giving the displacement field equation and also the strain displacement relationship. The fluid flow in the porous matrix was taken to be governed by simple Darcy's law. Dowson et.al [124-125] gave yet another simple formulation and accounted for viscosity variation with the hyaluronate concentration. The boosted squeeze time was found to be in good agreement with the experimental result. Ling [126] presented an analytical model to account for the non-linearity of the cartilage. It was pointed out that the two mechanisms of 'weeping', and 'boosted' are not exclusive. Higginson and Norman [127], Mansour and Mow [128,129] and Higginson [130] have given more rigorous mathematical models. They considered the elastic as well as the porous nature of the cartilage.

It is however observed that the present situation regarding joint lubrication is not very clear. Earlier works based on the classical continuum theory, could not explain the observed effective increase in viscosity near the solid boundary.

Little is known about the rheological nature and quantity of lubricant present in the human joints. Such knowledge is urgently required for the development of materials and designs and the better understanding of the tribological characteristics of

replacement bearings for the human body.

It would not be out of place to mention a little about the synovial fluid. Normal synovial fluid is generally clear or yellowish and viscous. It can be briefly described as a dialysate of blood plasma. It contains about one third of the protein concentration of the plasma. In addition the synovial fluid contains a very important polymer known as hyaluronic acid or sometimes called mucopolysaccharide. It is this hyaluronic acid molecule which gives synovial fluid its slippery and stringy behaviour. It also gives the characteristic non-Newtonian behaviour [131]. It was concluded by McCutchen [111] that the synovial fluid is a boundary lubricant. The synovial mucin are polymers of high molecular weight. Estimates of the molecular weight of the synovial mucin are as high as several million. Chemically, it is hyaluronic acid combined more or less firmly with less or more protein.

Thus in studying the human joint lubrication problem, one must examine not only the continuum behaviour of the synovial fluid but also the microscopic structure. In obtaining the constitutive equations one must, therefore, resort to the microcontinuum approach as the continuum approach will be less definite about the detail structure of the material.

This provides the motivation for the present work. The micropolar fluid model proposed by Eringen [44], serves as a

satisfactory model for the description of the flow behaviour of the polymer fluids and real fluid suspensions. It has already been pointed out that the micropolar fluid theory can be utilized to explain the rheological behaviour (increase in viscosity and boundary lubrication) of the lubricant. It also serves as a satisfactory model, when the fluid has long chain additive molecules.

It is, therefore, noted that the synovial fluid may be thought of as a micropolar fluid because of the long chain hyaluronic acid molecules. The increase in the concentration of the hyaluronate in the synovial fluid, which is the important feature of the boosted lubrication, causing an increase in the effective viscosity, can also be accounted for in this theory, by way of increase in the micromotions and the couple stress. In this analysis, it is assumed that the human joint can be approximated by a system of a porous spherical bearing. Micropolar fluid theory is applied. Slip which almost invariably occurs near the porous boundary is considered by using the Beavers and Joseph [132] velocity slip criterion. The elasticity of the cartilage, i.e. the porous matrix, is ignored to avoid the additional complexity in the already sufficiently complex model. Thus the present analysis may be termed as a first approximation to the human joint lubrication theory, using the microcontinuum approach. The only work in this direction is by Tandon and Jaggi [73,74] . Who have used, rather too simple a

geometry for the human joint. The validity of various equations is debatable as will be obvious from the present analysis. The coeffic ient of friction is calculated wrongly. Moreover the full potential of the micropolar fluid theory has not been realised.

8.2 ANATOMY OF A SYNOVIAL JOINT

The different forms of synovial joints in the Human body can not be readily reduced to a single model. For example, the hip joint is a close fitting ball and socket affair, to be approximated by an equivalent spherical bearing, while the ankle joint can be approximated by a cylinder-cylinder arrangement, resembling a close fitting journal bearing. Fig. 8.1, shows a joint illustrating the salient features encountered in synovial joints. In this schematic representation of a human joint, the load transmitting structural members are the bones. The ends of the bones which are usually globular in appearance, are covered with a layer of relatively soft and porous material called cartilage. The articular cavity contains the synovial fluid, which is responsible for the complex joint lubrication phenomenon.

8.3 THEORETICAL FORMULATION - ASSUMPTIONS AND EQUATIONS

Geometrically the system of synovial joint, especially the hip joint may be represented by a sphere on a porous surface. Both the sphere and porous surface are assumed to be rigid. The simplicity of the arrangement is shown in Fig. 8.2. The normal

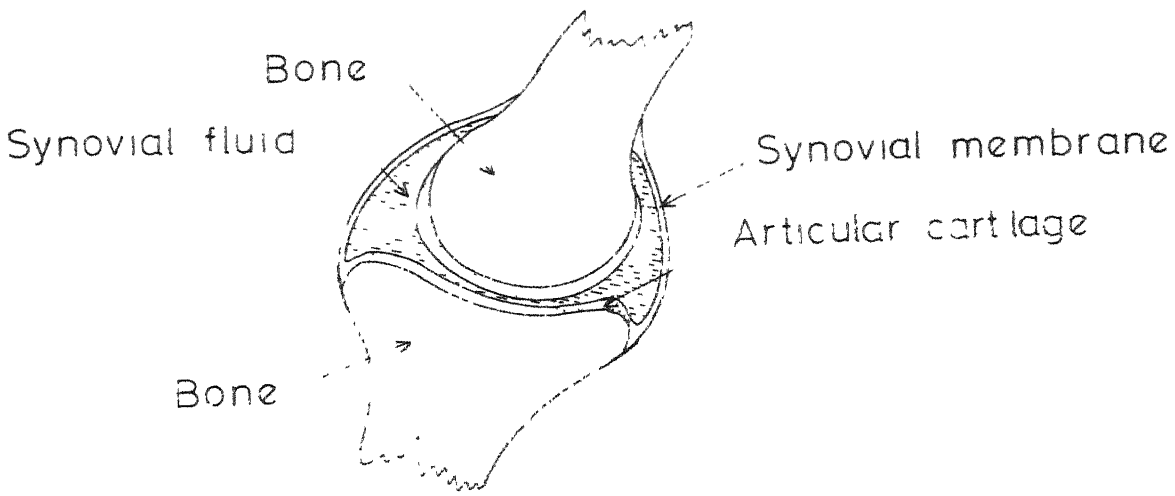

Fig 8.1(a) Synovial joint

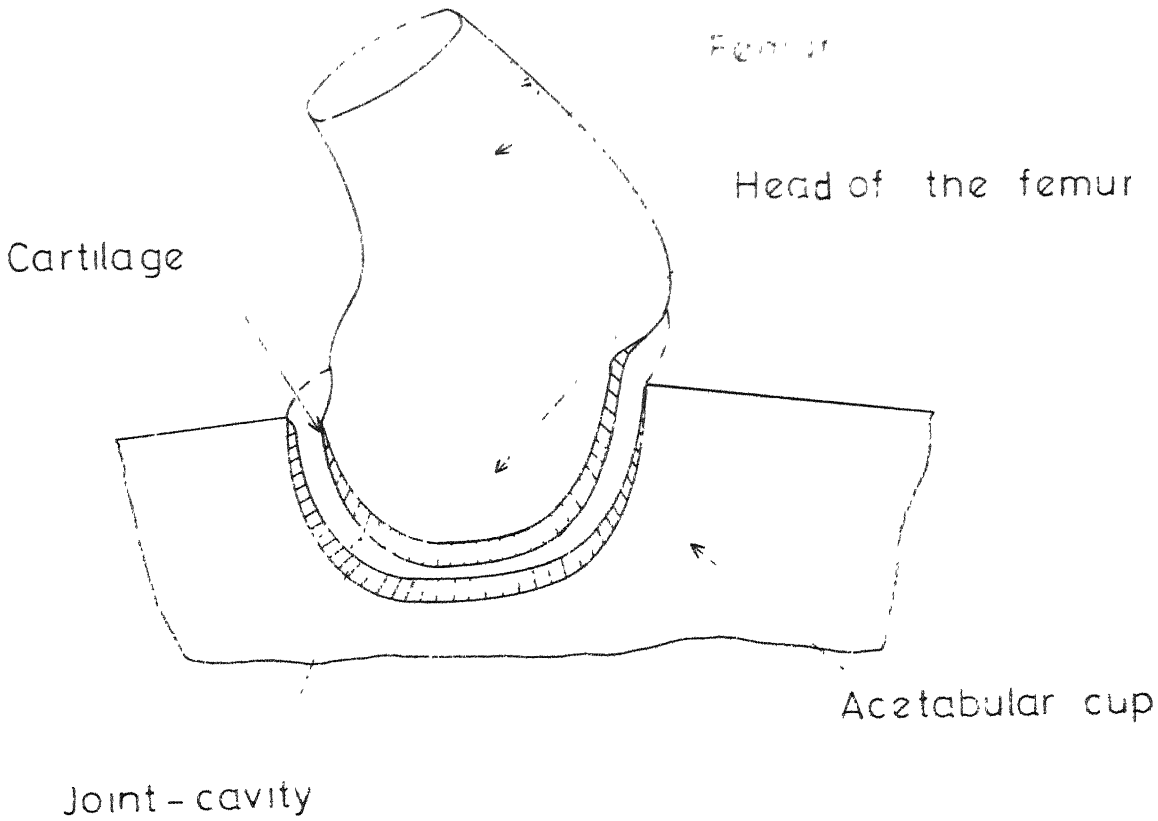

Fig 8.1(b) Hip joint

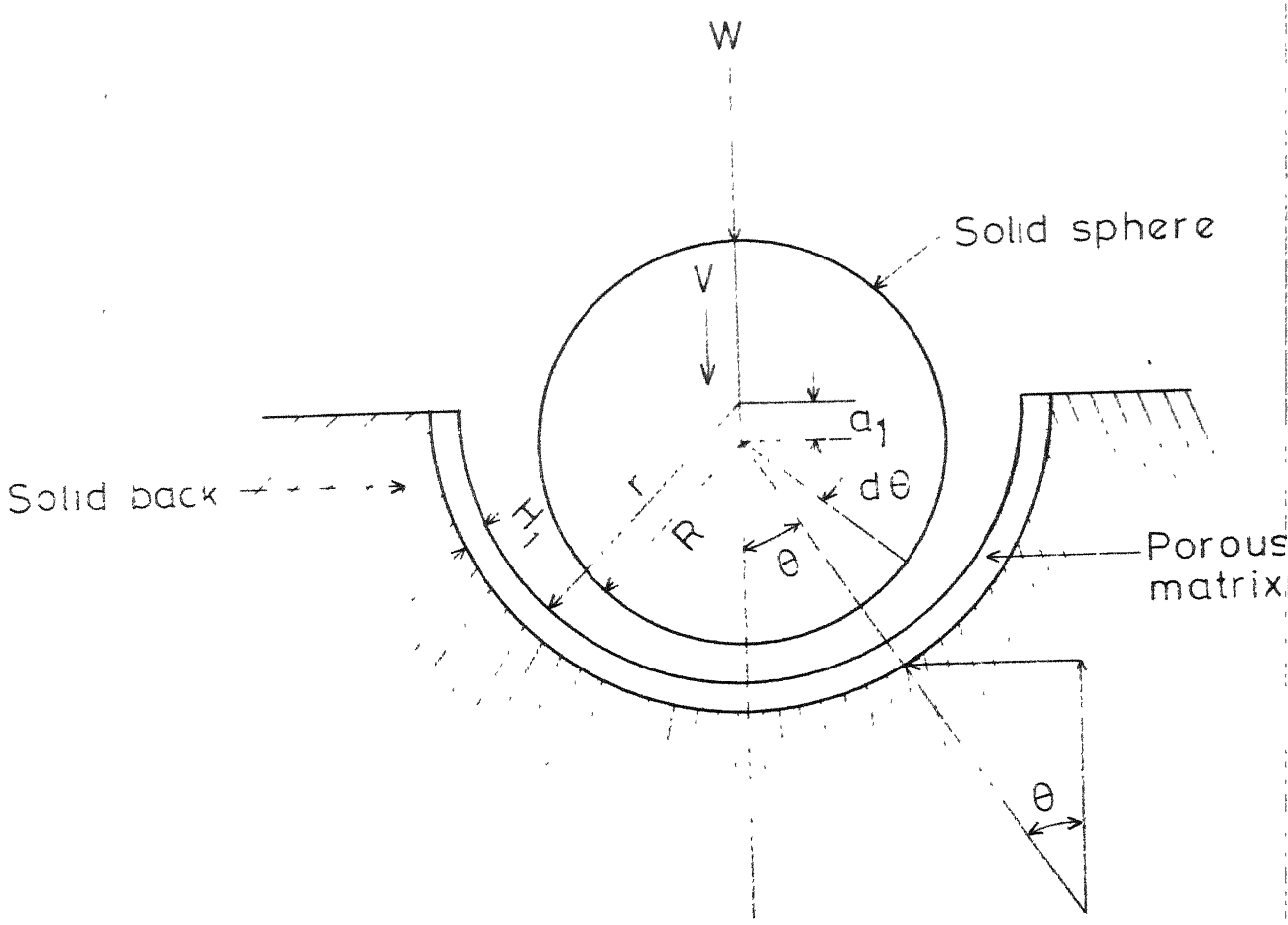

Fig 8.2 Configuration of spherical bearing as a model o
hip joint.

approach of the sphere is achieved by allowing it to fall under gravity on to the lower porous surface. The system is assumed to be lubricated by a highly non-Newtonian 'Synovial Fluid' which has long chain hyaluronate molecules. Micropolar fluid theory is assumed to govern the behaviour of the synovial fluid.

(i) Basic Equations

The basic governing equations for a three dimensional flow field under the assumptions stated in Chapter II, from eqns. (2.32) to (2.35), are

$$(\mu + \tfrac{1}{2}\chi)\frac{\partial^2 u}{\partial y^2} + \chi\frac{\partial \nu_3}{\partial y} - \frac{\partial p}{\partial x} = o \tag{8.1}$$

$$(\mu + \tfrac{1}{2}\chi)\frac{\partial^2 w}{\partial y^2} - \chi\frac{\partial \nu_1}{\partial y} - \frac{\partial p}{\partial z} = o \tag{8.2}$$

$$\gamma\frac{\partial^2 \nu_1}{\partial y^2} - 2\chi\nu_1 + \chi\frac{\partial w}{\partial y} = o \tag{8.3}$$

$$\gamma\frac{\partial^2 \nu_3}{\partial y^2} - 2\chi\nu_3 - \chi\frac{\partial u}{\partial y} = o \tag{8.4}$$

The boundary conditions are

$$u = U_{11},\ w = U_{12},\ \nu_1 = \nu_3 = o,\ \text{at } y = o \tag{8.5}$$

$$u = U_{21} - \frac{\sqrt{\phi_a}}{\Delta}\left.\frac{\partial u}{\partial y}\right|_{y=h},\ w = U_{22} - \frac{\sqrt{\phi_a}}{\Delta}\left.\frac{\partial w}{\partial y}\right|_{y=h},$$

$$\nu_1 = o,\ \nu_3 = o,\ \text{at } y = h \tag{8.6}$$

where ϕ_a is the porosity of the cartilage surface and Δ is the slip parameter. Condition (8.5) is the no-slip boundary condition for the velocity and microrotation velocity at the non-porous boundary and condition (8.6) is the slip boundary condition for velocity according to Beavers and Joseph [132] , however, the microrotation is assumed to vanish at the porous surface also.

(ii) Velocity Distribution

Solving equations (8.1) to (8.4) for velocity components u,w and microrotation velocity components ν_1, ν_3 ; with the boundary conditions (8.5) and (8.6), we obtain

$$u = \frac{1}{\mu}\left(\frac{y^2}{2} \frac{\partial p}{\partial x} - B_{11} y\right) - \frac{2N^2}{m} B_{11} y - \frac{2N^2}{m} (B_{31} \sinh my + B_{41} \cosh my) + B_{21} \tag{8.7}$$

$$w = \frac{1}{\mu}\left(\frac{y^2}{2} \frac{\partial p}{\partial z} - B_{12} y\right) - \frac{2N^2}{m} B_{12} y - \frac{2N^2}{m} (B_{32} \sinh my + B_{42} \cosh my) + B_{22} \tag{8.8}$$

$$\nu_1 = \frac{1}{2\mu}\left(y \frac{\partial p}{\partial z} - B_{12}\right) - B_{32} \cosh my - B_{42} \sinh my \tag{8.9}$$

$$\nu_3 = -\frac{1}{2\mu}\left(y \frac{\partial p}{\partial x} - B_{11}\right) + B_{31} \cosh my + B_{41} \sinh my \tag{8.10}$$

where

$$B_{1i} = \frac{\mu\left[(U_{i1} - U_{i2}) + \frac{h}{2\mu} \frac{\partial p}{\partial x_i}\left\{ 2\phi_1 (1 - N^2) + h - \frac{2N^2}{m} \tanh \frac{mh}{2}\right\}\right]}{\left\{\phi_1 (1 - N^2) + h - \frac{2N^2}{m} \tanh \frac{mh}{2}\right\}} \tag{8.11}$$

$$B_{2i} = U_{il} + \frac{N^2}{\mu m} \frac{1}{\sinh mh} \{B_{1i}(\cosh mh-1) + h \frac{\partial p}{\partial x_i}\} \qquad (8.12)$$

$$B_{3i} = -\frac{1}{2\mu} B_{1i} \qquad (8.13)$$

$$B_{4i} = \frac{1}{2\mu \sinh mh} \{B_{1i} (\cosh mh-1) + h \frac{\partial p}{\partial x_i}\} \qquad (8.14)$$

where

$$i = 1,2,\ x_1 = x,\ x_2 = z,\ N = \left(\frac{\chi}{2\mu + \chi}\right)^{\frac{1}{2}},\ m = \frac{N}{\ell},\ \ell = \left(\frac{\gamma}{4\mu}\right)^{\frac{1}{2}},$$

$$\phi_1 = \frac{\sqrt{\phi_a}}{\Delta} \qquad (8.15)$$

(iii) Generalized Reynolds Equation

Integrating the equation of continuity

$$\frac{\partial u}{\partial x} + \frac{\partial v}{\partial y} + \frac{\partial w}{\partial z} = o \qquad (8.16)$$

across the film, we get the generalized Reynolds equation as

$$\frac{\partial}{\partial x} \{F_{11}(N,\ell,h,\phi_1) \frac{\partial p}{\partial x}\} + \frac{\partial}{\partial z} \{F_{11}(N,\ell,h,\phi_1) \frac{\partial p}{\partial z}\}$$

$$= \frac{\partial}{\partial x} \{G_{11}(N,\ell,h,\phi_1)\} + \frac{\partial}{\partial z} \{G_{12}(N,\ell,h,\phi_1)\} + V + V_p \qquad (8.17)$$

where V is the relative normal velocity of the surfaces and V_p is the velocity of the fluid towards the porous region at the cartilage surface and

$$F_{11} = F_{11}(N,\ell,h,\phi_1) = \frac{1}{\mu}\,\frac{f_{31}\ \{f_{11}+\phi_1(1-N^2)(\frac{h^2}{2}-\frac{f_{21}}{f_{31}})\}}{\{\phi_1(1-N^2)+f_{31}\}} \qquad (8.18)$$

$$G_{1i}=G_{1i}(N,\ell,h) = \frac{\{\phi_1(1-N^2)h\,U_{1i}+\frac{h}{2}f_{31}(U_{1i}+U_{2i})\}}{\{\phi_1(1-N^2)+f_{31}\}},$$

$$i = 1,2 \qquad (8.19)$$

$$f_{11} = f_{11}(N,\ell,h) = \frac{h^3}{12}+\ell^2 h-\frac{N\ell h^2}{2}\coth\frac{NH}{2\ell} \qquad (8.20)$$

$$f_{21} = f_{21}(N,\ell,h) = \frac{h^3}{6}-\ell^2 h+\frac{N\ell h^2}{\sinh\frac{Nh}{2\ell}} \qquad (8.21)$$

$$f_{31} = f_{31}(N,\ell,h) = h-2N\ell\tanh\frac{Nh}{2\ell} \qquad (8.22)$$

Now the problem remains to find the velocity V_p of the fluid at the porous surface towards the porous region. For this purpose, let us recall that the hyaluronic acid is a long chain polymer compound. The molecular weight of hyaluronic acid molecule is 5×10^5 (approximately) and molecular length of the order $5 \times 10^{-5} - 10^{-4}$ cm, Dowson [115]. These molecules normally can not pass through the porous matrix which is the basis of boosted lubrication. Thus it can be assumed that the flow through the cartilage matrix is Newtonian, and hence the velocity of the lubricant through the porous matrix shall be governed by the usual Darcy's law [133].

Thus [133],

$$V_p = - \frac{\phi_a}{\mu} \frac{\partial p}{\partial y}\Big|_{y=h} \tag{8.23}$$

From the requirement of continuity we have for the porous matrix

$$\vec{\nabla} . \vec{q} = - \frac{\phi_a}{\mu} \nabla^2 p = o \tag{8.24}$$

so that, since $\frac{\phi_a}{\mu} \neq o$,

$$\nabla^2 p = o \tag{8.25}$$

The problem now reduces to get the solution of the Reynolds equation (8.17) for the pressure in the oil film, simultaneously with that of Laplace eqn. (8.25), for the porous matrix, with a common $\frac{\partial p}{\partial y}$ at the boundary.

Assuming the thickness of porous matrix to be very small as compared to the radius of the sphere ($H_1 << R$), the average pressure at any radial section of the porous matrix can be taken equal to the pressure in the lubricating film. It is further assumed that $\frac{\partial p}{\partial y}$ is linear across the matrix and is zero at the outer surface of the porous bearing shell.

This assumption leads to

$$\frac{\partial^2 p}{\partial y^2} = \text{constant} = K_1 \text{(say)} \tag{8.26}$$

Hence from Laplace equation

$$\frac{\partial^2 p}{\partial z^2} + \frac{\partial^2 p}{\partial x^2} = - K_1 \tag{8.27}$$

Integrating (8.26) , we get

$$\frac{\partial p}{\partial y} = K_1 y + K_2 \tag{8.28}$$

where K_2 is constant of integration.

With the boundary condition $\frac{\partial p}{\partial y} = o$ at $y = h + H_1$, we get

$$\frac{\partial p}{\partial y} = K_1 (y-h-H_1) \tag{8.29}$$

Hence

$$\left.\frac{\partial p}{\partial y}\right|_{y=h} = -K_1 H_1 \tag{8.30}$$

Substituting the value of K_1 from eqn. (8.27), we get

$$\left.\frac{\partial p}{\partial y}\right|_{y=h} = H_1 \left(\frac{\partial^2 p}{\partial x^2} + \frac{\partial^2 p}{\partial z^2} \right) \tag{8.31}$$

Thus

$$V_p = - \frac{\phi_a H}{\mu} \left(\frac{\partial^2 p}{\partial x^2} + \frac{\partial^2 p}{\partial z^2} \right) \tag{8.32}$$

Substituting the value of V_p in eqn. (8.17) and simplifying, we get

$$\frac{\partial}{\partial x} \left[\{ F_{11}(N,\ell,h,\phi_1) + \frac{\phi_a H_1}{\mu} \} \frac{\partial p}{\partial x} \right] + \frac{\partial}{\partial z} \left[\{ F_{11}(N,\ell,h,\phi_1) + \frac{\phi_a H_1}{\mu} \} \frac{\partial p}{\partial z} \right] = V + \frac{\partial}{\partial x} [\{ G_{11}(N,\ell,h,\phi_1) \}] + \frac{\partial}{\partial z} [\{ G_{12}(N,\ell,h,\phi_1) \}] \tag{8.33}$$

Equation (8.33) is the generalized Reynolds equation governing the pressure distribution in the cavity of the joint.

8.4 NORMAL MOTION OF THE HUMAN JOINT

Attention is now restricted to the study of normal motion of the joints. Therefore, the effects arising out of sliding are neglected, i.e. $U_{1i} = U_{2i} = o$, $i = 1,2$. Thus eqn. (8.33) takes the form

$$\frac{\partial}{\partial x}\left[\left\{F_{11}(N,\ell,h,\phi_1) + \frac{\phi a^{H_1}}{\mu}\right\}\frac{\partial p}{\partial x}\right] + \frac{\partial}{\partial z}\left[\left\{F_{11}(N,\ell,h,\phi_1) + \frac{\phi a^{H_1}}{\mu}\right\}\frac{\partial p}{\partial z}\right] = V \tag{8.34}$$

The film thickness is

$$h = c(1-\varepsilon\cos\theta) \tag{8.35}$$

and the velocity of squeezing is

$$V = \frac{dh}{dt} = -c\frac{d\varepsilon}{dt}\cos\theta \tag{8.36}$$

Using the spherical polar co-ordinates for the system under consideration, i.e. using

$$x = R\sin\theta\cos\zeta \tag{8.37}$$

$$y = R\cos\zeta \tag{8.38}$$

$$z = R\sin\theta\sin\zeta \tag{8.39}$$

eqn. (8.34) assumes the form

$$\frac{1}{R^2 \sin\theta} \frac{\partial}{\partial\theta} \left[\sin\theta \left\{ F_{11}(N,\ell,h,\phi_1) + \frac{\phi_a H_1}{\mu} \right\} \frac{\partial p}{\partial\theta} \right]$$

$$+ \frac{1}{R^2 \sin^2\theta} \frac{\partial}{\partial\zeta} \left[\left\{ F_{11}(N,\ell,h,\phi_1) + \frac{\phi_a H_1}{\mu} \right\} \frac{\partial p}{\partial\zeta} \right]$$

$$= - c \frac{d\varepsilon}{dt} \cos\theta \qquad (8.40)$$

It is reasonable to assume $\frac{\partial p}{\partial\zeta} = o$ (i.e. the pressure is constant along ζ direction). With this assumption, eqn. (8.40) reduces to

$$\frac{1}{R^2 \sin\theta} \frac{\partial}{\partial\theta} \left[\sin\theta \left\{ F_{11}(N,\ell,h,\phi_1) + \frac{\phi_a H_1}{\mu} \right\} \frac{\partial p}{\partial\theta} \right]$$

$$= - c \frac{d\varepsilon}{dt} \cos\theta \qquad (8.41)$$

To solve the Reynolds eqn. (8.41) the pressure boundary condition must be known. Since the pressure reaches a maximum at $\theta = o$, therefore the first condition becomes

$$\frac{dp}{d\theta} = o \text{ at } \theta = o \qquad (8.42)$$

However the other condition is debatable as the exact extension of lower cavity of bone is undetermined. If one assumes the lower cavity to terminate at some point $\theta = \pm \theta^*$, then the second condition would become

$$p = o \text{ at } \theta = \pm \theta^* \qquad (8.43)$$

But this again involves an unknown parameter θ^*. However it is reasonable to assume that $\theta^* = \frac{\pi}{2}$ (approximately). This assumption

may be justified because the pressure reaches a peak at $\theta = o$ and falls very sharply on both sides. Hence the influence of the boundary on pressure distribution is likely to be negligible after some distance from $\theta = o$.

Thus we have the second boundary condition as

$$p = o \text{ at } \theta = \pm \frac{\pi}{2} \tag{8.44}$$

Integrating eqn. (8.41) using the boundary conditions (8.42) and (8.44) the equations governing the pressure gradient and pressure distribution, are, respectively

$$\frac{dp}{d\theta} = -\frac{1}{2}\mu R^2 c \frac{d\varepsilon}{dt} \sin\theta \times \times \left[\frac{\{\phi_1(1-N^2) + f_{31}\}}{\phi_a H_1 \{\phi_1(1-N^2) + f_{31}\} + f_{31}\{f_{11} + (\frac{h^2}{2} - \frac{f_{21}}{f_{31}})(1-N^2)\phi_1\}} \right] \tag{8.45}$$

and

$$p(\theta) = \frac{1}{2}\mu R^2 c \frac{d\varepsilon}{dt} \times \times \int_o^{\pi/2} \sin\theta \left[\frac{\{\phi_1(1-N^2) + f_{31}\}\, d\theta}{\phi_a H_1 \{\phi_1(1-N^2)+f_{31}\} + f_{31}\{f_{11} + \phi_1(1-N^2)(\frac{h^2}{2} - \frac{f_{21}}{f_{31}})\}} \right] \tag{8.46}$$

The expression for load capacity is

$$W = 2\pi R^2 \int_0^{\pi/2} p \sin\theta \cos\theta \, d\theta \tag{8.47}$$

or

$$W = \frac{\pi R^4}{2} \mu c \frac{d\varepsilon}{dt} \times \times \int_0^{\pi/2} \sin^3\theta \left[\frac{\{\phi_1(1-N^2) + f_{31}\} \, d\theta}{\phi_a H_1 \{\phi_1(1-N^2)+f_{31}\} + f_{31}\{f_{11}+\phi_1(1-N^2)(\frac{h^2}{2} - \frac{f_{21}}{f_{31}})\}} \right]$$

(8.48)

Non-dimensionalizing, using

$$H = \frac{h}{c} = 1 - \varepsilon \cos\theta, \; L = \frac{c}{\ell}, \; \phi_s = \frac{\sqrt{\phi_a}}{c\Delta}, \; \phi_p = \frac{\phi_a H_1}{c^3} \tag{8.49}$$

where ϕ_p and ϕ_s are characterization of slip and porosity effects, respectively. Thus the non-dimensional load capacity is

$$\bar{W} = \frac{2c^2 W}{\pi R^4 \mu \frac{d\varepsilon}{dt}}$$

$$= \int_0^{\pi/2} \left[\frac{\sin^3\theta \{\phi_s(1-N^2) + F_{31}\} \, d\theta}{\phi_p \{\phi_s(1-N^2)+F_{31}\} + F_{31}\{F_{10}+\phi_s(1-N^2)(\frac{H^2}{2} - \frac{F_{21}}{F_{31}})\}} \right]$$

(8.50)

where,

$$F_{10} = \frac{H^3}{12} + \frac{H}{L^2} - \frac{NH^2}{2L} \coth \frac{NLH}{2} \tag{8.51}$$

$$F_{21} = \frac{H^3}{6} - \frac{H}{L^2} + \frac{NH^2}{L \sinh NLH} \tag{8.52}$$

$$F_{31} = H - \frac{2N}{L} \tanh \frac{NLH}{2} \tag{8.53}$$

The time of approach, t, from an initial film thickness to a final film thickness, in terms of corresponding eccentricity ratios, is given by

$$t = \frac{\pi R^4 \mu}{2c^2 W} \times$$

$$\times \int_{\varepsilon_o}^{\varepsilon_1} \left[\int_0^{\pi/2} \frac{\sin^3 \theta \{\phi_s(1-N^2) + F_{31}\} \, d\theta}{\phi_p \{\phi_s(1-N^2) + F_{31}\} + F_{31} \{F_{10} + \phi_s(1-N^2)(\frac{H^2}{2} - \frac{F_{21}}{F_{31}})\}} \right] d\varepsilon$$

(8.54)

The non-dimensional time of approach is

$$T = \frac{2c^2 Wt}{\pi 2\mu} \frac{1}{R^4} =$$

$$= \int_{\varepsilon_o}^{\varepsilon_1} \left[\int_0^{\pi/2} \frac{\sin^3 \theta \{\phi_s(1-N^2) + F_{31}\} \, d\theta}{\phi_p \{\phi_s(1-N^2) + F_{31}\} + F_{31} \{F_{10} + \phi_s(1-N^2)(\frac{H^2}{2} - \frac{F_{21}}{F_{31}})\}} \right] d\varepsilon$$

(8.55)

8.5 RESULTS AND DISCUSSION

(i) Dimensionless Parameters

Apart from the usual dimensionless numbers encountered in the classical theory four new parameters ϕ_s, ϕ_p, N and L, are of importance in the study of the present joint lubrication problem. The slip parameter ϕ_s and the permeability ϕ_p have since long been identified and discussed. It would suffice here to mention that a larger value of ϕ_s or ϕ_p signifies a greater slip or a greater permeability and a value of $\phi_s = o$ or $\phi_p = o$ signifies no slip or a non-porous body. It may be noted that for a non-porous body the slip is necessarily zero, however, a zero slip does not imply a non-porous case.

The parameters N and L have already been discussed in Chapter III. In the present context, it suffices to say that, N and L represent concentration and length parameter of the hyaluronic acid molecules, respectively, in synovial fluid. Higher is the value of N higher is the concentration of the molecules, and lower is the value of L higher is the chain length of molecules. Thus the joint lubrication characteristics would be prominent when N is higher and L is lower.

(ii) Diseased Joints

The properties of the synovial fluid undergo a marked variation with age, specially in case of a diseased or damaged joint. In a

rheumatoid arthritic patient, the synovial fluid may even loose its non-Newtonian behaviour, Bloch and Dintenfass [134] . This is characterized by the cases of $N = 0$ or $L \to \infty$. These cases actually correspond to the classical theory approach . Burch et. al [135] indicated that the concentration of hyaluronic acid molecule in synovial fluid decreases for a diseased joint. For old joints, the cartilage becomes softer, less resilient and may even wear out in certain cases. These two cases can be characterized by a decreasing value of N and ϕ_p respectively. Furthermore, it is seen that for a rheumatoid joint hyaluronic acid molecule has a lower molecular weight. A lower molecular weight corresponds to smaller length of the molecule. This, in this study, is depicted by a larger value of L.

Thus it is evident that, the present study is capable, through the parameters ϕ_s, ϕ_p , L and N , to analyse the behaviour of a diseased joint also.

(iii) Joint Characteristics

The non-dimensional load capacity $\bar{W}$ is given by equation (8.50). Even a casual glance, tells that the slip parameter ϕ_s is multiplied by the factor $(1-N^2)$, in the numerator as well as the denominator. The same is true for the expression of the dimensionless time of approach T, eqn. (8.55). This is an important result. This indicates that as N increases the effect of the slip will decrease, because

$\phi_s(1-N^2)$ will decrease. Increase in N, is a consequence of the Boosted lubrication. So as the concentration of the hyaluronic acid molecules increases, the effective viscosity becomes more and the effect of slip on the load and response time decreases.

Curves for dimensionless load capacity $\bar{W}$ vs. the various parameters involved are shown in Figures 8.3 to 8.9. Figures (8.3) to (8.5) show that the load decreases as the value of slip parameter increases. The qualitative trend is similar to that obtained by the classical theory approach. Of importance is the fact that load decreases as (a) the porosity increases ; Fig. 8.3, (b) the concentration decreases ; Fig. 8.4 and (c) the chain length of hyaluronic acid molecule decreases ; Fig. 8.5. These results establish theoretically that a diseased or a damaged joint will carry a lesser load.

Graphs for the load vs. ϕ_p ; Figs. 8.6 - 8.7, indicate a similar trend that the load decreases as ϕ_p increases for a fixed value of other parameters. Fig. 8.7 ; which is a plot of $\bar{W}$ vs. ϕ_p for different values of N, indicates that if ϕ_p increases and N decreases, simultaneously, the decrease in load will be very rapid.

Fig. 8.8 is a graph of $\bar{W}$ vs. N for the porous (indicated by continuous lines) and the non-porous (dotted lines) cases for various values of L. The curve for $L \to \infty$ gives the minimum load in both cases. This case corresponds either to the classical

theory approach or the reverse case of diseased joint where the synovial fluid might have lost its non-Newtonian characteristics. Obviously this curve is straight line, since it no longer is a function of N. Also, since the porosity of the cartilage has been established beyond doubt, the case of non-porous curves, in spite of their higher load capacity, are not of much significance. These curves are however given here only to illustrate the significant quantitative difference in the load capacity.

Dimensionless load $\bar{W}$ vs. L(Fig. 8.9) shows a very slow decrease in the load for low values of N. Indicating that for low concentration of the hyaluronic acid molecules in the synovial fluid the load is very low, even when the chain length of the molecule may be high. But as the concentration further increases, the capacity becomes higher for long chain length (low value of L) of the molecule. However, as the chain length decreases, the load capacity decreases rapidly, irrespective of the value of the concentration. This happens in the diseased rheumatoid joint.

The curves for the film thickness vs. the time of approach are shown in Figs. 8.10-8.13. The study of these curves is very vital for the joint lubrication problem because this would indicate the time it would take the two cartilage surfaces to come into intimate contact, which actually will happen if the film thickness becomes zero, i.e. all the fluid is squeezed out from between the two surfaces.

It is seen that the time of approach is sufficiently large for low values of the slip parameter ; Fig. 8.10 , but an increase in the slip decreases the time of approach ; thus preserving the qualitative trend of the classical theory approach. A similar result is visible from Fig. 8.11 ; that T decreases as the porosity increases. The time of approach for the slip case (continuous lines) and the no-slip case (dotted lines) is almost identical. The most important aspect of this figure is the fact that as the value of ϕ_p increases a finite time of approach is obtained. This becomes sufficiently small for high value of ϕ_p, which indicates that all of the synovial fluid is either squeezed out or passes into the pores, causing an intimate contact of the cartilage surfaces in a very short period of time. This may be a cause of consistent severe pain in the diseased rheumatoid joints.

Almost similar results are obvious from Figs. 8.12 - 8.13 ; wherein the results for the non-porous case are indicated by dotted lines and for that of the porous case by continuous lines. The time of approach is seen to decrease as either the chain length of the hyaluronic acid molecule decreases or as the concentration decreases (i.e. as L increases and N decreases). Finite value of T are once again indicated for high value of L (low chain length) and low value of N (low concentration).

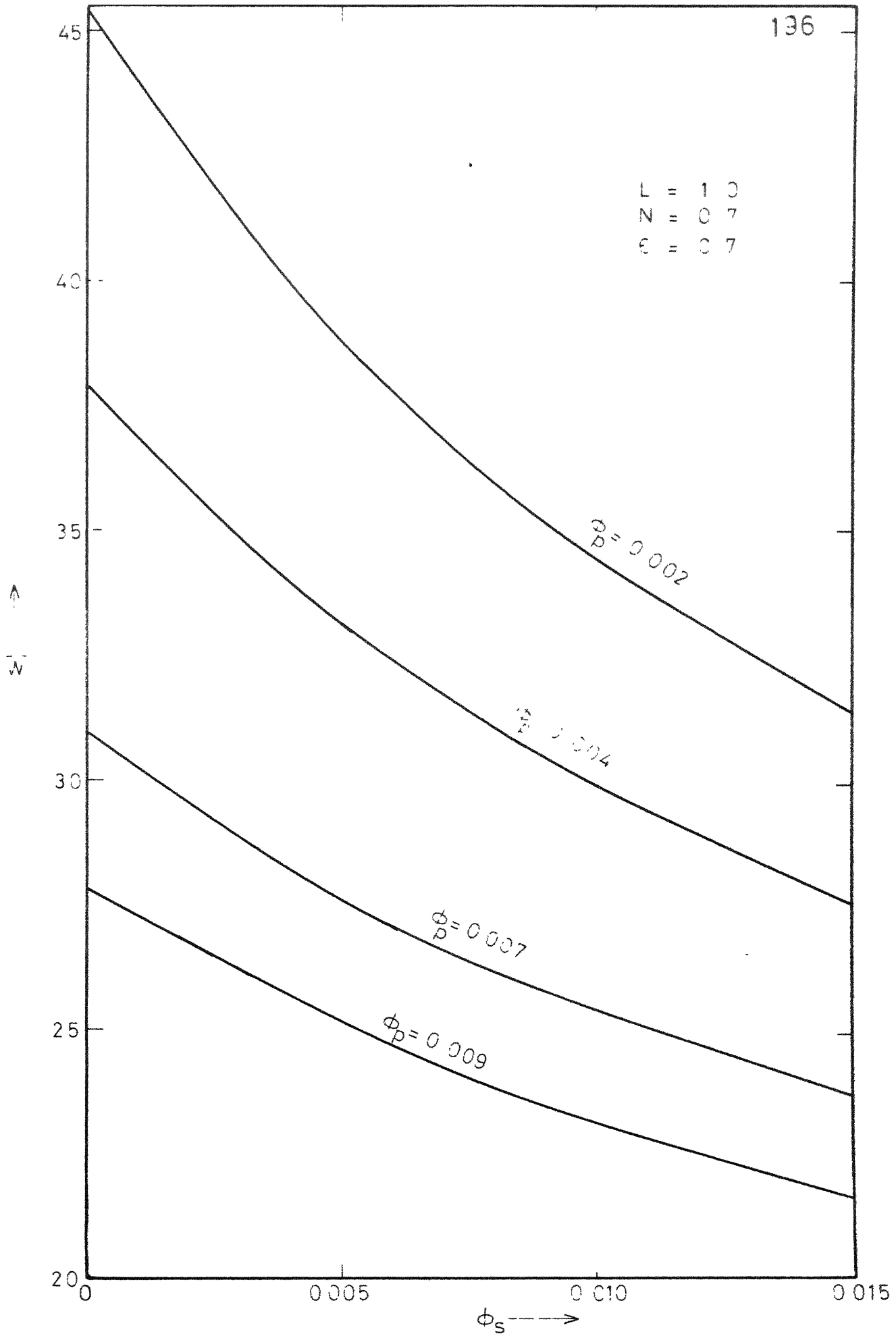

Fig 8 3 Non-dimensional load capacity vs. slip parameter for different values of porosity parameter

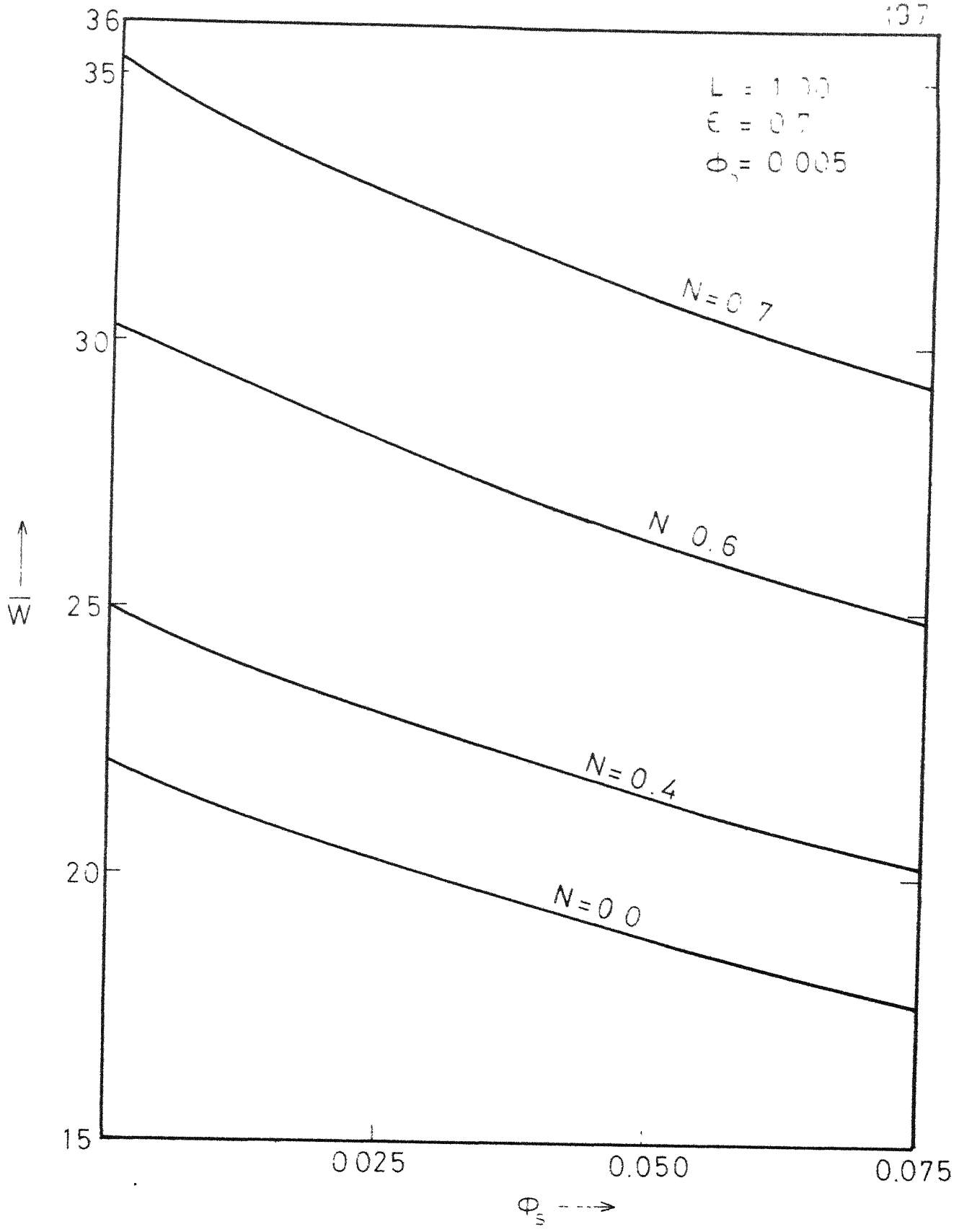

Fig 8.4 Non-dimensional load capacity vs slip parameter for different values of coupling number

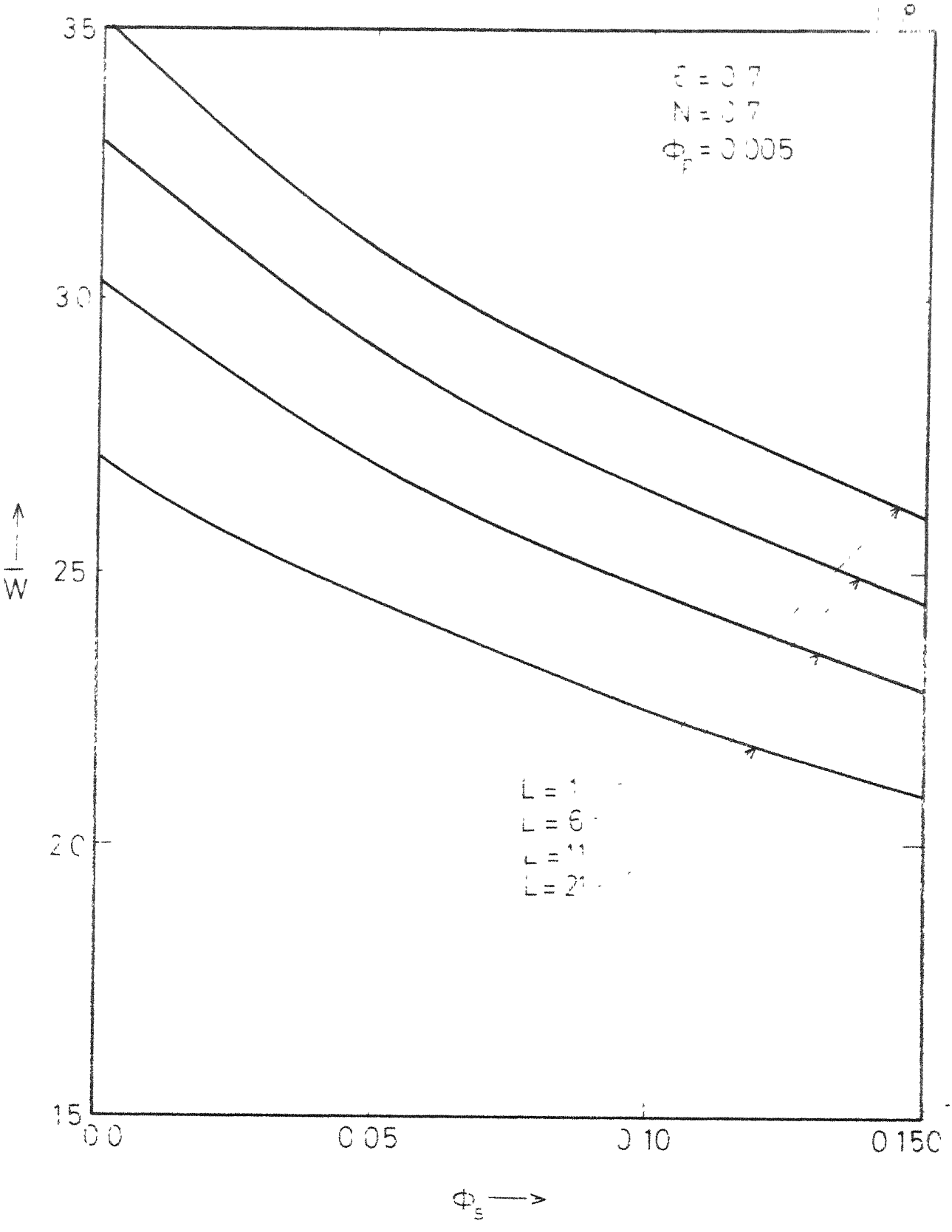

Fig 8 5 Non-dimensional load capacity vs slip parameter for different values of L

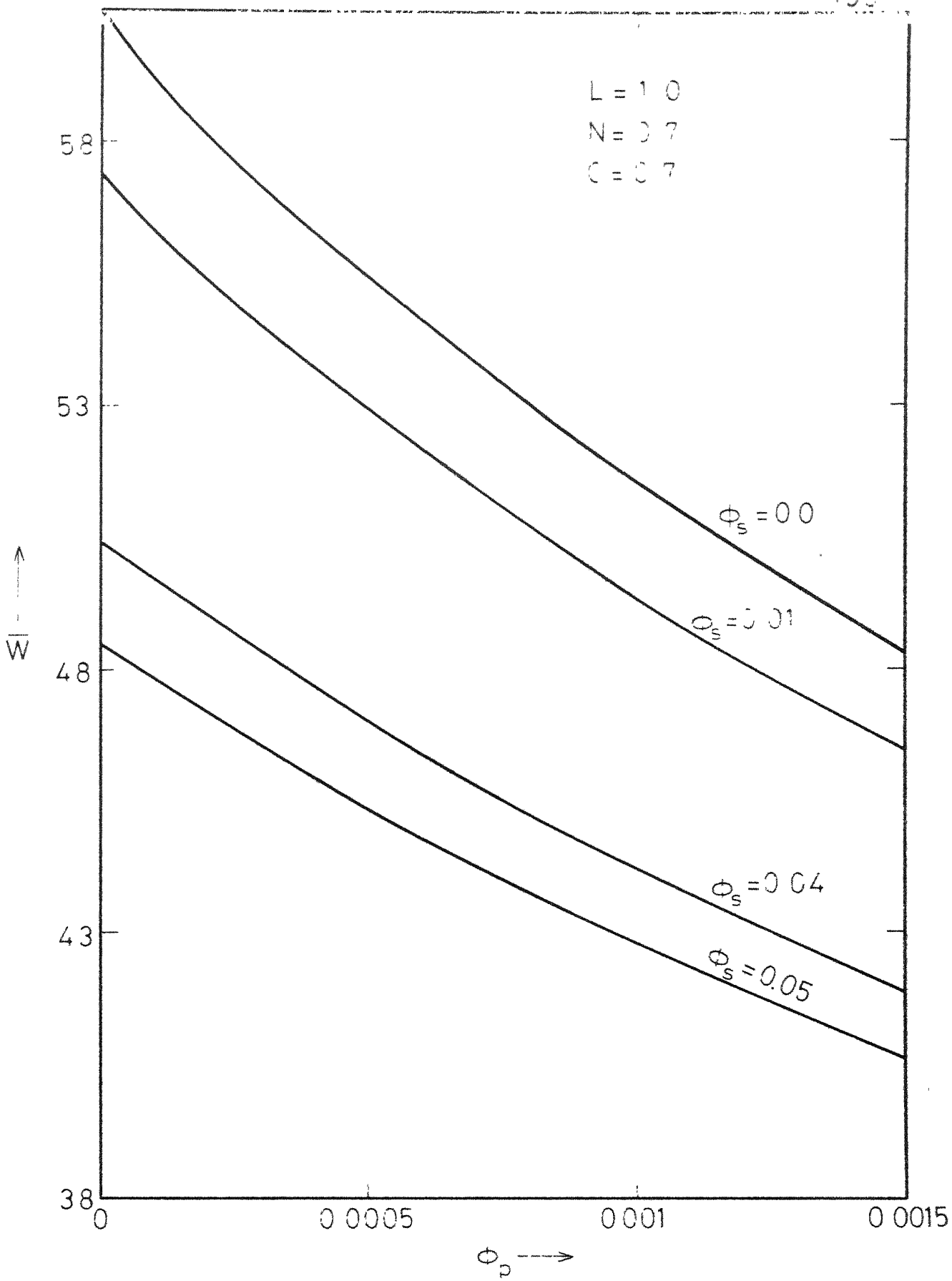

Fig 3 6 Non-dimensional load capacity vs porosity parameter for different values of slip parameter

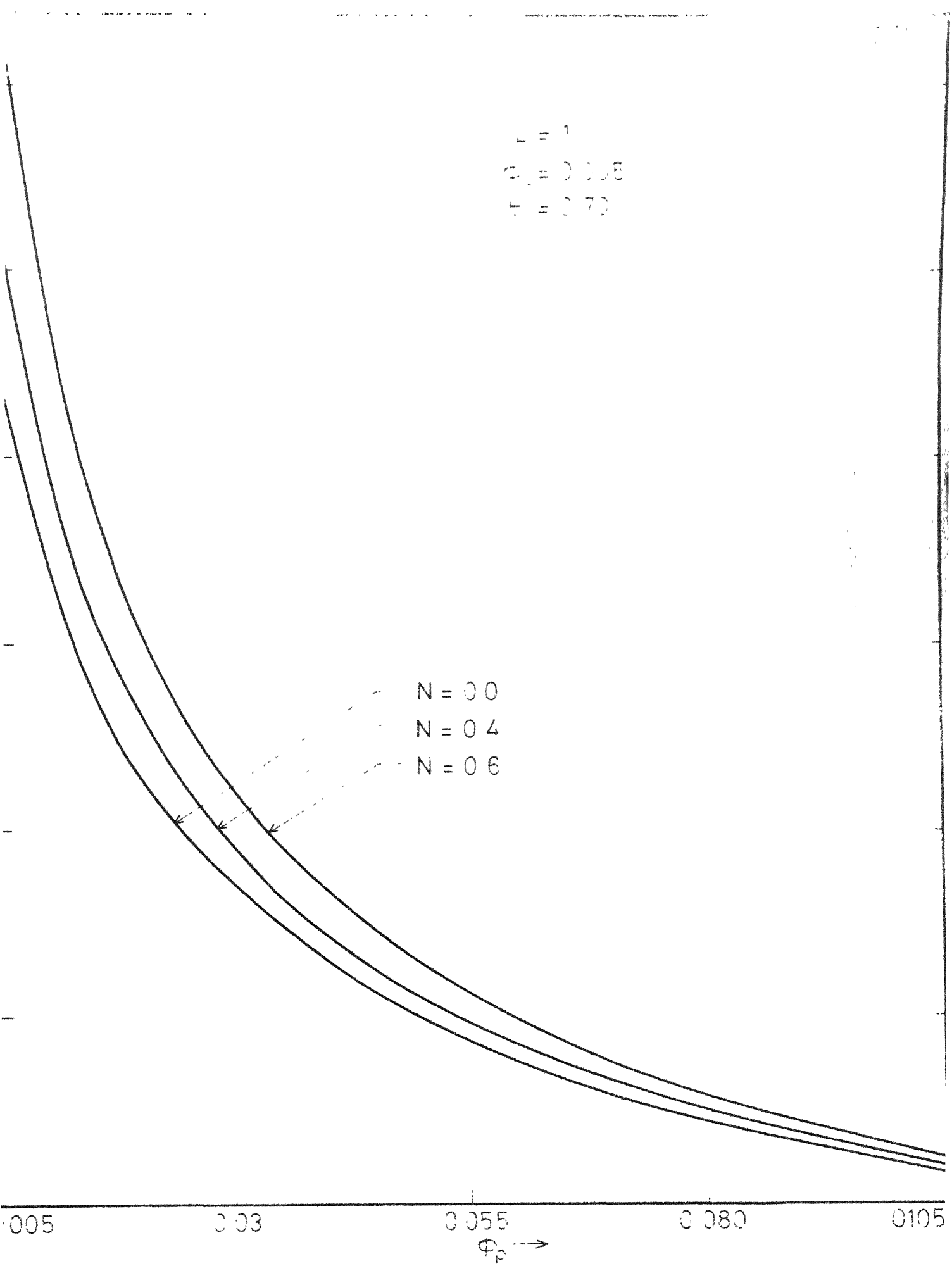

Fig 8.7 Non-dimensional load capacity vs porosity parameter for different [illegible] pumping number

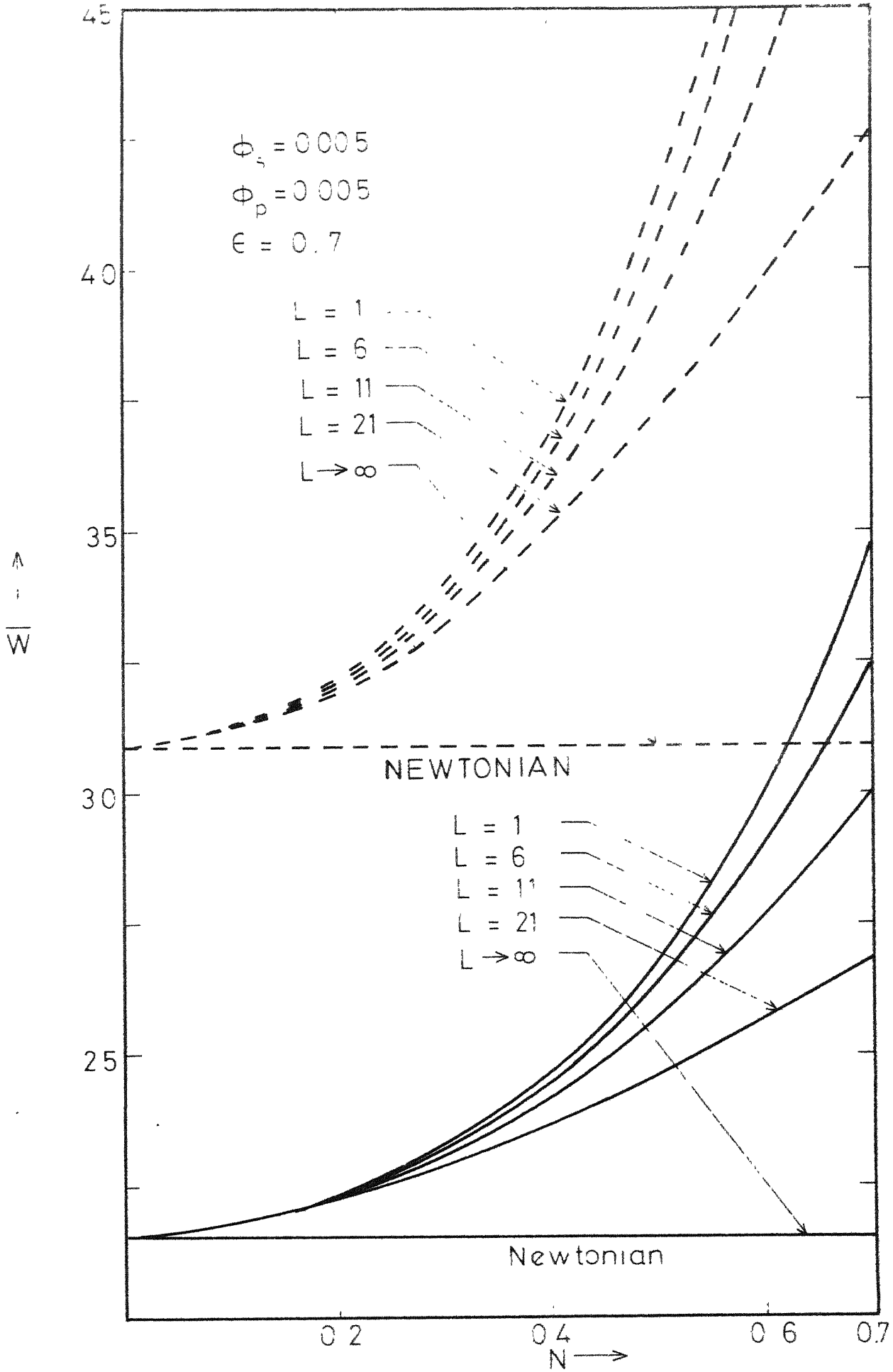

Fig 8.8 Non-dimensional load capacity vs coupling number for different values of L

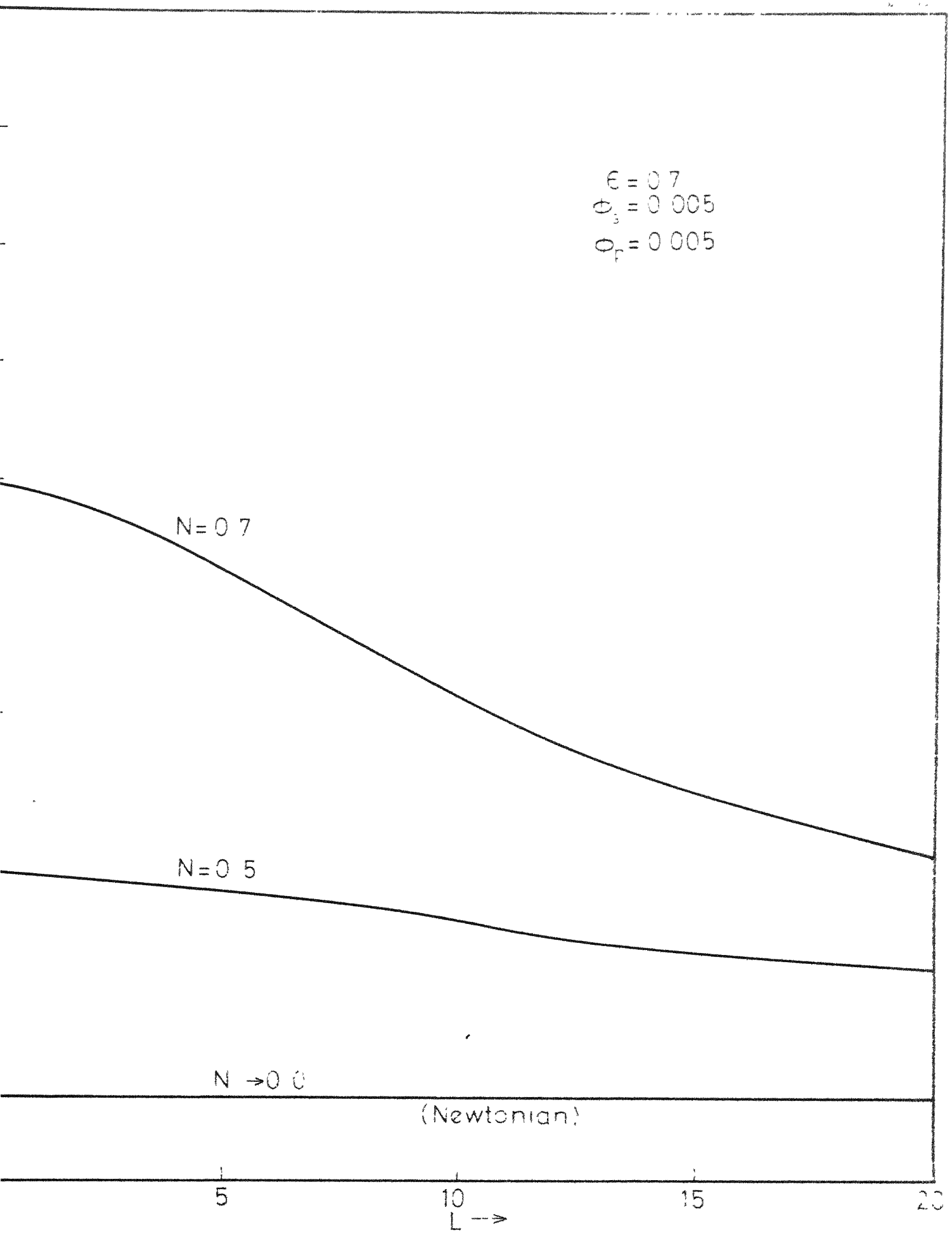

g 8.9 Non - dimensional load capacity vs. L for different values of coupling number

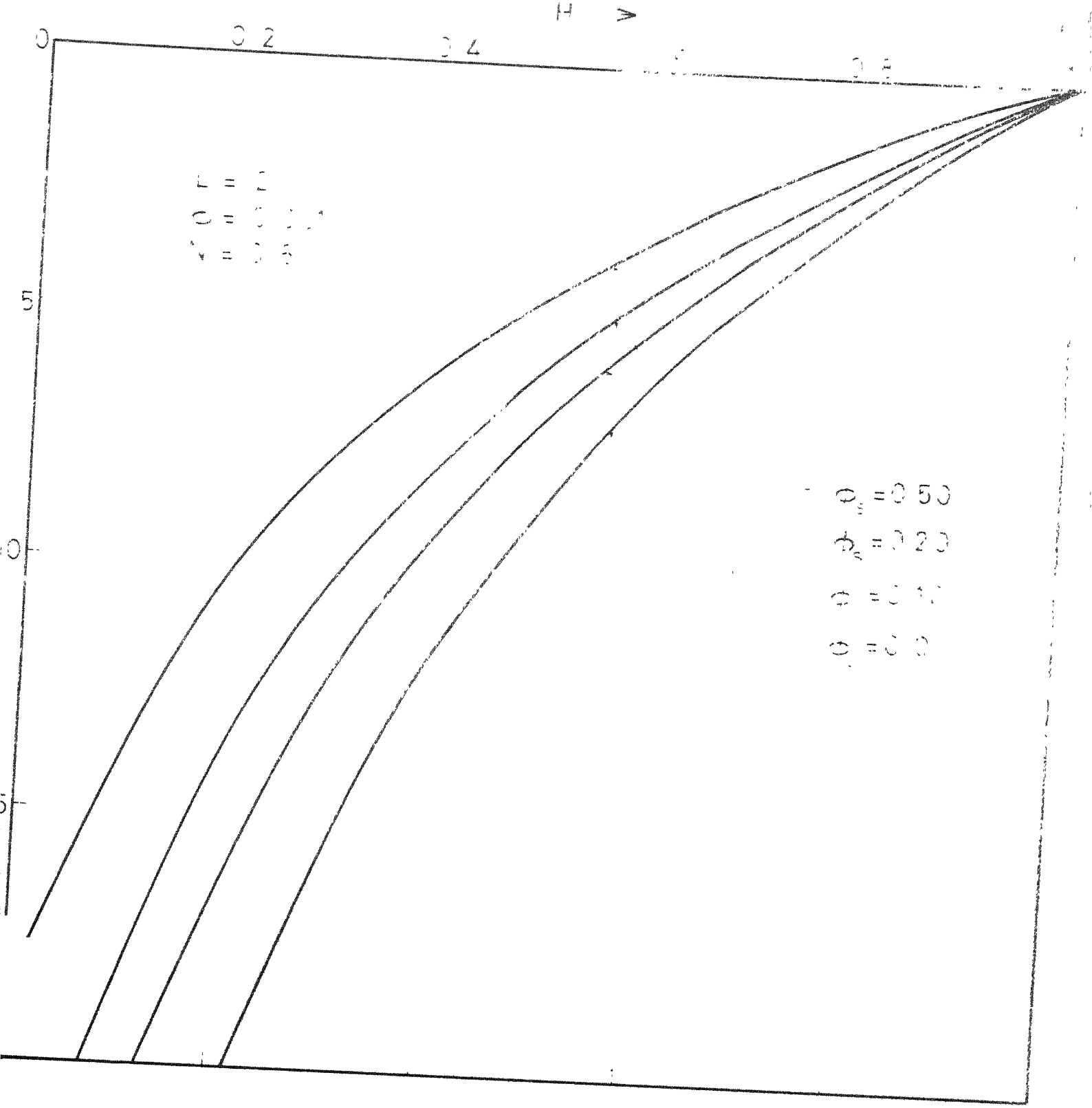

Fig 8.10 Non-dimensional film thickness vs non-dimensional time of approach for different values of slip parameter

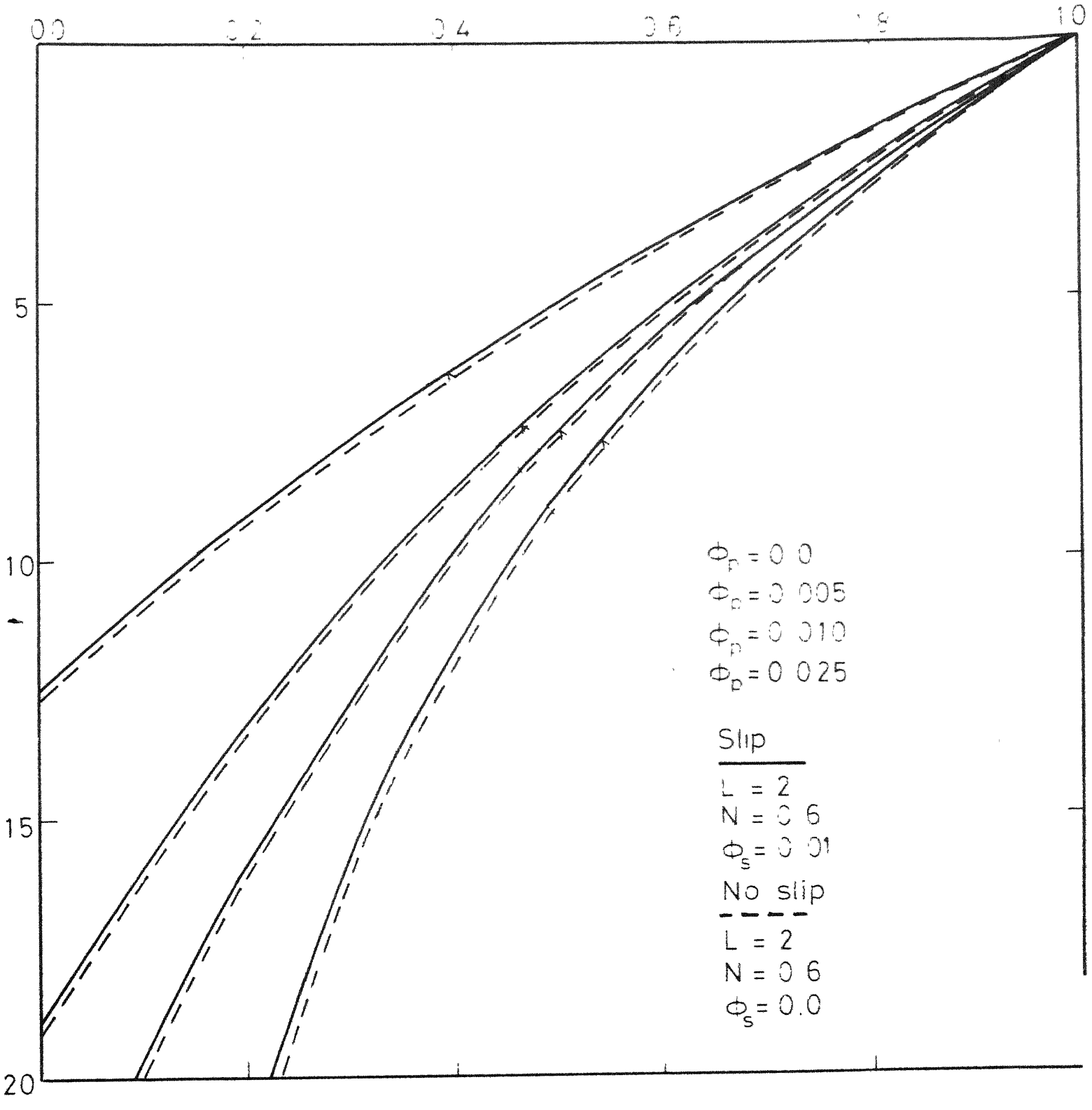

Fig. 8 11 Non-dimensional film thickness vs non-dimensional time of approach for different values of porosity parameter

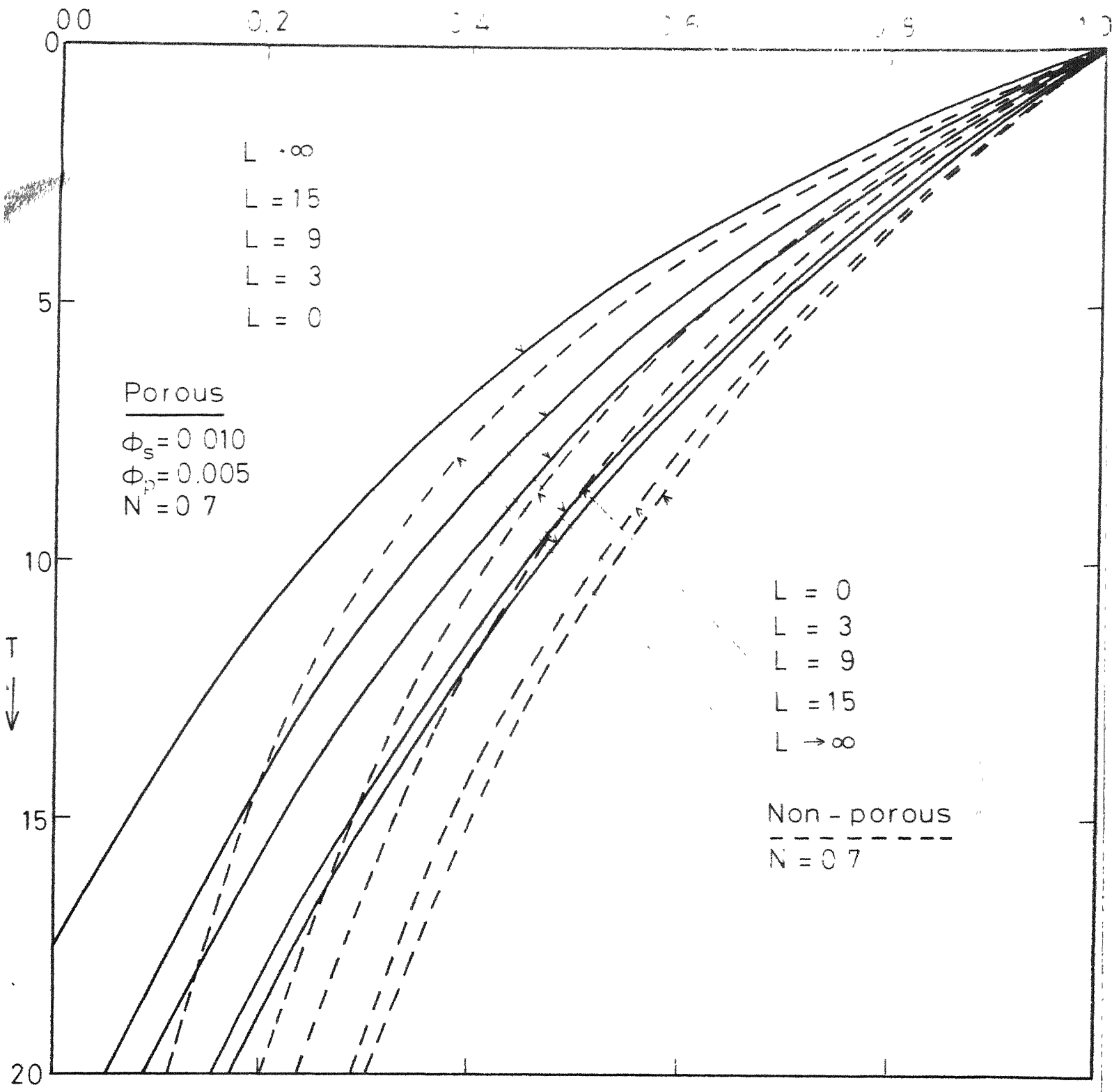

Fig 8.12 Non-dimensional film thickness vs non-dimensional time of approach for different values of L

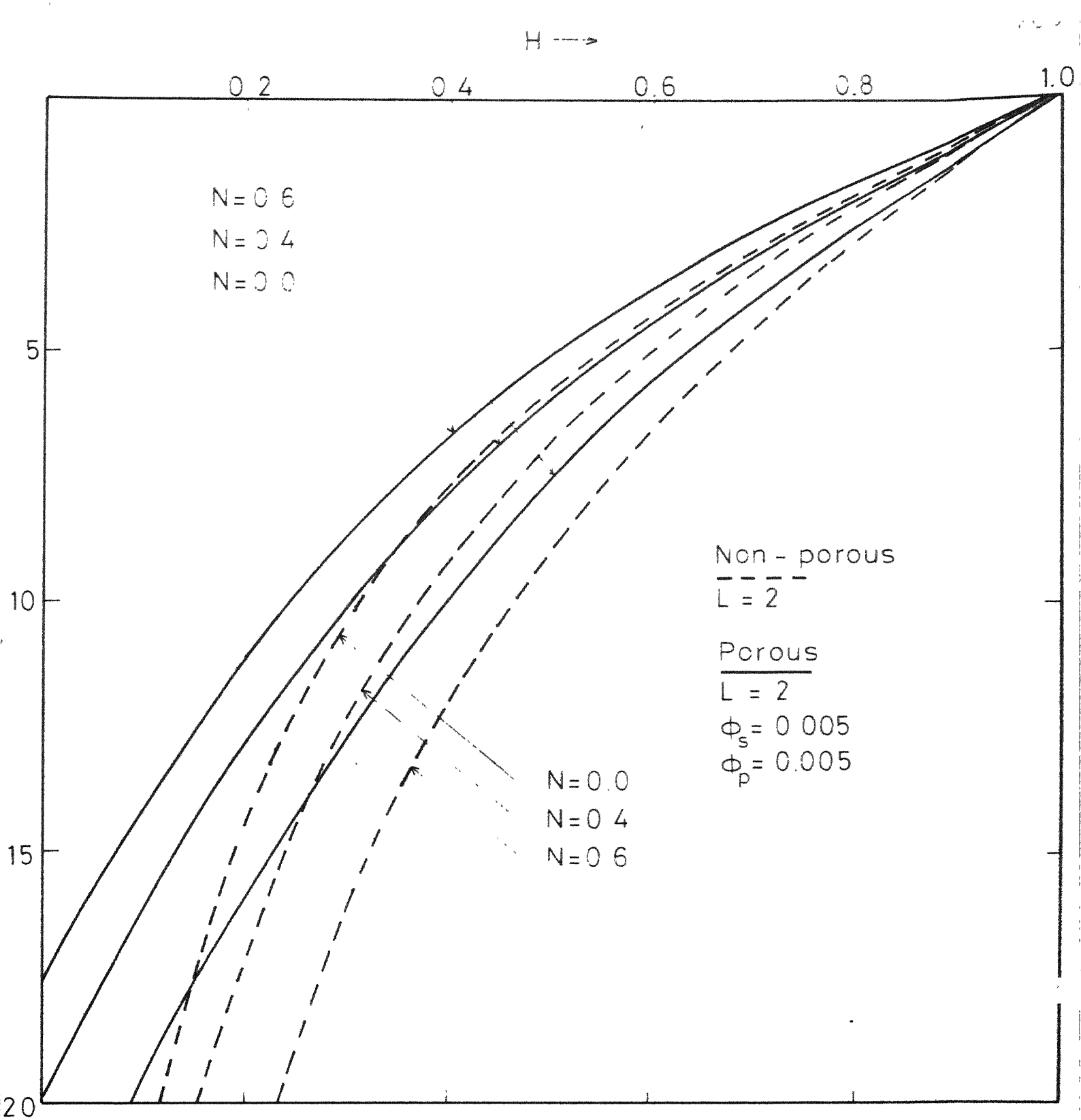

Fig 8 13 Non - dimensional film thickness vs non - dimensional time of approach for different values of coupling number

CHAPTER IX

SUMMARY AND CONCLUSIONS

The classical lubrication theory is based upon a fundamental assumption that the fluid film behaves in a Newtonian way, i.e. on the classical continuum theory. However, the atomistic models of the material, especially of fluids that possess coarse structure and fibres (such as colloidal fluids, liquid crystals and fluid containing additives) have shown that the mass density can fluctuate violently with the size of the volume element, when it is below a certain critical limit but still in the macroscopic range. Thus the continuum assumption for mass density is no longer applicable.

Another important class of problems where the classical theory is likely to give erroneous results is when the characteristic length scale is comparable to the average grain or molecule size contained in the medium. In such situations the molecular or the granular constituents of the medium are excited individually and the intrinsic motion of the material constituents must be taken into account. Typical of this class are the problem of flow through narrow passages, such as those found in human arteries and in lubrication theory.

The classical lubrication theory also contains no mechanism to explain the presence of the residual film so commonly observed by various workers [22,28,29,31,36] . Thus there is a strong

motivation for extending the range of applicability of continuum mechanics, particularly in the study of fluid flow of the type mentioned above, using the field theory approach to describe the macroscopic manifestation of microscopic events, i.e. micromotions and deformations.

Microscopic effects generated by the micromotions of particles in suspension of viscous fluids, or by the molecules in the proximity of a solid surface, drastically change the character of flow between narrow passages. The origin of the rheological abnormalities is then to be investigated on the basis of the theory of micro-mechanical motions.

One way of accounting for these micro-mechanical motions is through the so called theory of fluid microcontinua, advanced by Eringen [40] , in which the continuous media are now regarded as sets of structured particles, which not only contain mass and velocity but also a substructure, i.e. each material volume element contains microvolume elements which can translate, rotate and deform independently of the motion of the macrovolume. Thus a mechanism is provided in this theory to treat materials which are capable of supporting local stress moments and body moments and in addition are influenced by the microelement spin inertia.

The microfluid theory is however too complicated and the underlying theoretical problem is not easily amenable to the solution of non-trivial problems in this field. This led Eringen to postulate a subclass of these microfluids, called micropolar fluids [44] , which would still

exhibit effects arising from particle micromotion. For this class of fluids, the deformation of the fluid microelement is ignored, nevertheless, microrotation effects are still present and surface and body couples are permitted.

Physically the theory of micropolar fluids may serve as a satisfactory model for description of the flow behaviour of polymeric fluids and fluid suspensions, or wherever the microrotation may play an important role. One is then naturally inclined to apply this concept of the microcontinuum to the analysis of a wide variety of fluid flow problems wherever a further refined model of fluid behaviour is sought.

Motivated by these considerations the lubrication theory for micropolar fluids has been developed by many authors in the last decade. Various traditional lubrication problems have been reported. The results obtained are encouraging and illustrate the capabilities of this theory, in explaining the phenomenon of the enhancement of effective viscosity in thin films. Even after a decade, this study seems to be in a preliminary state. Scores of lubrication problems have yet to be solved from this view point. For example, little work has appeared on dynamically loaded bearings and porous bearings from the microcontinuum view point. Moreover, the problems of finite dimensional bearings and bearings with rough surfaces from this view point are yet to be analyzed.

Thus, in this thesis, these lubrication problems are studied from the microcontinuum point of view, in an attempt to explain theoretically the rheological abnormalities so frequently observed in fluids with additives, especially when confined to narrow passages.

The thesis begins with an introductory type Chapter, emphasizing the existence of the residual film in the proximity of a solid surface and laying the foundation for the application of the theory of micropolar fluids to certain hitherto untouched lubrication problems. Then in Chapter II, a generalized Reynolds equation applicable to finite lubrication problems, is derived, using the micropolar fluid theory. The equations obtained in Chapter II are applied in Chapter III, to a two-dimensional problem of squeeze film of a ball in a spherical seat and to some three dimensional non-cyclic squeeze films, assuming the characteristic coefficients to be constant, in an attempt to study the effects of rigid particle additives for the three dimensional micropolarity model. Increase in effective viscosity due to the micropolarity is established theoretically. It is also shown that the theoretical effects of the micropolarity on three dimensional lubrication are identical to the two dimensional problems, at least qualitatively.

A very important result of this study is the dependence of bearing characteristics on a non-dimensional length parameter $L(=\frac{c}{\ell}$, where c is the bearing clearance and $\ell = (\frac{\gamma}{4\mu})^{1/2}$, a fluid property having the dimensions of length). This parameter links the fluid with the bearing geometry and can be thought of as a number which

is inversely proportional either to the length of the molecule of a non-Newtonian lubricant or to the molecular size of the additive. It is found that smaller the L(i.e. larger the ℓ, or smaller the clearance) more pronounced are the micropolar effects.

This dependence of bearing characteristics, especially effective viscosity, on the geometry of the system, may also give a possible explanation for discrepancies in actual viscosity measurements made using viscometers of different designs or sizes.

It should also be noted that most of the earlier workers have used the relation $o \leq N^2 < 1$. However, in Chapter III it is shown that $o \leq N^2 < \frac{1}{2}$. Thus the results of those workers are grossly exaggerated due to non-admissible values of N.

The next problem (Chapter IV), deals with the dynamically loaded short journal bearings in which both wedge and squeeze films are active. The Reynolds equation for the general case of dynamically loaded infinitely short bearing is derived, where the lubricant is assumed to be micropolar. Detailed consideration is given to the dynamic behaviour of squeeze film in a short journal bearing under a sinusoidal load with no journal rotation. Various bearing characteristics are obtained assuming a full film to exist. The micropolarity of the fluid results in more resistance to journal motion, thereby allowing for smaller eccentricities for a constant load. The overall conclusion of this study is an increase in effective viscosity due to the micropolarity of the lubricant.

The next problem (Chapter V), is that of the roller bearings in combined rolling, sliding and normal motion analyzed under cavitation boundary conditions. Various bearing characteristics are obtained and represented graphically. The overall conclusion of the study, in conformity with the experimental results, is an increase in effective viscosity, resulting in an increase in load carrying capacity and a decrease in coefficient of friction, when analyzed from microcontinuum view point.

It has been experimentally observed [27] that there is a sudden decrease in the coefficient of friction on addition of long-chain polar compounds. A graph of the values of coefficient of friction plotted against molecular weight (see ref. 136, p.350) shows the greater the number of atoms and longer the molecule the lower the coefficient of friction will be. Holding h_o constant (where h_o is the minimum film thickness), and recalling that $L = \frac{h_o}{\ell}$ (L is defined in this way in Chapter V), L for the curves in Figs. 5.6 to 5.8 is seen therefore to depend only on the fluid, that is on the material characteristic length. Considering the length of molecules of the boundary lubricant to be proportional to the material characteristic length, it is observed that the portion of the curve (N = o.7) in Figs. 5.6 to 5.8, to the right of the minimum satisfies the result that an increase in the length of molecule (corresponding to a decrease in L) causes a decrease in coefficient of friction and vice-versa.

In the next problem (Chapter VI), micropolar fluid theory is applied to study the effects of surface roughness. Generalized forms of Reynolds equation are derived for three cases of roughness, namely, transverse roughness, longitudinal roughness and isotropic roughness, using the stochastic approach. For mathematical simplicity only the stationary part of the bearing is assumed to be rough. This theory is subsequently applied to the problem of infinitely long journal bearing in order to study the interaction of micropolarity with surface asperities, using the half Sommerfeld boundary conditions. Various bearing characteristics are obtained numerically and results are compared with smooth bearing using nominal film thickness concept. The results obtained are in qualitative agreement with Newtonian results for rough surfaces. However, it is shown that the effects of surface roughness are more pronounced, when analyzed from microcontinuum view point.

A number of experiments in which the evidence of rheological abnormalities, like enhancement of viscosity, has been rather extensive and convincing, are of squeeze film type [22,28,29,31,36] .

It has been suggested that the asperities on the solid surface might account for the rheological abnormalities and residual film [30] .

Motivated by these considerations, the next problem (Chapter VII) deals with the squeezing between rough parallel plates. Three standard geometries, namely, infinitely long parallel plates, circular plates

and finite rectangular plates, are considered. Various squeeze film characteristics are obtained for the three cases of roughness. The results are compared with the corresponding smooth plates. The rather important geometry, i.e. the finite rectangular plates squeeze film is analyzed in details. Since this geometry can distinguish between the one-dimensional roughness and isotropic roughness, a comparision is made between these two cases. Further, for a constant area bearing, it is observed that the aspect ratio (width/length) plays a vital role for one-dimensional roughness, i.e. the bearing characteristics, for a given roughness, may increase or decrease depending upon this parameter.

The last problem (Chapter VIII) is of synovial joint lubrication studied from microcontinuum view point. The synovial joints provided by the nature in the human body to carry out the trouble free motion of one bone past another, have long been identified as bearing systems. The present situation regarding joint lubrication is, however, not very clear. Earlier work, based upon the classical continuum theory, could not give a satisfactory explanation for the increased effective viscosity in synovial joints. The microcontinuum approach represents a more realistic model for explaining the complex mechanism occuring in human joints.

The behaviour of the synovial fluid, which has long chain hyaluronic acid molecules, is considered to be governed by the micropolar fluid theory. The porosity of the cartilage surface

and the slip at the porous boundary are taken into account and a modified form of Reynolds equation is derived. The joints are approximated by a spherical bearing and various bearing characteristics are obtained in details. The salient feature of this study, is an increase in effective viscosity. This theory also establishes theoretically, that for a diseased or a damaged joint the load capacity and the response time decrease . This decrease may result in pain in case of diseased rheumatoid joint.

The correlation of the results obtained in this thesis with various experimental studies may perhaps be believed coincidental and is definitely open to criticism since, in the light of these studies no experimental verification of the micropolar theory has been made. Nevertheless, at this early stage such criticisms are natural and in fact healthy for a crucial scrutiny of the theory and its ultimate acceptance. The results obtained are, however, interesting, and it is our strong belief that the micropolar fluid theory has the potentialities to explain the rheological anomalies in fluids containing additives through the parameters N and L when they flow through narrow passages.

Although the various results based on this theory are in perfect qualitative agreement with the experimentally observed results, an attempt for a quantitative fit would not be of any significance (since two undetermined parameters exist for curve fitting) unless some numerical values could be ascribed to the coefficient χ and γ.

A significant step in this direction is by Arimon et.al [137] who established a relationship between the microscopic coefficients and hematocrit concentration in blood samples. Further, Muglianello and Sevilla [138] , Goldsmith and Mason [139] , Zakhaveva et. al. [140] and Puks [28,29] established a relationship between the effective viscosity and the molecular weight (particle size).

It is hoped that these studies would raise the curiosity of serious research workers to this rich field. The most useful contribution in this direction would be a repetition of the past experimental studies, in the light of these microcontinuum effects and thereby providing a much needed correlation with the theory.

REFERENCES

1. Parish, W.F. (1929)
   Lubricants.
   Encyclopaedia Britannica, 14th Ed., Vol.14, 1929,p.451.

2. Adams, W.F. (1853)
   Railway axle lubrication.
   Proc.Instn.Mech.Engrs.,Vol.4,1853,p.57.

3. Petrov, N. (1883)
   Friction in machines and the effect of the lubricant. (in Roman).
   Engng.J.St.Petersb.,1883,p.71-140,228-279,377-436, 535-564.

4. Tower,B. (1883,1884,1885)
   (i) First report in friction experiments.
   (a) Proc.Instn.Mech.Engrs.,Vol.34,1883,p.632.
   (b) Proc.Instn.Mech.Engrs.,Vol.35,1884,p.29.
   (ii) Second report on friction experiments.
   Proc.Instn. Mech.Engrs.,Vol.36,1885,p.58.

5. Reynolds,O. (1886)
   On the theory of lubrication and its application to Mr. Beauchamp Tower's experiments including an experimental determination of the viscosity of Olive oil.
   Phil.Trans.Roy.Soc.,London.,Series A, Vol.177, 1886,p.137.

6. Sommerfeld,A.(1904)
   Zur hydrodynamischen theorie der schmiermi-Helreiburg.
   Z.Angew.Math.U.Phys.,Vol.50,1904,p.97.

7. Boswall,R.O. (1928)
   The theory of film lubrication,Longmans, London, 1928.

8. Henniker,J.C. (1949)
   The depth of the surface zone of a liquid.
   Rev.Mod.Phys.,Vol.21,1949,p.322.

9. Allen,C.M. and Drauglis,E. (1969)
   Boundary layer lubrication : Monolayer or multilayer.
   Wear, Vol.14, 1969,p.363.

10. Kingsbury, A. (1903)
A new oil-testing machine and some of its results.
TRANS.ASME, Vol.24, 1903, p.144.

11. Hardy, W. and Nottage, M. (1926)
Studies in adhension-I.
Proc.Roy.Soc., London, Series A, Vol.112, 1926, p.64.

12. Hardy, W. and Nottage, M. (1928)
Studies in adhension-II.
Proc.Roy.Soc., London, Series A., Vol.118, 1928, p.225.

13. Hardy, W. and Nottage, M. (1930)
The analysis of commercial lubricating oils by physical methods.
Lubrication Research Technical Paper No.1.
Department of Scientific and Industrial Research, London, 1930, p.2.

14. Wilson, R.E. and Barnard, D.P. (1922)
The mechanism of lubrication-II :
Methods of measuring the properties of oilness.
J.Ind.Engng.Chem., Vol.14, 1922, p.683.

15. Bulkley, R. (1931)
Viscous flow and surface films.
J.Research Nat. Bur. Stand., Vol.6, 1931, p.89.

16. Bastow, S.H. and Bowdon, F.P. (1931)
On the contact of smooth surfaces.
Proc.Roy.Soc., London, Series A, Vol.134, 1931, p.404.

17. Bastow, S.H. and Bowdon, F.P. (1935)
Physical properties of surfaces-II : Viscous flow of liquid films.
Proc.Roy. Soc., London, Series A, Vol.151, 1935, p.220.

18. Griffiths, A.A. (1921)
The phenomena of rupture and flows in solids.
Trans.Roy.Soc., London, Series A, Vol.221, 1921, p.163.

19. Tausz, J. and Szekley, P. (1933)
Erod u Teer, Vol. 9, 1933, p.331.

20. Terzaghi, C. (1924)
Zeets.f. Angew. Math.Mech., Vol.4, 1924, p.107.

21. Macauly, J.M. (1936)
Range of action of surface forces.
Nature, Vol. 138, 1936, p.587.

22. Needs, S.J. (1940)
Boundary film investigations.
TRANS.ASME, Vol.62, 1940, p.331.

23. Adamson, A.W. (1960)
Physical Chemistry of Surfaces.
New York, Interscience, 1960.

24. Wells, H.M. and Southcombe, J.E. (1920)
The theory and Practice of lubrication -
The germ process.
J.Soc.Chem.Ind.(London), Vol.39, 1920, p.51.

25. Hardy, W.B. and Doubleday, I. (1921)
Boundary lubrication - The paraffin series.
Proc.Roy.Soc., London, Series A, Vol.100, 1921,
p.550.

26. Hardy, W.B. and Doubleday, I. (1923)
Boundary lubrication - The latent period
and mixture of two lubricants.
Proc.Roy.Soc., London, Series A, Vol.104,
1923, p. 25.

27. Beeck, O., Givens, I.W. and Smith, A.E. (1940)
On the mechanism of boundary lubrication I. The
action of long-chain polar compounds.
Proc.Roy.Soc., London, Series, A, Vol.177,
1940, p.90.

28. Fuks, G.I. (1960)
The properties of solutions of organic acids
in liquid hydrocarbons at solid surface ,
Research in Surface Forces, Ed. Deryagin,
B.V., Vol.1, 1960, p.79.

29. Fuks, G.I. (1964)
The polymolecular component of the lubricating
boundary layer.
ibid., Vol.2, 1964, p.159.

30. Hayward, A.T.J. and Isdale, J.D. (1969)
The rheology of liquids very near to solid
boundaries.
Brit.J. Appl.Phys., Vol.2, 1969, p.251.

31. Drauglis,E., Lucas,A.A. and Allen,C.M. (1970)
Thin film rheology of boundary lubricating surface films, Part I Battelle Memorial Institute Report,1970.

32. Derjaguin,B.V. (1933)
Z. Phys.Vol.84,p.657,1933.

33. Derjaguin,B.V.,Karasev,V.V., Zakhavaeva,N.N. and Lazarev, U.P. (1957).
Soviet Phys. - JEPT, Vol.27, 1957, p. 980.

34. Cameron,A. and Crouch, R.F. (1963)
Interaction of hydrocarbon and surface active agent.
Nature, London, Vol.198, 1963,p.475.

35. Gohar,R. and Cameron, A. (1963)
Optical measurement of oil film thickness under elastohydrodynamic lubrication.
Nature,London, Vol.200,1963,p.458.

36. Askwith,T.C.,Cameron,A. and Crouch,R.F. (1966)
Chain length of additives in relation to lubricants in thin film and boundary lubrication.
Proc.Roy.Soc.,London,Series A, Vol.291,1966, p.500.

37. Cameron,A. and Gohar,R. (1966)
Theoretical and experimental studies of the oil film in lubricated point contact.
Proc.Roy.Soc.,London,Series A, Vol.291,1966,p.520.

38. Drauglis,E, Lucas,A.A. and Allen,C.M. (1971)
Smectic model for liquid films on solid substrates.
Spec.Disc.Far.Soc.,Vol.1,1971,p.251.

39. Ariman,T.,Turk, M.A. and Sylvester,N.D. (1973)
Microcontimuum fluid mechanics - A Review.
Intern.J. Engng. Sci., Vol.11,1973,p.905.

40. Eringen,A.C. (1964)
Simple microfluids.
Intern.J.Engng.Sci.,Vol.2,1964,p.205.

41. Eringen,A.C. (1964)
Mechanics of micromorphic materials.
Proc.XI Intern.Cong.Appl.Mech.,Munich, Germany,1964,p.131.

42. Eringen,A.C. and Suhubi, E.S., (1964)
Non-linear theory of simple microelastic solids-I.
Intern.J.Engng.Sci.,Vol.2,1964,p.189.

43. Suhubi,E.S. and Eringen,A.C. (1964)
Non-linear theory of simple microelastic solids-II.
Intern.J.Engng.Sci.,Vol.2,1964,p.389.

44. Eringen,A.C. (1966)
Theory of micropolar fluids.
J.Math.Mech.,Vol.16,1966,p.1.

45. Ariman,T.,Turk, M.A. and Sylvester,N.D. (1974)
Application of microcontinuum fluid mechanics.
Intern.J.Engng.Sci.,Vol.12,1974,p.273.

46. Kline,K.A. and Allen,S.J. (1970)
Fluid suspensions flow formation in Couette motion.
Z.Angew.Math.Phys.,Vol.21,1970,p.26.

47. Kline,K.A. and Allen,S.J. (1971)
A thermodynamic theory of fluid suspensions.
Physics of Fluids,Vol.14,1971,p.1863.

48. Kline,K.A. and Allen,S.J. (1970)
Non-steady flows of fluids with microstructure.
Physics of Fluids,Vol.13,1970,p.263.

49. Cowin,S.C. (1968)
Polar Fluids.
Physics of Fluids,Vol.11,1968,p.1919.

50. Pennington,C.J. and Cowin,S.C. (1969)
Couette flow of a polar fluid.
Trans.Soc.Rheol.,Vol.13,1969,p.387.

51. Pennington,C.J. and Cowin,S.C. (1970)
The effective viscosity of polar fluids.
Trans.Soc.Rheol.,Vol.14,1970,p.219.

52. Willson,A.J. (1970)
Boundary layers in micropolar fluids.
Proc.Camb.Phil.Soc.,Vol.67,1970,p.469.

53. Peddieson (Jr.), J. and McNitt,R.P. (1970)
Boundary-layer theory for a micropolar fluid.
Recent Advances in Engineering Sciences, Vol.5, 1970, p.405.

54. Allen,S.J. and Kline,K.A. (1971)
Lubrication theory for micropolar fluids.
Trans.ASME, J. Appl. Mech., Vol.38, 1971,p.646.

55. Agrawal,V.K., Ganju, K.L. andJethi,S.C. (1972)
Squeeze films and externally pressurized bearings micropolar fluid lubricated.
Wear,Vol.19, 1972,p.259.

56. Balaram,M. and Shastri,V.U.K. (1972)
Micropolar lubrication.
Trans.ASME, J. Appl.Mech.,Vol.39, 1972,p.834.

57. Shukla, J.B. and Isa, M. (1975)
Generalized Reynolds equation for micropolar lubricants and its application to optimum one-dimensional slider bearings : Effects of solid particle additives in solution.
J. Mech. Engng. Sci., Vol. 17, 1975, p.280.

58. Prakash, J. and Sinha, P. (1975)
Lubrication theory for micropolar fluids and its application to a journal bearing.
Intern. J. Engng. Sci., Vol.13, 1975, p.217.

59. Datta,A.B. (1972)
Pivoted slider bearing with convex pad surface in micropolar fluids.
Japanese J. Appl. Phys. Vol.11, 1972, p.98.

60. Maiti,G. (1973)
Composite and step slider bearing in micropolar fluid.
Jap.J. Appl. Phys.,Vol.12, 1973,p.1058.

61. Isa,M. and Zaheeruddin, K. (1978)
Analysis of step bearings with a micropolar fluid lubricant.
Wear., Vol. 47, 1978, p. 211.

62. Verma,P.D.S., Agrawal, V.K. and Bhatt, S.B. (1979)
Porous inclined slider bearing lubricated with micropolar fluid.
Wear,Vol.53,1979, p.101.

63. Sinha, P. and Singh, C. (1981)
The effect of additives in the lubricant of a composite bearing with an inclined stepped surface.
Wear,Vol.66,1981,p.17.

64. Prakash, J. and Sinha, P. (1977)
Theoretical effect of solid particle on the lubrication of journal bearing considering cavitation.
Wear,Vol.41,1977,p.104.

65. Prakash, J. and Sinha, P. (1975)
Micropolar fluid lubricated journal bearings with smooth out flow.
Letters in Applied and Engineering Sciences, an International Journal, Vol.3, No.3, 1975, p.213.

66. Mahanti,A.C. (1976)
A theoretical study of the effect of solid particles in the lubricant of a partial journal bearing.
Wear, Vol.39, 1976, p. 45.

67. Isa, M. and Zaheeruddin, K. (1978)
Micropolar fluid lubrication of one-dimensional journal bearing.
Wear,Vol.50, 1978,p.211.

68. Balaram, M. (1975)
Micropolar squeeze films.
TRANS.ASME,J.Lub.Tech.,Vol.97,1975,p.565,

69. Prakash,J. and Sinha, P. (1976)
Squeeze film theory for micropolar fluids.
Trans.ASME,J. Lub. Tech.,Vol.98,1976,p.139.

70. Prakash, J. and Sinha, P. (1976)
A study of squeeze flow in micropolar fluid lubricated journal bearing.
Wear,Vol.38,1976,p.17.

71. Ramanaiah,G. and Dubey,J.N. (1975)
Micropolar fluid lubricated squeeze films and thrust bearings.

72. Zaheeruddin,K. and Isa, M. (1978)
Characteristics of a micropolar lubricant in squeeze film porous spherical bearing.
Wear,Vol. 51, 1978, p.1.

73. Tandon, P.N. and Jaggi, S. (1979)
A polar model for synovial fluid with reference to human joints.
Intern. J. Mech. Sci., Vol.21, 1979, p.161.

74. Tandon, P.N. and Jaggi, S. (1977)
Lubrication of porous solids in reference to human joints.
Proc.Indian Acad.Sci., Vol.85, 1977, p.144.

75. Prakash, J. and Sinha, P. (1976)
Cyclic squeeze films in micropolar fluid lubricated journal bearings.
Trans.ASME, J. Lub. Tech., Vol.98, 1976, p.412.

76. Sinha, P. (1977)
Dynamically loaded micropolar fluid lubricated journal bearings with special reference to squeeze film under fluctuating loads.
Wear, Vol.45, 1977, p.279.

77. Khader, M.S. and Vachon, R.I. (1973)
Theoretical effects of solid particles in hydrostatic bearing lubricant.
Trans. ASME, J. Lub. Tech., Vol.95, 1973, p.104.

78. Shukla, J.B. and Isa, M. (1975)
Externally pressurized optimum bearing with micropolar fluid as lubricant.
Jap. J. Appl. Phys., Vol. 14, 1975, p. 275.

79. Isa, M. and Zaheeruddin, K. (1977)
Hydrostatic step seal and externally pressurized conical step bearing with micropolar lubricant.
Japanese J. Appl. Phys., Vol.66, 1977, p.1577.

80. Prakash, J. and Christensen, H., (1976)
Rheological anomalies in thin hydrodynamic films- A microcontinuum view.
Presented at the Symposium on Lubricant Properties in Thin Lubricating Films, April 4-9, 1976, Centennial ACS meeting, New York, ACS Preprint, Vol.21, 1976, p.79.

81. Sinha, P. (1977)
Effect of rigid particles in the lubrication of rolling contact bearings considering cavitation.
Wear, Vol.44, 1977, p.295.

82. Prakash, J. and Christensen, H. (1977)
A microcontinuum theory for the elastohydrodynamic inlet zone.
Trans. ASME, J. Lub. Tech., Vol.99, 1977, p.24.

83. Mahanti, A.C. and Ramanaiah, G. (1976)
Inertia effects of micropolar fluid in squeeze bearings and thrust bearings.
Wear, Vol. 39, 1976, p.227.

84. Tipei, N. (1979)
Lubrication with micropolar liquids and its application to short bearings.
Trans. ASME, J. Lub. Tech., Vol.101, 1979, p.356.

85. Pinkus, O. and Sternlicht, B. (1961)
Theory of hydrodynamic lubrication.
McGraw-Hill, Inc., New York, 1961.

86. Cameron, A. (1966)
The principles of lubrication.
Longmans Green and Co. Ltd., 1966.

87. Sinha, P. and Singh, C. (1981)
Theoretical effects of rigid particle additives in non-cyclic squeeze films.
Trans. ASME, J. Lub. Tech., (To appear, 1981).

88. Archibald, F.R. (1956)
Load capacity and time relation for squeeze films.
Trans. ASME, Vol. 78, 1956, p.29.

89. Ocvirk, F.W. (1952)
Short bearing approximation for full journal bearings.
NASA, Washington, D.C., TN 2808, 1952.

90. Sasaki, T., Mori, H. and Okino, N. (1962)
Fluid lubrication theory of roller bearings.
Trans. ASME, J. Basic Engng., Series D, No.1, Part I, p. 166 ; Part II , 1962, p.175.

91. Dowson, D., Markho, P.H. and Jones, D.A. (1976)
Lubrication of lightly loaded cylinders in combined rolling, sliding and normal motion. Part I - Theory.
Trans. ASME, J. Lub. Tech., Vol. 98, 1976, p.509.

92. Markho, P.H. and Dowson, D. (1976)
The lubrication of lightly loaded cylinders in combined rolling, sliding and normal motion. Part - II, Experiment.
Trans.ASME, J. Lub. Tech.,Vol.98,1976, p.517.

93. Dowson,D. and Higginson, G.R. (1966)
Elastohydrodynamic lubrication : The fundamentals of roller and gear lubrication.
Pergamon Press, Oxford.

94. Floberg, L. (1961)
Lubrication of two cylindrical surfaces considering cavitation.
Transactions of Chalmers University of Technology, 234, No. 14, Institute of Machine Elements,1961.

95. Burton,R.A. (1963)
Effects of two dimensional, sinusoidal roughness on the load support characteristics of a lubricant film.
Trans. ASME, J. Basic Engng., Series D, Vol. 85, 1963, p.258.

96. Tzeng,S.T. and Saibel, E. (1967)
Surface roughness effect on slider bearing lubrication.
ASLE, Trans.,Vol. 10, 1967, p.334.

97. Tzeng,S.T. and Saibel, E. (1967)
On the effects of surface roughness in the hydrodynamic lubrication theory of a short journal bearing.
Wear, Vol.10, 1967,p.179.

98. Ostvik, R. and Christensen, H. (1968-69)
Changes in surface topography with running - in.
Proc. Instn. Mech. Engrs., Vol. 183 (Pt. 3P), 1968-69, p.59.

99. Christensen, H. and Tonder,K. (1969)
Tribology of rough surfaces :
Stochastic models of hydrodynamic lubrication.
SINTEF Report 10/69-18,1969.

100. Christensen, H. and Tonder, K. (1969)
Tribology of rough surfaces : Parametric study and comparison of lubrication models.
SINTEF Report 22/69-18,1969.

101. Christensen, H. (1969-70)
Stochastic models for hydrodynamic lubrication of rough surfaces.
Proc. Instn. Mech. Engrs., Vol.184, (Pt.1), 1969-70, p.1013.

102. Elrod, H.G. (1973)
Thin-film lubrication theory for Newtonian fluids with surfaces possessing striated roughness or grooving.
Trans.ASME, J. Lub. Tech., Vol.95, 1973, p.485.

103. Tonder, K. (1976)
Lubrication of surfaces having area distributed Isotropic roughness.
Joint ASME - ASLE Lubrication Conference Oct. 1976, Boston.

104. Prakash, J. and Tonder, K. (1978)
Roughness effects in circular squeeze-plates.
ASLE, Trans., Vol.20, 1978, p.257.

105. Prakash, J. and Christensen, H. (1978)
Squeeze film between two rough rectangular plates.
J. Mech. Engng. Sci., Vol.20, 1978, p.183.

106. Moore, D.F. (1965)
Drainage criteria for runway surface roughness.
J. Roy. Aeron. Soc., Vol. 69, No.653, 1965, p.337.

107. MacConaill, M. A. (1932)
The function of intra-articular fibrocartilages with special reference to the knee and inferior redioular joints.
J. Anat., Vol.66, 1932, p.210.

108. Charney, J. (1959)
The lubrication of animal joints.
Proc. Symp. Biomechanics, Instn. Mech. Engrs., London, Paper No. 12.

109. McCutchen, C.W. (1959)
Mechanism of animal joints.
Nature, Vol. 184, 1959, p.1284.

110. McCutchen, C.W. (1962)
The frictional properties of animal joints.
Wear, Vol. 5, 1962, p.1.

111. McCutchen, C.W. (1966)
Boundary lubrication by synovial fluid : Demonstration and possible osmotic explanation.
Fed.Proc., Vol.25(3), 1966, p.1061.

112. McCutchen, C.W. (1967)
Physiological lubrication.
Proc.Instn. Mech. Engrs., Vol.181(3J), 1967, p.55.

113. Dintenfass, L. (1963)
Lubrication in synovial joints : A theoretical analysis.
J.Bone. Jnt. Surg., Vol.45A(6), 1963, p.1241.

114. Tanner, R.I. (1966)
An alternative mechanism for the lubrication of synovial joints.
Phys.Med.Biol., Vol.11(1), 1966, p.119.

115. Dowson, D. (1967)
Modes of Lubrication in human joints.
Proc.Instn. Mech. Engrs., Vol.181 (3J), 1967, p.45.

116. Walker, P. S. , Dowson, D., Longfield, M.D. and Wright, V. (1968)
Boosted lubrication in synovial joints by fluid entrapment and enrichment.
Ann. Rheum. Dis., Vol.27(6), 1968, p.512.

117. Negami, S. (1964)
Dynamic Mechanical properties of synovial fluid.
M.S. thesis, Lehigh University, Penn., U.S.A., 1964.

118. Maroudas, A. (1966-67)
Hyaluronic acid films : Research report 2. Lubrication and wear in living and artificial human joints.
Proc. Instn. Mech. Engrs., Vol. 181 (Pt. 3J), 1966-67, p.122.

119. Higginson, G.R. and Norman, R. (1974)
The lubrication of porous elastic solids with reference to the functioning of human joints.
J. Mech. Engng. Sci. , Vol.16, 1974, p.250.

120. Unsworth, A., Dowson, D. and Wright, V. (1975)
Some new evidence on human joint lubrication.
Ann. Rheum. Dis., Vol.34,1975,p.277.

121. Wright,V. and Dowson, D. (1976)
Lubrication and cartilage.
J. Anat.,Vol.121,1976,p.107.

122. Fein, R.S. (1967)
Are synovial joints squeeze -film lubricated ?
Proc. Instn. Mech. Engrs., Vol.181 (Pt.3J),1967,
p.125.

123. Mow,M.C. and Ling, F.F. (1969)
On weeping lubrication theory.
ZAMP, Vol.20, 1969, p.156.

124. Dowson, D., Walker, P.S., Longfield, M.D. and Wright,V. (1970).
A joint simulating machine for load Bearing joints.
Med.Biol.Engng.,Vol.8,1970,p.37.

125. Dowson,D.,Unsworth, A. and Wright, V. (1970)
Analysis of boosted lubrication in human joints.
J. Mech. Engng. Sci.,Vol.12,1970,p.364.

126. Ling,F.F. (1974)
A new model of articular cartilage in human
joints.
TRANS.ASME,J.Lub. Tech., Vol.96, 1974,p.449.

127. Higginson, G.R. and Norman,R. (1974)
A model Investigation of squeeze film
lubrication in animal joint.
Phy.Med. Biol.,Vol.19,1974,p.785.

128. Mansour,J.M. and Mow, V.C. (1976)
The permeability of articular cartilage
under compressive strain and at high pressure.
J.Bone.Jnt.Surg.,Vol.58(A),1976,p.509.

129. Mansour, J.M. and Mow, V.C. (1976)
On the natural lubrication of synovial joints.
Presented at the Joint ASME - ASLE
Conference, Boston Paper No. 76-Lub-1, 1976.

130. Higginson, G.R. (1978)
Elastohydrodynamic lubrication in human joints.
Engng. in Med. ,Vol.7, 1978, p.1.

131. Mow,V.C. (1969)
The role of lubrication in biomechanical joints.
TRANS.ASME, J.Lub.Tech.,Vol.91,1969,p.320.

132. Beavers,G.S. and Joseph,D.D. (1967)
Boundary conditions at a naturally permeable wall.
J.Fluid Mech.,Vol.30,1967,p.197.

133. Scheidigger,A.E. (1957)
The physics of flow through porous media.
The MacMillan Company,New York,N.Y.,1957,p.54-69.

134. Bloch,B. and Dintenfass, L. (1963)
Rheological study of human synovial fluid.
Australian - New - Zealand J. of Surgery, Vol. 33, 1963, p. 108.

135. Burch, G.E., Love, W.D. and Jeffrey (1960)
The waning joints.
Progress of Medical Sciences, Volume of January,1960.

136. Fuller,D.D. (1956)
Theory and practice of lubrication for engineers.
Wiley,1956.

137. Ariman, T., Turk, M.A. and Sylvester, N.D. (1974)
On steady and pulsatile flow of blood.
TRANS.ASME, J. Appl.Mech.,Vol.96,1974,p.1.

138. Bugliarello, G. and Sevilla, J. (1970)
Velocity distribution and other characteristics of steady and pulsatile blood flow in fine glass tubes.
Bio-rheology, Vol.7, 1970,p.85.

139. Goldsmith, H.L. and Mason, S.G. (1967)
The microrheology of dispersions.
Rheology - Theory and Applications, R.F. Elrich, ed., Academic Press, New York,1967,p.86-250.

140. Zakhaveva,N.N., Deryagin, B.V., Khomutov, A.M. and Andreev, S.V. (1964)
The effect of molecular weight and structure on the viscosity and stability of the thin liquid film.
Research in Surface Forces,B.V. Deryagin,ed.,Vol.2,